Naphthalene Based Conjugated Materials

Dissertation

zur Erlangung des akademischen Grades

Doktor der Naturwissenschaften
(Dr. rer. nat.)

eingereicht im Fachbereich C – Mathematik und Naturwissenschaften der
Bergischen Universität Wuppertal

von

Benjamin S. Nehls

aus Remscheid

Wuppertal, 2005

„Der erste Trunk aus dem Becher der Naturwissenschaften macht atheistisch, aber auf dem Grund des Bechers wartet Gott.“

Werner Heisenberg

„Never, never, never ever give up!“

Winston Churchill

Die vorliegende Arbeit wurde in der Zeit von Dezember 2003 bis Juli 2005 am Lehrstuhl für Makromolekulare Chemie des Fachbereiches C – Mathematik und Naturwissenschaften der Bergischen Universität Wuppertal unter Anleitung von Prof. Dr. U. Scherf durchgeführt.

Mein besonderer Dank gilt Herrn Prof. Dr. U. Scherf für die Überlassung des interessanten und fruchtbaren Themas dieser Arbeit, seine stete Diskussionsbereitschaft sowie seine vielfältige persönliche Unterstützung.
Ein weiterer Dank gilt dem Verband der chemischen Industrie für die freundlich gewährleistete finanzielle Unterstützung.

1. Gutachter: Prof. Dr. U. Scherf (BU Wuppertal)
2. Gutachter: Prof. Dr. S. Ramakrishnan (IISc, Bangalore, India)
Eingereicht am: 03.08.2005
Mündliche Prüfung am: 30.09.2005

Meinen Eltern in Dankbarkeit.

Abstract

The relationship between the chemical structure of π – conjugated polymers or oligomers and their macroscopic optical and electrooptical properties is complex in nature and not fully understood at the present. Fused aromatic rings are often incorporated into semiconducting organic materials in order to realize a more extended π – conjugation. The simplest example of fused rings is naphthalene with two condensed phenyl rings. Naphthalene has a versatile and well – developed substitution chemistry, which provides different patterns for both polymerization and side – chain attachment. Therefore, utilizing the naphthalene unit should allow some tuning of the electronic and optical properties of the resulting materials. The work presented in this thesis is focused on incorporating naphthalene units into conjugated poly – and oligomers.

In chapter 2, naphthalene is incorporated into alternating copolymers as the simplest way of introducing new building blocks into new polymers. To get a better understanding different model compounds have been synthesized and compared with the polymers. Some of the model compounds are under investigation as active layers in organic field effect transistors (OFETs).

Chapter 3 presents a series of novel polyarylene – type ladder polymers containing 1,5- and 2,6- linked naphthalene units. This includes the first example of such ladder polymers consisting exclusively of six membered rings. The substitution patterns and linkage positions allow some fine tuning of the optical properties. One of the ladder polymers is also utilized as the gain material of a distributed feedback (DFB) polymer laser.

The polymers in chapter 4 utilize the 1,1'-binaphthyl unit as the central unit of a new class of potentially helical, conjugated ladderpolymers. Due to the interrupted conjugation across the binaphthyl moiety, some tuning of the optical properties is possible. To investigate the substitution patterns two model compounds have been synthesized and characterized via NMR and X-ray crystallography.

Chapter 5 introduces novel statistical copolymers of (9,9-dioctylfluorene) containing various amounts of binaphthyl units. Herein the binaphthyl unit shows its capability to suppress side chain crystallization and leads to completely amorphous materials. Second order (DFB) polymer lasers based on thin films of these materials showed extremely low lasing thresholds. The materials allow a dramatic improvement of polyfluorene based solid state lasers.

In the last chapter a new family of star – shaped oligoaryl dimers based on binaphthyl or biphenyl cores are described. An extensive investigation of their structure and electronic properties including UV/Vis and NMR spectroscopy as well as X – ray analysis is presented, especially related to intramolecular π - π – interactions.

Table of Contents

1. General Introduction

1.1. Conjugated Polymers and Organic Semiconductors

Since the beginning of mankind people have used natural macromolecular materials, like wood, leather, wool and many more. The start of industrialization in the last century has led to the use of modified natural polymers and new synthetic materials. Since then the area of macromolecular materials has become more and more important accompanied with an enormous broad spectra of new features.[1] The advantages of polymeric materials compared with other "classic" materials like glass, ceramic or metal are the low specific weight, high form and corrosion stability and good processibility. The addition of additives opens furthermore the option of fine-tuning of properties.

Today it is hard to picture what the world would look like without polymeric materials which is reflected by a yearly production of more than 10^8 tons of synthetic polymers.[2] Besides mass production polymers like polypropylene (PP), polyethylene (PE) or polystyrene (PS) polymers for special applications are the focus of modern research like liquid crystalline polymers,[3;4] polymer implantats,[5] or conducting and semiconducting materials.[6;7]

Most plastics are known as electrical insulators except for the class of conjugated polymers, which have been discovered by Shirakawa et al.[8] in 1977 and were awarded in 2000 with the Nobel Prize in Chemistry for Heeger, Shirakawa and Mac Diarmid. Their work describes the observation that polyacetylene can be converted into an electrically conductive material by reduction or oxidation of the conjugated backbone. This process is called "doping" in analogy to the doping of n - or p - inorganic semiconductors.[9]

Conjugated polymers or to be more exact π-conjugated polymers differ from other polymers in having a backbone of alternating single, double or triple bonds. They are also termed as "organic semiconductors" with respect to the fact that they can be described similar to inorganic semiconductors. Both have electrons organized in bands rather than in discrete levels and both have their ground state energy bands either completely filled or completely empty.[10] Analogue to their inorganic relatives their highest energy occupied band is called the valence band, while the lowest energy unoccupied band is called conduction band. The energy difference E_g between these two levels is called the band gap energy. While the discovery of electrical conductivity in doped π-conjugated polymers already triggered the

interest of many scientists, the real breakthrough was established in 1990 with the observation of electroluminescence in the semiconducting polymer poly(*p*-phenylenevinylene) (PPV) by the Friend group (Cambridge).[6] The search for polymers and small organic molecules as the active layer in light emitting diodes has advanced rapidly. Even when the display market is still dominated by Cathode – Ray – Tubes (CRT) and Liquid – Crystal – Displays (LCD) the impact of organic light emitting diodes (OLEDs) is getting stronger, so that the first mass products are hitting the market. Products containing the first displays using semiconductive organic materials are being sold, e.g. a Kodak digital camera with a five centimeter OLED view screen and the "James Bond shaver" of Phillips.

Figure 1.1: OLED displays in commercial products (Photos: Kodak, Phillips).

However, the use of π-conjugated materials is not limited to their application in OLEDs.[11-14] Due to their interesting optical and electronic properties, resulting from the extensive π-electron delocalization along the polymeric backbone, these polymers can also be applied as the active material in a vast number of applications e.g. field effect transistors[15-18], photodiodes[19], sensors[20], polymer lasers[21-25], and organic solar cells.[26-28]

For highly stable and efficient materials of such applications semiconducting polymers with smart designed and optimized properties are greatly desired. The toolbox of organic chemistry hereby opens a broad variety of suitable reactions and easily accessible target compounds. The optimization of the target structures results thereupon in smart materials with fine – tuned optical and electronic properties. Figure 1.2 shows the chemical structures of some of the most intensively studied π-conjugated polymers. Besides that plenty of structural combinations lead to statistical, alternating and block copolymers with new attributes.

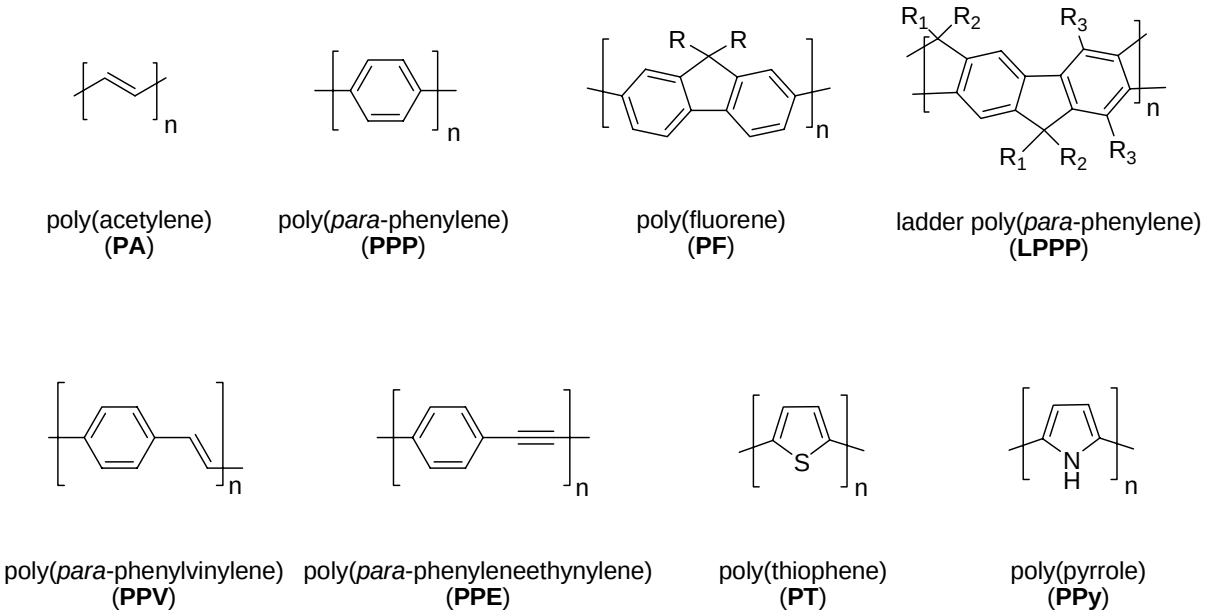

Figure 1.2: Chemical structures of some popular π-conjugated polymers

Poly(*p*-phenylene) (PPP) can be seen as the ark-type of conjugated polymers. Nevertheless, pure PPP is insoluble and therefore very difficult to process. To overcome this shortcoming, flexible sidechains have been attached which solubilize the polymer. Admittedly, a new problem arises due to the fact that the sidechains force the backbone benzene rings to twist away from coplanarity and disturb the interring conjugation. Therefore the resulting solubilized PPPs behave remarkably different from the unsubstituted PPPs. To prohibit the twisting of the benzene rings, the polymers can be partly or fully planarized as realized in polyfluorenes (PF) or PPP – type ladder-polymers (LPPP).[29;30]

1.2. Synthetic Methods

1.2.1. Metal Catalyzed Coupling Reactions

Transition metal catalyzed reactions have revolved the area of organic synthesis within the last two decades. In general, cross-coupling reactions are known as reactions between an active R-X compound (-X, -Cl, -I, -OTf, -OTos) with a suitable leaving group and a carbanion or carbanion equivalent counterpart to form a new carbon – carbon bond under transition – metal catalysis.

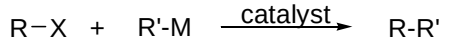

While bromides iodides, chlorides or triflates normally are used as the activating group -X, the choice of the "metal" M of the carbanion species is much more manifold.[31] The most popular examples use boron (Suzuki-Miyaura), magnesium (Kumada-Tamao), lithium (Murahashi), zinc (Negishi), tin (Stille), silicon (Hiyama) and copper (Normant) organyls. A wide range of transistion metal complexes have been used as catalysts in these coupling reactions, attention has particularly paid to palladium and nickel complexes. The extensive research within the last decades have led to an unmanageable variety of reaction conditions and even completly new cross coupling reactions like carbon-heteroatom couplings.[32-34]
Unique for all these reactions is their mechanism, described as a catalytic cycle. Great effort has been contributed to get a deeper understanding of the single steps resulting in a lot of detailed, and mostly very complicated theories.[35;36] Despite its shortcomings the so - called "textbook-mechanism" still gives the simplest description of the different elementary steps and the occurring problems.[37]

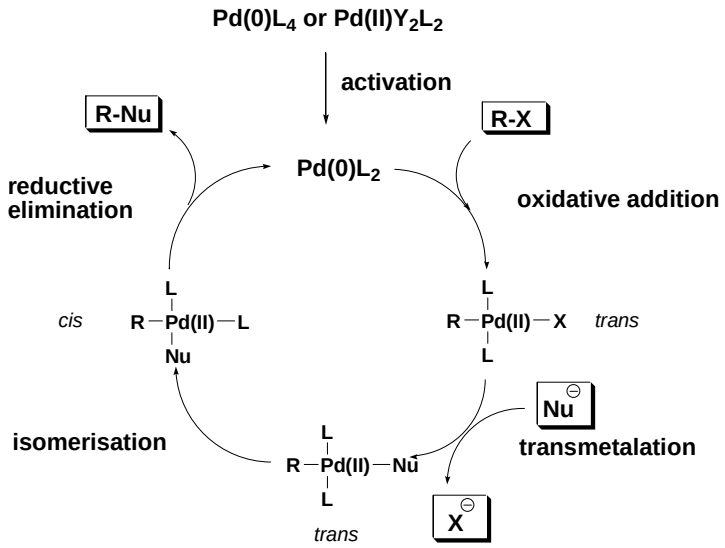

Figure 1.3: "Textbook mechanism" of palladium - catalyzed cross coupling reactions.

The oxidative addition of aryl halides to palladium (0) complexes under formation of aryl-palladium(II) species is the initial step in all catalytic cross coupling reactions. It has been proposed that under distinct reaction conditions coordinatively unsaturated $Pd(0)L_2$ species are formed from Pd(0)-phosphine complexes or alternatively from Pd(II) salts and complexes by reduction. These catalytic species should then react with the aryl halide under formation of a stable *trans* - configured complex. Admittedly, this exact procedure seems doubtful due to the fact that isolated *trans*-complexes have been found to couple only very slowly with

organometallic reagents.[38] The rate of the oxidative addition strongly depends on the chemical environment of R and the leaving halide. In general, electron-poor rests R react faster than electron-rich ones, and iodides react faster than bromides or chlorides. The later point can easily be seen by comparing the energy of dissociation of the respective C-X bonds. Due to their high energy of about 96 kcal/mol, chlorides have been known to be unreactive for a very long time up to the introduction of extremely electron – rich ligands to the field of catalysis.[39] The addition of R-X is followed by a transmetalation in which the catalyst is attacked by an organic nucleophil. The strength of the nucleophil is determined by the corresponding metal. In most cases, zinc-compounds are more reactive than tin or boron compounds. Before a new carbon – carbon or carbon – heteroatom bonds can be formed, a rearrangement on the central transistion metal is necessary, which is usually described as isomerisation. Finally, the catalytic core undergoes a reductive cleavage in which subsequently the new formed compound R-Nu is eliminated.

Among all these cross coupling reactions the Suzuki coupling is probably the most established procedure.[31;40-43] Its popularity ranges from natural product synthesis[44] over material science[45] to industrial process[46] and is based on many factors – e.g., the commercial availability of boronic acids and esters, their high stability, and non-toxiticity. An anomaly of the Suzuki coupling compared with other transition metal catalyzed reactions is the required use of a base. Interestingly, even after more than two decades of reaction development the function of the base is still not fully clear. The predominating theory throughout scientific literature is that the base quarternerizes the boronic-compound and, therefore, increases its reactivity.[47]

Another very useful transistion metal - mediated reaction is the Ni(0) - mediated Yamamoto homo - coupling reaction, which undergoes a different reaction cycle. Semmelhack *et al.* have been the first who observed the coupling of two arylhalides towards biaryls utilizing bis(1,5-cyclooctadiene)nickel(0) ($Ni(COD)_2$).[48;49] Due to the mild conditions, this reaction has been developed as a valuable alternative to the copper - catalyzed Ullmann-coupling, which requires quite drastic conditions.[50] During their studies towards conjugated polymers the group of Yamamoto extended the scope of this coupling reaction to polymerizations and applied 2,2'-bipyridyl (bpy) as a supporting ligand guiding to pronounced increased yields and mild conditions.[51-53] Detailed studies concerning the mechanism of this reactions have been carried out by Semmelhack[48], Yamamoto[54] and Kochi[55] and are depicted in Figure 1.4. After the ligand exchange between COD and bipyridyl, the oxidative addition of the arylhalide (depicted as a bromide) occurs and directs to complex **2**. The addition of

bipyridyl accelerates the reaction drastically as the bipyridyl complex undergoes the oxidative addition much faster. Complex **2** disproportionates within the follwing step into the complexes **3** and **4**. While **3** leaves the reaction cycle, the formed biaryl is set free via reductive elimination of **4**.

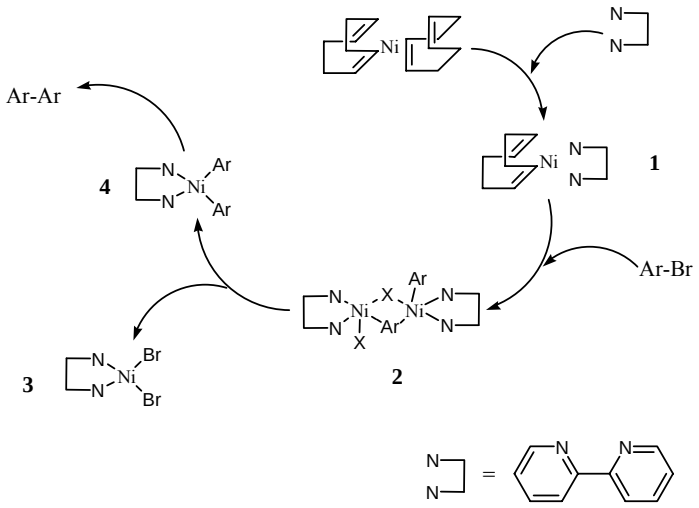

Figure 1.4: Schematic progression of a aryl-aryl coupling via Yamamoto-coupling.

Most Yamamoto - type coupling reactions, carried out within this thesis, are variations of a synthetic protocol developed by Pei and Yang.[56;57] For the completeness it should be mentioned that, furthermore, a multitude of related catalytic Ni(0)-mediated reactions exists which utilize reducting reagents such as zink[56;58] or electrochemical support.[59] However, applied to the herein presented systems, they gave lower yields and decreased molecular weights.

1.2.2. Microwave Assisted Synthesis

High speed synthesis with microwaves has attracted widespread interest, reflected by more than 2000 articles in the area of microwave-assisted organic synthesis.[60-65] Even though the effect of microwaves is known for more than 50 years, the first reported example in synthetic chemistry appeared in 1986 by Gedye and Giguere.[66;67] However, it took a long time until microwaves became more and more a standard tool in synthetic laboratories. This can clearly be attributed to the lack of controllability and reproducibility of the early results, which have been usually conducted in modified household microwave ovens. In addition, the risks associated with the flammability of organic solvents and explosions accompanied by nearly no temperature and pressure control were of major concern. Due to these problems, the current trend is to use so - called “mono-mode microwave reactors”, which allow computer

aided reaction control. These systems heat only one reaction vessel at a time which is centered on a point of a defined radiation. Most of these microwaves use septum - sealed standard reaction vessels. In the case of the CEM®-Discovery machine, this septum is penetrated by a pressure probe allowing a constant pressure measuring. The temperature is detected by an IR sensor that is directed towards the bottom of the reaction vessel. Depending on this online monitoring, the irriadiation power may be adjusted to maintain the desired conditions. Figure 1.5 shows the schematic design of a monomode microwave reactor.

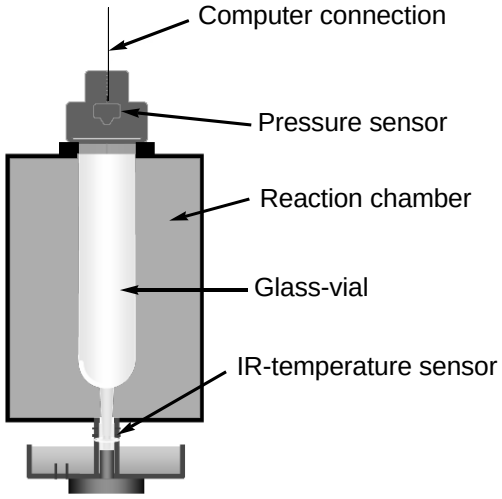

Figure 1.5: Structure of a monomode microwave system.

Unique for all reported microwave assisted reactions are the drastically shortened reaction times and often altered product distributions compared to conventionally heated control experiments. These sometimes drastic changes have often led to speculations on the existence of so called “specific microwave effects” or “nonthermal effects”.[68;69] Meanwhile, most scientists agree that in the majority of cases the reasons for the enhanced rates are the consequence of thermal/kinetic effects. In addition to the thermal/kinetic effects there are some effects that are caused by the uniqueness of the microwave dielectric heating mechanisms, which are essentially still thermal effects. For example, this may be superheating phenomenons of heterogeneous catalysts, selective heating of reactive centers or the formation of “molecular radiators”.[70]

However, the application of microwaves to polymerization reactions barely survived in a shadowy existence. These days, step-growth polymerizations are the most extensively investigated polymerization reactions under microwave irradiation because of the close relationship between polymer and organic chemistry. Figure 1.6 shows the drastic increase of

microwave assisted polymerizations within the last years. The class of special interest for this thesis is the group of C-C cross coupling reactions, which has attracted attention only very recently.[71-75]

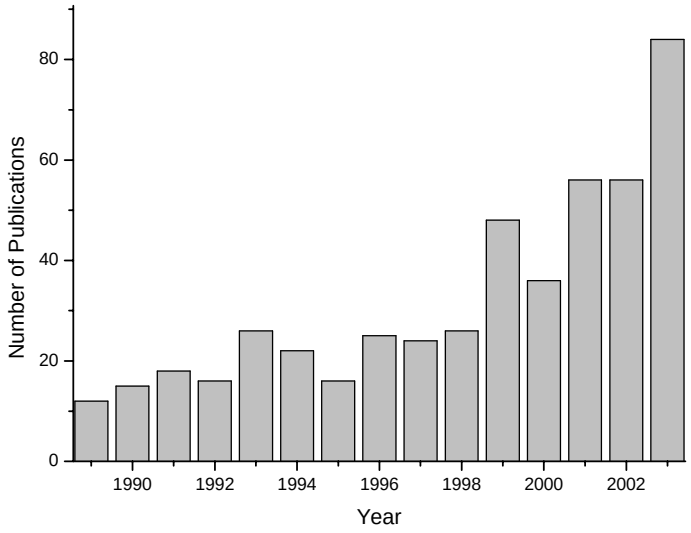

Figure 1.6: Number of publications dealing with microwaves and polymer-synthesis.

Up to the year 2002, only one paper dealing with the synthesis of polyphenylacetylens under microwave irradiation had been reported, describing a metathesis procedure conducted in a household microwave oven.[76] Carter of the IBM Almaden group reported the nickel(0)-mediated coupling of 2,7-dibromo-9,9-dihexylfluorene in toluene within 10 min.[71] While standard procedures often suffer from low reproducibility and very long reaction times up to five days, their results showed very good yields and molecular weights even after short heating periods. Subsequently, the groups of Yamamoto and Scherf reported similar reaction times and in the latter case even better molecular weights by changing the solvent to THF.[77;78]

The first examples of Suzuki– and Stille cross coupling polymerizations were shown by the Scherf group in 2004. Reaction times for the preparation of five representative polymers have been developed and were found to decrease from more than three days in the case of conventional heating down to ca. 10 minutes. Besides the mentioned drastic reduction of the reaction times, it is has also been found that some polymers show drastically higher molecular weights under microwave assisted conditions.[79;80] Almost simultaneously, the first description of a Sonogashira coupling polymerization by Hecht and coworker was published,

which still requires longer reaction times than the herein presented polymerizations.[81] Scheme 1.1 shows some of the most popular examples.

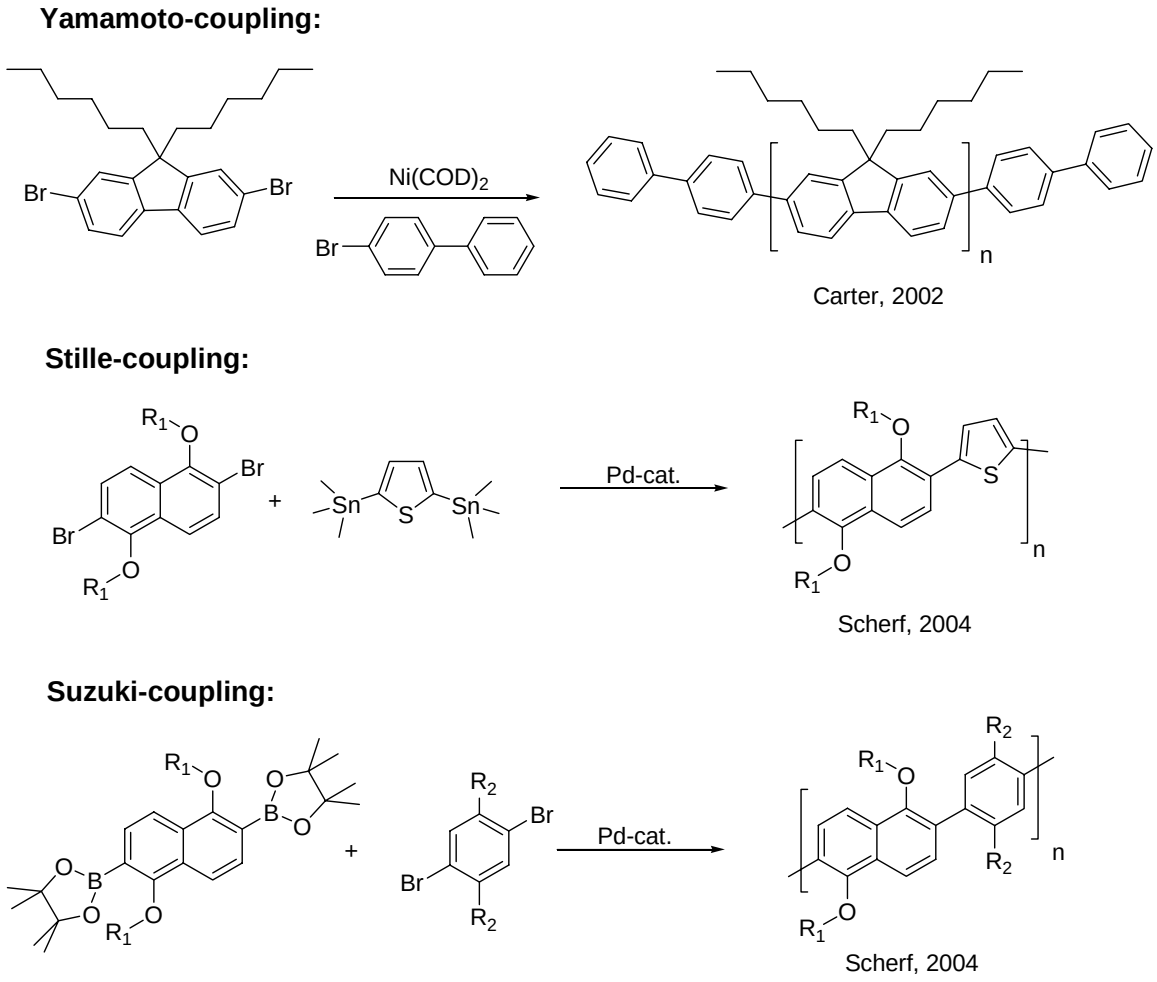

Scheme 1.1: Examples of the first polymerizations via microwave assisted cross coupling reactions.

1.3. Aim and Scope

The relationship between the chemical structure of π – conjugated polymers or oligomers and their macroscopic optical and electrooptical properties is complex in nature and not fully understood at the present. Fused aromatic rings are often incorporated into semiconducting organic materials in order to realize a more extended π – conjugation. The simplest example of fused rings is naphthalene with two condensed phenyl rings. Naphthalene has a versatile and well – developed substitution chemistry, which provides different patterns for both polymerization and side – chain attachment. Therefore, utilizing the naphthalene unit should allow some tuning of the electronic and optical properties of the resulting materials. The work

presented in this thesis is focused on incorporating naphthalene units into conjugated poly – and oligomers.

In chapter 2, naphthalene is incorporated into alternating copolymers as the simplest way of introducing new building blocks. To get a better understanding different model compounds have been synthesized and compared with the polymers. Some of the model compounds are under investigation as active layers in organic field effect transistors (OFETs).

Chapter 3 presents a series of novel polyarylene – type ladder polymers containing 1,5- and 2,6- linked naphthalene units. This includes the first example of such ladder polymers consisting exclusively of six membered rings. The substitution patterns and linkage positions allow some fine tuning of the optical properties. One of the ladder polymers is also utilized as the gain material of a distributed feedback (DFB) polymer laser.

The polymers in chapter 4 utilize the 1,1'-binaphthyl unit as the central unit of a new class of potentially helical, conjugated ladder polymers. Due to the interrupted conjugation across the binaphthyl moiety, some tuning of the optical properties is possible. To investigate the substitution patterns two model compounds have been synthesized and characterized via NMR spectroscopy and X-Ray crystallography.

Chapter 5 introduces novel statistical copolymers of (9,9-dioctylfluorene) and various amounts of binaphthyl units. Herein the binaphthyl unit shows its capability to suppress side chain crystallization and leads to completely amorphous materials. Second order (DFB) polymer lasers based on thin films of these materials showed extremely low lasing thresholds. The materials allow a dramatic improvement of polyfluorene based solid state lasers.

In the last chapter a new family of star – shaped oligoaryl dimers based on binaphthyl or biphenyl cores are described. An extensive investigation of their structure and electronic properties including UV/Vis and NMR spectroscopy as well as X – Ray analysis is presented, especially related to intramolecular π - π – interactions.

References and Notes

[1] H. G. Elias, *Makromoleküle*, Hüthig und Wepf Verlag, Basel, Heidelberg, New York **1990**.

[2] M. D. Lechner, K. Gehrke, E. H. Nordmeier, *Makromolekulare Chemie*, Birkenhäuser Verlag, **1993**.

[3] R. Zentel, *Adv.Mater.* **1989,** *101*, 1437.

[4] H. Finkelmann, *Angew.Chem.* **1987,** *99*, 840.

[5] J. C. Wheeler, W. A. Woods, M. J. Cox, R. W. Cantrell, F. H. Watkins, R. F. Edlich, *J.Long Term Eff.Med.Impl.* **1996,** *6*, 207.

[6] J. H. Burroughes, D. D. C. Bradley, A. R. Brown, P. L. Burn, R. N. Marks, K. Mackey, R. H. Friend, A. B. Holmes, *Nature* **1990,** *347*, 539.

[7] A. J. Heeger, *Angew.Chem.Int.Ed.* **2001,** *40*, 2591.

[8] H. Shirakawa, E. J. Louis, A. G. MacDiarmid, C. K. Chiang, A. J. Heeger, *Chem.Commun.* **1977,** 578.

[9] C. K. Chiang, C. R. Fincher, Y. W. Park, A. J. Heeger, H. Shirakawa, E. J. Lewis, S. C. Gau, A. G. MacDiarmid, *Phys.Rev.Lett.* **1977,** *39*, 1098.

[10] T. A. Skotheim, R. L. Elesenbaumer, J. R. Reynolds, *Handbook of Conducting Polymers*, 2ed ed. (Ed.: Marcel Dekker) New York **1998**.

[11] A. Kraft, A. C. Grimsdale, A. B. Holmes, *Angew.Chem.Int.Ed.* **1998,** *37*, 402.

[12] Y. Shirota, *J.Mater.Chem.* **2000,** *10*, 1.

[13] U. Mitschke, P. Bäuerle, *J.Mater.Chem.* **2000,** *10*, 1471.

[14] R. H. Friend, R. W. Gymer, A. B. Holmes, J. H. Burroughes, R. N. Marks, C. Taliani, D. D. C. Bradley, D. A. Dos Santos, J. L. Bredas, M. Logdlund, W. R. Salaneck, *Nature* **1999,** *397*, 121.

[15] Z. N. Bao, *Adv.Mater.* **2000,** *12*, 227.

[16] G. Horowitz, *Adv.Mater.* **1998,** *10*, 365.

[17] H. Sirringhaus, N. Tessler, R. H. Friend, *Science* **1998,** *280*, 1741.

[18] C. D. Dimitrakopoulos, P. R. L. Malenfant, *Adv.Mater.* **2002,** *14*, 99.

[19] H. Imahori, S. Fukuzumi, *Adv.Funct.Mater.* **2004,** *14*, 525.

[20] D. T. McQuade, A. E. Pullen, T. M. Swager, *Chem.Rev.* **2000,** *100*, 2537.

[21] C. Kallinger, M. Hilmer, A. Haugeneder, M. Perner, W. Spirkl, U. Lemmer, J. Feldmann, U. Scherf, K. Müllen, A. Gombert, V. Wittwer, *Adv.Mater.* **1998,** *10*, 920.

[22] M. D. McGehee, A. J. Heeger, *Adv.Mater.* **2000,** *12*, 1655.

[23] V. G. Kozlov, S. R. Forrest, *Current Opinion in Solid State & Materials Science* **1999,** *4*, 203.

[24] U. Scherf, S. Riechel, U. Lemmer, R. F. Mahrt, *Current Opinion in Solid State & Materials Science* **2001,** *5*, 143.

[25] N. Tessler, G. J. Denton, R. H. Friend, *Nature* **1996,** *382*, 695.

[26] H. Hoppe, N. S. Sariciftci, *Journal of Materials Research* **2004,** *19*, 1924.

[27] C. J. Brabec, N. S. Saricifti, J. C. Hummelen, *Adv.Funct.Mater.* **2001,** *11*, 15.

[28] J. J. M. Halls, A. C. Arias, J. D. MacKenzie, W. S. Wu, M. Inbasekaran, E. P. Woo, R. H. Friend, *Adv.Mater.* **2000,** *12*, 498.

[29] U. Scherf, *J.Mater.Chem.* **1999,** *9*, 1853.

[30] U. Scherf, E. J. W. List, *Adv.Mater.* **2002,** *14*, 477.

[31] F. Diederich, P. J. Stang, *Metal-catalyzed Cross Coupling Reactions*, Wiley-VCH, Weinheim **1998**.

[32] J. P. Wolfe, S. Wagaw, J. F. Marcoux, S. L. Buchwald, *Acc.Chem.Res.* **1998,** *31*, 805.

[33] J. F. Hartwig, *Acc.Chem.Res.* **1998,** *31*, 852.

[34] J. F. Hartwig, *Pure Appl.Chem.* **1999,** *71*, 1417.

[35] C. Amatore, A. Jutand, *Acc.Chem.Res.* **2000,** *33*, 314.

[36] L. J. Gooßen, D. Koley, H. Hermann, W. Thiel, *Chem.Comm.* **2004,** 2141.

[37] C. Elschenbroich, A. Salzer, *Organometallchemie*, Teubner-Studienbücher, **1990**.

[38] L. J. Gooßen, Skript, Katalyse und metallorganische Synthese, **2004**.

[39] G. C. Fu, A. F. Littke, *Angew.Chem.* **2002,** *114*, 4350.

[40] A. Suzuki, *J.Organomet.Chem.* **1999,** 147.

[41] N. Miyaura, A. Suzuki, *Chem.Rev.* **1995,** *95*, 2457.

[42] S. P. Stanforth, *Tetrahedron* **1998,** *54*, 263.

[43] S. R. Chemler, D. Trauner, S. J. Danishefsky, *Angew.Chem.* **2003,** *113*, 4676.

[44] K. C. Nicolaou, E. J. Sorensen, *Classics in Total Synthesis*, Wiley-VCH, Weinheim **1996**.

[45] A. D. Schlüter, *J.Polym.Sci.Part A* **2001,** *39*, 1533.

[46] G. B. Smith, G. C. Dezeny, D. L. Hughes, A. O. King, T. R. Verhoeven, *J.Org.Chem.* **1994,** *59*, 8151.

[47] J. W. Canary, *J.Am.Chem.Soc.* **1994,** *116*, 6985.

[48] M. F. Semmelhack, P. M. Helquist, L. D. Jones, L. Keller, L. Mendelsohn, L. S. Ryono, J. G. Smith, R. D. Stauffer, *J.Am.Chem.Soc.* **1981,** *103*, 6460.

[49] P. W. Jolly, G. Wilke, in *The Organic Chemistry of Nickel*, Academic Press Inc., London **1974**.

[50] F. Ullmann, J. Bielecki, *Chem.Ber.* **1901,** *34*, 2174.

[51] T. Yamamoto, *Prog.Polym.Sci.* **1992,** *17*, 1153.

[52] T. Yamamoto, *J.Synth.Org.Chem.Jpn.* **1995,** *53*.

[53] T. Yamamoto, T. Ito, K. Kubota, *Chem.Lett.* **1988,** 153.

[54] T. Yamamoto, S. Wakabayashi, K. Osakada, *J.Organomet.Chem.* **1992,** *428*, 222.

[55] T. T. Tsou, J. K. Kochi, *J.Am.Chem.Soc.* **1979,** *101*, 7547.

[56] Q. B. Pei, Y. Yang, *J.Am.Chem.Soc.* **1996,** *118*, 7416.

[57] S. C. Chang, Y. Yang, Q. B. Pei, *Applied Physics Letters* **1999,** *74*, 2081.

[58] M. Zembayashi, K. Tamao, J. Yoshida, M. Kumada, *Tetrahedron Lett.* **1977,** *18*, 4089.

[59] M. Troupel, Y. Rollin, S. Sibille, J. Perichon, *J.Organomet.Chem.* **1980,** *202*, 435.

[60] L. Perreux, A. Loupy, *Tetrahedron* **2001,** *57*, 9199.

[61] P. Lidström, J. Tierney, B. Wathey, J. Westman, *Tetrahedron* **2001,** *57*, 9225.

[62] S. Caddick, *Tetrahedron* **1995,** *51*, 10403.

[63] D. Adams, *Nature* **2003,** *421*, 571.

[64] B. L. Hayes, *Microwave Synthesis - Chemistry at the Speed of Light*, CEM - Publishing, Matthews, NC **2002**.

[65] C. O. Kappe, *Angew.Chem.Int.Ed.* **2004,** *43*, 6250.

[66] R. N. Gedye, F. Smith, K. Westaway, H. Ali, L. Baldisera, L. Laberge, J. Roussel, *Tetrahedron Lett.* **1986,** *27*, 279.

[67] R. J. Giguere, T. L. Bray, S. M. Duncan, G. Majetich, *Tetrahedron Lett.* **1986,** *27*, 4945.

[68] N. Kuhnert, *Angew.Chem.Int.Ed.* **2002,** *41*, 1863.

[69] C. R. Strauss, *Angew.Chem.* **2002,** *114*, 3741.

[70] C. O. Kappe, A. Stadler, in *Microwaves in Organic Synthesis*Ed.: A. Loupy), Wiley-VCH, Weinheim **2002**, p. pp. 405-433.

[71] K. R. Carter, *Macromolecules* **2002,** *35*, 6757.

[72] M. Larhed, A. Hallberg, *J.Org.Chem.* **1996,** *61*, 9582.

[73] M. Larhed, G. Lindeberg, A. Hallberg, *Tetrahedron Lett.* **1996,** *37*, 8219.

[74] M. Larhed, C. Moberg, A. Hallberg, *Acc.Chem.Res.* **2002,** *35*, 717.

[75] O. Navarro, H. Kaur, P. Mahjoor, S. P. Nolan, *J.Org.Chem.* **2004,** *69*, 3173.

[76] K. Dhanalakshmi, G. Sundararajan, *Polym.Bull.* **1997,** *39*, 333.

[77] T. Yamamoto, Y. Fujiwara, H. Fukumoto, Y. Nakamura, S. Koshihara, T. Ishikawa, *Polymer* **2003,** *44*, 4487.

[78] F. Galbrecht, X. H. Yang, B. S. Nehls, D. Neher, T. Farrell, U. Scherf, *Chem.Commun.* **2005,** 2378.

[79] B. S. Nehls, U. Asawapirom, S. Füldner, E. Preis, T. Farrell, U. Scherf, *Adv.Funct.Mater.* **2004,** *14*, 352.

[80] B. S. Nehls, Diplomarbeit, Mikrowellenunterstützte Synthese von Polyarylenen, Bergische Universität Wuppertal, **2003**.

[81] S. Hecht, B. Block, *Chem.Commun.* **2004,** 300.

2. Naphthalene – Thiophene Alternating Copolymers

2.1. Introduction and Motivation

The dynamic development in advanced materials research has led to organic conjugated materials with tailored photophysical properties. In alternating copolymers two structurally different conjugated segments can be combined leading to novel materials with properties which are not simply related to the individual components. Semiconducting polyarylenes are usually prepared via palladium-catalyzed cross coupling reactions by reacting either aryl bis(boronic ester) (Suzuki-coupling) or distannyl derivatives (Stille-coupling) with dihaloarenes.[1-5] Generally the Suzuki route has attained more importance and is potentially more versatile than the Stille route. This is mainly due to the fact that boronic acid derivatives are easy to handle, tolerant to a large number of functional groups, and non-toxic. However, alternating copolymers with electron rich thiophene units are usually prepared via the Stille procedure which is favourable in terms of molecular weight and yield.[2;6;7] Up to now alternating poly(heteroarylene-arylene)s dominantly contain substituted benzenes as the arylene components.

One application of conjugated materials is the use in organic field effect transistors (OFETs) as a low cost product alternative to amorphous Si technology.[8;9] Typically, these materials are divided into two major classes: conjugated polymers and corresponding oligomers. In both classes it has been shown that efficiency of charge transport is directly linked to the low range ordering. Today, OFETs have been fabricated incorporating a wide variety of organic structure classes.[10;11] The most promising performance has been observed for oligo – and polythiophenes and linearly fused polycyclic aromatic compounds such as pentacene and its derivatives.[12-19] Naphthalene is the simplest fused aromatic ring system. Furthermore, the naphthalene unit can be modified in various ways with respect to solubility and processibility of the resulting oligomers and polymers. In principle naphthalene could be linked in three different ways to allow a non – interrupted backbone conjugation, through their 1,4 -, 1,5 – or the 2,6 – positions, respectively (see Scheme 2.1). While literature holds several reports of

copolymers with 2,6 – or 1,4 - linked naphthalene units[4;20;21] only few examples of copolymers with 1,5 – conjugated naphthalenes have been reported.[22-24] To combine the favourable features of both classes mentioned before, (oligo)thiophene units were choosen as the heteroarylene part, to prepare alternating (oligo)thiophene/naphthalene copolymers.

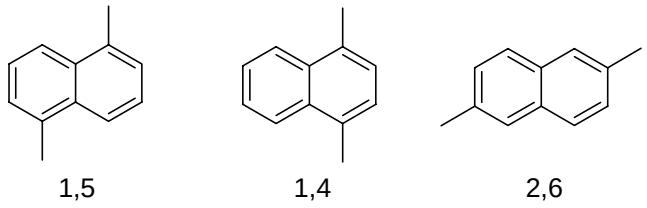

Scheme 2.1: Possible linking positions of the naphthalene unit.

Despite the simple access and the obvious potential, examples of thienylene/naphthalene copolymers are very rare, no matter in what kind of linkage. Only two examples dealing with similar polymers are reported in the literature so far.

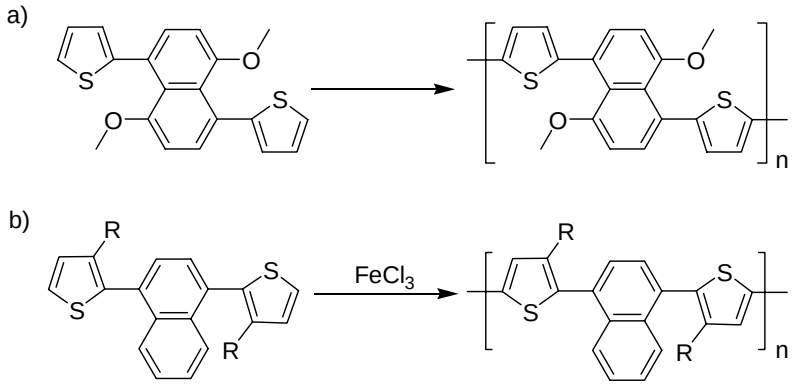

Scheme 2.2: Examples of naphthalene - oligothiophene copolymers.

The first one is reported by the Tan group (see Scheme 2.2 a) using a electropolymerization protocol, which leads to insoluble polymers. Thus no GPC results were given and the polymers were just characterized by elemental analysis.[25] A second paper was contributed by the Lai group which followed a related approach, but utilized more soluble monomers and a chemical oxidative polymerization procedure.[24] However, both protocols do not lead to soluble polymers which restrict the processabillity drastically.

More recent reports have shown a type of “competition” between oligomeric monodisperse molecules and related polymers for OFET applications. Both have their special advantages

and disadvantages.[11;26] Conjugated polymers usually fit the criteria to facilate simple manufacturing procedures and the ability to form homogenous films directly from solution.[27] However, structural imperfections within chains, coupled with the statistical nature of polymerization reactions provide materials that are not as well defined as low mass organic molecules.[28] Furthermore, materials based on lowmolecular weight monodisperse systems can be purified by standard organic methodologies.[29;30]

Another important aspect of conjugated oligomers is that they can be considered as models for conjugated polymers. They allow to establish reliable structure – property relationships with respect to electronic, photonic and thermal properties. This chapter describes the synthesis, characterization, and optical properties of three alternating naphthalene (oligo)thiophene copolymers as well as the preparation and characterization of two related model-compounds. Initial OFET investigations reflect a tremendous effect of the alkoxy sidechains on the charge carrier mobility.

2.2. Results and Discussion

2.2.1. Monomer and Polymer Synthesis

The Synthesis of three different (oligo)thiophene monomers (monomer, dimer, trimer) is outlined in Scheme 2.3. Terthiophene **3** was prepared via a Nickel-mediated aryl – aryl coupling, while thiophene and bithiophene are commercially available. The bis(trimethylstannyl)-oligothiophenes (**4-6**) were prepared by metalation of oligothiophenes with BuLi and subsequent quenching with trimethyltinchloride.

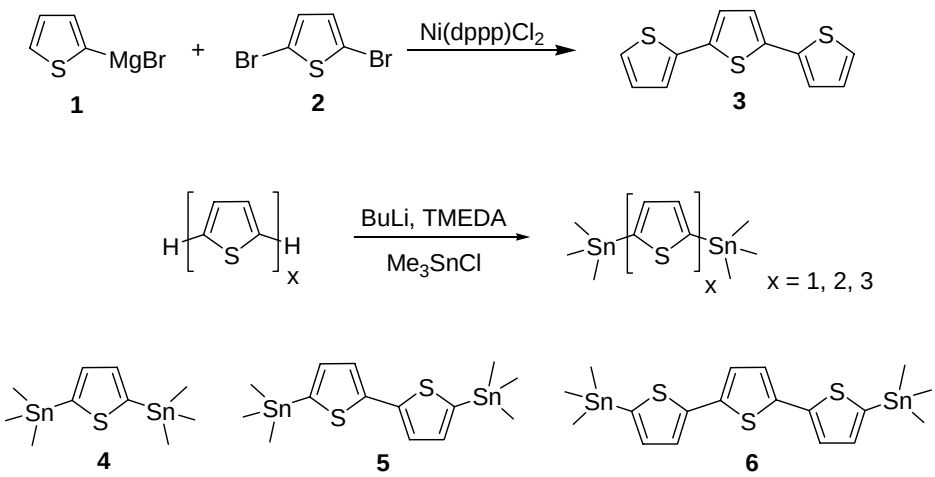

Scheme 2.3: Synthesis of the distannylated thienylene monomers **4-6**.

The crude products were recrystallized from ethanol to afford monomers **4-6** in 80-60 % yield.

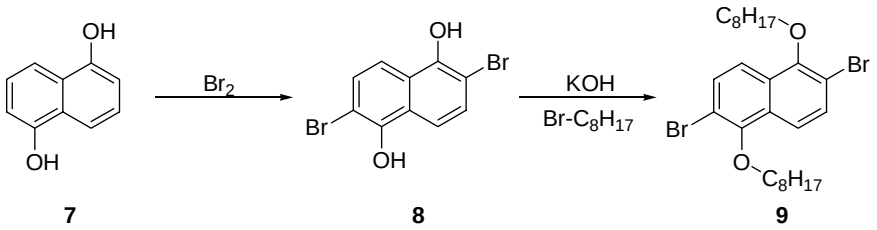

Scheme 2.4: Synthesis of the naphthalene monomer **9**.

The naphthalene monomer depicted in Scheme 2.4 was obtained starting from 1,5-dihydroxy-naphthalene (**7**). Bromination under acidic conditions gave 2,6-dibromo-1,5-dihydroxynaphthalene (**8**), which was subsequently converted to 2,6-dibromo-1,5-dioctyloxynaphthalene (**9**).[31]

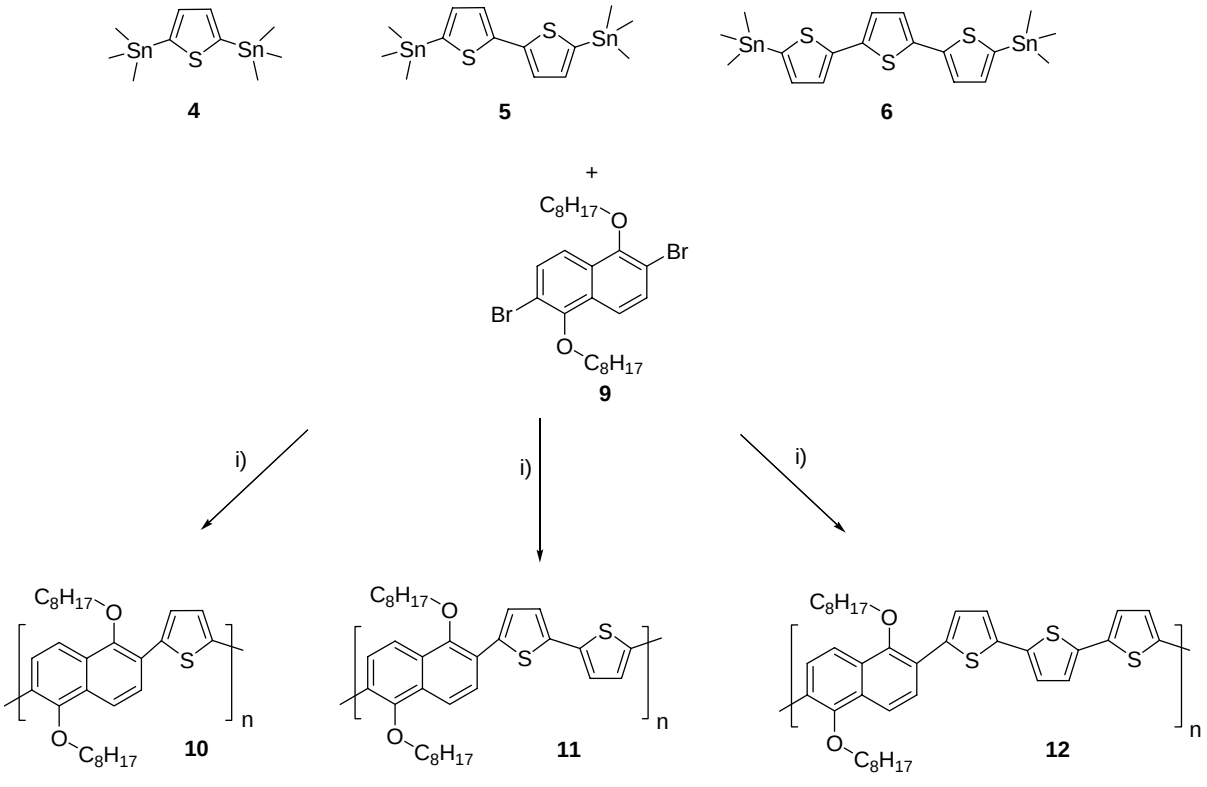

i) $Pd(PPh_3)_4$, toluene, µW (300 W, 250°C, 9 min)

Scheme 2.5: Synthesis of alternating naphthalene-thiophene copolymers (**10-12**) via a Stille – type cross – coupling.

The desired alternating copolymers were prepared via a microwave assisted Stille-type cross coupling reaction in dry degassed toluene, using $Pd(PPh_3)_4$ as a catalyst.[4;32] The microwave-assisted protocol has to be found superior compared to conventional variants. All reactions were carried out in sealed 10 mL vials which were filled under glovebox conditions.

Previous studies have shown that the amount of microwave energy is of immense importance for the reactions. Although at an energy of 300 W there was no noticeable decomposition of the palladium catalyst on the vessel walls.[4] The molecular weights differ between M_n = 21,100 to 6,600 by going from **10** to **12** (see Table 2.1) and are in good agreement with earlier studies on alternating fluorene-thiophene copolymers, which have also shown a significant decrease in yields and chain length by extending the thienylene part.[1] The polymers readily dissolve in common organic solvents such as chloroform, THF, or toluene. Polymers **10-12** have been fully characterized by ^1H and ^{13}C NMR spectroscopy. All ^1H NMR spectra show the typical signal at $\delta \sim 4$ ppm, corresponding to the O-CH_2 group of the naphthalene moiety.

Table 2.1: Molecular weights and yields of polymers **10-12**.

Polymer	Mn	PD	Yield (%)
10	21,100	1.9	70
11	11,800	2.5	62
12	6,600	1.9	55

2.2.2. Synthesis and Characterization of the Model Compounds

In recent years π-conjugated oligothiophenes have received much attention as model compounds for the related polymers. Since these oligomers are well - defined chemical systems, investigations of their size - dependent properties have been conducted towards a better understanding of conjugated polymers. Previous studies have shown that phenylene-thiophene oligomers are a promising class of semiconductors, which have been employed in organic light emitting diodes (OLEDs)[33;34] as well as in p-channel OFETs.[35;36] The reported studies suggest that the solubilizing effect and the ability to form ordered films is more substantial for oligomers with terminal n-alkyl chains.[37;38] Two different model compounds have been synthesized and completely characterised. Structure **14** was targeted as a model compound to polymer **11**. The terminal n-hexyl side chains were introduced for solubility reasons. Compound **16** was synthesized as a lower substituted model compound to test the influence of the alkoxy side chains.[35;39-41]

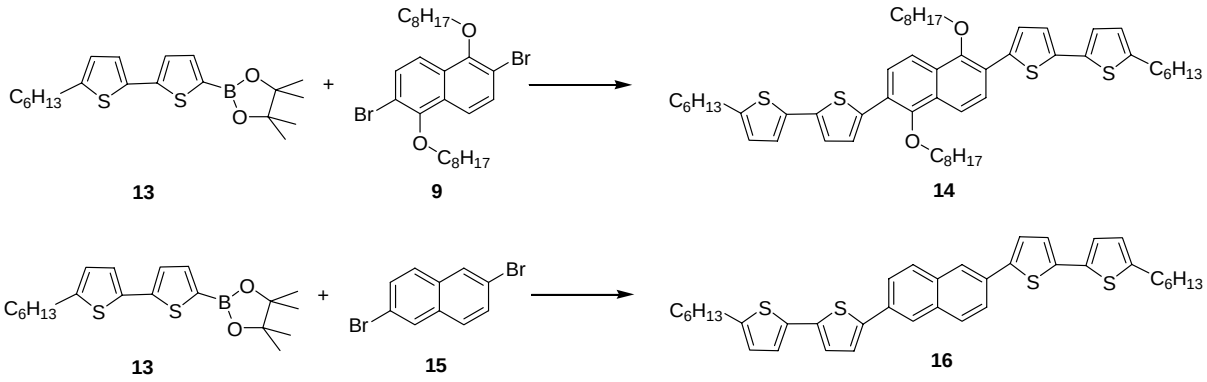

Scheme 2.6: Synthetic scheme towards thiophene/naphthalene oligomers **14** and **16**.

Both oligomers were prepared via microwave assisted palladium (0)-catalyzed Suzuki-coupling of the appropriate bromo derivative with the corresponding boronic ester derivatives, as shown in Scheme 2.6.[31] While the synthesis of **9** is explained above (Scheme 2.4) compounds **13** and **15** are commercially available and have been used without further purification. **14** was afforded in weak yields of about 50 % after aqueous work-up and subsequent chromatography on silica as a yellow powder. Whereas, **16** could be isolated in yields over 70 % after two recrystallization cycles from hot toluene.

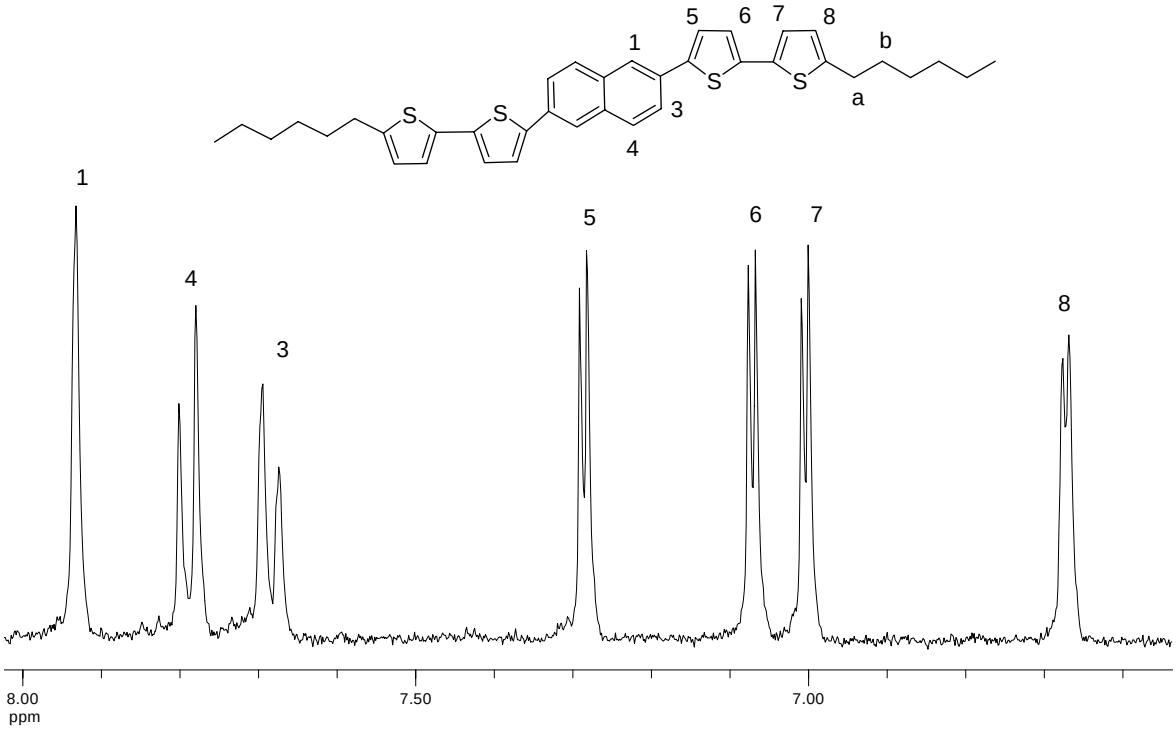

Figure 2.1: ^{1}H NMR spectrum (aromatic region) of **16** in $C_2D_2Cl_4$.

The chemical structures of both model compounds were verified by ^{1}H and ^{13}C NMR studies, as well as by mass spectrometry measurements. All signals could clearly be assigned by using ^{1}H-^{1}H ROESY and ^{1}H-^{1}H COSY experiments. To exemplify the modus operandi the aromatic region of compound **16** in the ^{1}H NMR spectrum is shown in Figure 2.1. The ^{1}H-^{1}H COSY (Figure 2.2) as well as the ^{1}H-^{1}H COSY-LR mode show a pronounced coupling between alkyl proton (a) and the closest thiophene proton (8). Taking this as a starting point all thiophene protons could be assigned via the ^{1}H-^{1}H COSY spectrum. Further ^{1}H-^{1}H ROESY and ^{1}H-^{1}H COSY-LR experiments also allow an exact assignment of the naphthalene protons.

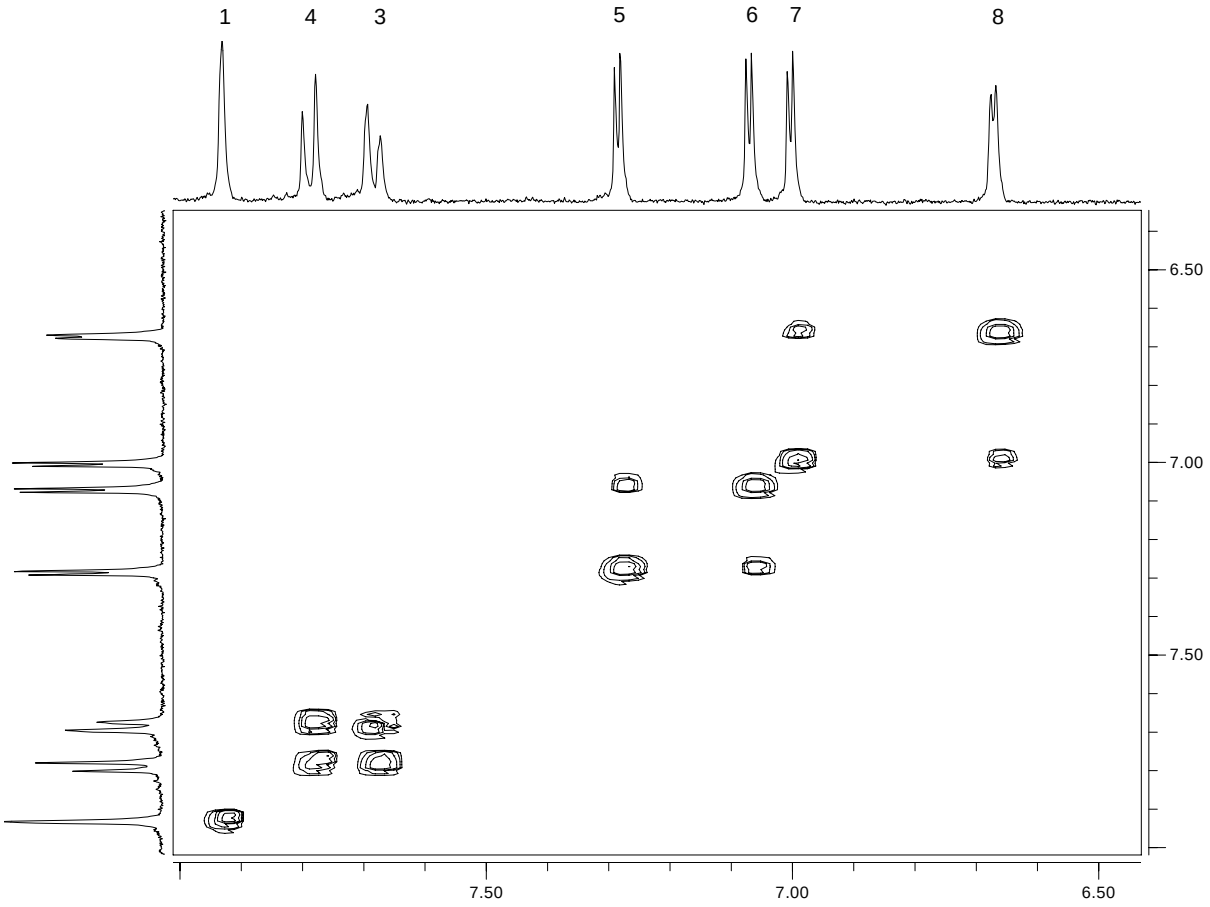

Figure 2.2: ^{1}H-^{1}H COSY spectrum of **16** in $C_2D_2Cl_4$.

The assignment of compound **14** followed a similar procedure. In both cases all expected ^{13}C NMR signals were found.

2.2.3. Optical Spectroscopy

The optical properties of the polymers have been investigated both in chloroform solution as well as in thin films. It is unique for all polymers that the UV/Vis spectra are unstructured

with broad absorption bands centred at λ_{max} = 427 nm (**10**), 449 nm (**11**), and 456 nm (**12**). To give a clue, regioregular poly(3-alkylthiophene) has an absorption maximum at circa 450 nm. Even more interesting is the comparison with the class of alternating fluorene oligothiophene copolymers, which show very similar absorption maxima in comparison with the corresponding naphthalene derivatives (see Table 2.2).[1] Especially in solution the spectra are almost identical.

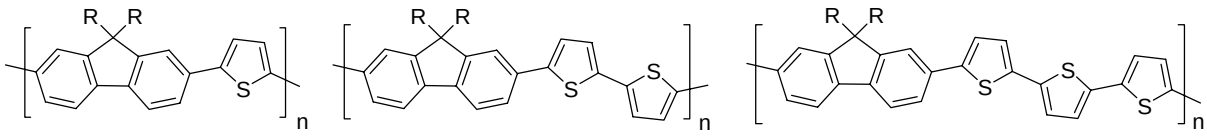

R = 3,7,11-trimethyldodecyl **PFFaT** | R = n-octyl **PF8TT** | R = 2-ethylhexyl **PF26TTT**

Scheme 2.7: Alternating fluorene-oligothiophene copolymers.[1]

The influence of the alkoxy substituted naphthalene unit as replacement of the fluorene moiety seems to be negligible and reflects that the optical properties are mainly governed by the oligothiophene blocks. The spectra of **10 – 12** in chloroform solution are shown in Figure 2.3.

Table 2.2: Absorption and emission maxima of polymers **10 – 12**.

Polymer	$\lambda_{max.}$ ($CHCl_3$-solution) (nm)		$\lambda_{max.}$ (film) (nm)	
	abs.	em.	abs	em.
10	427	472, 497	437, 457	508
11	449	498, 530	460, 488	548
12	456	515, 552	472	572
PFFaT	427	473, 500	427	504, 531
PF8TT	447	497, 530	452	551, 581
PF26TTT	453	515, 547	471	567, 602

The emission spectra of **10 – 12** show an increasing fine structure of the π – π transition when elongating the thiophene units, which is explained by the easier opportunity to planarize the excited state. Furthermore, it can be concluded that the solubilizing sidechains of the naphthalene unit do not significantly affect the solid state arrangement of (oligo)thiophene based copolymers. The absorption maxima of the bi – and terthiophene based copolymers show a very similar shape and shift. Extension of the oligothiophene units shifts the emission maxima towards lower energies, which is indicated by a pronounced red shit. In solution the

PL maximum shifts about 23 nm by going from a thiophene (**10**) to a bithiophene (**11**) and another 12 nm by extending it to a terthiophene block (**12**).

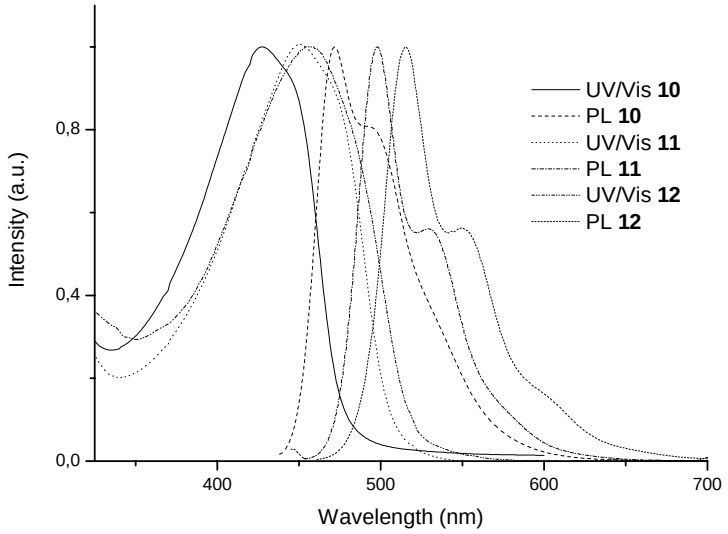

Figure 2.3: UV/Vis and PL spectra of **10**, **11** and **12** in chloroform solution.

All solid state PL spectra are remarkably red-shifted compared to their solution spectra. In the case of **10** the shift is rather weak with only 36 nm. However, in the case of **12** a particular shift of 57 nm is observed, which is explained by the good ability of the terthiophene based copolymers to form π – stacked aggregates.

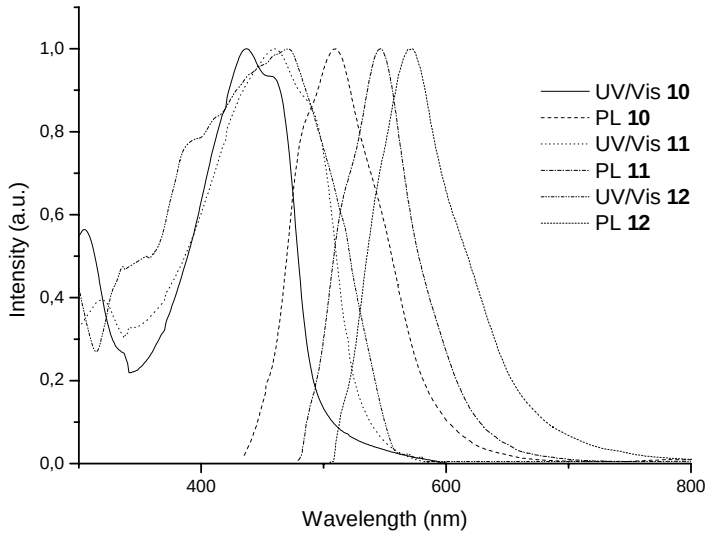

Figure 2.4: UV/Vis and PL spectra of **10**, **11** and **12** in thin films.

To get a better understanding of the optical spectra and to investigate furthermore the influence of the substitution pattern on the naphthalene unit the corresponding model compounds have also been examined both in chloroform solution and drop casted thin films from chloroform.

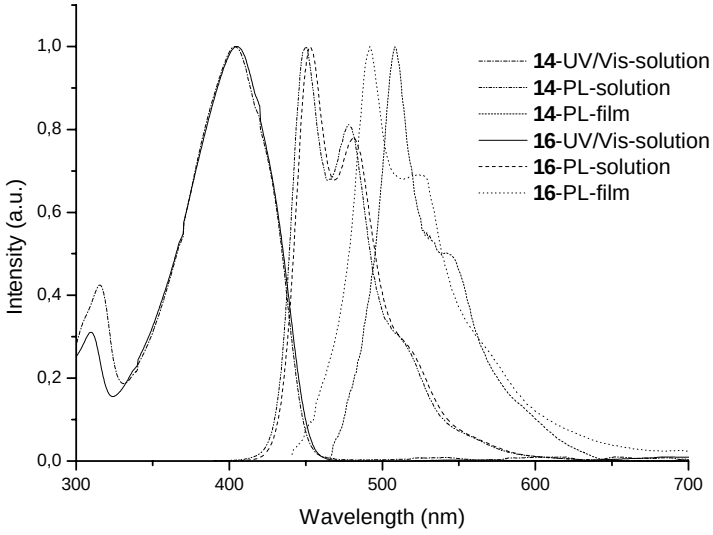

Figure 2.5: Absorption and emission of **14** and **16** in chloroform solution and thin films.

As expected and in good agreement with the corresponding polymers the solution absorption spectra are structureless and broad with a maximum at 405 nm. Due to the shorter conjugation the maxima are blue – shifted compared to polymer **11**. The solution PL spectra are nearly identical with two transitions at around 450 and 480 nm, which indicates no distinct influence of the peripherical alkoxy sidechains in solution. Nevertheless, the solid state spectra are much more red – shifted. The alkoxy - substituted derivative **14** undergoes a redshift of 39 nm by going from solution to films, the corresponding compound **16**, without the alkoxy groups, experiences a shift of 57 nm. This finding indicates an increased intermolecular interaction towards aggregates for **16** as expected. The alkoxy substituents of **14** seem to suppress a closer π – stacked arrangement in the solid state.

2.2.4. FET Investigations

Model compounds **14** and **16** and polymer **11** are under intensive investigation as the active layer in OFETs, in corporation with the Bao – group (Stanford, USA). All materials have been spincoated from chloroform solutions onto a highly doped n – silicon wafer under

standard laboratory conditions. Even under these basic device design reached **16** a charge carrier (hole) mobility of 1.35×10^{-2} cm^2/Vs and an on/off ratio of around 200. The values of **14** display a dramatically decreased mobility by circa three orders of magnitude, reflecting the strong influence of the alkoxy sidechains.

Table 2.3: OFET data (Average of two individual devices).

Material	μ (cm^2/Vs)	on/off
11	2.90×10^{-8}	249
14	4.35×10^{-5}	2795
16	1.35×10^{-2}	199

Therefore, it is easy to understand that the mobilities of the corresponding polymer **11** are again considerably lower with values of about 10^{-8} cm^2/Vs. At the present stage detailed studies towards an enhanced OFET performance of **16** are underway and will be reported elsewhere.

2.3. Application as a "Bubble Array" Matrix Polymer

Micro- and nanostructuring of organic semiconductors is of critical importance in the fabrication of photonic bandgap materials and heterojunction devices such as photovoltaic cells.[42-44] Therefore, a variety of templating methods based on self-assembly have been developed to create micro – and submicrometer structures. These include templating using emulsions,[45] honeycomb structures formed by polymers with rod-coil architectures,[46] and self organized surfactants.[47] These templating approaches allow the preparation of three - dimensional ordered pores with dimensions of tens to thousands of nanometers.

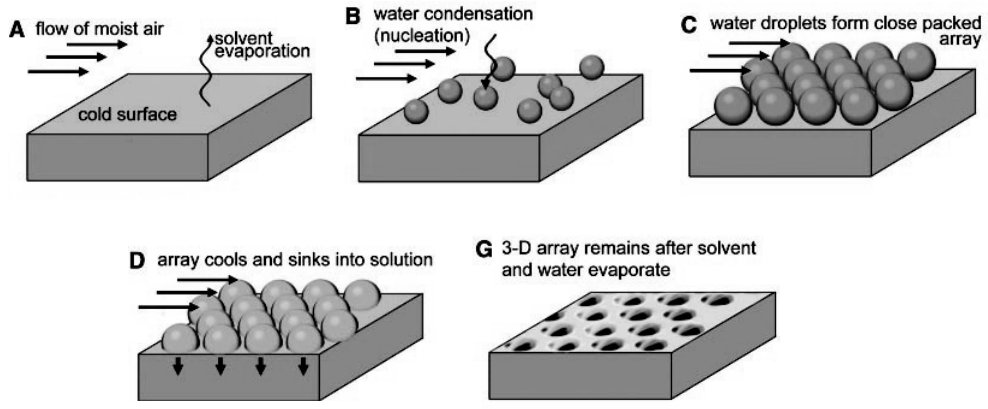

Figure 2.6: Mechanism of "bubble – array" formation utilizing the "breath figure – method".

However, the micro - nanostructuring of organic semiconductors is under investigation and often requires lengthy procedures. With exception of the Neher-Scherf-Landfester microemulsion method[42;43] and a nanotemplating approach by Martin,[48;49] there are not many generally applicable methods for the microstructuring of polymers. Srinivasarao and Bunz applied a technique which is known as "breath figure- method",[50] which was first reported by Lord Rayleigh,[51;52] to rigid – rod conjugated polymers.[53-55] "Breath figures" form if warm moist air comes in contact with a cold surface. Lord Rayleigh showed that "breath figures" are hexagonally arranged microscopic water droplets that condense onto the cold support. They are formed not only on cold solids but as well on liquid surfaces. A spectacular use for "breath figures" stems from the discovery that polymers dissolved in a low boiling point solvent such as carbon disulfide form "bubble arrays" when moist air is used to evaporate the solvent. The remaining polymer matrix shows highly ordered "bubble arrays", fossilized versions of the "breath figures" (Figure 2.6).[50] In collaboration with Prof. M. Srinivasarao and Prof. U. H. F. Bunz (Georgia Institute of Technology, USA) it was shown that polymer **11** is able to form high quality "bubble array" areas at ambient temperature. **11** was dissolved in carbon disulfide and a drop of this solution was placed on a untreated glass slide. Evaporation of the solvent in the presence of moist air leaded to the structures shown in Figure 2.7 and Figure 2.8. Usually these polymer scaffolds can be dissolved again in organic solvents.

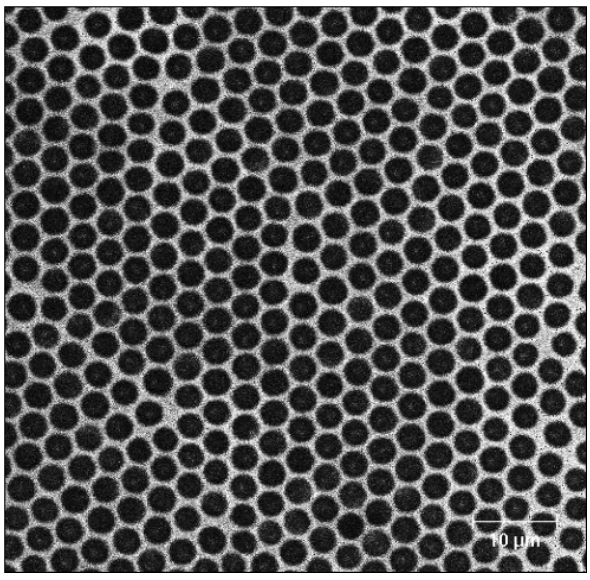

Figure 2.7: SEM image of a macroscopic "bubble arrays" formed by evaporation of dilute solutions of **11** in carbon disulfide.

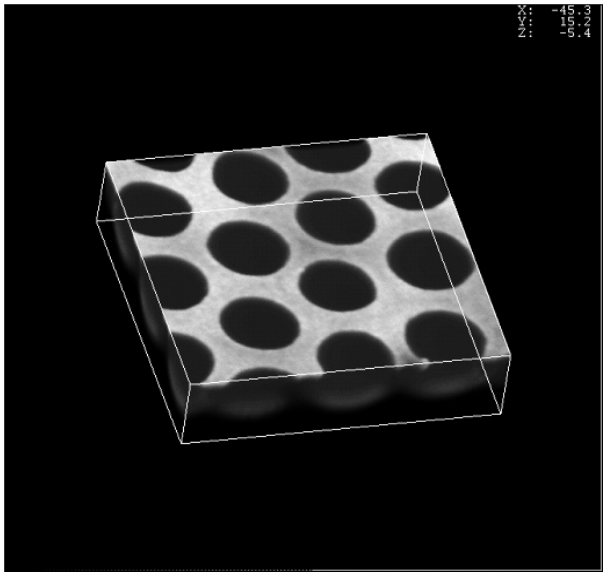

Figure 2.8: 3D view of a "bubble array" made by confocal laser microscopy of polymer **11**.

However, to allow a convenient way to fill these "picoliter beaker" structures, insoluble "bubble arrays" are highly desired. Therefore, Srinivasarao and Bunz presented a facile way to fabricate stable, noninterconnected, and insoluble "bubble array" areas by using crosslinkable polymers.[53] These easily generated structures strongly resemble lithographically microfabricated "picoliter beaker" arrays. The fact that linear rigid – rod polymers form highly ordered arrays refutes the notion that branched or coiled polymers, e.g. polystyrene are necessary to form these arrays. Further studies will investigate the possibility to fill these holes with different "guest" materials and to examine the energy and charge transfer within these arrays. These materials have great potential as microanalytical tools and as matrices for the fabrication of microlenses.

2.4. Conclusion

A series of new alkoxy-substituted, alternating naphthalene thiophene copolymers and related model compounds have been synthesized and characterized. The absorption and emission bands are subsequently red – shifted with increasing length of the oligothienylene segments. The solid state optical spectra indicate strong π – interactions between parallelly arranged oligomer or polymer chains. The solid state behaviour is of particular interest for utilization in OFETs. Initial results show tremendously decreased charge carrier mobilities when attaching alkoxy side-chains to the naphthalene units. Therefore, especially compound **16** will be further investigated as the active organic material of OFETs. Polymers **10**-**12** have been

investigated as matrix materials in so called “bubble arrays”, prepared via the “breath figure” method. Subsequent experiments deal with the conversion towards insoluble arrays, as well as with the filling of the structures.

2.5. Experimental Section

2.5.1. General Methods

Unless otherwise indicated, all starting materials were obtained from commercial suppliers (Aldrich, Fischer, EM Science, Lancaster, ABCR, Strem) and were used without further purification. All reactions were carried out under an argon atmosphere. Analytical thin-layer chromatography (TLC) was performed on Kieselgel F-254 pre-coated TLC plates. Visualization was performed with an 254 nm ultraviolet lamp. Silica gel column chromatography was carried out with Silica Gel (230-400 mesh) from EM Science. ^{1}H- and ^{13}C-NMR data were obtained on a Bruker ARX 400-spectrometer. Chemical shifts are expressed in parts per million (δ) using residual solvent protons as internal standards. Splitting patterns are designated as s (singlet), d (doublet), t (triplett), q (quartet), bs (broad singlet), m (multiplet). Low-resolution mass spectrometry was obtained on a Varian MAT 311A operating at 70 eV (Electron Impact, EI) and reported as m/z and percent relative intensity. FD masses were obtained on a ZAB 2-SE-FDP. Elemental analysis were performed by the University of Wuppertal, Department of Analytical Chemistry, using a Perkin Elmer 240 B. Molecular weight determinations via Gel Permeation Chromatography (GPC) were performed using a Spectra 100 GPC column (5 µm particles) eluted with THF at 30°C (flow rate of 1 mL/min and concentration of the polymer: ca. 1.5 g/L. The calibration was based on polystyrene standards with narrow molecular weight distribution. All GPC analyses were performed on solutions of the polymers in THF at 30°C. Phase transitions were studied by differential scanning calorimetry (DSC) with a Bruker Reflex II thermosystem at a scanning rate of 10 K min^{-1} for both heating and cooling cycles. The UV-Vis and fluorescence spectra were recorded on a Jasco V-550 spectrophotometer and a Varian-Cary Eclipse spectrometer respectively (concentration of the polymer: ca. 1.5 g/L). Infrared spectroscopy (IR) was performed on a Nicolet Protégé 460 spectrometer in chloroform solution or in bulk. Microwave assisted synthesis were performed using a CEM – Discovery monomode microwave utilizing a IR-temperature sensor, magnetic stirrer and sealed 10 mL glass vials. All reactions were monitored and controlled using a personal computer.

2.5.2. Synthesis

2,2':5',2'' Terthiophene (3)

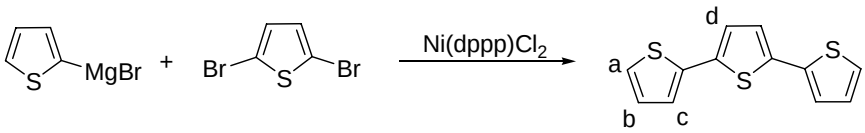

2-bromothiophene (14.7 g, 90 mmol) was slowly added to stirred, refluxing mixture of magnesiumturnings (2.2 g, 90 mmol) with a trace of iodine in anhydrous diethylether (40 mL). The mixture was heated to reflux for one hour. After complete dissolution of the magnesium the resulting Grignard compound was transferred to a second three-necked flask containing 2,5-dibromothiophene (9.7 g, 40 mmol) and [1,3-bis(diphenylphosphino)-propane]nickel (II) ($Ni(dppp)Cl_2$) (48 mg, 0.09 mmol) in anhydrous diethylether and stirred at room temperature for 48 h. The solution was poured into water and extracted with ether. The organic layer was washed with brine and dried over Na_2SO_4. After evaporation of the solvent the remaining residue was recrystallized from ethanol. Yield: 82%. ^1H NMR (400 MHz, $C_2D_2Cl_4$, 25 °C): δ = 7.18 (d, 2H, J = 5.0 Hz, H-a), 7.12 (d, 2H, J = 3.7 Hz, H-c), 7.03 (s, 2H, H-d), 6.97 (dd, 2H, J = 3.7 Hz, J= 5.0 Hz, H-b) ppm. ^{13}C NMR (100 MHz, $C_2D_2Cl_4$, 25 °C): δ = 137.2, 136.4, 128.3, 125.0, 124.7, 124.1 ppm. LR-MS (EI, 70eV): m/z = 248 [M^+] (100.0), 249 (16.5), 250 (16.7). Anal. Calcd. for $C_{12}H_8S_3$: C, 58.03; H, 3.25; S, 38.73. Found: C, 57.88; H, 3.74; S, 38.24.

General Procedure for distannylated Oligothiophenes:

A mixture of *sec*-butyllithium (22.6 mL, 1.3 M in hexanes, 29.3 mmol) was added dropwise to a stirred, cooled (-78°C) mixture of the (oligo)-thiophene (12.6 mmol), N,N,N',N'-tetra-methyldiamine (4.15 g, 27.9 mmol) hexanes (10 mL) and THF (20 mL) were added. The solution was warmed to 50°C and again cooled to – 78°C. A solution of trimethyltinchloride (29 mL, 1 M in THF, 29 mmol) was added at once and the mixture again warmed up to room temperature and stirred for 10 h. The reaction was quenched by adding an ammoniumchloride solution (90 mL, 2 M). The mixture was extracted into chloroform, washed with water, brine, dried over Na_2SO_4 and the solvent was removed via rotary evaporation. The residue was recrystallized from ethanol.

2,5-Bis(trimethylstannyl)-thiophene (4)

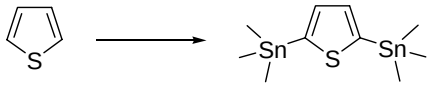

Yield: 72%. ^{1}H NMR (400 MHz, $C_2D_2Cl_4$, 25 °C): δ = 7.37 (s, 2H), 0.37 (s, 18H) ppm. ^{13}C NMR (100 MHz, $C_2D_2Cl_4$, 80 °C): δ = 143.4, 136.2, -7.7 ppm. FD-MS: 409.8 (100.0). Anal. Calcd. for $C_{10}H_{20}SSn_2$: C, 29.32; H, 4.92; S, 7.83. Found: C, 29.25; H, 5.09; S, 7.45.

5,5'-Bis(trimethylstannyl)-2,2'-bithiophene (5)

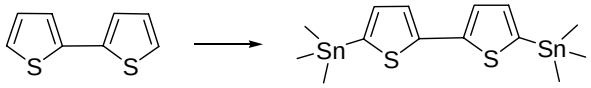

Yield: 75 %. ^{1}H NMR (400 MHz, $C_2D_2Cl_4$, 25 °C): δ = 7.20 (d, 2H, J = 3.3 Hz), 7.02 (d, 2H, J = 3.3 Hz), 0.32 (s, 18H) ppm. ^{13}C NMR (100 MHz, $C_2D_2Cl_4$, 80 °C): δ = 143.1, 137.5, 136.3, 125.0, - 7.7 ppm. FD-MS: 491.8 (100.0). Anal. Calcd. for $C_{14}H_{22}S_2Sn_2$: C, 34.19; H, 4.51; S, 13.04. Found: C, 34.01; H, 4.06; S, 12.45.

5,5''-Bis(trimethylstannyl)-2.2':5,2''-terthiophene (6)

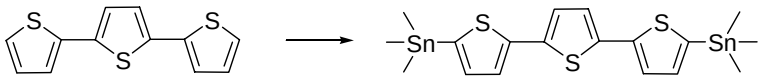

Yield: 75 %. ^{1}H NMR (400 MHz, $C_2D_2Cl_4$, 25 °C): δ = 7.21 (d, 2H, ^{3}J = 3,3 Hz), 7.04 (d, 2H, J = 3.3 Hz), 7.00 (s, 2H) 0.33 (s, 18H, -CH_3) ppm. ^{13}C NMR (100 MHz, $C_2D_2Cl_4$, 25 °C): δ = 142.5, 138.0, 136.1, 134.9, 125.0, 124.3, -7.9 ppm. FD-MS: 573.9 (100.0). Anal. Calcd. for $C_{14}H_{22}S_3Sn_2$: C, 37.67; H, 4.21; S, 16.76. Found: C, 37.55; H, 3.66; S, 16.74.

1,5-Dihydroxy-2,6-dibromonaphthalene (8)

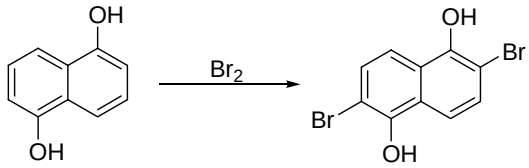

A solution of 1,5-dihydroxynaphthalene (10 g, 0.06 mol) in glacial acetic acid (100 mL) with a few crystals of iodine was heated to 80°C. Bromine (6.9 mL, 0.13 mol) in glacial acetic acid (30 mL) was added slowly over 1 hour. The mixture was stirred for a further hour and then cooled to 0°C. Greenish crystals occured which were filtered of, washed with hexanes and dried. Yield: 85 %. ^{1}H NMR (400 MHz, d-DMSO, 25 °C): δ = 7.64 (d, 2H, J = 9.2 Hz), 7.53 (d, 2H, J = 9.2 Hz), 9.6-10.2 (bs, 2H) ppm. ^{13}C NMR (100 MHz, d-DMSO, 25 °C): δ =

149.48, 129.64, 126.30, 115.24, 105.84 ppm. LR-MS (EI, 70eV): m/z = 75 (29.2), 101 (53.2), 208 (33.7), 210 (31.8), 316 (57.1), 318 [M^+] (100.0), 320 (55.5).

1,5-Dioctyloxy-2,6-dibromonaphthalene (9).

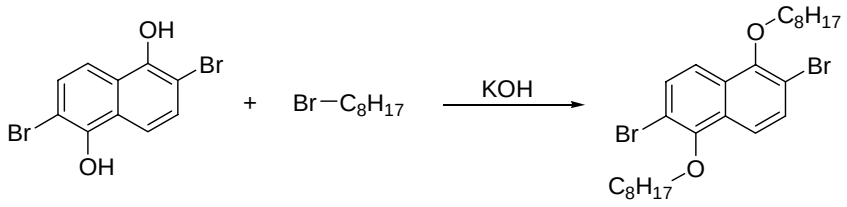

A solution of 2,6-dibromo-1,5-dihydroxynaphthalene (**8**) (10.0 g, 31.5 mmol) and KOH (5.3 g, 94.5 mmol) in anhydrous ethanol (200 mL) was degassed with argon and heated to reflux. Octylbromide (16.5 mL, 95.2 mmol) was added slowly and the solution was refluxed for 12 hours. The reaction mixture was cooled and filtered. The solid was then stirred in water (200 mL) for 1 hour, filtered and dried under vacuum. Yield: 77 %. ^{1}H NMR (400 MHz, $CDCl_3$, 25 °C): δ = 7.75 (d, 2H, J = 9.0 Hz), 7.61 (d, 2H, J = 9.0 Hz), 4.07 (t, 4H, J = 6.6 Hz), 1.95 (m, 4H), 1.59 (m, 4H), 1.37 (m, 16H), 0.92 (t, 6H) ppm. ^{13}C NMR (100 MHz, $CDCl_3$, 25 °C): δ = 152.8, 131.0, 130.1, 119.3, 113.8, 74.6, 31.8, 30.3, 29.5, 29.3, 29.0, 22.7, 14.1 ppm. LR-MS (EI, 70eV): m/z = 44 (90.3), 57 (58.34), 316 (45.9), 318 (100.0), 320 (44.7), 540 (6.9), 542 [M^+] (13.3), 544 (7.2).

General Procedure for Microwave-Assisted Stille Polymerizations:

An equimolar quantity (0.18 mmol) of bis(trimethylstannyl)oligothiophene and **9** and [$Pd(PPh_3)_4$] (9 mg, 0.008 mmol) were added to a 10 mL vial under glove-box conditions. Dry toluene (4 mL) was added and the solution was irradiated with microwaves (300 W, maximum temperature) for 9 minutes. The reaction mixture was diluted with chloroform and washed with 2M HCl, saturated aqueous NaEDTA and $NaHCO_3$ solutions. The organic phase was dried over Na_2SO_4 and the solvent was removed. The residue was dissolved in chloroform precipitated into methanol and filtered. The solid material was extracted for 2 days in a soxhlet apparatus with acetone, the resulting polymer was collected and dried under vacuum.

Poly[2,6-(1,5-dioctyloxy)naphthalene]-*alt*-2,5-thienylene (10)

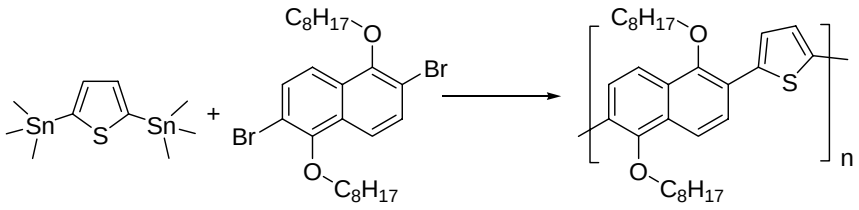

Yield: 70 %. GPC (vs. polystyrene standards in THF): M_n = 21,100, M_w/M_n = 1.9. ^{1}H NMR (400 MHz, $CDCl_3$, 25°C): δ =8.12 (d, 2H, J = 7.8 Hz), 7.99 (d, 2H, J = 8.2 Hz), 7.81 (d, 2H, J = 5.8 Hz), 4.11 (m, 4H), 2.13 (m, 4H), 1.68 (m, 4H), 1.45 (m, 16H), 1.00 (m, 6H) ppm. ^{13}C NMR (100 MHz, $CDCl_3$, 25°C): 151.7, 140.1, 129.7, 126.6, 126.2, 123.6, 119.0, 74.3, 31.9, 30.5, 29.6, 29.3, 26.2, 22.7, 14.1 ppm.

Poly[2,6-(1,5-dioctyloxy)naphthalene]-*alt*-2,5-bithienylene (11)

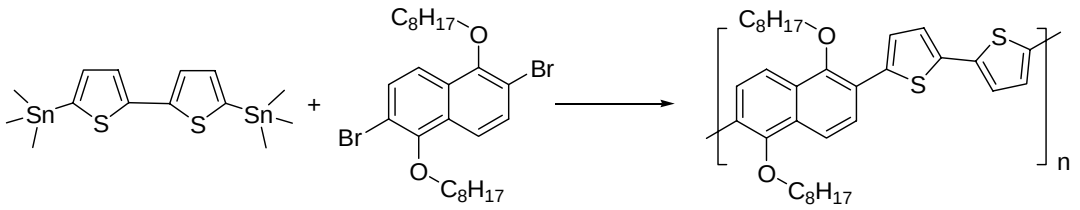

Yield: 62 %. GPC (vs. polystyrene standards in THF): M_n = 11,800, M_w/M_n = 2.5. ^{1}H NMR (400 MHz, $C_2D_2Cl_4$, 25 °C): δ =7.94 (d, 2H, J = 8.1 Hz), 7.76 (d, 2H, J = 8.2 Hz), 7.54 (m, 2H), 7.28 (m, 2H), 4.01 (m, 4H), 1.98 (m, 4H), 1.57 (m, 4H), 1.33 (m, 16H), 0.89 (m, 6H) ppm. ^{13}C NMR (100 MHz, $C_2D_2Cl_4$, 25 °C): δ = 152.0, 138.9, 138.4, 130.0, 127.1, 126.7, 123.9, 123.6, 119.2, 74.8, 32.0, 30.6, 29.7, 29.4, 26.4, 22.7, 14.1 ppm.

Poly[2,6-(1,5-dioctyloxy)naphthalene]-*alt*-5,5’’-(2,2’:5’,2’’-terthiophene) (12)

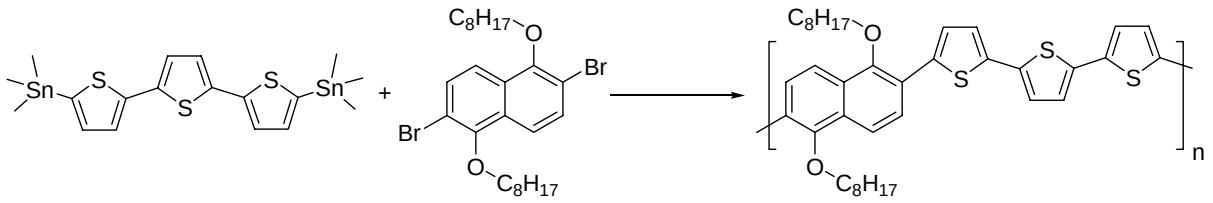

Yield: 55 %. GPC (vs. polystyrene standards in THF): M_n = 6,600, M_w/M_n = 1.9. ^{1}H NMR (400 MHz, $C_2D_2Cl_4$, 80 °C): δ = 7.90 (m, 2H), 7.75 (m, 2H), 7.48 (m, 2H), 7.21 (m, 2H), 7.15 (m, 2H), 3.9-4.1 (m, 4H, O-CH_2), 1.95 (m, 4H), 1.54 (m, 4H), 1.25-1.42 (m, 16H), 0.87 (m,

6H, CH_3) ppm. ^{13}C NMR (100 MHz, $C_2D_2Cl_4$, 80 °C): δ = 151.9, 138.9, 137.9, 136.9, 129.9, 127.0, 126.6, 124.6, 124.1, 123.5, 119.3, 74.8, 32.0, 30.7, 29.7, 29.4, 26.4, 22.8, 14.3 ppm.

2,6-Bis(5-*n*-hexyl-2,2'-bithiophene-5'-yl)-1,5-di-*n*-octyloxy-naphthalene (14)

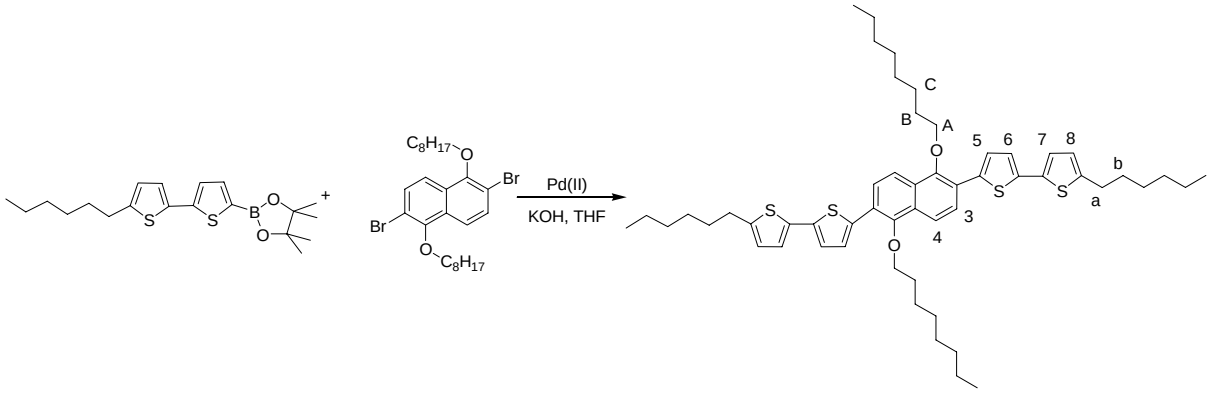

A dried 10 mL microwave tube was charged with 1,5-dioctyloxy-2,6-dibromo-naphthalene (**9**) (0.189 g, 0.35 mmol), 5-*n*-hexyl-2,2'-bithiophene-5'-(4,4,5,5-tetramethyl-1,3,2-dioxaborolane) (**13**) (0.33 g, 0.87 mmol), KOH (0.24 g, 4.19 mmol), $PdCl_2(PPh_3)_2$ (0.05 g, 0.07 mmol) and sealed under argon. Dry THF (4 mL) was added and the reaction was irradiated with microwaves (300 W) for 12 min at a temperature of 120°C. The mixture was poured into water and then extracted with dichloromethane, which was subsequently washed with water and brine, dried over Na_2SO_4 and the solvent was removed by rotary evaporation. The residue was washed with hot ethanol and recrystallized from toluene to afford **14** in 52 % yield. ^{1}H NMR (400 MHz, $C_2D_2Cl_4$, 25 °C): δ = 7.82 (d, 2H, J = 8.9 Hz, H3/H4), 7.71 (d, 2H, J = 8.9 Hz, H3/H4), 7.43 (d, 2H, 3.8 Hz, H-5), 7.07 (d, 2H, 3.7 Hz, H-6), 6.99 (d, 2H, J = 3.4 Hz, H-7), 6.66 (d, 2H, J = 3.2 Hz, H-8), 3.88 (t, 4H, J = 6.5 Hz, H-A), 2.74 (t, 4H, J = 7.5 Hz, H-a), 1.91 (q, 4H, J = 7.5 Hz, J = 14.4 Hz), 1.62 (q, 4H, J = 7.5Hz, J = 14.4 Hz), 1.49 (q, 4H, J = 7.0 Hz, J = 14.0Hz), 1.27 (m, 28H), 0.83 (m, 12H) ppm. ^{13}C NMR (100 MHz, $C_2D_2Cl_4$, 25 °C): δ = 151.3, 145.9, 138.7, 137.5, 135.1, 129.6, 126.7, 126.4, 125.2, 123.5, 123.4, 123.2, 119.1, 74.7, 32.1, 31.8, 30.7, 30.4, 30.0, 29.8, 29.6, 29.0, 26.4, 23.0, 22.9, 14.5, 14.4 ppm. LR-MS (EI, m/z): 767 (57.0), 879 [M^+] (100.0).

2,6-Bis(5-*n*-hexyl-2,2'-bithiophene-5'-yl)-naphthalene (16)

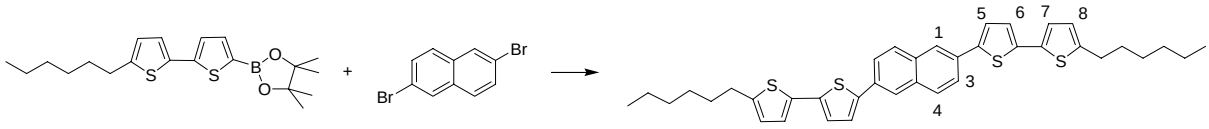

Compound **16** was prepared by a method similar to that used for **14** utilizing 2,6-dibromo-naphthalene. The residue was purified via two recrystallization cycles from hot toluene to afford **16** in 70 % yield. ^{1}H NMR (400 MHz, $C_2D_2Cl_4$, 25 °C): δ = 7.93 (d, 2H, J = 1.3 Hz), 7.79 (d, 2 H, J = 8.5Hz), 7.69 (dd, 2 H, J = 1.3 Hz, J = 8.5 Hz), 7.29 (d, 2 H, J = 3.7 Hz), 7.07 (d, 2 H, J = 3.8Hz), 7.00 (d, 2 H, J = 3.5 Hz), 6.67 (d, 2 H, J = 3.5 Hz), 2.77 (t, 4 H, J = 7.6 Hz), 1.67 (q, 4 H, J = 7.1 Hz, J = 7.4 Hz), 1.34 (m, 12 H), 0.87 (t, 6 H, J = 7.0 Hz).^{13}C NMR (100 MHz, $C_2D_2Cl_4$, 25 °C): δ = 146.2, 142.6, 138.1, 134.9, 133.2, 132.1, 128.9, 125.1, 125.1, 124.6, 124.3, 123.9, 123.9, 31.7, 317, 30.4, 29.0, 22.7, 14.2. LR-MS (EI, m/z): 553 (42.4), 624 (100.0), 625 [M^+] (39.3), 626 (29.6).

References and Notes

[1] U. Asawapirom, R. Güntner, M. Forster, T. Farrell, U. Scherf, *Synthesis* **2002,** *9*, 1136.

[2] M. Forster, K. O. Annan, U. Scherf, *Macromolecules* **1999,** *32*, 3159.

[3] M. Jayakannan, J. L. J. van Dongen, R. A. J. Janssen, *Macromolecules* **2001,** *34*, 5386.

[4] B. S. Nehls, U. Asawapirom, S. Füldner, E. Preis, T. Farrell, U. Scherf, *Adv.Funct.Mater.* **2004,** *14*, 352.

[5] L. Yu, Z. Bao, R. Cai, *Angew.Chem.Int.Ed.* **1993,** *32*, 1345.

[6] A. Devasagayaraj, J. M. Tour, *Macromolecules* **1999,** *32*, 6425.

[7] Q. T. Zhang, J. M. Tour, *J.Am.Chem.Soc.* **1997,** *119*, 9624.

[8] G. Horowitz, *J.Mater.Res.* **2004,** *19*, 1946.

[9] Z. Bao, *Adv.Mater.* **2000,** *12*, 227.

[10] H. E. Katz, *Chem.Mater.* **2004,** *16*, 4748.

[11] M. M. Ling, Z. Bao, *Chem.Mater.* **2004,** *16*, 4824.

[12] R. J. Kline, M. D. McGehee, E. N. Kadnikova, J. Liu, J. M. Frechet, *Adv.Mater.* **2003,** *15*, 1519.

[13] H. Meng, F. Sun, M. B. Goldfinger, G. D. Jaycox, Z. Li, W. J. Marshall, G. S. Blackman, *J.Am.Chem.Soc.* **2005,** *127*, 2406.

[14] A. Zen, D. Neher, U. Asawapirom, U. Scherf, *Adv.Funct.Mater.* **2004,** *14*, 757.

[15] M. Mushrush, A. Facchetti, M. Lefenfeld, H. E. Katz, T. J. Marks, *J.Am.Chem.Soc.* **2003,** *125*, 9414.

[16] A. Facchetti, M. Mushrush, M. Yoon, G. R. Hutchison, M. Ratner, T. J. Marks, *J.Am.Chem.Soc.* **2004,** *126*, 13859.

[17] C. D. Sheraw, T. N. Jackson, D. L. Eaton, J. E. Anthony, *Adv.Mater.* **2003,** *15*, 2009.

[18] Q. Miao, T. Nguyen, T. Someya, G. B. Blanchet, C. J. Nuckolls, *J.Am.Chem.Soc.* **2003,** *125*, 10284.

[19] F. Garnier, A. Yassar, R. Hajlaoui, G. Horowitz, F. Deloffre, B. Servet, S. Ries, P. Alnot, *J.Am.Chem.Soc.* **1993,** *115*.

[20] S. Tasch, W. Graupner, G. Leising, L. Pu, M. W. Wagner, R. H. Grubbs, *Adv.Mater.* **1995,** *7*, 903.

[21] M. Hanack, J. L. Segura, H. Spreitzer, *Adv.Mater.* **1996,** *8*, 663.

[22] B. Behnisch, P. Martinez-Ruis, K. H. Schweikart, M. Hanack, *Eur.J.Org.Chem.* **2000,** 2541.

[23] N. G. Pschirer, T. Miteva, U. Evans, R. S. Roberts, A. R. Marshall, D. Neher, M. L. Myrick, U. H. F. Bunz, *Chem.Mater.* **2001,** *13*, 2691.

[24] C. Z. Zhou, W. L. Wang, K. K. Lin, Z. K. Chen, Y. H. Lai, *Polymer* **2004,** *45*, 2271.

[25] B. Sankaran, M. D. Jr. Alexander, L. S. Tan, *Synth.Met.* **2001,** *123*, 425.

[26] Z. Bao, J. A. Rogers, H. E. Katz, *J.Mater.Chem.* **1999,** *9*, 1895.

[27] A. Kraft, A. C. Grimsdale, A. B. Holmes, *Angew.Chem.Int.Ed.* **1998,** *110*, 416.

[28] G. Odian, *Principles of Polymerization*, Wiley, New York **1991**.

[29] J. C. Ostrowski, R. A. Hudack, M. R. Robinson, S. Wang, G. C. Bazan, *Chem.Eur.J.* **2001,** *7*, 4500.

[30] Y. J. Miao, W. G. Herkstroeter, B. J. Sun, A. G. Wong-Foy, G. C. Bazan, *J.Am.Chem.Soc.* **1995,** *117*, 407.

[31] B. S. Nehls, E. Preis, S. Füldner, T. Farrell, U. Scherf, *Macromolecules* **2005,** *38*, 687.

[32] B. S. Nehls, Diplomarbeit, Mikrowellenunterstützte Synthese von Polyarylenen, Bergische Universität Wuppertal, **2003**.

[33] H. Yanagi, T. Morikawa, S. Hotta, K. Yase, *Adv.Mater.* **2001,** *13*, 313.

[34] H. Yanagi, T. Morikawa, S. Hotta, *Appl.Phys.Lett.* **2002,** *81*, 1512.

[35] X. M. Hong, H. E. Katz, A. J. Lovinger, B. C. Wang, K. Raghavachari, *Chem.Mater.* **2001,** *13*, 4686.

[36] S. Hotta, M. Goto, *Adv.Mater.* **2002,** *14*, 498.

[37] F. Garnier, A. Yasar, R. Hajilaoui, G. Horowitz, F. Deloffre, B. Servet, S. Ries, P. Alnot, *J.Am.Chem.Soc.* **1993,** *115*, 8716.

[38] X. M. Hong, H. E. Katz, A. J. Lovinger, B. C. Wang, K. Raghavachari, *Chem.Mater.* **2001,** *13*, 4686.

[39] G. Horowitz, *J.Mater.Chem.* **1999,** *9*, 2021.

[40] H. E. Katz, X. M. Hong, A. Dodabalapur, R. Sarpeshkar, *J.Appl.Phys.* **2002,** *91*, 1572.

[41] M. Mushrush, A. Facchetti, M. Lefenfeld, H. E. Katz, T. J. Marks, *J.Am.Chem.Soc.* **2003,** *125*, 9414.

[42] T. Kietzke, D. Neher, K. Landfester, R. Montenegro, R. Güntner, U. Scherf, *Nat.Mater.* **2003,** *2*, 406.

[43] K. Landfester, R. Montenegro, U. Scherf, R. Güntner, U. Asawapirom, S. Patil, D. Neher, T. Kietzke, *Adv.Mater.* **2002,** *14*, 651.

[44] S. A. Jehnekhe, X. L. Chen, *Science* **2005,** *283*, 372.

[45] A. Imhof, D. J. Pine, *Nature* **1997,** *389*, 948.

[46] G. Widawski, B. Rawiso, B. Francois, *Nature* **1994,** *369*, 387.

[47] A. Monnier, F. Schüth, Q. Huo, D. Kumar, D. Margolese, R. S. Maxwell, G. D. Stucky, M. Krishnamurty, P. Petroff, A. Firouzi, M. Janicke, B. F. Chemelka, *Science* **1993,** *261*, 1299.

[48] C. R. Martin, *Acc.Chem.Res.* **1995,** *28*, 61.

[49] C. R. Martin, *Chem.Mater.* **1996,** *8*, 1739.

[50] M. Srinivasarao, D. Collings, A. Philips, S. Patel, *Science* **2001,** *292*, 79.

[51] Lord Rayleigh, *Nature* **1911,** *86*, 416.

[52] Lord Rayleigh, *Nature* **1912,** *90*, 436.

[53] B. Erdogan, L. Song, J. N. Wilson, J. O. Park, M. Srinivasarao, U. H. F. Bunz, *J.Am.Chem.Soc.* **2004,** *126*, 3678.

[54] L. Song, R. K. Bly, J. N. Wilson, S. Bakbak, J. O. Park, M. Srinivasarao, U. H. F. Bunz, *Adv.Mater.* **2004,** *16*, 115.

[55] B. C. Englert, S. Scholz, P. J. Leech, M. Srinivasarao, U. H. F. Bunz, *Chem.Eur.J.* **2005,** *11*, 995.

3. 1,5 – and 2,6 – Linked Naphthylene Based Ladder Polymers

3.1. Introduction and Motivation

Among the class of semiconducting polymers the family of *para*-phenylene ladder polymers possesses a very protrude and unique set of optical and electronic properties.[1] The limited conformational freedom is a particularly relevant property of conjugated ladder - type materials since the steric inhibition of electron delocalization is drastically reduced. Twisting of the conjugated main chain induced by bulky side-chains often leads to a reduction of the conjugation length accompanied with drastic changes in optical properties. On the other hand the introduction of solubilizing side-chains is necessary to guarantee a sufficient processibility. LPPP – type Ladder polymers combine both an extended π – conjugation and sufficient solubility.

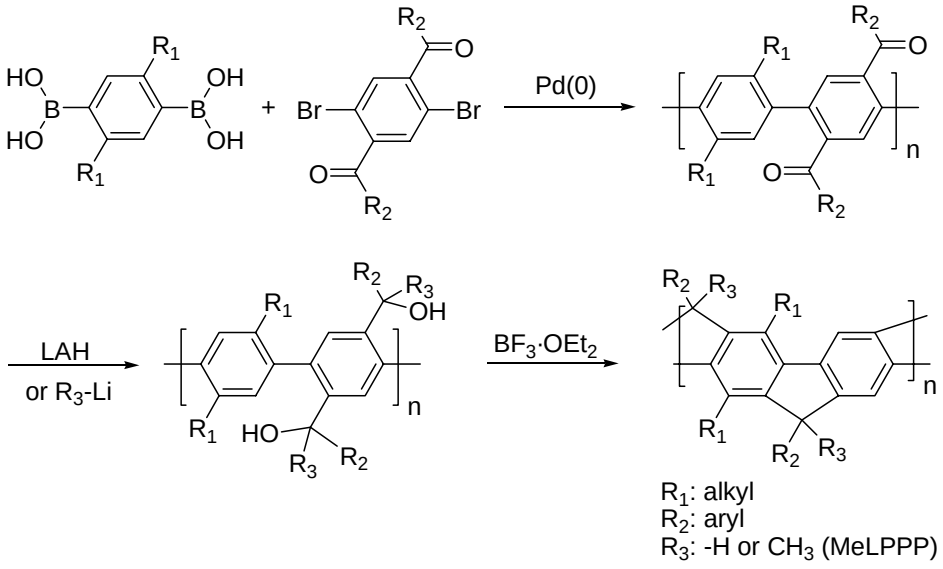

Scheme 3.1: Synthesis of ladder-type poly(*p*-phenylenes) LPPP according to Scherf and Müllen.[2]

Today two general routes to prepare ladder materials exist.[3;4] (i) the polymerization of multifunctional monomers under simultaneous generation of both strands of the ladder structure, or (ii) the cyclization of suitably functionalized, single chain precursor polymers. Ladder polymers incorporating a poly(phenylene)-structure (LPPP) are one of the most often examined class of semiconducting polymers and have attracted widespread attention as components for organic light emitting diodes[5], solid state laser [6-8], and two photon pumped fluorescence devices.[9-11] LPPP materials were first described in 1991 by Scherf and Müllen (Scheme 3.1).[2] The original LPPP showed an unstructured broad emission of yellow color in the solid state compared to the sharp blue fluorescence band in solution. The low energy emission was first attributed to interchain interactions (π-π stacking) between planar segments.[12] Related LPPP - type derivatives such as the MeLPPP with a methyl group on the bridging carbon have overcome these drawbacks.[13] However, a recent, detailed study focused on the origin of the broad solid – state emission feature has shown that emissive keto defects cause the low energy fluorescence band.[14] Related ladder polymers incorporating higher benzoid building blocks or extended aromatic systems are rare and limited for antracene – containing structures.[15-17] Naphthalene with its well – developed substitution chemistry opens the possibility to create different patterns of aryl – aryl connection and side-chain attachment. The different backbone structure should allow some tuning of the electronic and optical properties of the resulting ladder polymers.

3.2. Results and Discussion

3.2.1. Synthesis and Characterization

The initial targets towards the desired naphthalene ladder polymers were the corresponding diboronic ester monomers as shown in Scheme 3.2. 2,6-dibromo-1,5-dihydroxynaphthalene (**1**) and 1,5-dibromo-2,6-dihydroxynaphthalene (**4**) were obtained via treatment of the corresponding dihydroxynaphthalenes with bromine under acidic conditions.[18] Subsequent treatment with KOH and octylbromide in ethanol gave the resultant dioctyloxy compounds **2** and **5** in yields about 80 %. In the case of the 1,5-dibromo-4,8-dialkoxynaphthalene derivative (**8**) a n-propyloxy group was choosen to ensure good solubility and to avoid unfavourable steric hinderance. Therefore, 1,5-dihydroxynaphthalene was reacted with KOH and propylbromide in ethanol to achieve the dipropyloxy derivative **7** in a Williamson - type ether

formation in high yields of about 90 %. The conversion of **7** to the dibromo derivative **8** was carried out in acetonitrile using NBS as the brominating reagent.[19]

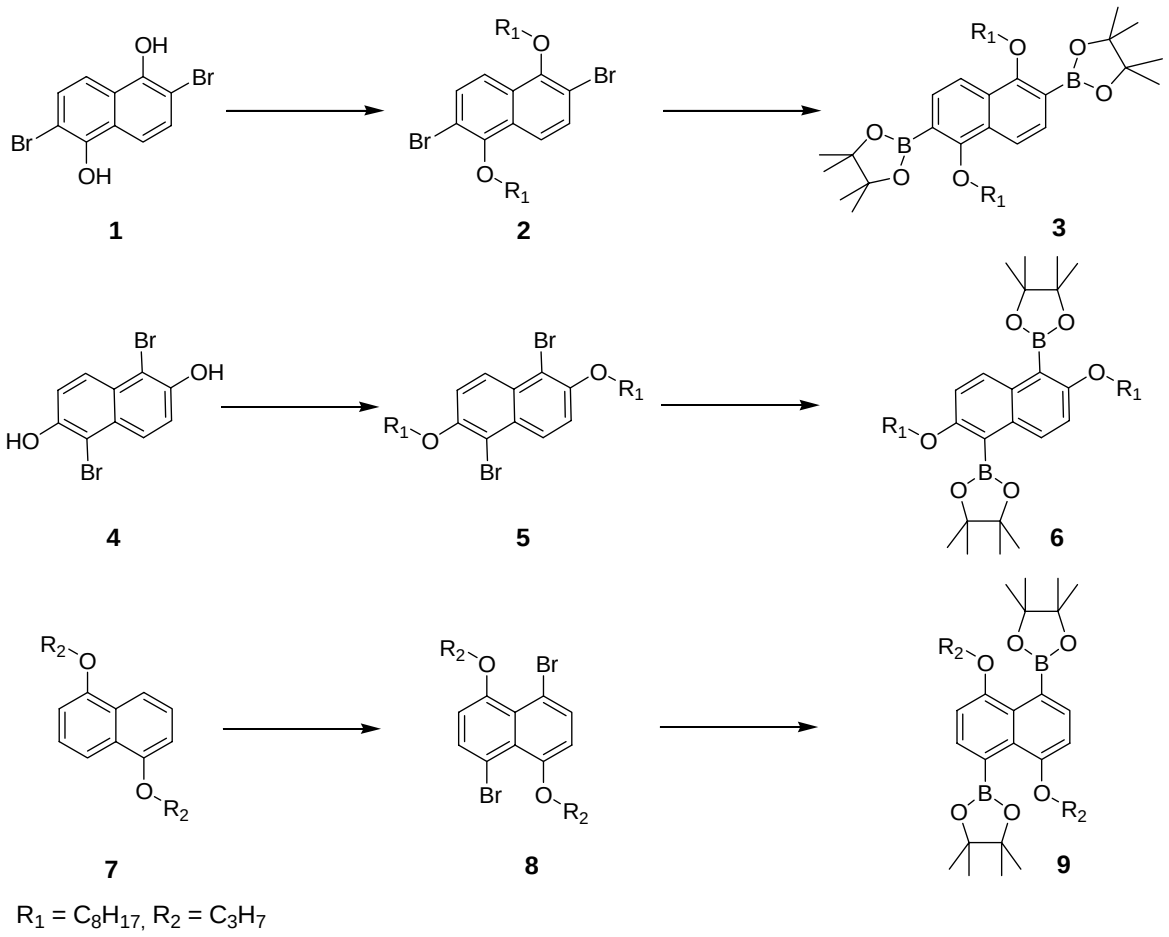

Scheme 3.2: Synthetic route towards the naphthalene boronic-ester monomers

The bisboronic ester derivatives **3**, **6** and **9** were obtained in yields between 60 and 70 % from a reaction of the dibromo derivatives with 1.25 equivalents (per halide) of BuLi at – 78°C and subsequent quenching with 2-isopropoxy-4,4,5,5-tetramethyl-1,3,2-dioxaborolane in THF/hexane.

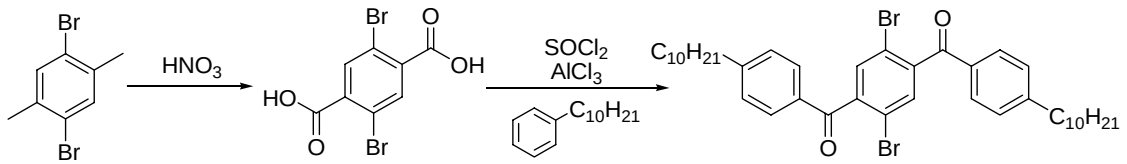

Scheme 3.3: Synthetic route towards monomer **11**

The synthesis of the dibromo counter monomer **11** started with the oxidation of 2,5-dibromo-1,4-dimethylbenzene to the related 2,5-dibromo-terephthalic-acid (**10**). **10** was converted to the (not isolated) diaciddichloride by treatment with thionyl chloride and further converted in a Friedel – Crafts – type acylation to afford 1,4-bis(4',4''-decylbenzoyl)-2,5-dibromobenzene (**11**). The synthetic protocol towards the desired ladder polymers bases on the general procedure depicted in Scheme 3.1. First, the single stranded polyketone precursors have to be prepared (Scheme 3.4).

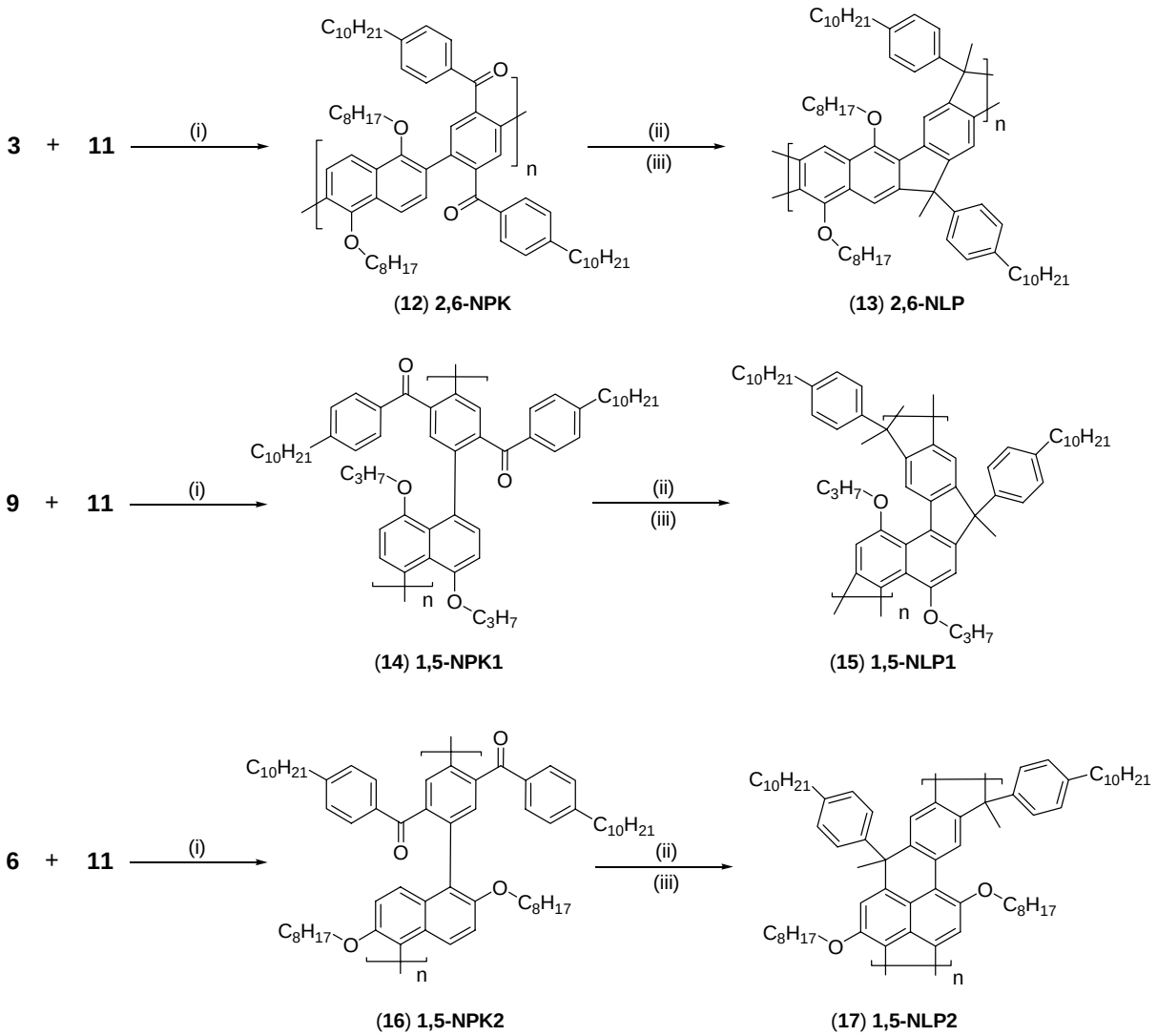

i) THF, KOH, Pd(II), μW (110°C); ii) toluene/THF, MeLi; iii) dichloromethane, $BF_3 \cdot OEt_2$

Scheme 3.4: Structure of the synthesized naphthalene based ladder polymers and their open – chain precursors.

The first polyketone in the series of the novel target structures was **2,6-NPK** (**12**), which was synthesized from **3** and **11** under a standard toluene/aq. K_2CO_3 - Suzuki protocol utilizing tetrakis(triphenylphosphino)-Pd as the catalyst.[2] Further investigations showed that a THF/ aq. K_2CO_3/$Pd(PPh_3)_2Cl_2$ system was more suitable and gave **2,6-NPK** in reasonable yields after three days (molecular weight $M_n = 11{,}300$, with a polydispersity PD = 1.8). The obtained polymer was characterized by IR, ^1H and ^{13}C NMR spectroscopy. The characteristic keto group showed a strong absorption band in the IR at 1661 cm^{-1} and also gave a characteristic signal in the ^{13}C spectrum at $\delta = 195.9$ ppm. The other twelve aromatic and eighteen alkyl/alkoxy resonances in the ^{13}C spectrum are in agreement with the expected polymer structure.

Due to the time consuming polymer synthesis and the resulting difficulties predicting the optimum conditions microwave assisted coupling protocols were applied. As mentioned in chapter 1 the use of microwave – assisted heating in cross – coupling reactions for polymers was solely described by our group.[20] Therefore, we started with some general investigations of the coupling conditions. When microwaves were applied to the "standard reaction mixture" (toluene/aqueous base) boiling spots were generated leading to strong erratic heating curves (Figure 3.1). This effect could be minimized when THF/aqueous base – mixtures or non-aqueous systems (dry THF/base) were applied.

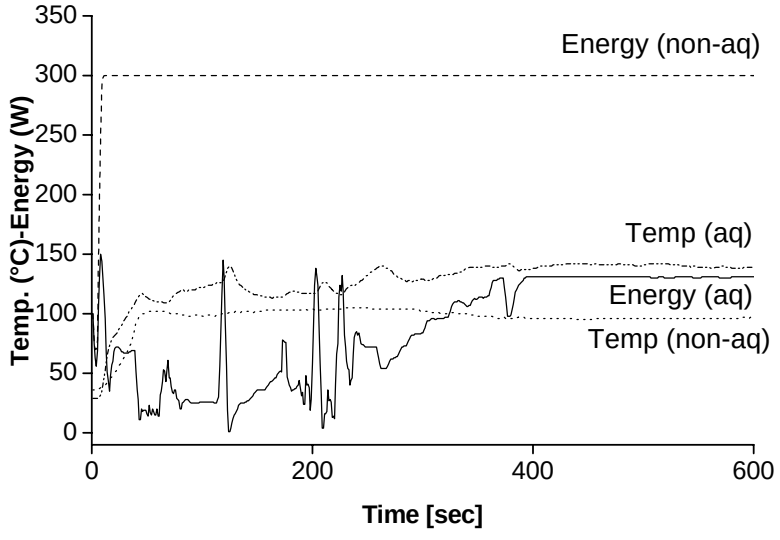

Figure 3.1: Temperature – energy profiles of the microwave – assisted preparation of **2,6-NPK** via aqueous (aq) (THF/aq. K_2CO_3) and non – aqueous (non-aq) (THF/KOH) Suzuki protocols.

An overview showing the tested conditions is given in Table 3.1. The best result was achieved when the reactants were heated in a THF/aq. K_2CO_3 system with 150 Watts at ~140°C for eleven minutes. Polymer **2,6-NPK** showed a molecular weight M_n = 14,200 and a polydispersity PD = 1.8 in 61 % yield. This result shows a good comparability to polymers obtained by conventional heating.

Table 3.1: Optimization of the reaction conditions

No.:	Solvent.	Catalyst	Base	Eq. Base	Mn (univ.)	PD	yield [%]
1	toluene	$Pd(PPh_3)_4$	H_2O/K_2CO_3	10	2,800	1.7	65
2	THF	$PdCl_2(PPh_3)_2$	H_2O/K_2CO_3	10	14,200	1.8	61
4	THF	$PdCl_2(PPh_3)_2$	KF	10	monomers	-	-
5	THF	$PdCl_2(PPh_3)_2$	K-O-*t*-But.	10	monomers	-	-
6	THF	$PdCl_2(PPh_3)_2$	DBU	10	monomers	-	-
7	THF	$PdCl_2(PPh_3)_2$	Na_2CO_3/TBAB	10/2,2	monomers	-	-

However, when these conditions were adopted to the preparation of the polyketones **1,5-NPK1** (**14**) and **1,5-NPK2** (**16**) no product was formed. Therefore, again an optimization of the microwave-assisted heating protocol was carried out. Again, non-aqueous conditions seem to be beneficial in the case of the sterically hindered boronic esters.[21-23]

Table 3.2: Molecular weights and yields of the polyketones and ladder polymers

Polymer	Heating	M_n[(a)]	PD[(a)]	Yield (%)
2,6-NPK	conventional[(b)]	11,300	1.7	80
2,6-NPK	conventional[(c)]	3,800	2.5	83
2,6-NPK	μW[(d)]	14,200	1.8	60
2,6-NPK	μW[(e)]	29,900	2.3	72
1,5-NPK1	μW[(e)]	13,600	2.4	89
1,5-NPK2	μW[(e)]	9,000	1.9	78
2,6-NLP	---	18,400	1.5	77
1,5-NLP1	---	12,900	2.0	70
1,5-NLP2	---	13,700	1.6	71

(a) Determined by gel permeation chromatography using narrow molecular weight polystyrenes as standards, (b) aq K_2CO_3/THF 3 days, (c) aq K_2CO_3/THF 1 day, (d) aq K_2CO_3/THF microwave heating for 12 min (μW 150W), (e) solid KOH/THF microwave heating for 10 min (μW 300W)

Investigations showed that the best results were now obtained under heterogeneous conditions using grinded KOH in dry THF in the microwave – apparatus at a temperature of 115°C for ten minutes. The reaction proceeded smoothly (Figure 3.1) and gave the desired polymers in good yields with high molecular weigths (Table 3.2). In the last microwave – assisted heating protocol an increasing amount of base (in this case KOH) causes higher yields and molecular weights (Figure 3.2). If two equivalents KOH per boronic ester were used polymer **1,5-NPK1** was obtained with a M_n of 3,500 and a PD = 1.9. Increasing the amount to six equivalents KOH led nearly to a trebling of the molecular weight up to M_n = 13,600 and PD = 2.4. Polyketone **1,5-NPK2** linked in the 1,5 – positions was obtained with M_n = 9,000 and PD = 1,9. Using these conditions it was also possible to prepare the already described **2,6-NPK** in 72 % yield with a significant increased molecular weight M_n = 29,900 (PD = 2.3). After overnight extraction with ethanol molecular weights of M_n = 38,500 (PD = 1.8) were obtained. Why such a big excess of base is necessary can not be explained sufficiently at that stage. In general it is known that the transmetallation between organopalladium complexes and boronic esters is favoured when the nucleophilicity of the boronic ester – component is increased. However, the exact mechanism of this is still under investigation. Two possible ways are discussed at the present time. (i) The quarternization of the boroncenter leads to an enhanced nucleophilicity; or (ii) a hydroxopalladium complex is formed which just needs a weak nucleophil.[24-26]

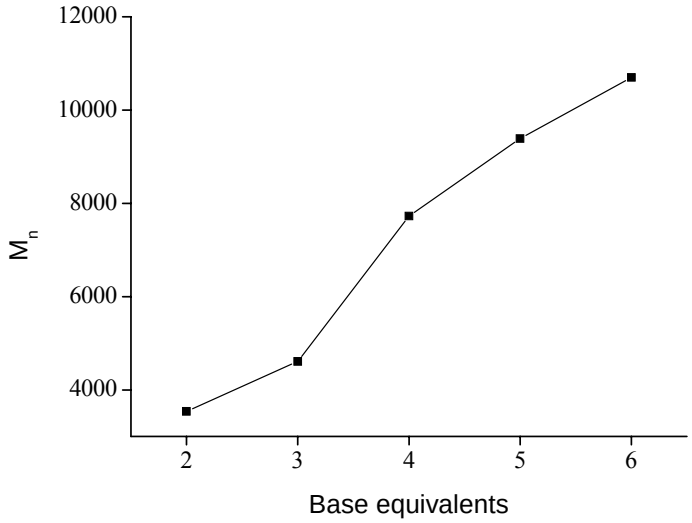

Figure 3.2: Molecular weight of **1,5-NPK** versus equivalents of KOH used in the coupling.

However, (i) and (ii) cannot explain the strong dependence from the amount of base sufficiently. Another possibility which has to be taken into account is the influence of ions in microwave assisted reactions. In general it is desirable to use unpolar solvents for polymer synthesis to assure solubility of the products. Nonetheless, these media have low dielectric constants and loss tangents, so that they absorb the microwave radiation just negligible.[27] To increase the microwave absorption factor a good absorber can be added such as salts or ionic liquids.[28-30] Even when the effect of KOH in the presented experiments (Figure 3.3) is not so dramatic as the effect of ionic liquids, the heating pattern changes in comparison to the heating of pure THF.

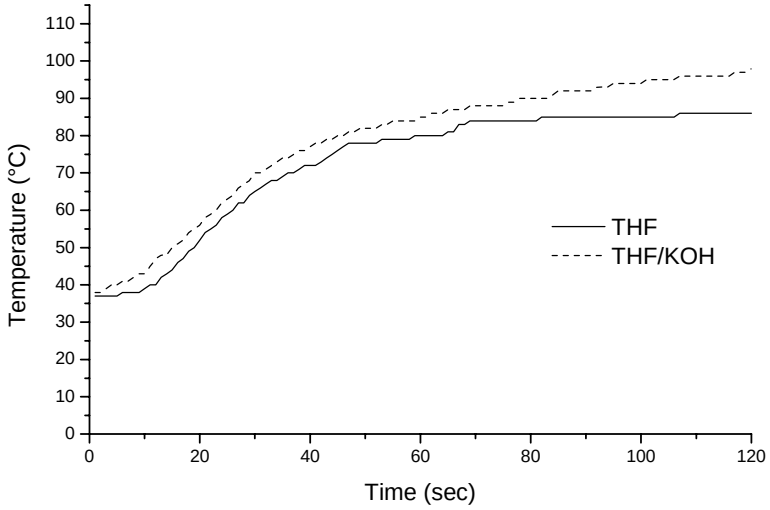

Figure 3.3: Heating curves for THF and THF/KOH under identical microwave conditions

After two minutes a difference of about twenty degrees could be observed. Therefore, it is proposed that the interaction of the base with the microwaves results in the generation of "hot spots" within the reaction mixture. The concentration of such "hot spots" increases as more KOH is added, and this thermal effect expedites the cross-coupling reaction.

The next step in the preparation of the desired ladder-polymers was the transformation of the keto groups into tertiary alcohols by reaction with methyl lithium. Prior to this transformation the polyketones were purified by soxhlet extraction with ethanol to remove low molecular components. The completeness of the conversion was monitored via IR – spectroscopy by the disappearance of the carbonyl band. The final ring closure to the ladder polymers was achieved by addition of an excess of $BF_3 \cdot OEt_2$ to a solution of the polyalcohol in

dichloromethane. The conversion was indicated by the immediate appearance of a blue fluorescence. All three polyketones could be cyclized quantitatively to afford the corresponding ladder structures. To eliminate the low molecular parts all ladder polymers were again extracted with ethanol. All molecular weights and yields are listed in Table 3.2. All ladder polymers were fully characterized by GPC, UV/Vis, PL, ^{1}H and ^{13}C NMR spectroscopy. Exemplary the ^{13}C NMR spectrum of **2,6-NLP** is depicted in Figure 3.4, showing the complete ring closure. The ^{13}C NMR spectrum reveals the expected twelve signals in the aromatic region, no other signals were observed within the detection limit which would indicate structural defects or incomplete ring closure. Furthermore, also the complete disappearances of the carbonyl signal of the polyketones at $\delta = 195.9$ ppm can be noticed. Two new signals at $\delta = 54.5$ (Signal a) and 27.5 (Signal b) ppm corresponding to the bridging quaternary carbon and the methyl group occur.

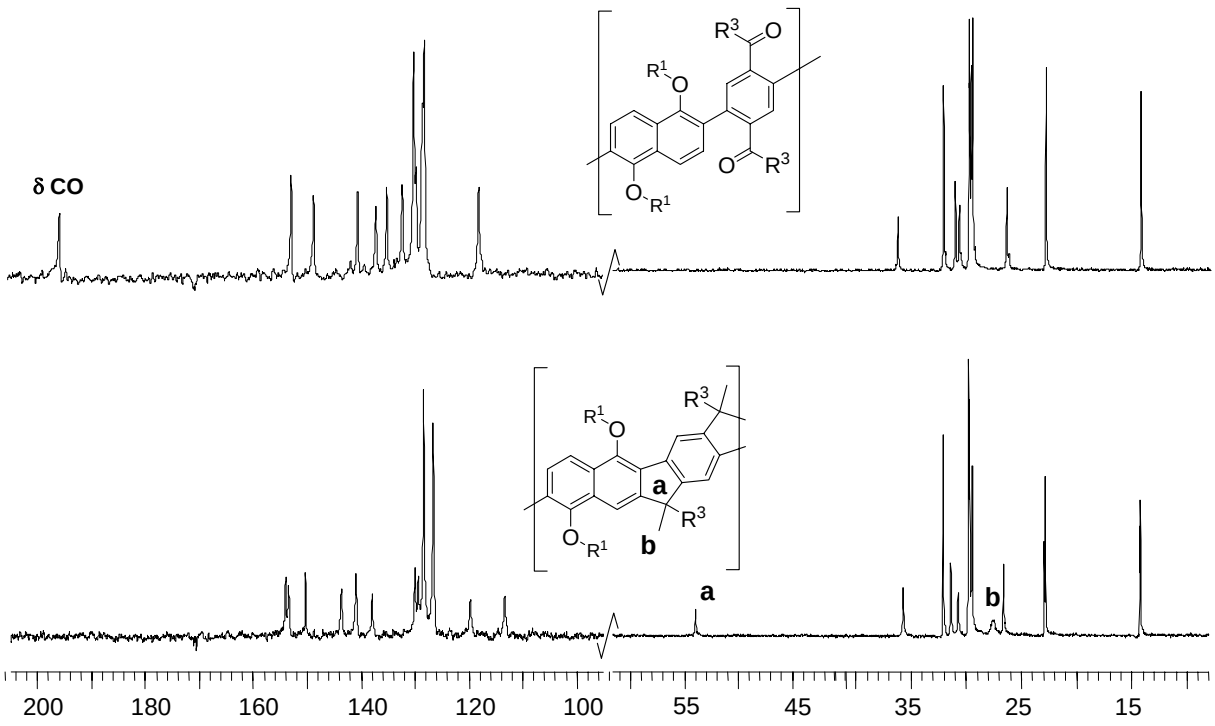

Figure 3.4: ^{13}C NMR spectra of **2,6-NPK** (top) and **2,6-NLP (**bottom) in $C_2D_2Cl_4$.

3.2.2. Optical Properties

All three novel ladder-polymers were investigated for their optical properties, both in solution and thin films. The transition from the conformationally twisted polyketone precursor to the double – stranded ladder polymer is accompanied by a drastic change in the optical properties.

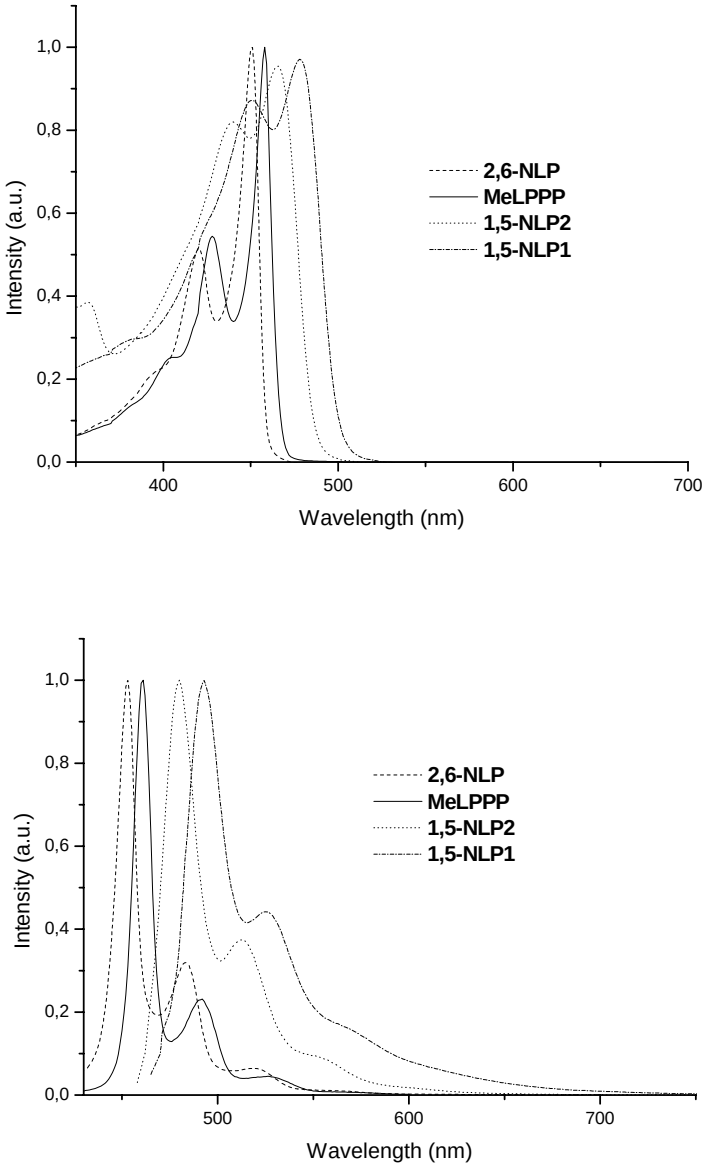

Figure 3.5: (a) UV/Vis and (b) photoluminescence spectra of dilute chloroform solutions of **2,6-NLP**, **1,5-NLP1**, **1,5-NLP2**, and **MeLPPP**.

The well resolved vibronic structure and the sharp edge of the solution absorption spectra testify the rigidity of the ladder polymers and indicate a complete cyclization. Figure 3.5a depicts the UV/Vis spectra of the three novel ladder polymers compared to **MeLPPP**. For clarity the UV/Vis and PL spectra are depicted separately. **2,6-NLP** displays the highest energy absorption with a maximum at 448 nm, which is blue – shifted in relation to **MeLPPP** with its maximum at 458 nm. Polymers **1,5-NLP1** and **1,5-NLP2** both exhibit broader spectra and obviously bathochromically shifted maxima at 480 and 466 nm, respectively. In the photoluminescence spectra (Figure 3.5b) **2,6-NLP** again exhibits the highest energy PL with a maximum at 453 nm and well resolved vibronic sidebands at 483 and 519 nm. The two 1,5 naphthalene-based substituted ladder polymers are characterized by red – shifted maxima at 493 nm for **1,5-NLP1** and 480 nm for **1,5-NLP2,** respectively (Table 3.3). The latter two polymers also show well resolved 0-1 sidebands at 525 and 513 nm and lower resolved 0-2 transitions at 554 and 572 nm. **2,6-NLP** shows the typical behavior of arylene- type ladder polymers with a very small Stokes shift of only 246 cm^{-1} in solution. Stokes shifts of this magnitude can be interpreted as a consequence of geometrically constrained, rigid π – electron systems with a small structural difference between the electronic ground and the first excited state. The Stokes shifts of **1,5-NLP1** (549 cm^{-1}) and **1,5-NLP2** (626 cm^{-1}) are slightly increased compared to **2,6-NLP** (246 cm^{-1}) or **MeLPPP** (95 cm^{-1}) and indicate a somewhat reduced intrachain order due to a stronger distortion within the polymer backbone. All Stokes shifts were derived from the solution data given in Table 3.3.

Table 3.3: Absorption and emission data of the naphthalene based ladder polymers.

Polymer	$\lambda_{max.}$ ($CHCl_3$-solution) (nm)		$\lambda_{max.}$ (film) (nm)	
	abs.	em.	abs	em.
2,6-NLP	420, 448	453, 485, 523[(a)]	419, 450	458, 486, 518[(a)]
1,5-NLP1	451, 480	493, 525, 572[(b)]	449, 476	508, 532[(b)]
1,5-NLP2	439, 466	480, 513, 554[(a)]	438, 465	485, 510, 545[(a)]
MeLPPP	428, 458	460, 491, 531[(c)]	426, 456	464, 494, 530[(c)]

(a) λ_{ex} = 440 nm, (b) λ_{ex} = 460 nm, (c) λ_{ex} = 450 nm

The way from isolated molecules in dilute solutions to molecular assemblies in the solid state is often accompanied by changes of the optical spectra. So – called coorperative phenomena become important and can change the electronic and optical properties very drastically. These changes are often documented by the occurence of a low – energy emission band in the range between 2 - 2.5 eV. This turns the blue luminescence into a greenish emission. This change was originally attributed to excimer or aggregate formation.[12;31] More recent studies of List,

Scherf and Bredas point towards ketonic defects as source of the low – energy emission in ladder – type PPPs.[14]

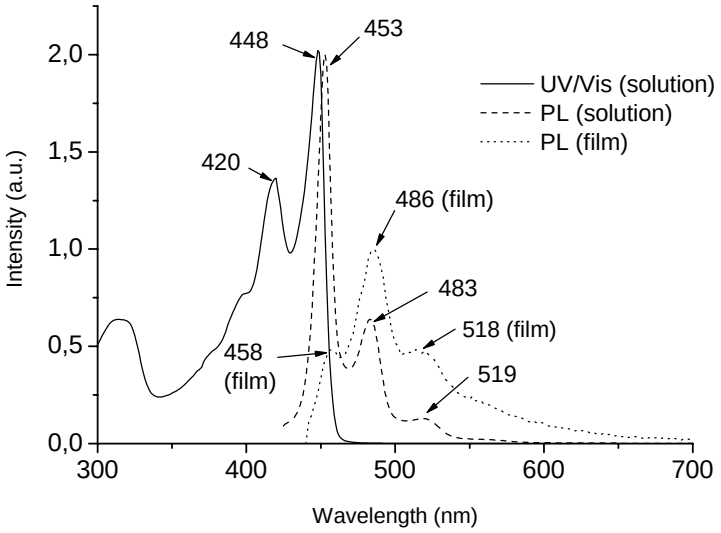

Figure 3.6: Absorption and emission spectra of **2,6-NLP** in solution and thin film.

The comparison of optical spectra of the three ladder polymers in thin films reveals only small bathochromic shifts of the maxima. As an example the absorption and emission of **2,6-NLP** are depicted in Figure 3.6. The diminished 0 – 0 emission band of **2,6-NLP** in the film is caused by self absorption effects.

For a deeper insight into the geometrical structure of the ladder polymers geometry optimizations utilizing the B3LYP method with a 6 – 31G** basis set have been carried out. Figure 3.7a and b show the calculated structures of the repeating units of **2,6-NLP** and **1,5-NLP2** as front and edge – on views. For the **1,5-NLP2** unit (Figure 3.7b) the edge – on view documents a pronounced deviation from planarity. The octyloxy groups were shortened to methoxy units and the bridge was reduced to $–CH_2$ unit to decrease the calculation times. The geometry of the third derivative **1,5-NLP1** was also calculated (not depicted) and displays an intermediate picture with a slightly distorted geometry.

These results also confirm the decreasing photostability by going from **2,6-NLP** to **1,5-NLP1** to **1,5-NLP2**. Degradation tests of all ladder polymers were performed with sunlight under atmospheric conditions. While **2,6-NLP** showed no bleaching solutions of **1,5-NLP1** and **1,5-NLP2** were significantly bleached after a few hours. It has been previously reported that

structurally related hydrocarbons such as terylenes and perylenes that are substituted in the bay position with considerable deviations from planarity showed a reduced photostability.[32]

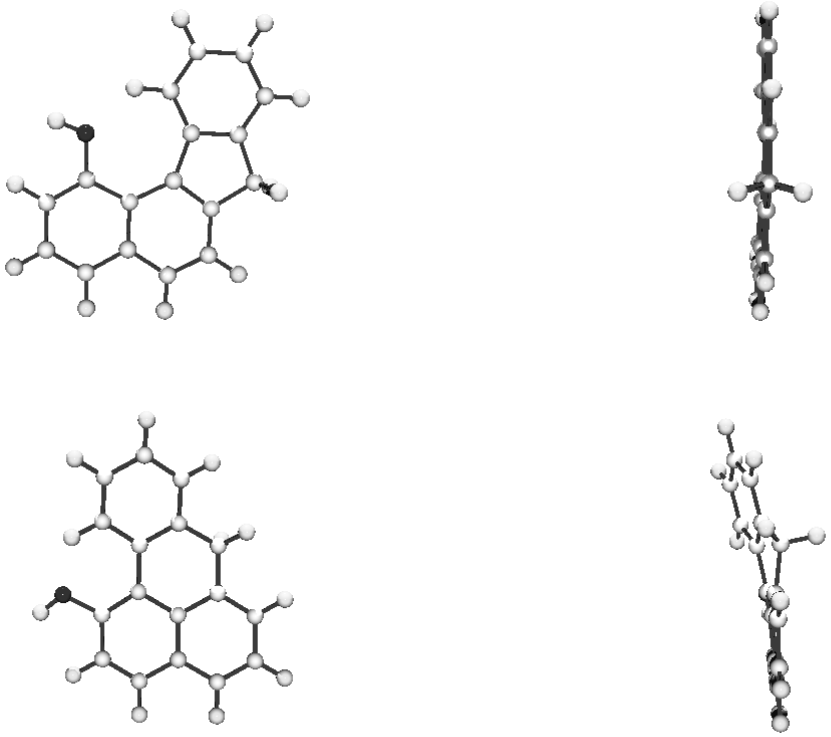

Figure 3.7: B3LYP/6-31G** calculations of the repeating units in **2,6-NLP** and **1,5-NLP2** (front and edge – on view).

Previous studies on naphthalene – based oligo – and polymers have suggested a sequential hypsochromic shift in absorption and emission on going from 1,4 – to 2,6 – and 1,5 – linked oligonaphthalenes. Furthermore, these variations in the optical properties have been attributed to backbone distortion and/or steric effects.[33-38] Nevertheless, it is very difficult to derive clear and reliable trends due to the interplay of geometry – and substitution – related effects. In contrast, the herein presented molecules are geometrically fixed. The optical properties are primarily governed by the linking postion and substitution pattern. A clear blue shift in the absorption maxima of 32 and 18 nm, respectively, is observed when going from **1,5-NLP1** to **1,5-NLP2** and **2,6-NLP**. This trend would imply that 1,5-linked naphthalene units are more favourable for main – chain π – conjugation compared to their 2,6 – linked pendants. As expected, within the same 1,5- linkage pattern motif, changing the position of the

electron – donating alkoxy substituents from *ortho* (**1,5-NLP2**) to *para* (**1,5-NLP1**) results in a bathochromic shift of 14 nm in absorption and 13 nm in emission.

3.3. Second Order Distributed Feedback Lasing in Naphthylene Based Ladder Polymers

Since the discovery of stimulated emission in organic solid state films, much effort has been made towards the realization of an organic solid state injection laser. One of the most promising candidates for such a device is **MeLPPP**.[13] This polymer offers a large material gain of around 2000 cm^{-1}, excellent film – forming properties and a high charge carrier mobility with low trap densities.[39-41] To examine the potential as lasing materials of the new naphthalene – based ladder polymers the most stable polymer (**2,6-NLP**) was investigated as the gain material in a second order distributed feedback laser by the group of Prof. W. Kowalsky (TU Braunschweig).[42]

3.3.1. Introduction

A prerequisite for lasing is the presence of stimulated emission, quantified by the wavelength - dependent cross section for stimulated emission $\sigma(\lambda)$. Fortunately, most conjugated polymers form a so called four – level system which is schematically depicted in Figure 3.8. When a material in its ground state (GS) is photopumped the effect of ground state absorption (GSA) occurs and a manifold of excited state vibrational levels become populated.

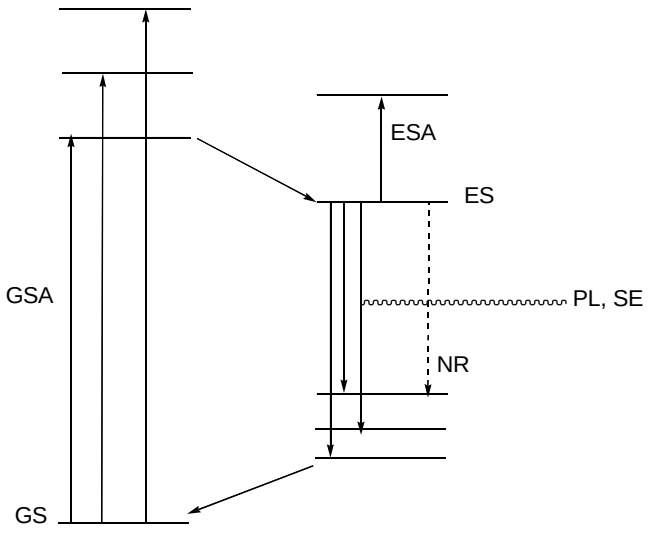

Figure 3.8: Schematic diagram of a four - level energy system.

Within a very short time period (femtoseconds) relaxation into the lowest vibronic state occurs which also explains the energy shift (Stokes – shift) of the excited state (ES). At low photon densities, photoluminescence (PL) or non - radiative recombinations (NR) are the dominant processes. If the photon density of pumping increases, population reversal is reached and stimulated emission (SE) can become the dominating deactivation process. Another way of loss besides PL and NR is the excited state absorption (ESA) which can be avoided by large Stokes – shifts. Once light has started travelling through the amplifying medium its intensity starts growing exponentially according to

$$I = I_0 \exp[(g - \alpha)l]$$

where I_0 is the initial intensity, g the (power) gain coefficient, α the loss coefficient and l the distance travelled in the gain medium. In general active laser materials have to fulfil the following criteria

1. high luminescence efficiency,
2. formation of aggregates has to be avoided,
3. no spectral overlap between stimulated emission and residual or excited state absorption, and
4. high mobility of electrons and holes (only for injection lasers)

Need 1 is fulfilled by most conjugated polymers, while point 2 can be reached by chemical design of side chains or the choice of suitable solvents for spin – casting the films.[43;44] However, point 3 is a more critical point. Problematic are the absorption from the excited state (ESA) and the triplett absorption. Auspiciously the triplett absorption of polymers is often located at much lower energies than the singlet emission.[45;46] On the other hand (ESA) can be a serious problem.

One very promising candidate for solid state lasing is **MeLPPP** (Scheme 3.1) which offers large material gain values.[39;41] To obtain solid state lasing a huge variety of resonator laser structures have been developed. Figure 3.9 features the most popular geometries that have been explored in the past years using optical excitation.

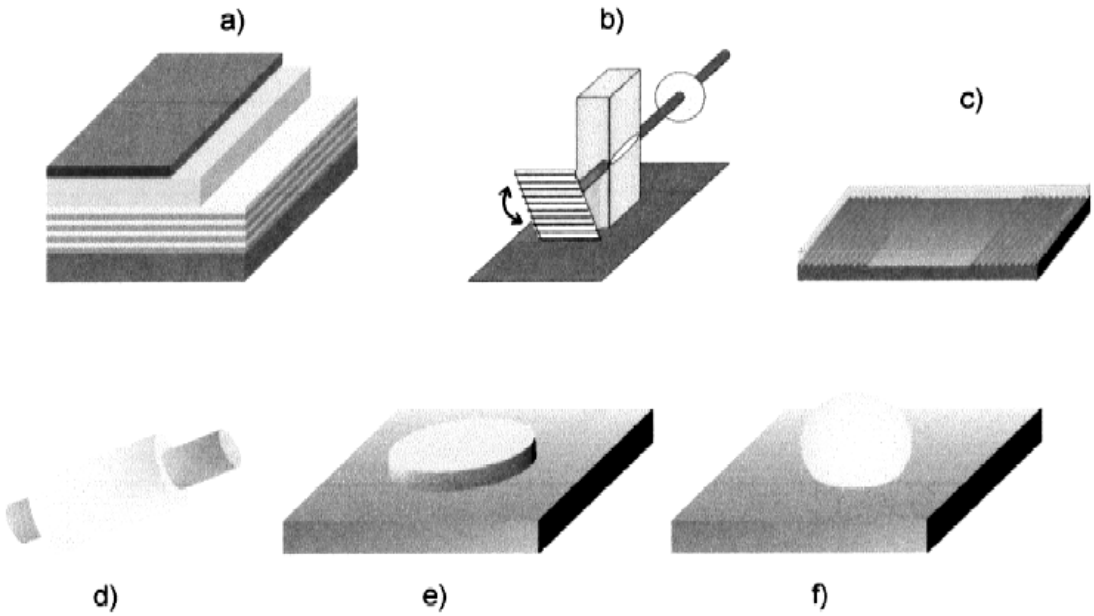

(a) microcavity, (b) tunable external cavity, (c) planar waveguide (distributed Bragg resonator), (d) microring, (e) microdisk, (f) microdroplet.

Figure 3.9: Scheme of various resonator structures for conjugated polymer lasers.[6]

The herein presented results are utilizing the concept of distributed feedback resonators (DFB) which was introduced in the early 1970s by Kogelnik et al.[47] Solid state lasing of **MeLPPP** has been shown in surface emitting second order (DFB) structures or in two dimensional DFB structures.[48-51] Regarding a future application in solid state injection lasers a low lasing threshold seems desirable. Therefore, the known **MeLPPP** and the novel **2,6-NLP** were examined in second order lasing geometries, and **MeLPPP** also in a first order geometry.

3.3.2. Results and Discussion

Of substantial importance is the quality of the used gratings, which have been fabricated by e-beam lithography and dry etching. For second order lasing substrates with grating periods varying from 290 to 340 nm (in 10 nm steps) were used. The depth of the grooves was 100 nm. The active layer was confined by the quartz substrate ($n_{SiO_2} \sim 1.46$) on the bottom and air ($n_{\mathrm{Air}} \sim 1$) on the top. For first order lasing grating periods of about 150 nm would be required,

utilizing the same procedure of manufacturing. Figure 3.10 shows a SEM image of a grating with a 150 nm period.

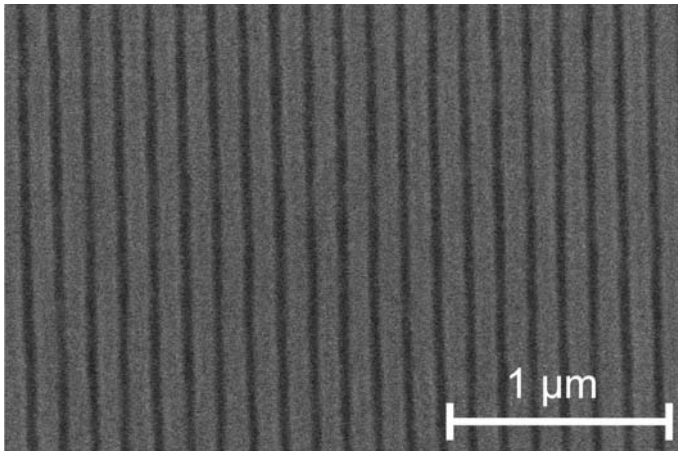

Figure 3.10: SEM image of a grating with a grating period of 150 nm.

All laser samples were optically excited using a pulsed nitrogen laser (30 Hz repetition rate, 500 fs pulses at λ = 337 nm) as the pump source. For second order lasing the pump beam was focused on the surface of the sample under an incident angle of about 30°.

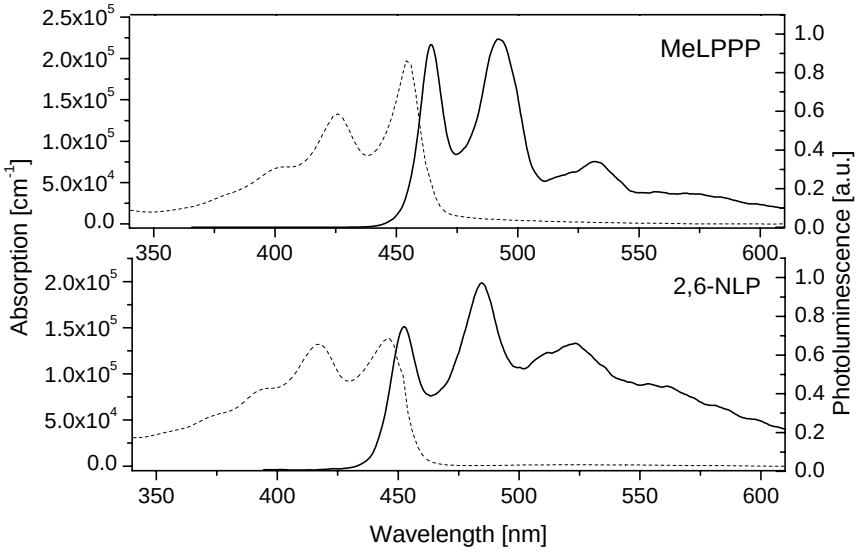

Figure 3.11: Absorption and photoluminescence of the investigated polymers as thin films.

Figure 3.11 shows the normalized UV/Vis and PL spectra of the two ladder polymers in thin films. Like already mentioned in the previous paragraphs, the emission of **2,6-NLP** is slightly

blue shifted compared to **MeLPPP**. The emission characteristics change dramatically when the pump intensity is increased. Gain narrowing occurs indicating amplified spontaneous emission. The half – width of the resulting ASE band was 2.3 nm in **MeLPPP** and 2.4 nm in **2,6-NLP**, respectively. Similar to the PL results the ASE peak maximum is slightly blue shifted for **2,6-NLP** by 5.3 nm when compared to **MeLPPP**.

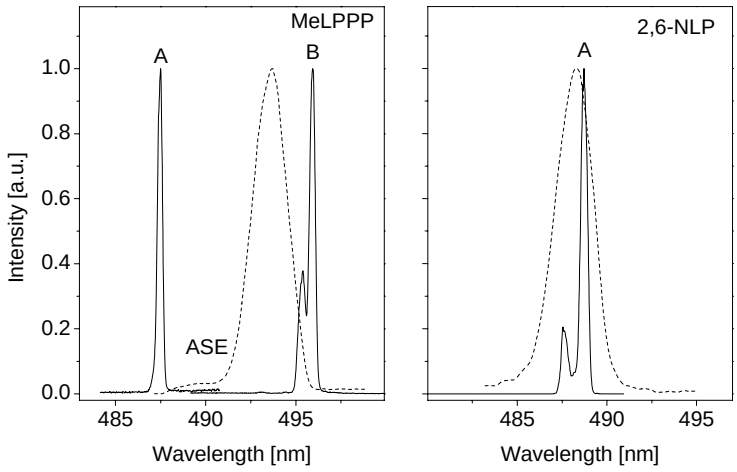

Figure 3.12: ASE (dashed line) and observed laser intensity spectra of **MeLPPP** and **2,6-NLP**.

Both ladder polymers show laser action on suitable DFB substrates. **MeLPPP** shows second order lasing with grating periods of 290 and 300 nm at wavelength of 487.5 and 495.9 nm, respectively. **2,6-NLP** only shows lasing peaking at 488.7 nm on a substrate with 290 nm as the grating period (Figure 3.12). Figure 3.13 compares the threshold energies for second order lasing. **MeLPPP** exhibits minimum threshold energy of 232 μJ/cm² at 495.9 nm. The lasing threshold of **2,6-NLP** is considerable higher with 477 μJ/cm² at 488.7 nm. Related to the significantly lower lasing threshold of **MeLPPP** only this polymer was used to design a first order DFB device. As expected the threshold could further be reduced to a energy density of 25.9 μJ/cm² which stands for a threshold reduction by a factor of nine compared to the second order device. Further details can be found in the literature.[42]

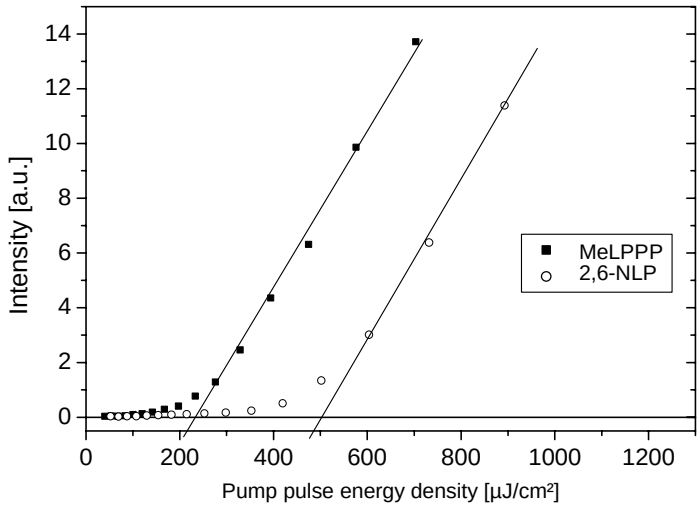

Figure 3.13: Laser output characteristics for second order DFB resonators for **MeLPPP** and **2,6-NLP**

3.4. Conclusion

New non-aqueous microwave – assisted Suzuki – type cross coupling protocols for the generation of polyketone precursors towards novel naphthalene – based ladder polymers have been developed. While **2,6-NLP** could be synthesized both via conventional and microwave - assisted heating, the sterically more hindered 1,5-linked polyketones **1,5-NPK1** and **1,5-NPK2** could only be attained by non-aqueous microwave – assisted heating protocols. **1,5-NLP2** is the first example of a polyarylene ladder polymer consisting exclusively six membered rings. The optical properties of all ladder polymers have been investigated. The results show an increased Stokes shift for the 1,5 – linked naphthalene based ladder polymers coupled with a decreased photostability. These results are in agreement with geometry optimization on a B3LYP/6-31G** level.

With regard of a possible utilization as active components in solid state polymer lasers the most stable polymer **2,6-NLP** has been used to fabricate a second order DFB laser device. A sharp laser emission at 488.7 nm could be observed for **2,6-NLP** with a lasing threshold energy of ca. 480 µJ/cm².

3.5. Experimental Section

3.5.1. General Methods

For a general section concerning spectroscopic techniques and chemicals the reader is referred to chapter 2 of this thesis.

Synthesis of compounds **1** and **2** has already been described in chapter 2.

3.5.2. Synthesis

1,5-Dioctyloxynaphthalene-2,6-bis(4,4,5,5-tetramethyl-1,3,2-dioxaborolane) (3).

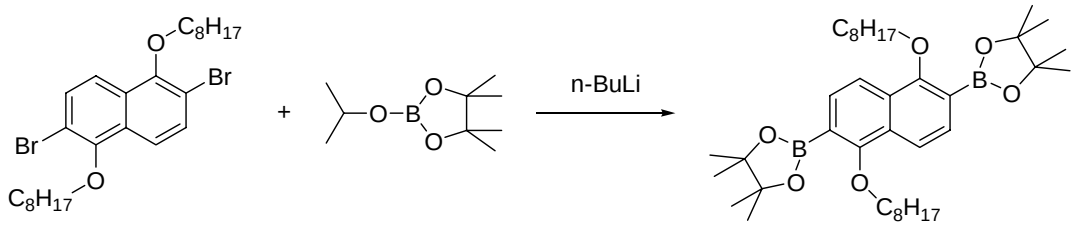

n-Buli (4.8 mL of 2.5M solution, 12 mmol) was added dropwise to a solution of **2** (3.0 g, 5.4 mmol) in THF (80 mL) at – 78 ^{o}C. The solution was stirred at – 78 ^{o}C for 30 minutes and then at – 10 ^{o}C for 10 minutes. The temperature was again lowered to – 78 ^{o}C and 2-isopropoxy-4,4,5,5-tetramethyl-1,3,2-dioxaborolane (4.0 mL, 19.6 mmol) was added all at once. The solution was allowed to return to room temperature slowly and then stirred overnight before being poured into water. The aqueous phase was then extracted with dichloromethane, which was subsequently washed with water and brine, dried over $MgSO_4$ and the solvent was removed by rotary evaporation. The residue was purified by column chromatography on silica gel with ethyl acetate/hexanes (1:9) as eluent to give **3** as a yellow solid (52 %). ^{1}H NMR (400 MHz, $C_2D_2Cl_4$, 25 °C): δ = 7.82 (d, J = 8.4 Hz, 2H), 7.64 (d, J = 8.4 Hz, 2H), 3.98 (t, J = 6.8 Hz, 4H), 1.84 (m, 4H), 1.44 (m, 4H), 1.32 (s, 24H), 1.24 (m, 16H), 0.83 (m, 6H) ppm. ^{13}C NMR (100 MHz, $C_2D_2Cl_4$, 25 °C): δ = 162.5, 131.6, 131.7, 118.4, 117.8, 84.1, 77.3, 32.1, 31.8, 30.7, 29.9, 29.6, 25.2, 23.0, 14.5 ppm. MS (EI, 70eV): m/z = 44 (47.7), 55 (49.0), 83 (100.0), 635 (43.9), 636 [M^+] (97.9), 637 (39.6). Anal. Calc. for $C_{38}H_{62}B_2O_6$: C, 71.70; H, 9.82. Found: C, 70.88; H, 9.85.

1,5-Dibromo-2,6-dihydroxynaphthalene (4)

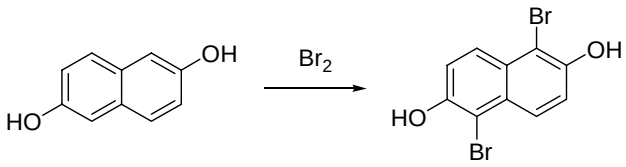

A solution of 2,6-dihydroxynaphthalene (10 g, 0.06 mol) in glacial acetic acid (100 mL) with a few crystals of iodine was heated to 80°C. Bromine (6.9 mL, 0.13 mol) in glacial acetic acid (30 mL) was added slowly over a period of 1 hour. The mixture was stirred for a further hour and then cooled to 0°C. Yellow crystals occur which were filtered of, washed with hexane and dried under vacuum. Yield: 82 %. ^{1}H NMR (400 MHz, d_6-DMSO, 25 °C): δ = 7.20 (d, J = 9.2 Hz, 2H), 7.31 (d, J = 9.2 Hz, 2H), 10.3 (bs, 2H) ppm. ^{13}C NMR (100 MHz, d_6-DMSO, 25 °C): δ = 150.5, 127.8, 125.9, 119.6, 104.9 ppm. MS (EI, 70eV): m/z = 75 (29.2), 101 (53.2), 208 (33.7), 210 (31.8), 316 (57.1), 318 [M^+] (100.0), 320 (55.5).

1,5-Dibromo-2,6-dioctyloxynaphthalene (5).

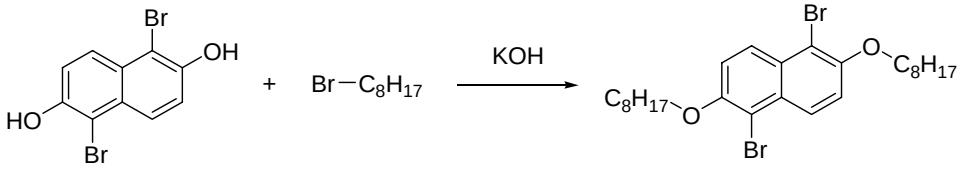

A solution of 1,5-dibromo-2,6-dihydroxynaphthalene (**4**) (10.0g, 31.5 mmol) and KOH (5.3g, 94.5 mmol) in anhydrous ethanol (200 mL) was degassed with argon and heated to reflux. Octylbromide (16.5 mL, 95.2 mmol) was added slowly and the solution was refluxed for 12 hours. The reaction mixture was cooled down and the precipitate filtered off. The solid was then stirred in water (200 mL) for 1 hour, filtered and dried under vacuum. Yield: 83 %. ^{1}H NMR (400 MHz, $CDCl_3$, 25 °C): δ = 8.19 (d, J = 9.3 Hz, 2H), 7.29 (d, J = 9.3 Hz, 2H), 4.15 (t, J = 6.6 Hz, 4H), 1.87 (m, 4H), 1.54 (m, 4H), 1.33 (m, 16H), 0.90 (m, 6H) ppm. ^{13}C NMR (100 MHz, $CDCl_3$, 25 °C): δ = 152.4, 129.3, 127.2, 116.8, 109.5, 70.4, 31.8, 29.4, 29.3, 29.2, 26.0, 22.6, 14.1 ppm. MS (EI, 70eV): m/z = 316 (59.0), 318 (100.0), 320 (58.1), 540 (12.4), 542 [M^+] (22.3), 544 (12.8).

2,6-Dioctyloxynaphthalene-1,5-bis-(4,4,5,5-tetramethyl-1,3,2-dioxaborolane) (6).

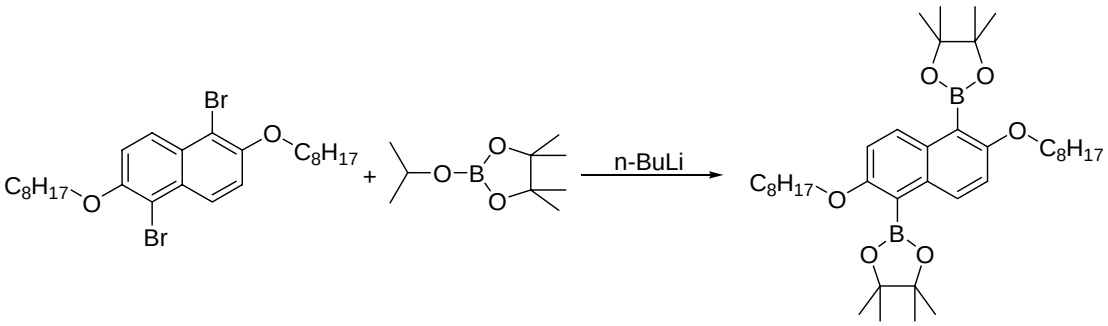

The compound was prepared by the same method used for **3**, employing a solution of **5** (3.0 g, 5.4 mmol). White crystals were obtained in 67 % yield after column chromatography on silica gel with ethylacetate/hexane (1:9) as the eluent. ^{1}H NMR (400 MHz, $C_2D_2Cl_4$, 25 °C): δ = 7.83 (d, J = 9.1 Hz, 2H), 7.13 (d, J = 9.1 Hz, 2H), 4.0 (t, 4H), 1.71 (m, 4H), 1.41 (s, 28H), 1.28 (16H), 0.91 (t, 6H) ppm. ^{13}C NMR (100 MHz, $C_2D_2Cl_4$, 25 °C): δ = 159.5, 132.6, 130.5, 115.3, 114.8, 84.1, 70.0, 32.1, 30.0, 29.8, 29.6, 26.5, 25.3, 23.0, 14.5 ppm. MS (EI, 70eV): m/z = 44 (54.1), 55 (55.9), 57 (59.0), 83 (100.0), 635 (66.3), 636 [M^+] (100.0), 637 (63.3). Anal. Calc. for $C_{38}H_{62}B_2O_6$: C, 71.70; H, 9.82. Found: C, 69.61; H, 9.76.

1,5-Dipropyloxynaphthalene (7).

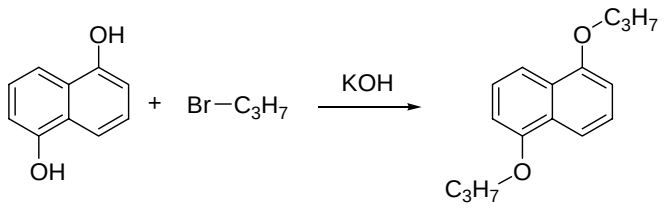

A solution of 1,5-dihydroxynaphthalene (10.0 g, 62.4 mmol) and KOH (10.5 g, 187 mmol) in anhydrous ethanol (200 mL) was degassed with argon and heated to reflux. Propylbromide (17 mL, 187 mmol) was added slowly and the solution was refluxed for 12 hours. The reaction mixture was cooled down and the precipitate filtered off. The solid was then stirred in water (200 mL) for 1 hour, filtered and dried under vacuum. Yield: 88 %. ^{1}H NMR (400 MHz, $CDCl_3$, 25 °C): δ = 7.20 (d, J = 8.3 Hz, 2H), 6.73 (dd, 2H), 6.23 (d, J = 7.7 Hz, 2H), 3.48 (t, 4H), 1.33 (m, 4H), 0.53 (t, 6H) ppm. ^{13}C NMR (100 MHz, $CDCl_3$, 25 °C): δ = 153.0, 125.2, 123.8, 112.5, 104.0, 68.1, 21.1, 9.4 ppm. MS (EI, 70eV): m/z = 160 (100.0), 244 [M^+] (43.7).

1,5-Dipropyloxy-4,8-dibromonaphthalene (8).

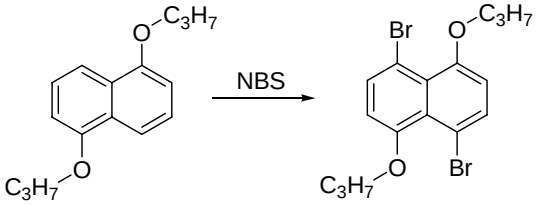

To a suspension of **7** (3.0 g, 12.3 mmol) in acetonitrile (40 mL) cooled in an ice bath a solution of *N*-bromsuccinimide (4.8 g, 27 mmol) in acetonitrile was added dropwise. The ice bath was removed and the resulting solution stirred at room temperature overnight. The solid was collected by filtration, washed with acetonitrile (50 mL) and then with methanol (100 mL) to give **8** in 63% yield. ^{1}H NMR (400 MHz, $CDCl_3$, 25 °C): δ = 7.68 (d, J = 8.6 Hz, 2H), 6.68 (d, J = 7.7 Hz, 2H), 4.0 (t, 4H), 1.98 (m, 4H), 1.15 (t, 6H) ppm. ^{13}C NMR (100 MHz, $CDCl_3$, 25 °C): δ = 154.6, 133.6, 126.2, 108.5, 106.9, 71.4, 22.4, 11.0 ppm. MS (EI, 70eV): m/z = 44 (63.4), 238 (53.8), 316 (52.6), 318 (100.0), 320 (48.7), 400 (38.2), 402 [M^+](79.9), 404 (37.1).

1,5-Dipropyloxynaphthalene-4,8-bis(4,4,5,5-tetramethyl-1,3,2-dioxaborolane) (9).

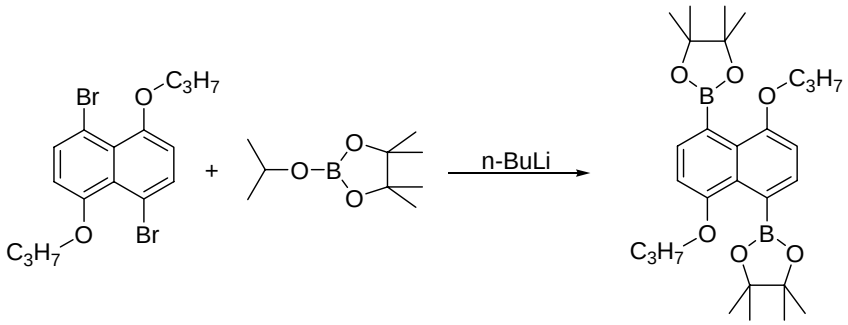

The compound was prepared by the same method used for **3**, employing a solution of **8** (3.0 g, 7.5 mmol). A yellow powder was obtained in 59 % yield after column chromatography on silica gel with ethylacetate/hexane (1:9) as the eluent. ^{1}H NMR (400 MHz, $C_2D_2Cl_4$, 25 °C): δ = 7.33 (d, J = 7.6 Hz, 2H), 6.68 (d, J = 7.6 Hz, 2H), 4.22 (t, 4H), 1.78 (m, 4H), 1.35 (s, 24H), 0.91 (t, 6H) ppm. ^{13}C NMR (100 MHz, $C_2D_2Cl_4$, 25 °C): δ = 155.2, 130.7, 129.4, 118.7, 106.0, 83.4, 25.4, 70.1, 21.7, 10.7 ppm. MS (EI, 70eV): m/z = 44 (44.8), 55 (40.9), 83 (100.0), 495 (25.4), 496 [M^+] (60.0), 497 (16.0). Anal. Calc. for $C_{28}H_{42}B_2O_6$: C, 67.77; H, 8.53. Found: C, 67.75; H, 8.37.

2,5-Dibromoterephthalic acid (10)

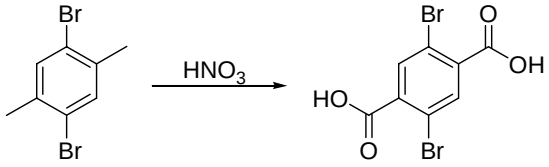

2,5-dibromo-1,4-dimethylbenzene (100 g, 0.38 mol) was stirred in 300 mL of HNO_3 (~ 40%) and refluxed for 5 days. The reaction was cooled to room temperature and neutralized with aqueous KOH solution. $KMnO_4$ (150 g, 0.95 mmol) was added and the mixture refluxed for further 24 h. Then again $KMnO_4$ (50 g, 0.32 mmol) was added and the reaction refluxed for additional 24 h. The reaction mixture was cooled down to room temperature and acidified with sulphuric acid (pH = 1). After addition of Na_2SO_3 the solution cleared and the colorless precipitate could be separated, washed and dried. Yield: (74 %)

^{1}H NMR (400 MHz, d_6-DMSO, 80 °C): δ = 15.3-12.7 (bs, 2H), 7.98 (s, 2H) ppm. ^{13}C NMR (50 MHz, d_6-DMSO, 80 °C): δ = 165.8, 137.3, 135.2, 119.0 ppm. MS (EI, 70eV): m/z = 307 (43.4), 322 (50.8), 324 [M^+] (100.0), 326 (47.5).

4',4''-didecyl-2,5-dibromoterephthalophenone (11)

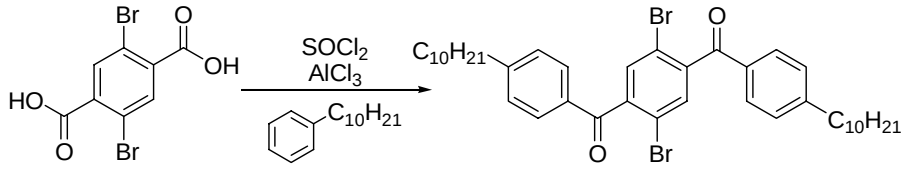

2,5-dibromoterephthalic acid (20 g, 0.046 mol) was refluxed in thionyl chloride (30 g, 0.25 mol) for 8 h. The excess of thionyl chloride was distilled off and the residue recrystallized from heptane, filtered and dried. The dichloride was used for the next step without any further purification. To a solution of 2,5-dibromoterephthaloyl dichloride (3.6g, 10 mmol) in dichlormethane (100 mL) aluminiumtrichloride (3.4 g, 26 mmol) was added at 0°C. After 15 min., a solution of n - decylbenzene (9 g, 41 mmol) in dichloromethane (25 mL) was added and stirred for 24 h at room temperature. The reaction was quenched with aqueous HCl and extracted into dichlormethane. The organic phase was washed with water, brine, dried over Na_2SO_4, and the solvent evaporated till dryness. The crude product was recrystallized from acetone. Yield: 75 %. ^{1}H NMR (400 MHz, $C_2D_2Cl_4$, 25 °C): δ = 7.67 (d, 2H, J = 8.2Hz), 7.52 (s, 2H), 7.25 (d, 2H, J = 8.2Hz), 2.62 (t, 4H, J = 8.86), 1.56 (m, 32H), 0.80 (t, 6H, J = 6.8Hz) ppm. ^{13}C NMR (100 MHz, $C_2D_2Cl_4$, 25 °C): δ = 193.62 (C=O), 151.01, 143.53, 133.27, 133.06, 130.74, 129.32, 118.75, 36.47, 32.19, 32.15, 31.24, 29.90,

29.84, 29.74, 29.61, 23.01, 14.52 ppm. MS (EI, 70eV): m/z = 245 (100.0), 507 (21.5), 724 [M^+] (53.2), 725 (20.5).

Synthesis of (2,6-NPK) (12).

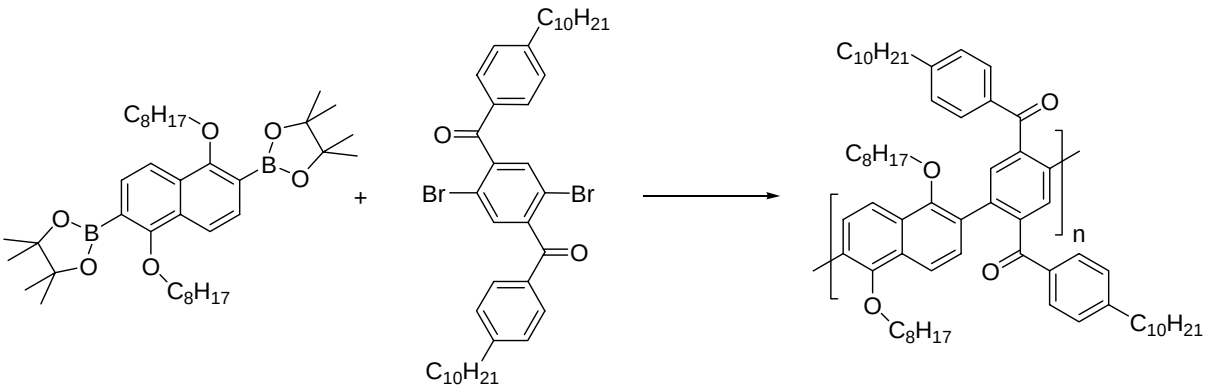

Conventional synthesis (12A):

A 100 mL flask was charged with 4',4''-didecyl-2,5-dibromoterephthalophenone (**11**) (0.3 g, 0.47 mmol), **3** (0.34 g, 0.47 mmol), $PdCl_2(PPh_3)_2$ (0.015 mg, 0.021 mmol) and dissolved in degassed THF (20 mL). K_2CO_3 (0.6g, 4.34 mmol in 5 mL degassed water) was added and the reaction mixture was refluxed for three days. The polymer was extracted into chloroform and the organic phase was washed with water, dried over $MgSO_4$ and the solvent was removed by rotary evaporation. The residue was redisolved in chloroform and precipitated into methanol to give **2,6-NPK** in 80% yield with molecular weight data M_n = 11,300, PD = 1.7. After extracting the crude solid with ethanol and reprecipitation, the polyketone was obtained in 72% yield. M_n = 13,700, PD = 1.3. ^{1}H NMR (400 MHz, $C_2D_2Cl_4$, 80 °C): δ = 7.75 (2H), 7.69 (6H), 7.25 (2H), 7.11 (4H), 3.76 (4H), 2.55 (4H), 1.57 (8H), 1.24 (48H), 0.85 (12H) ppm. ^{13}C NMR (100 MHz, $C_2D_2Cl_4$, 80 °C): δ = 195.9 (CO), 153.0, 148.9, 140.7, 137.3, 135.3, 132.5, 130.4, 129.9, 128.8, 128.7, 128.4, 118.4, 74.7, 36.2, 32.1, 31.9, 31.0, 30.6, 30.5, 29.8, 29.7, 29.6, 29.4, 29.2, 26.3, 26.1, 22.8, 22.7, 14.2 ppm. IR($CHCl_3$): ν = 2926, 2855, 1661 (C=O), 1605, 1215, 755, 668 cm^{-1}.

Microwave assisted synthesis via an aqueous method (12B):

A stock solution of an equimolar quantity of the monomers **3** and **11** in degassed THF was prepared and added to a 10 mL vial in a glove-box and sealed under argon. To this the monomer stock solution was added followed by a 10 – molar excess of a degassed 4M K_2CO_3 solution. The mixture was then irradiated with microwaves (150 W) for 12 min. The workup

followed the procedure of the conventional synthesis to afford the polymer in 60 % yield and molecular weights of M_n = 14,200, PD = 1.8.

Microwave assisted synthesis via a non-aqueous method (12C):

Equimolar quantities of the monomers **3** and **11**, $PdCl_2(PPh_3)_2$ (10 %) and powdered KOH (12 mol equivalents) were added to a 10 mL vial and sealed under argon. THF was then added and the solution irradiated with microwaves (115°C) for 12 min. The workup followed the procedure of the conventional synthesis to afford the polymer in 72 % yield and molecular weights of M_n = 29,900, PD = 2.3.

Synthesis of (2,6-NLP) (13).

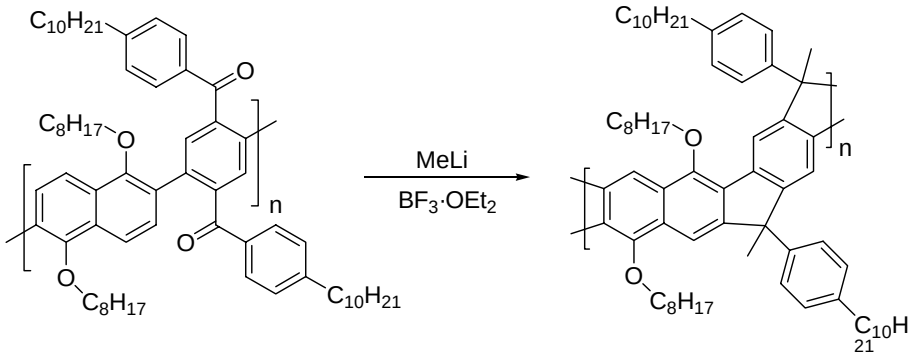

An excess of MeLi (1.6 M solution) was added to a solution of **2,6-NPK (12A)** in toluene (40 mL) and stirred for 10 min. THF (20 mL) was added and the mixture was stirred for 16 h at room temperature. Chloroform was added and the solution washed with 2M HCl. The organic phase was dried with Na_2SO_4 and the solvent was removed under reduced pressure. The polyalcohol was dissolved in dichloromethane (30 mL) and treated with an excess of borontrifluoride etherate. The solution was stirred for 2 h and then an EtOH/water mixture (70 mL 2:5) was added and the organic layer was extracted several times with water. The organic phase was dried with Na_2SO_4 and the solvent was removed by rotary evaporation. The residue was dissolved in chloroform and precipitated into methanol to give **2,6-NLP** in 70% yield with M_n = 18,400, PD = 1.5. ^{1}H NMR (400 MHz, $C_2D_2Cl_4$, 80 °C): δ =8.00 (2H), 7.76 (2H), 7.21 (4H), 7.01 (4H), 3.76 (4H), 2.55 (4H), 1.8-2.1 (7H), 1.2-1.6 (52H), 0.8-1.0 (12H) ppm. ^{13}C NMR (100 MHz, $C_2D_2Cl_4$, 80 °C): δ = 154.0, 153.4, 150.3, 143.7, 141.0, 138.0, 130.0, 129.4, 128.4, 126.6, 119.8, 113.4, 74.3, 54.5, 35.7, 32.1, 31.4, 30.7, 29.9, 29.8, 29.7, 29.6, 29.5, 29.4, 27.5, 26.6, 26.5, 22.9, 22.8, 14.3, 14.2 ppm.

Synthesis of 1,5-NPK1 via non-aqueous microwave procedure (14).

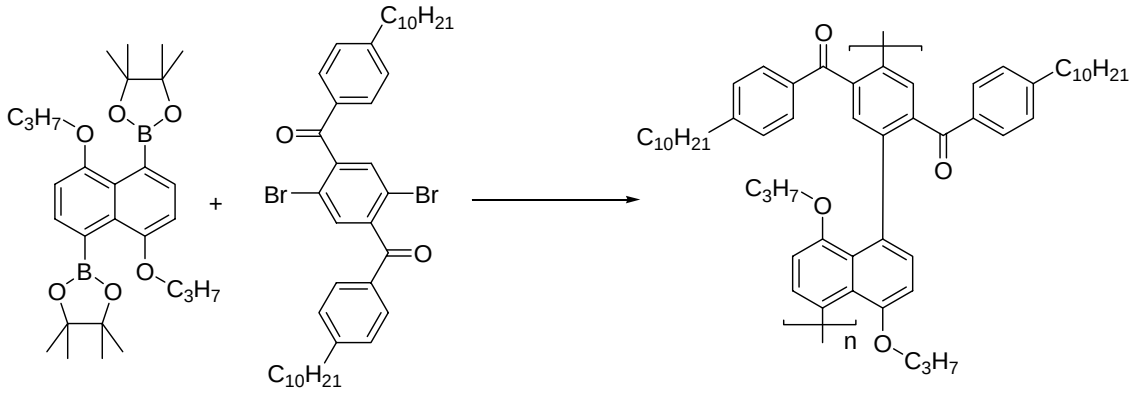

Equimolar quantities of the monomers **9** and **11**, $PdCl_2(PPh_3)_2$ (10 %) and powdered KOH (12 mol equivalents) were added to a 10 mL vial and sealed under argon. THF was then added and the solution irradiated with microwaves (115°C) for 12 min. The workup followed the procedure of the conventional synthesis of (**12A**) to afford the polymer in 89 % yield with molecular weights of M_n = 13,600, PD = 2.4. ^{1}H NMR (400 MHz, $C_2D_2Cl_4$, 80 °C): δ = 7.7-6.7 (14H), 3.8 (4H), 2.5 (4H), 1.3 (36H), 0.9 (12H). ^{13}C NMR (100 MHz, $C_2D_2Cl_4$, 80 °C): δ = 200.5 (CO), 158.4, 150.3, 145.4, 142.4, 138.9, 132.5, 132.1, 131.4, 130.8, 130.4, 128.8, 109.1, 70.5, 36.2, 36.0, 32.0, 31.0, 29.7, 29.5, 29.4, 25.4, 22.8, 22.5, 14.2, 11.0. IR($CHCl_3$): ν = 2920, 2850, 1649 (C=O), 1604, 1584, 1518, 1223, 1063, 941, 814 cm^{-1}.

Synthesis of 1,5-NLP1.

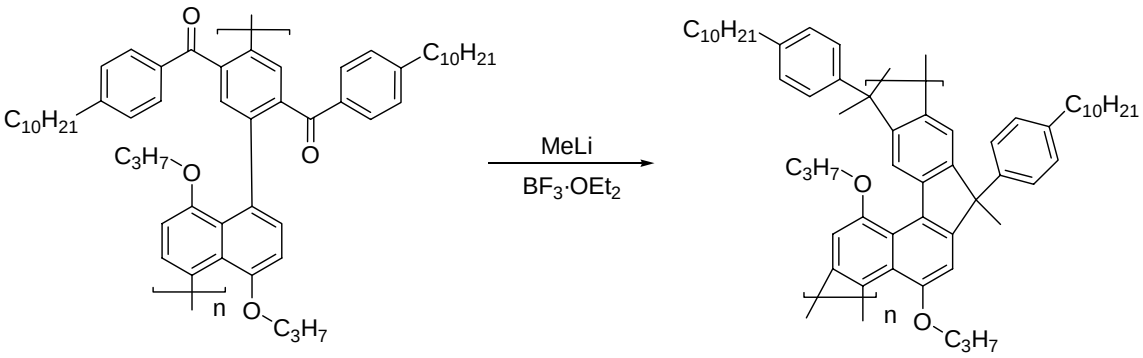

The preparation followed the procedure described for the cyclisation of **2,6-NPK**. After the work-up the residue was dissolved in chloroform and precipitated into methanol to give **1,5-NLP1** in 70% yield with M_n = 12,900, PD = 2.0. After extracting the crude solid with ethanol for two days and reprecipitation the ladder polymer was obtained in 38% yield. M_n = 21,400, PD = 1.5. ^{1}H NMR (400 MHz, CD_2Cl_4, 80 °C): δ =8.00 (2H), 7.18 (4H), 7.00 (4H), 6.72 (2H), 3.87 (4H), 2.51 (6H), 1.90 (4H), 1.55 (4H), 1.25 (32H), 0.86 (6H), 0.57 (6H) ppm. ^{13}C

NMR (100 MHz, CD_2Cl_4, 80 °C): δ = 156.1, 154.5, 153.2, 142.9, 140.5, 128.3, 126.9, 124.3, 121.8, 105.3, 71.4, 54.3, 35.7, 32.1, 31.4, 31.3, 29.9, 29.8, 29.7, 29.5, 25.5, 22.8, 21.7, 14.2, 10.5 ppm.

Synthesis of 1,5-NPK2 via non-aqueous microwave procedure.

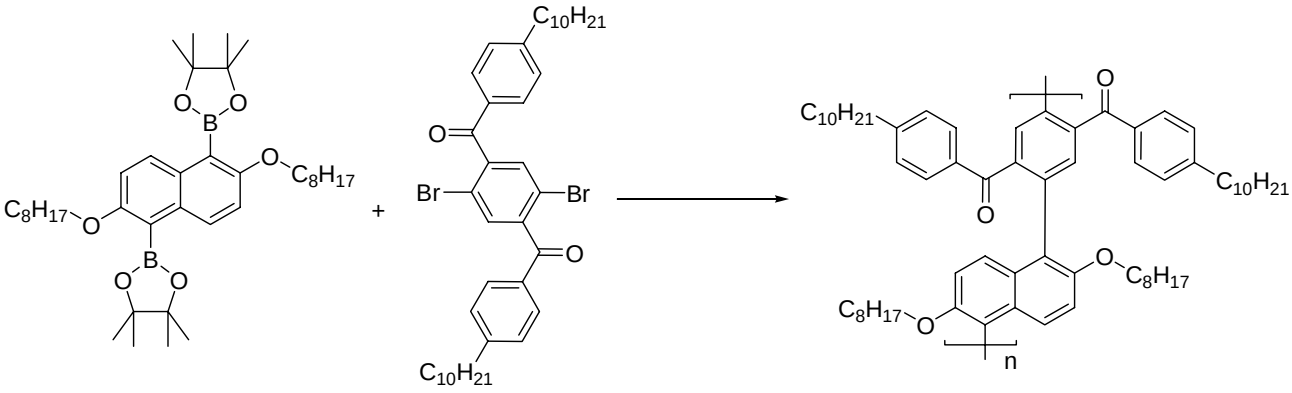

The preparation followed the procedure described for the non-aqueous synthesis of **1,5-NPK1**. After the work-up the residue was dissolve in chloroform and precipitated into methanol which gave polyketone in 78% yield with M_n = 9,000, PD = 1.9. After extracting the crude solid with ethanol for one day and reprecipitation the polyketone was obtained in 61% yield. M_n = 13,000, PD = 1.6. ^{1}H NMR (400 MHz, $C_2D_2Cl_4$, 80 °C): δ = 7.7-6.7 (14H), 3.9 (4H), 2.5 (4H), 0.4-1.8 (68H) ppm. ^{13}C NMR (100 MHz, $C_2D_2Cl_4$, 80 °C): 151.5, 151.1, 148.5, 141.9, 135.4, 133.4, 130.1, 129.2, 128.0, 126.7, 122.7, 114.9, 69.7, 36.3, 32.3, 32.2, 31.4, 30.0, 29.9, 29.8, 29.7, 26.2, 26.1, 23.0, 14.5 ppm. IR($CHCl_3$): ν = 2952, 2920, 2851, 1662 (C=O), 1604, 1508, 1464, 1433, 1242, 1178, 1079, 928, 806 cm^{-1}.

Synthesis of 1,5-NLP2.

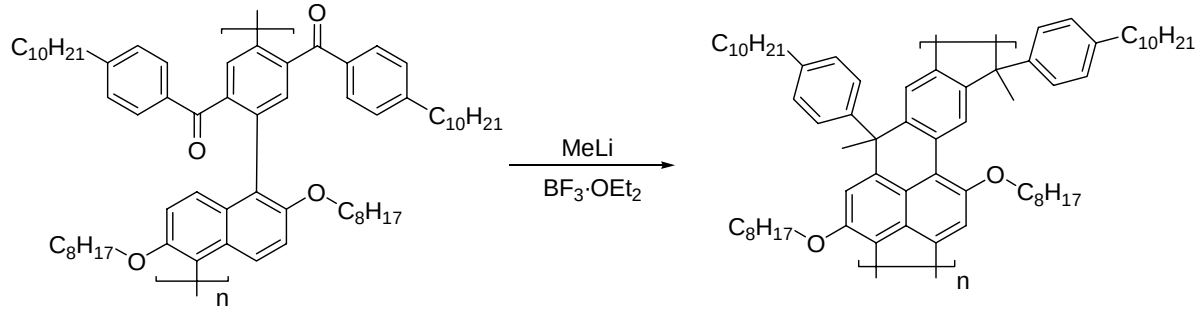

The preparation followed the procedure described for the cyclisation of **2,6-NPK**. After the usual work-up the residue was taken up in chloroform and precipitated into methanol to give **1,5-NLP1** in 71% yield with M_n = 13,700, PD = 1.6. ^{1}H NMR (400 MHz, $C_2D_2Cl_4$, 80 °C): δ

=8.5 (2H), 6.5-7.7 (10H), 3.7 (4H), 2.5 (4H), 0.4-2.0 (74H) ppm. ^{13}C NMR (100 MHz, $C_2D_2Cl_4$, 80 °C): δ = 153.2, 148.5, 142.0, 140.3, 134.9, 129.2, 129.1, 128.9, 127.9, 125.1, 118.6, 70.4, 49.4, 35.8, 34.5, 32.1, 31.5, 31.4, 29.8, 29.6, 29.5, 29.4, 29.3, 28.7, 26.2, 26.1, 22.8, 14.2 ppm.

3.5.3. Geometry Optimization

Geometry optimizaions were carried out by Dr. Peter Friedel from the Institut für Polymerforschung in Dresden. The geometries were roughly determined utilizing the AM1 method. The obtained geometries were used in a second set of minimizations to determine the equilibrium structure utilizing B3LYP with a 6-31G** basis set.

References and Notes

[1] U. Scherf, *J.Mater.Chem.* **1999,** *9*, 1853.

[2] U. Scherf, K. Müllen, *Macromol.Rapid Commun.* **1991,** *12*, 489.

[3] U. Scherf, K. Müllen, *Adv.Polym.Sci.* **1995,** *129*, 1.

[4] U. Scherf, in *Handbook of Conducting Polymers*Eds.: T. Skotheim, R. L. Elsenbaumer, J. R. Reynolds), Marcel Dekker, New York, Basel, Hong Kong **1998**, p. p. 363.

[5] A. Kraft, A. C. Grimsdale, A. B. Holmes, *Angew.Chem.Int.Ed.* **1998,** *37*, 402.

[6] U. Scherf, S. Riechel, U. Lemmer, R. F. Mahrt, *Current Opinion in Solid State & Materials Science* **2001,** *5*, 143.

[7] W. Graupner, G. Leising, M. Lanzani, M. Nisoli, S. D. Silvestri, U. Scherf, *Phys.Rev.Lett.* **2004,** *76*, 847.

[8] M. D. McGehee, A. J. Heeger, *Adv.Mater.* **2000,** *12*, 1655.

[9] M. G. Harrison, G. Urbasch, R. F. Mahrt, H. Giessen, H. Bässler, U. Scherf, *Chem.Phys.Lett.* **1999,** *313*, 755.

[10] A. Hohenau, C. Cagran, G. Kranzelbinder, U. Scherf, G. Leising, *Adv.Mater.* **2001,** *13*, 1303.

[11] C. Bauer, H. Giessen, B. Schnabel, E. B. Kley, U. Scherf, R. F. Mahrt, *Adv.Mater.* **2002,** *14*, 673.

[12] U. Lemmer, S. Heun, R. F. Mahrt, U. Scherf, M. Hopmerier, U. Siegner, E. O. Göbel, K. Müllen, H. Bässler, *Chem.Phys.Lett.* **1995,** *240*, 373.

[13] U. Scherf, A. Bohnen, K. Müllen, *Makromol.Chem.* **1992,** *193*, 1127.

[14] L. Romaner, G. Heimel, H. Wiesenhofer, P. Scandiucci de Freitas, U. Scherf, J. L. Bredas, E. Zojer, E. J. W. List, *Chem.Mater.* **2004,** *16*, 4667.

[15] S. Zheng, J. Shi, *Polymer Preprints* **2002,** *43*, 599.

[16] Zheng, S. and Shi, J. US 6,613,457 B2. 2002. US-Patent.

[17] S. Qui, P. Lu, F. Shen, L. Liu, Y. Ma, J. Shen, *Macromolecules* **2003,** *36*, 9823.

[18] A. S. Wheeler, D. R. Ergle, *J.Amer.Chem.Soc.* **1930,** *52*, 4872.

[19] Y. Pan, Z. Peng, *Tetrahedron Lett.* **2000,** *41*, 4537.

[20] B. S. Nehls, U. Asawapirom, S. Füldner, E. Preis, T. Farrell, U. Scherf, *Adv.Funct.Mater.* **2004,** *14*, 352.

[21] A. N. Cammidge, K. V. L. Crepy, *J.Org.Chem.* **2003,** *68*, 6832.

[22] A. N. Cammidge, K. V. L. Crepy, *Chem.Comm.* **2000,** 1723.

[23] T. Watanabe, N. Miyaura, A. Suzuki, *Synlett* **1992,** 207.

[24] J. W. Canary, *J.Amer.Chem.Soc.* **1994,** *116*, 6985.

[25] G. B. Smith, *J.Org.Chem.* **1994,** *59*, 8151.

[26] M. Moreno-Manas, *J.Org.Chem.* **1996,** *61*, 2346.

[27] C. Gabriel, S. Gabriel, B. S. J. Halstead, D. M. P. Mingos, *Chem.Soc.Rev.* **1998,** *27*, 213.

[28] S. Garbacia, B. Desai, O. Lavastre, C. O. Kappe, *J.Org.Chem.* **2003,** *68*, 9136.

[29] N. E. Leadbeater, H. M. Torenius, *J.Org.Chem.* **2004,** *67*, 6314.

[30] S. Ley, A. G. Leach, R. I. Storer, *J.Chem.Soc.Perkin Trans.I* **2001,** 358.

[31] W. Graupner, S. Eder, S. Tasch, G. Leising, G. Lanzani, M. Nisoli, S. de Silvestri, U. Scherf, K. Müllen, *J.Fluorescence* **1995,** *7*, 195.

[32] U. Anton, C. Gölter, K. Müllen, *Chem.Ber.* **1992,** *125*, 2325.

[33] B. Sankaran, M. D. Alexander, L. T. Tan, *Synthetic Metals* **2001,** *123*, 425.

[34] C. Z. Zhou, W. L. Wang, K. K. Lin, Z. K. Chen, Y. H. Lai, *Polymer* **2004,** *45*, 2271.

[35] B. Behnisch, P. Martinez-Ruis, K. H. Schweikart, M. Hanack, *Eur.J.Org.Chem.* **2000,** 2541.

[36] P. Martinez-Ruis, B. Behnisch, K. H. Schweikart, M. Hanack, L. Lüer, D. Oelkrug, *Chem.Eur.J.* **2000,** *6*, 1294.

[37] S. Tasch, W. Graupner, G. Leising, L. Pu, M. W. Wagner, R. H. Grubbs, *Adv.Mater.* **1995,** *7*, 903.

[38] J. L. Segura, N. Martin, M. Hanack, *Eur.J.Org.Chem.* **1999,** 643.

[39] D. Hertel, U. Scherf, H. Bässler, *Adv.Mater.* **1998,** *10*, 1119.

[40] E. J. W. List, C. H. Kim, J. Shinar, A. Pogantsch, G. Leising, W. Graupner, *Appl.Phys.Lett.* **2000,** *76*, 2083.

[41] G. Wegmann, B. Schweitzer, D. Hertel, H. Giessen, M. Oestreich, U. Scherf, K. Müllen, R. F. Mahrt, *Chem.Phys.Lett.* **1999,** *312*, 376.

[42] D. Schneider, T. Rabe, T. Riedl, W. Kowalsky, T. Farrell, S. Füldner, B. S. Nehls, U. Scherf, T. Weimann, J. Wang, P. Hinze, *Optical Lett.* **2005,** submitted.

[43] T. Nguyen, I. B. Martini, J. Liu, B. J. Schwartz, *J.Phys.Chem.B* **2000,** *104*, 237.

[44] T. Nguyen, V. Doan, B. J. Schwartz, *J.Chem.Phys.* **1999,** *110*, 4068.

[45] L. Smilowitz, A. J. Heeger, *Synthetic Metals* **1992,** *48*, 193.

[46] B. Kraabel, D. Moses, A. J. Heeger, *J.Chem.Phys.* **1995,** *103*, 5102.

[47] H. Kogelnik, C. V. Shank, *Appl.Phys.Lett.* **1971,** 152.

[48] A. Haugeneder, M. Hilmer, C. Kallinger, M. Perner, W. Spirkl, U. Lemmer, J. Feldmann, U. Scherf, *Appl.Phys.B* **1998,** *66*, 389.

[49] S. Riechel, U. Lemmer, J. Feldmann, T. Benstem, W. Kowalsky, U. Scherf, A. Gombert, V. Wittwer, *Appl.Phys.B* **2000**, 71.

[50] C. Bauer, H. Giessen, B. Schnabel, E. B. Kley, C. Schmitt, U. Scherf, R. F. Mahrt, *Adv.Mater.* **2001,** *13*, 1161.

[51] S. Riechel, C. Kallinger, U. Lemmer, J. Feldmann, A. Gombert, V. Wittwer, U. Scherf, *Appl.Phys.Lett.* **2004,** *77*, 2310.

4. Binaphthyl Based Step – Ladder Polymers

4.1. Introduction and Motivation

The successful integration of the naphthalene – units into a series of alternating co - and ladder polymers[1] (see chapter 2 and 3) led to the idea to incorporate similar binaphthyl building blocks. Chiral 1,1'-linked binaphthyls are a well – known building block of chiral ligands and sensors, and of optically active materials.[2-5] The characteristic feature is the C_2 symmetry of the binaphthyl unit which can be used to design chiral chromophores.[6;7] Chiral polymers and oligomers gain some interest as emitters of circularly polarized light. Potential applications are in the area of optical data storage[8-12] or as background illumination for liquid crystal (LC) displays.[13] Here, at the present stage the use of passive polarization filters is quite common. However, the direct generation of circularly polarized light could be beneficial towards an increased energy conversion efficiency. Many chiral materials used so far attain the chirality from chiral side-chains or chiral dopants. The binaphthyl unit on the other hand opens the way to incorporate main-chain chirality into the conjugated backbone.

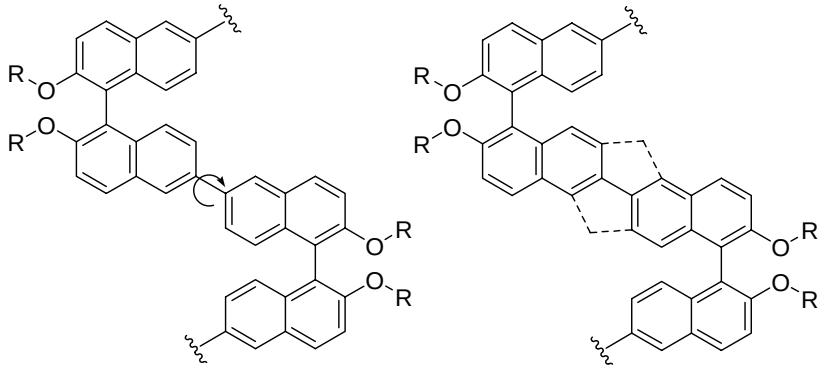

Scheme 4.1: Unrestricted vs. restricted rotation for single – stranded and step - ladder polymers.

As indicated in Scheme 4.1 a single bond linkage within the aromatic building blocks between two binaphthyls allows the π – system to rotate away from the planar conformation. Double stranded building blocks lead to so called step – ladder polymers with restricted conformational freedom. For such polymers a helical backbone structure is expected. Most of the known helical polymers receive their helicity from secondary interactions such as hydrogen bonding or van der Waals interactions.[14-18] Thus, many of the helical polymers can undergo conformational changes and therefore loose their helical information.[19] The CD spectra of such polymers are therefore, often similar to isolated binaphthyl chromophores. That is because each unit in the polymer acts nearly independently without an extended helical structure. During our project also a paper by Zhang and Pu was published, which dealt with a related topic.[5] However, their synthetic strategy towards helical Stepp – ladder polymers follows a different protocol utilizing a CF_3COOH - induced cyclization starting from the corresponding dialkyne compounds, leading to fused polyaromatic compounds (see Scheme 4.2).

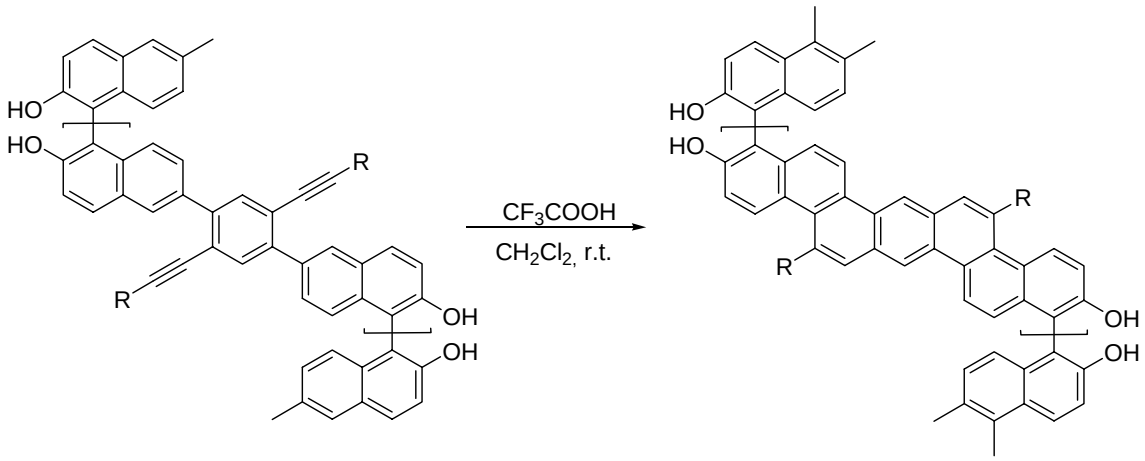

Scheme 4.2: Cyclization method used by Pu et al. towards helical step – ladder polymers.

However, this synthetic strategy is known to be difficult and often leads to structural defects.[20] Therefore, it seemed to be challenging to apply our already discussed favourable cyclization method (see chapter 3) for the synthesis of binaphthyl based step – ladder polymers. Despite the access to helical polymers the incorporation of binaphthyl units offers the option to disturb the planarity of polyarylenes. This strategy can suppress aggregation phenomena and leads to improved optical and electrooptical properties as demonstrated herein for polyfluorenes with statistically incorporated binaphthyl units (see chapter 5).[2;21]

The dihedral angle within the 1,1'-binaphthyl unit can vary from 60° to more than 120° for different substitution patterns (especially if substituted in the 2,2' – positions). As result, the π - conjugation through the binaphthyl unit is weak, so that the binaphthyls act as efficient conjugation barriers. Varying the amount of the binaphthyl units therefore allows some tuning of the optical and electronic properties.

4.2. Results and Discussion

4.2.1. Monomer and Polymer Synthesis

Our synthetic entry to binaphthyl-based step – ladder polymers starts with 6,6'-dibromo-2,2'-dihydroxy-1,1' – binaphthyl (**1**), which is commercially available or can be prepared in almost quantitative yields from 2,2'-dihydroxy-1,1'-binapthyl.[22;23] Treatment of **1** with n-octylbromide under basic conditions according to literature afforded **2** in good yields (> 90 %).[24-26] The corresponding boronic ester derivative was obtained in high yields via a Suzuki-Miyaura coupling utilizing Pd(dppf)Cl_2, bis(pinacolato)diboron and KOAc in THF.[27] Purification of **3** was obtained via coloumn chromatography and gave **3** as a yellow oil which solidified after six to eight weeks under atmospheric conditions as a white powder. The enantiomerically pure diboronic ester (R)-**3** was prepared in a similar fashion to racemic **3** [(R/S)-**3**].

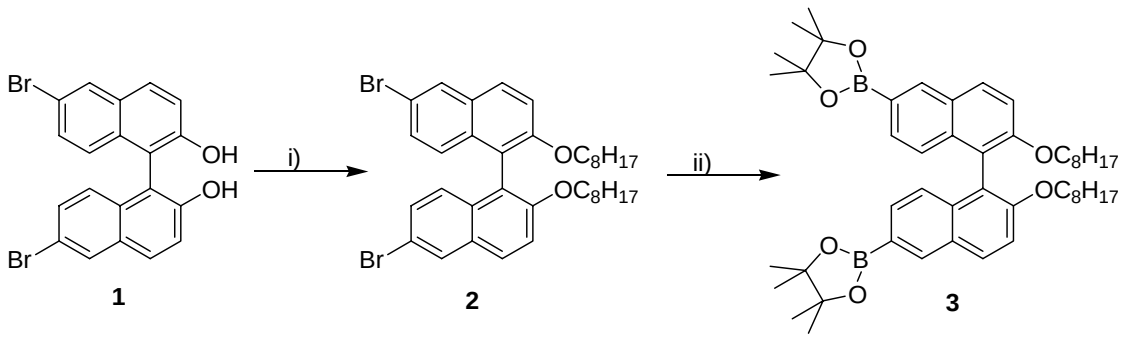

i) n-octylbromide, K_2CO_3, acetone, reflux, 24 h. ii) bis(pinacolato)diboron, Pd(dppf)Cl_2, KOAc, THF, 80°C, 24 h.

Scheme 4.3: Synthetic protocol towards monomer **3**.

The monomers **4** and **7** have already been described in Chapter 3 and in the literature, respectively.[28] All used molecules were characterized by standard methods such as NMR spectroscopy and mass spectrometry. **3** and **4** were coupled following a microwave – assisted

Suzuki type cross – coupling utilizing KOH as the base.[1] The polyketone (R/S)-**5** was formed in reasonable yields and molecular weights of $M_n = 13{,}250$ according to gel permeation chromatography (GPC, vs. polystyrene standard) after extracting with ethanol for one day. The enantiomeric pure (R)-**5** was obtained in similar yields and molecular weights ($M_n = 13{,}900$; PD = 1.6).

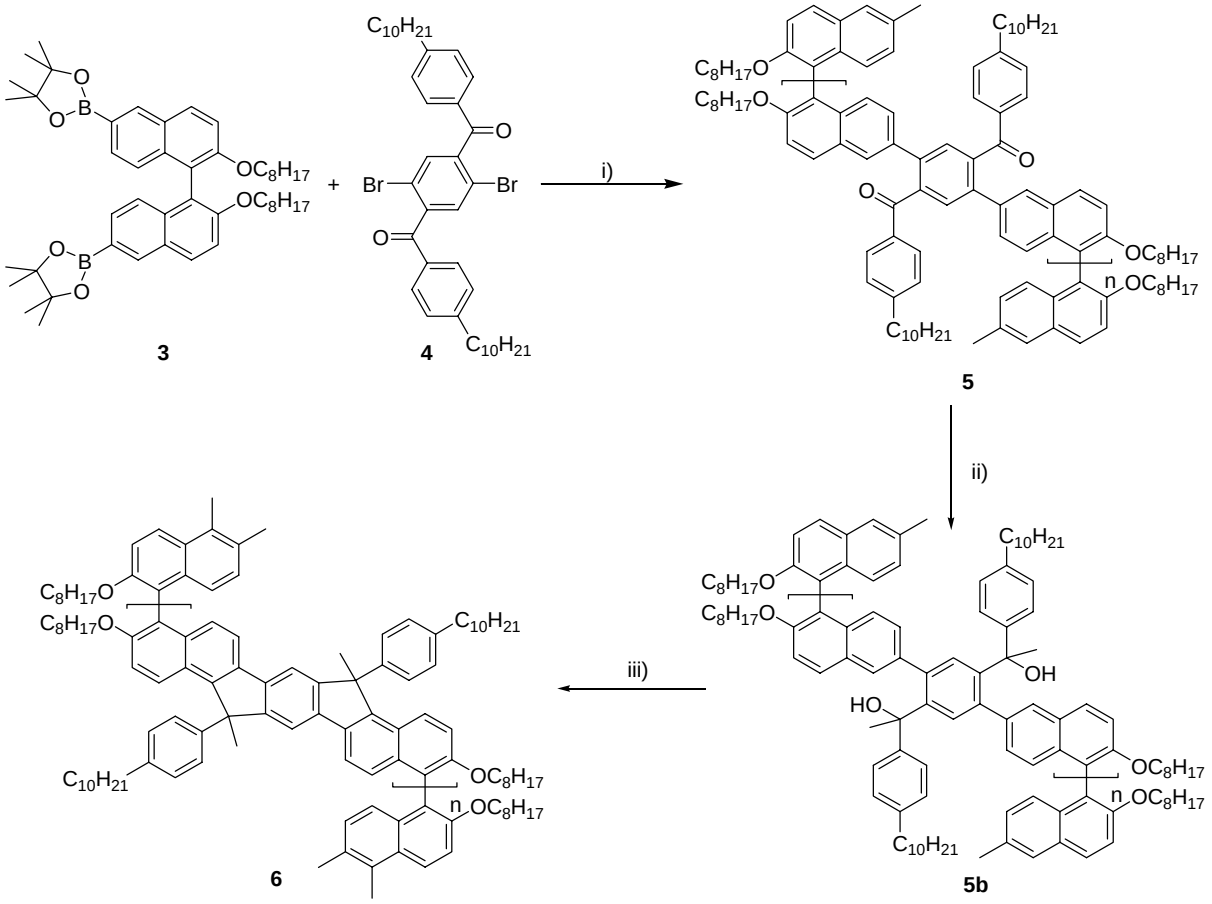

i) $Pd(PPh_3)_2Cl_2$, KOH, THF, µW (300W, 115°C). ii) MeLi, THF, 24 h. iii) $BF_3{\cdot}OEt_2$, dichloromethane.

Scheme 4.4: Synthesis of step-ladder polymer **6** and its precursor polyketone **5**.

The next step towards the desired step-ladder polymer was the transformation of the carbonyl function to a tertiary alcohol (**5b**) by treatment with methyllithium. The complete conversion was monitored by IR spectroscopy through the complete disappearance of the carbonyl band. Subsequent ring closure was achieved by addition of an excess of borontrifluoride etherate to a dichloromethane solution of **5b**. The resulting polymer was precipitated into methanol to afford **6** in yields of > 95 %. The product was very good soluble in several organic solvents. GPC analysis displayed a molecular weight for the racemic polymer of $M_n = 20{,}100$

(PD = 2.0) and for the chiral (R)-**6** a molecular weight of M_n = 16,500 (PD = 1.6). It should be noted that in contrast to linear rod – like conjugated polymers[29;30] GPC analyses of binaphthyl – based polymers versus polystyrene standards may give distinctly underestimated molecular weights by as much as a factor 2.5.[2]

Thermogravimetric (TGA) investigations on the polymers (R/S)-**6** and (R)-**6** have shown that both are stable up to temperatures of 350°C and show an onset decomposition temperature close to 400°C in good agreement with former investigations on phenyl-binaphthyl copolymers.[31]

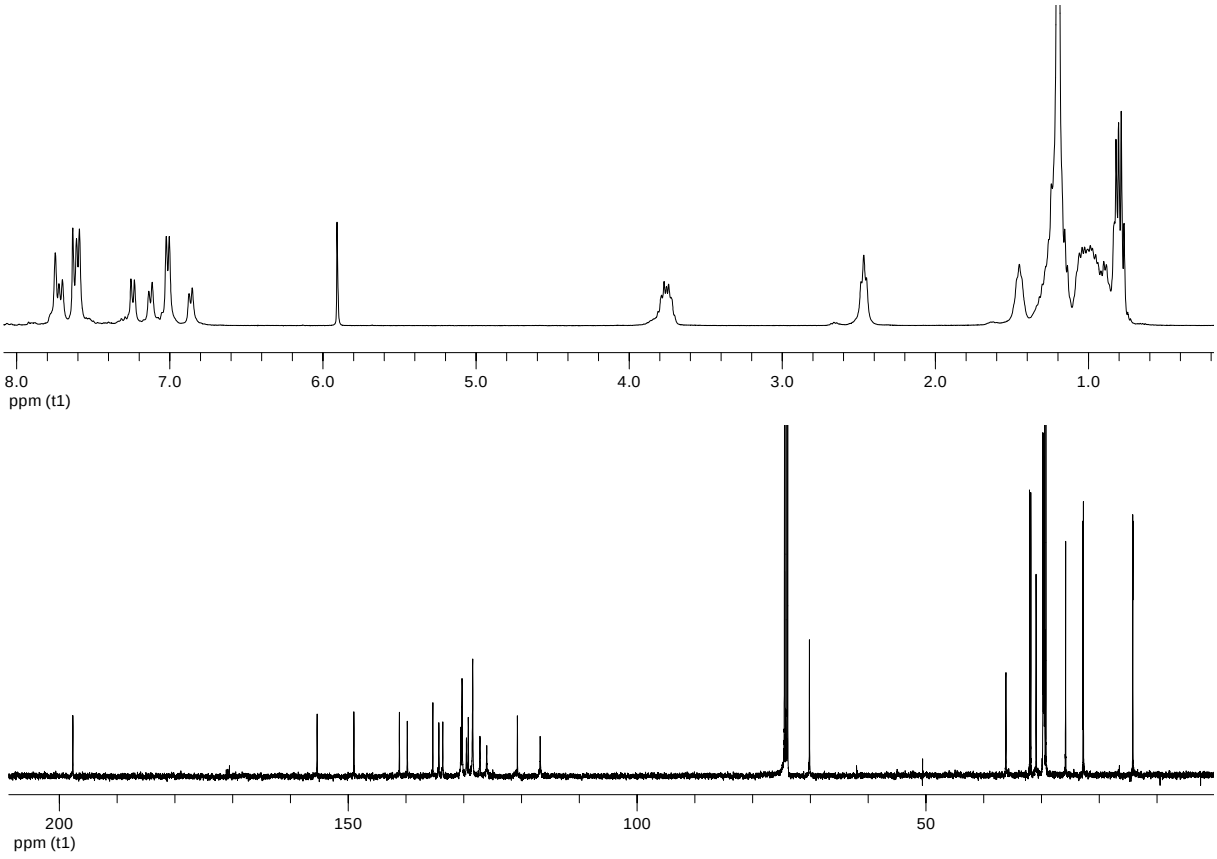

Figure 4.1: a) ^{1}H NMR and b) ^{13}C spectrum of (R/S)-**5** in $C_2D_2Cl_4$.

Polymers **5** and **6** were fully characterized by IR, ^{1}H and ^{13}C NMR spectroscopy. (R/S)-**5** gives an unusually good resolved ^{1}H NMR spectrum in $C_2D_2Cl_4$ (see Figure 4.1 a). The aromatic signals are clearly resolved and all measured integrals fit exactly. The ^{13}C NMR spectrum is also very good resolved (Figure 4.1 b) and displays the carbon signal of the carbonyl group at 197.6 ppm. Out of 17 expected ^{13}C signals in the aromatic region 16 can be easily found, while the broader signal at δ = 128.4 indicates the superposition of two signals.

Such good resolved NMR spectra are quite unusual for aromatic polymers. The NMR spectra of the chiral (R)-**5** are similar to (R/S)-**5**.

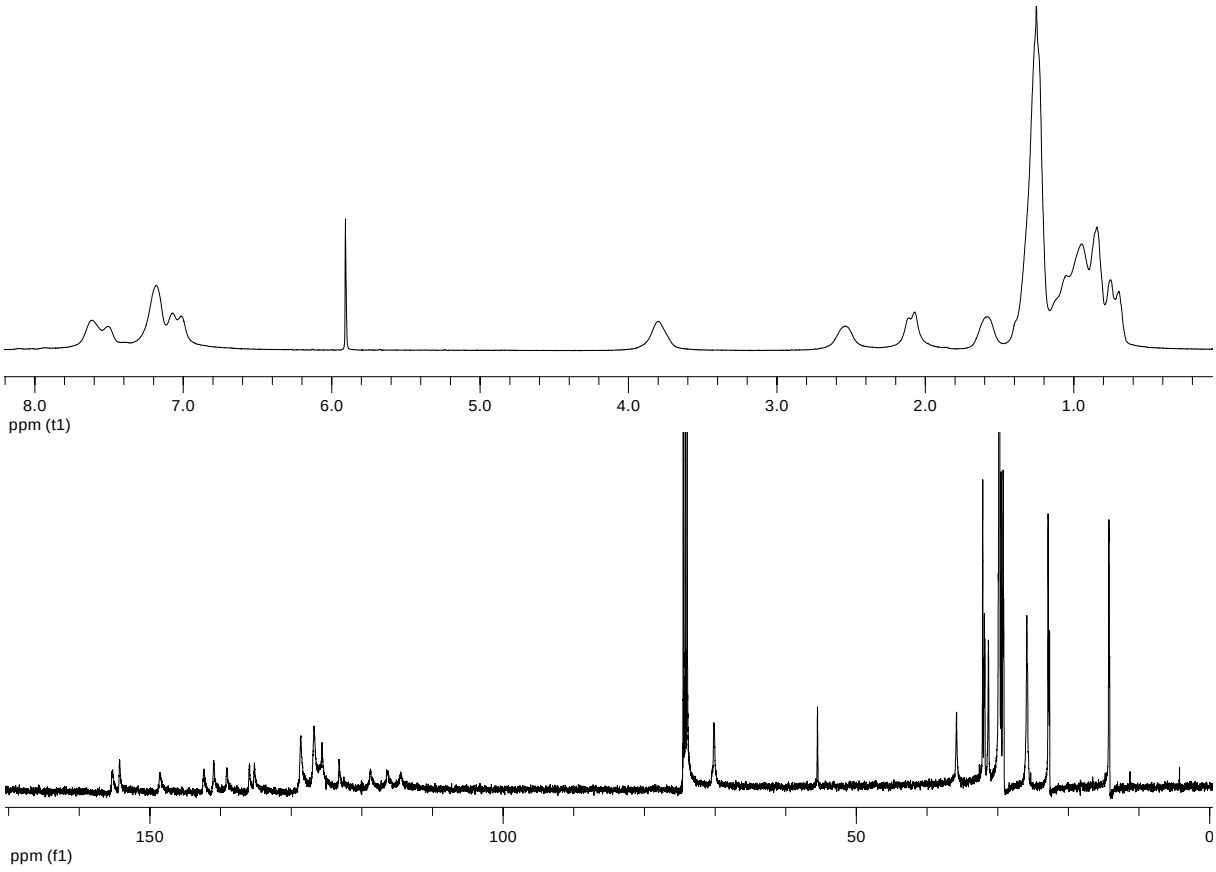

Figure 4.2: a) ^{1}H NMR and b) ^{13}C spectrum of (R/S)-**6** in $C_2D_2Cl_4$.

In the ^{1}H NMR spectra of both (R/S)-**6** and (R)-**6** the signals are relatively broad which makes it difficult to assign the aromatic hydrogens. The ^{13}C NMR aromatic signals are significantly broadend because of the much more rigid ladder structure. Complete cyclization can be assured by the complete vanishing of the carbonyl signal at δ = 197.6 ppm and the appearance of the bridging carbon at 55.5 ppm. To examine the influence of elongated ladder segments a statistical copolymer was synthesized (Scheme 4.5) by using a certain amount of 2,5-dihexyl-1,4-phenylene-diboronic acid (**7**) as comonomer. The synthesis was carried out following the same route as used for **5** and **6**. The concentration of the binaphthyl comonomer was 10 %. The actual percentage of the binaphthyl unit incorporated was calculated by comparing the relative intensities of the O-CH_2 proton signal at δ = 3.9 ppm from the binaphthyl unit to the sum of the aryl protons giving exactly the desired 10 % ratio.

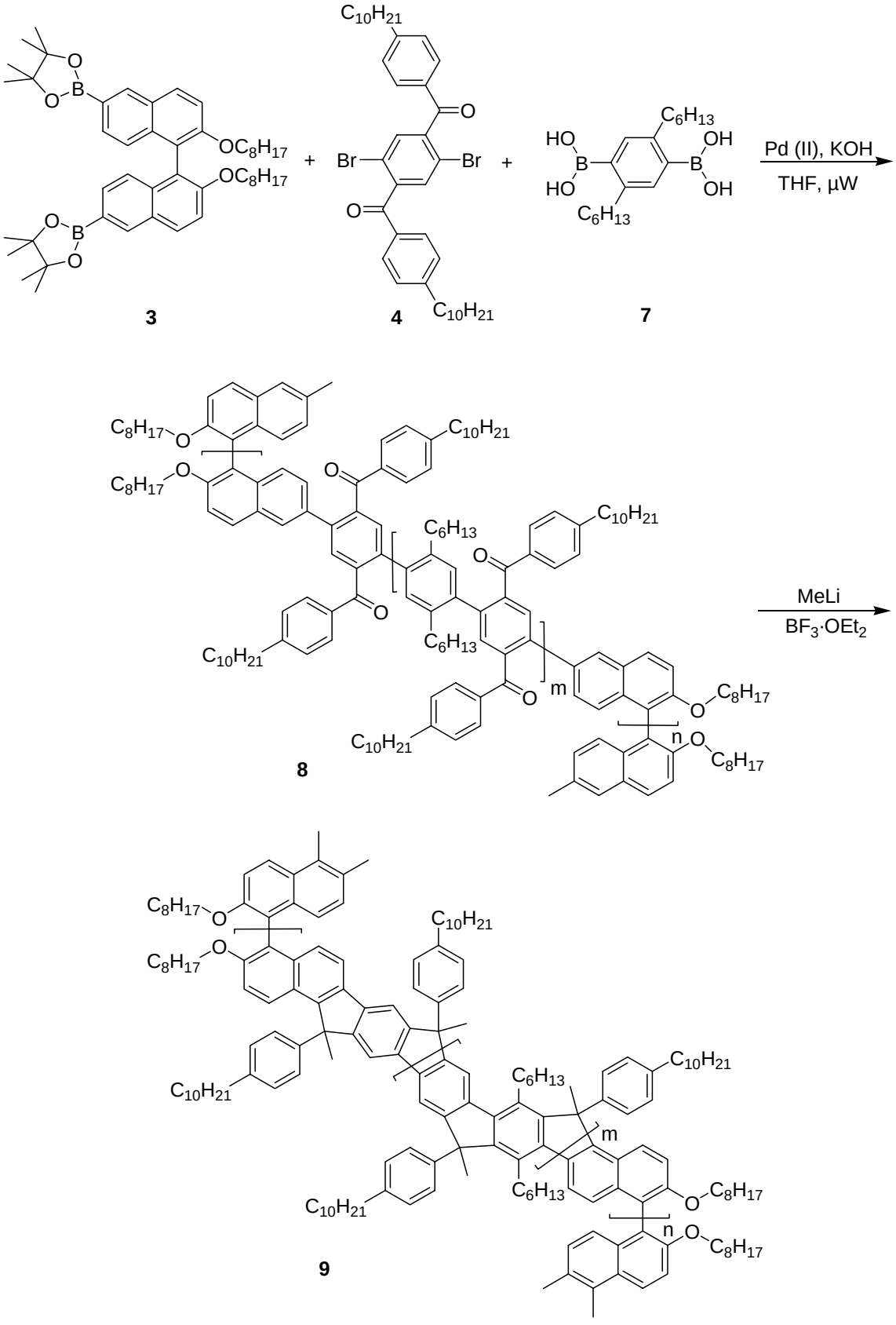

Scheme 4.5: Synthesis of a statistical step – ladder copolymer (R/S)-**9**.

Besides the weak carbonyl signal at δ = 196.8 ppm only 10 aromatic carbons and 16 alkyl signals could be found for **8** which shows that the ^{1}H NMR and even more the ^{13}C NMR spectrum of **8** are dominated by the elongated poly ketone segments. Treatment of **8** with methyl lithium and subsequent cyclization with $BF_3 \cdot OEt_2$ gives the step – ladder copolymer **9**. As already discussed for **6** the NMR signals broaden drastically after the transformation to the step – ladder polymer **9**.

4.2.2. Synthesis and Characterization of Model Compounds

To investigate the cyclization pattern at the binaphthyl unit after the polymer analogue ring closing reaction the synthesis of corresponding model compounds was performed. In principle, the cyclization can happen either in the 1- or the 3- position of the naphthyl unit as shown in Scheme 4.7 (**15a** or **15b**). The preparation of the essential starting materials is depicted in Scheme 4.6.

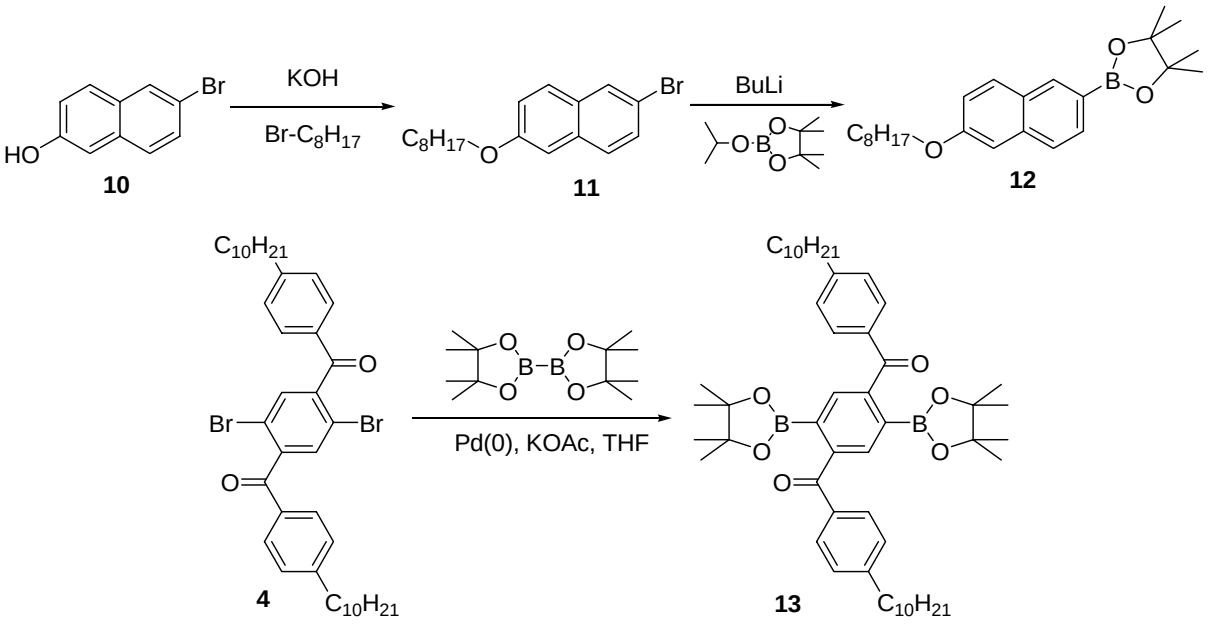

Scheme 4.6: Synthesis of **12** and **13**.

11 was obtained by alkylation of commercially available 2-bromo-6-naphthol (**10**) in good yields of about 80 %. Further treatment with n-butyllithium and subsequent "quenching" with isopropoxyborolane gave the boronic ester **12** in yields of 50 % (after chromatography). Synthesis of **4** has already been described in chapter 3, while the corresponding diboronic

ester **13** was obtained in a Palladium-catalyzed Suzuki-Miyaura coupling as described in the synthesis of **3**.

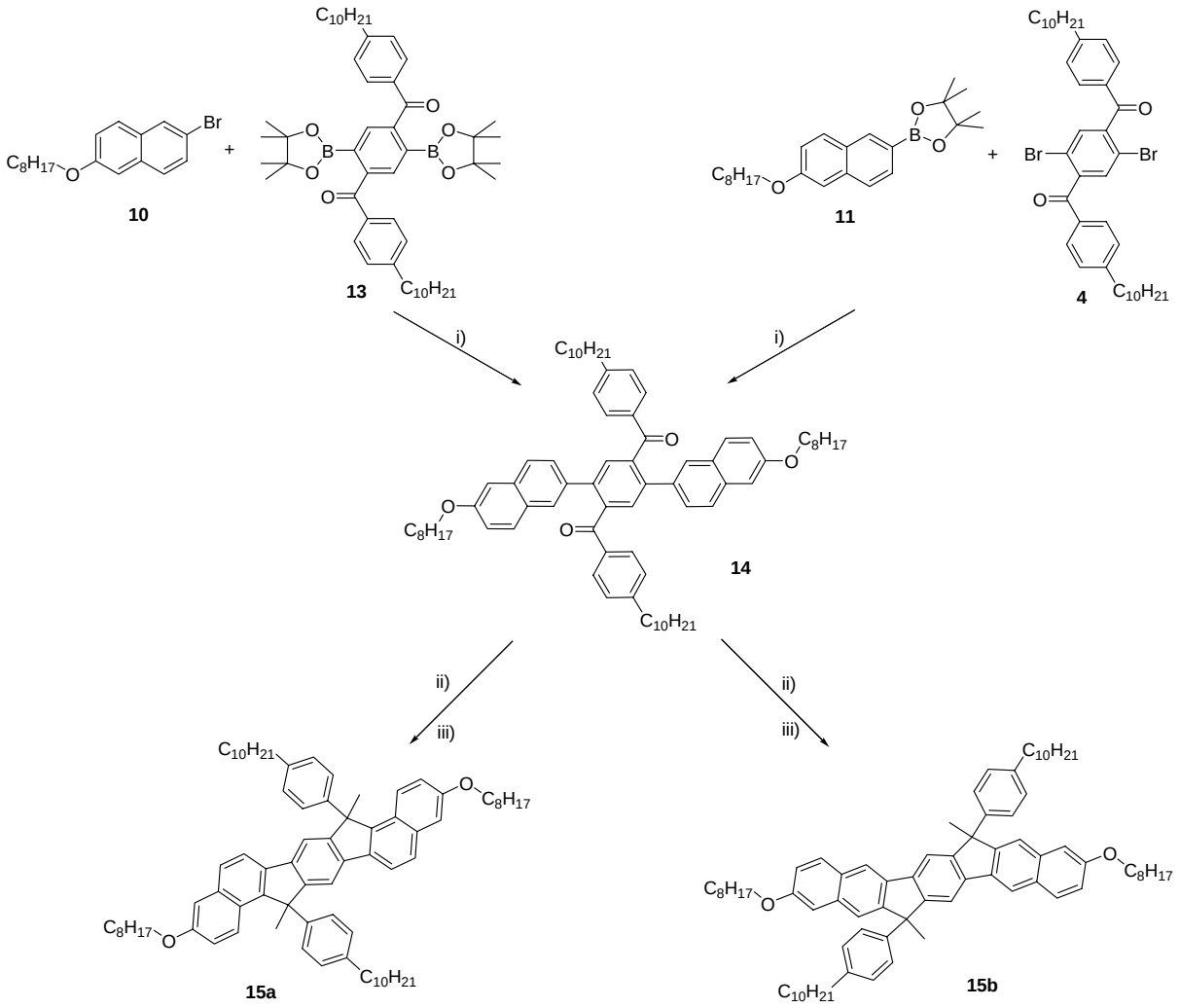

i) $Pd(PPh_3)_2Cl_2$, KOH, THF, µW (300W, 115°C). ii) MeLi, THF, 24 h. iii) $BF_3{\cdot}OEt_2$, dichloromethane.

Scheme 4.7: Synthetic route towards the model-compounds **15a**/**15b**.

Scheme 4.7 shows the synthesis of the model compounds **15a/b**. The diketone **14** was obtained via microwave assisted Suzuki cross – coupling of **10** and **13** or **11** and **4** without notably differences in yield or purity (60 – 65 % after chromatography). Structural identification of **14** and **15a/b** was obtained via MS and NMR studies. Figure 4.3 shows the aromatic region in the ^1H NMR spectrum of **14** in $CDCl_3$. The typical coupling constant and the shape of the signals allow the identification of the three phenyl protons. (a) gives a singlet,

while (b) and (c) result in doublets. Additional ^{1}H-^{1}H ROESY and ^{1}H-^{1}H COSY - LR spectra show a distinct coupling between the α - methylene triplet at δ = 2.5 ppm and (c).

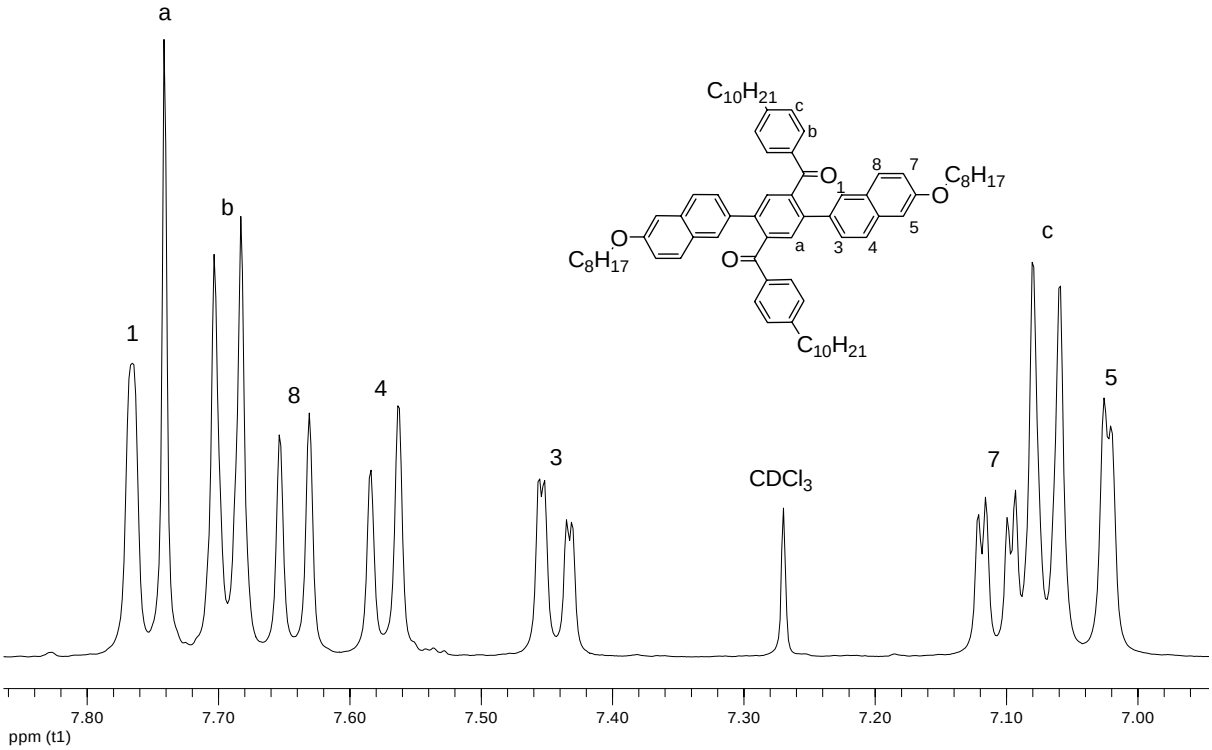

Figure 4.3: ^{1}H NMR spectrum (aromatic region) of **14** in $CDCl_3$.

Hereby, (b) is more downfield shifted due to the influence of the neighboring carbonyl function. For the naphthyl signals (5) reveals a small and typical coupling of about 2 Hz to (7). (5) also shows a lucid ^{1}H-^{1}H ROESY signal connected to the O-CH_2 alkoxy group at δ = 4.0 ppm. Furthermore (4) can be identified via a through space coupling to (5). The corresponding partners of (4) and (7), (3) and (8), can be identified in the ^{1}H-^{1}H COSY spectrum. Hereby, (1) is much more downfield shifted then (5).

The transformation of **14** to **15a/b** follows the usual procedure of the polymer analogue cyclization. Full reduction of the carbonyl function with methyl lithium was checked via the complete disappearance of the carbonyl band at 1656 cm^{-1} in the IR - spectrum. The resulting tertiary dialcohol was directly transformed into the ladder oligomer by treatment with $BF_3{\cdot}OEt_2$. Ring closure is accompanied by the appearance of a strong blue fluorescence. The crude mixture was purified via filtration over silica gel and gave **15a/b** in about 90 % yield as colourless oil. To prove the structure different NMR techniques have been applied. Figure 4.4 depicts the aromatic region in the ^{1}H spectrum of **15a**.

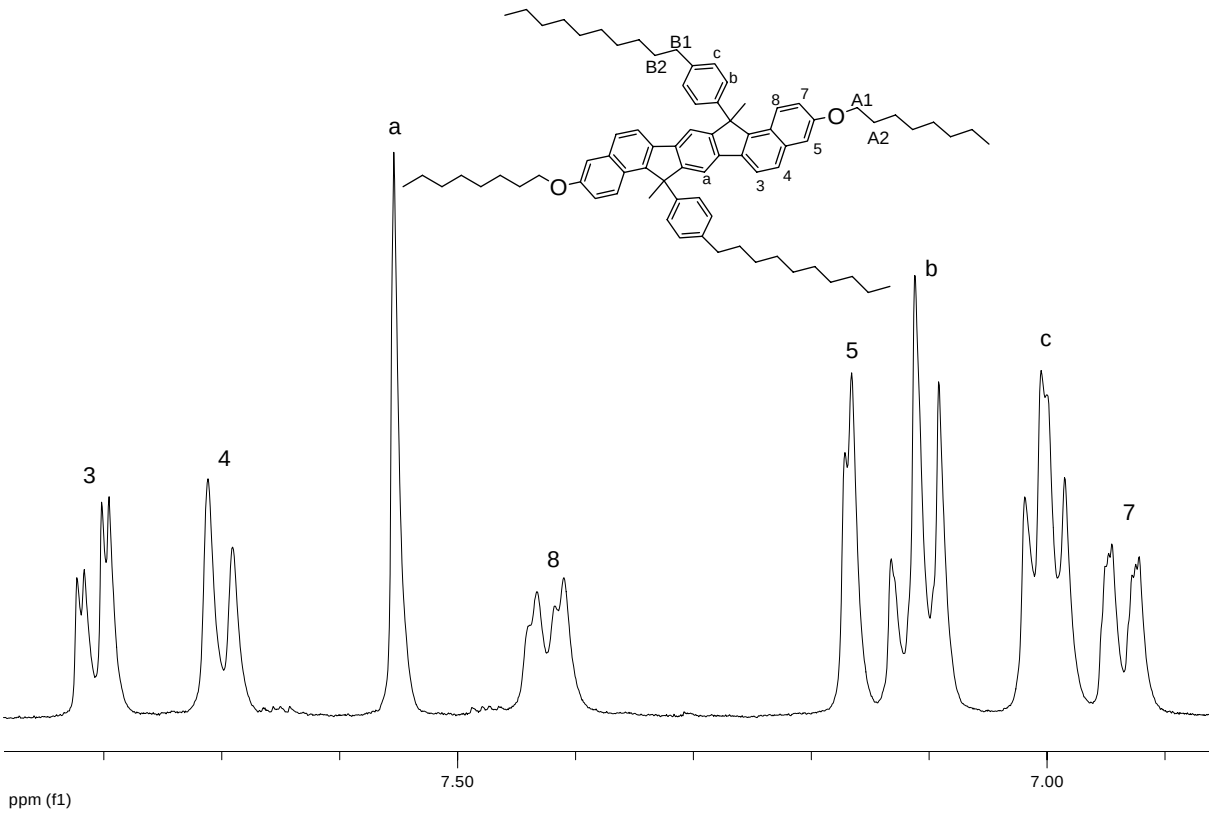

Figure 4.4: ^{1}H NMR spectrum (aromatic region) of **15a** in $C_2D_2Cl_4$.

The NMR spectrum clearly indicates a cyclization exclusively to the regioisomer **15a**. Again the phenyl signals can be clearly assigend via ^{1}H-^{1}H ROESY and ^{1}H-^{1}H COSY-LR investigations showing couplings between (c) and the α – methylene carbon (B1). (5) shows a strong ^{1}H-^{1}H COSY-LR coupling to (7) with identical coupling constances of about 2 Hz, which are as mentioned before, typical for $^{4}J_{(1-3)}$ couplings in naphthalene units. Once (7) is identified proton (8) can be recognized by a strong ^{1}H-^{1}H COSY coupling to (7). Protons (3) and (4) can be assigned via ^{1}H-^{1}H ROESY investigations, showing a coupling of (a) to (3) and of (4) to (5). However, despite the fact that all proton signals can be clearly assigned, the spectrum shows some untypical signal doubling. For example, proton (8) appears as a doublet of doublets which should just be a doublet in theory. Similar doubling effects can also be observed at a couple of signals in the ^{13}C spectra. The methyl group at the methylene – bridge appears as a well – resolved doublet at 25.6 and 25.7 ppm (see inset in Figure 4.6). The emersion of some smaller signals in Figure 4.6. is due to some not seperatable impurities, which do not belong to compound **15a**. Apparently, the NMR spectra are complicated by the

occurrence of two diastereoisomers, which are generated upon formation of the two methylene bridging groups in *syn* or *anti* configuration (see Figure 4.7).

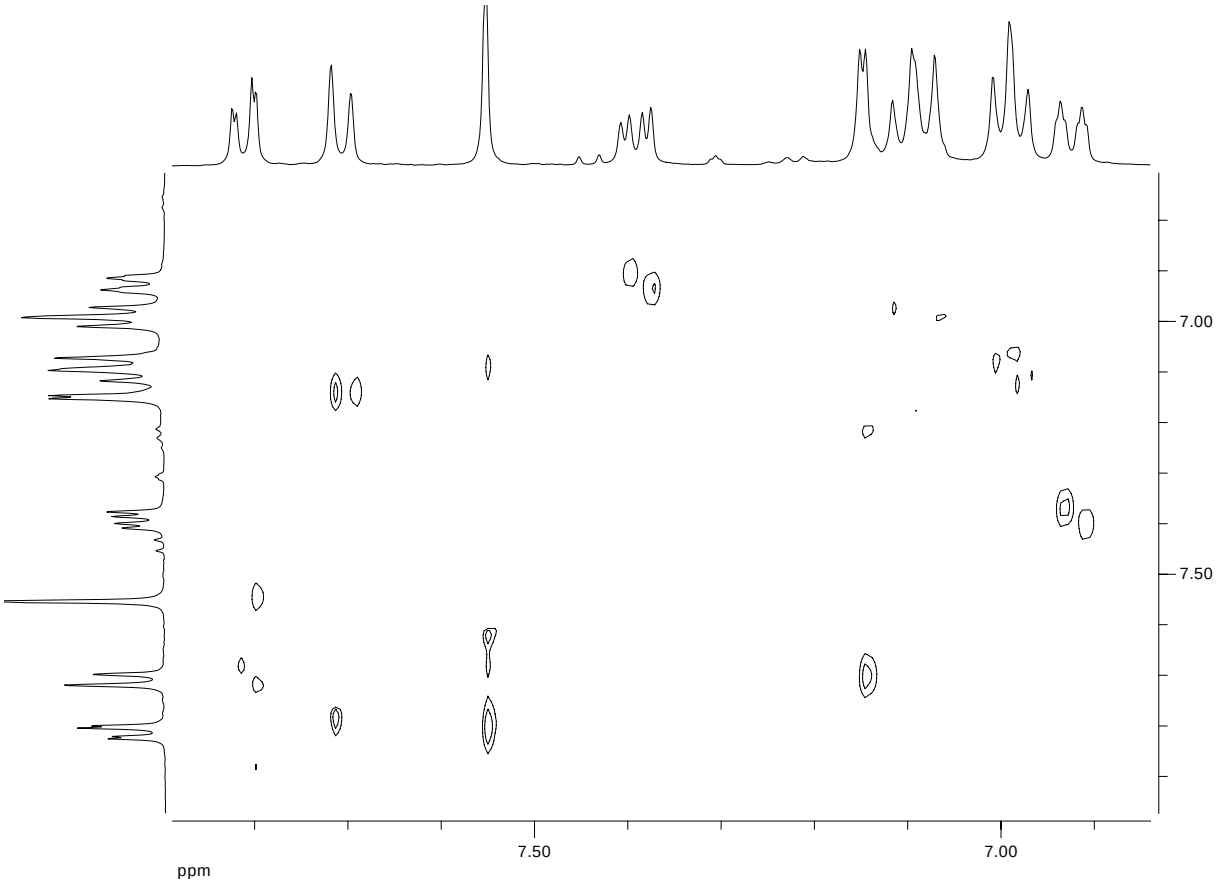

Figure 4.5: ^{1}H-^{1}H ROESY spectrum (aromatic region) of **15a** in $C_2D_2Cl_4$.

If all "doubled" signals are counted as single signals the desired number of 17 aromatic carbons for **15a** is found. It was not possible to separate the two diastereomers by column chromatography.

DSC examinations showed that **15a** possesses a glass transition temperature T_g of $\sim 0°C$ without crystallization. To circumvent the formation of diastereoisomers a model compound with two identical side chains at the methylene bridge was synthesized.

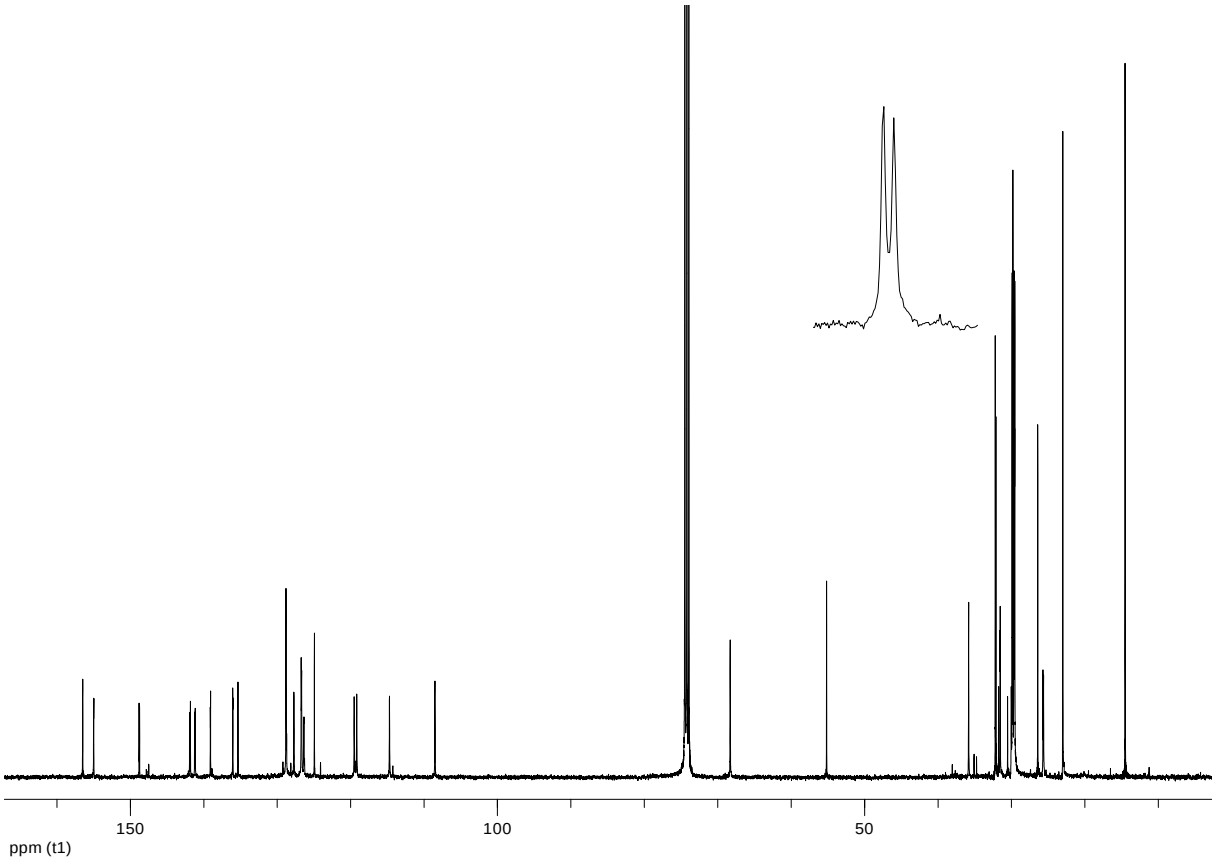

Figure 4.6: ^{13}C NMR spectrum of **15a** in $C_2D_2Cl_4$ (the inset shows the signal of the methyl group at the methylene bridge at 25.6/25.7 ppm).

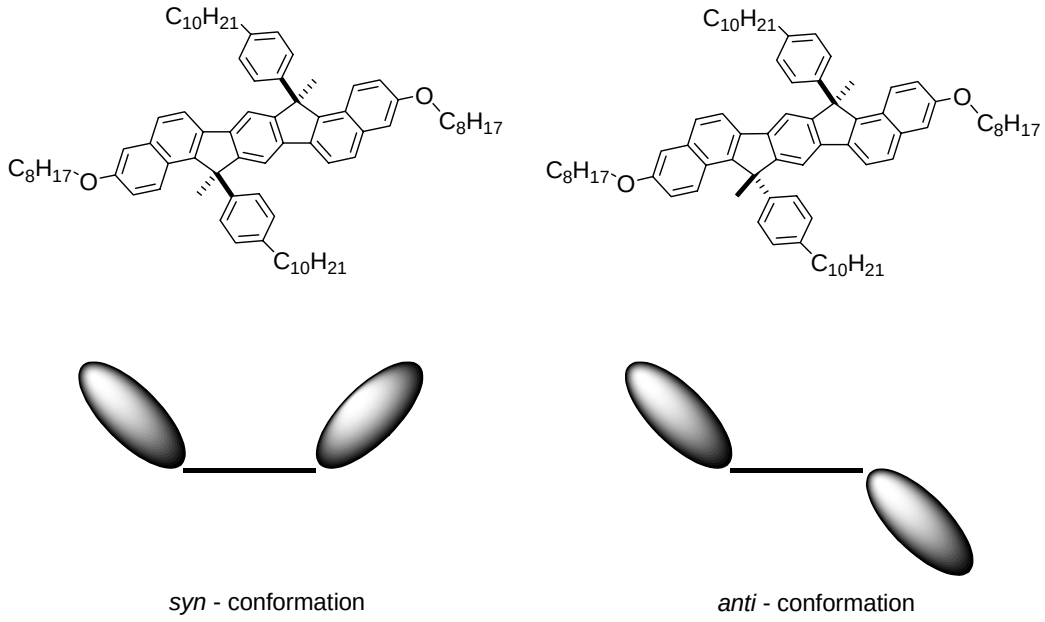

Figure 4.7: Schematic illustration of the two possible diastereoisomers of **15a.**

Hereby, a diester precursor **19** was reacted twice with the n-hexyllithium nucleophile.[32] Scheme 4.9 shows the access to the desired model compound **20**.

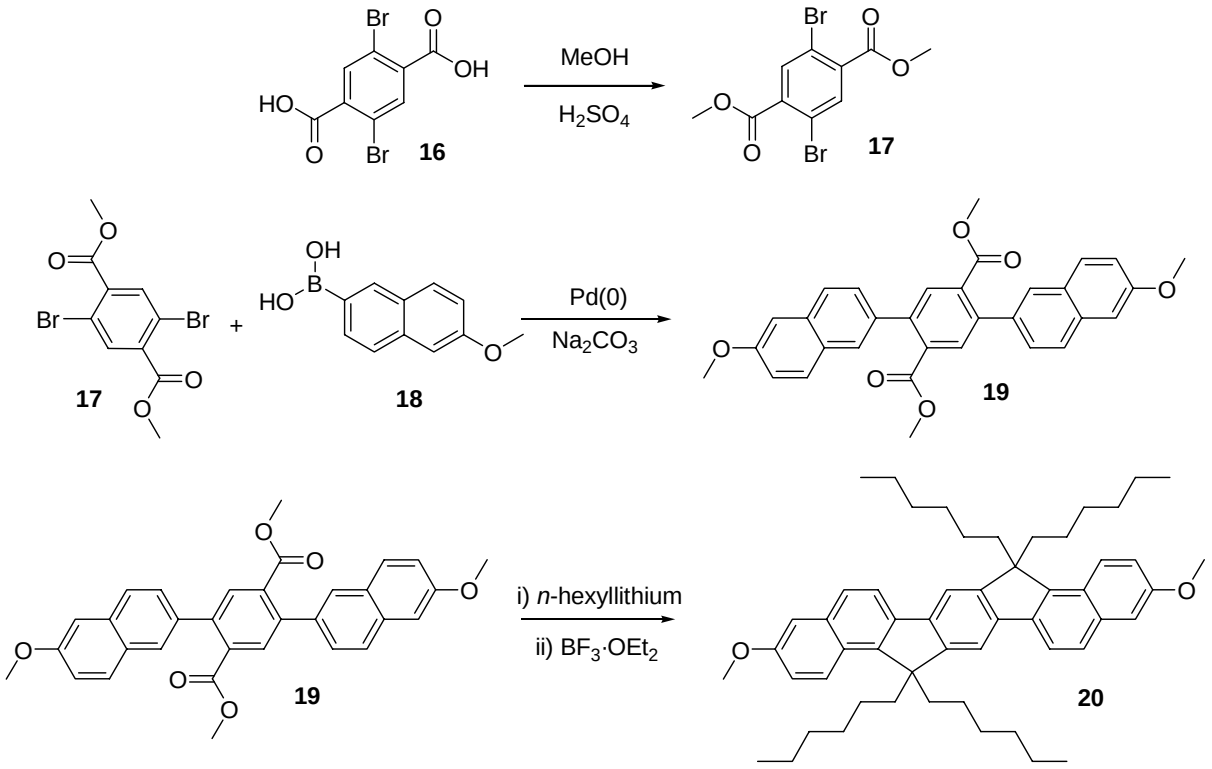

Scheme 4.9: Synthesis of the symmetric model compound **20**.

The terephthalic diester **17** was achieved in yields over 90 % in an acid catalysed esterification of 2,5-dibromo-terephthalic acid (**16**) in methanol. Suzuki – coupling of the diester **17** with 6-methoxy-naphthalene -2-boronic acid (**18**) proceeded smoothly and gave the dinaphthyl-diester **19** in 84 % yield after recrystallization. Addition of an excess of n-hexyllithium in dry THF gave the diol intermediate, which was subsequently cyclized to the model compound **20** in a Friedel-Crafts ring-closure reaction. The terminal alkoxy chains were shortened to methoxy groups, as this should favour the tendency to crystallize, which should allow an additional X-ray analysis.

Structural integrity of **20** was proved by NMR spectroscopy and MS studies. Figure 4.8 shows the ^{1}H NMR spectrum of **20** in $C_2D_2Cl_4$ (aromatic region). Again, as shown for compounds **13** and **14** the protons (5) and (a) could be used as the starting point for the ^{1}H NMR assignment. Examination of the ^{1}H-^{1}H ROESY spectrum (Figure 4.9) indicates clearly the through space coupling of (a) to (3) as well as the coupling of (5) to (4).

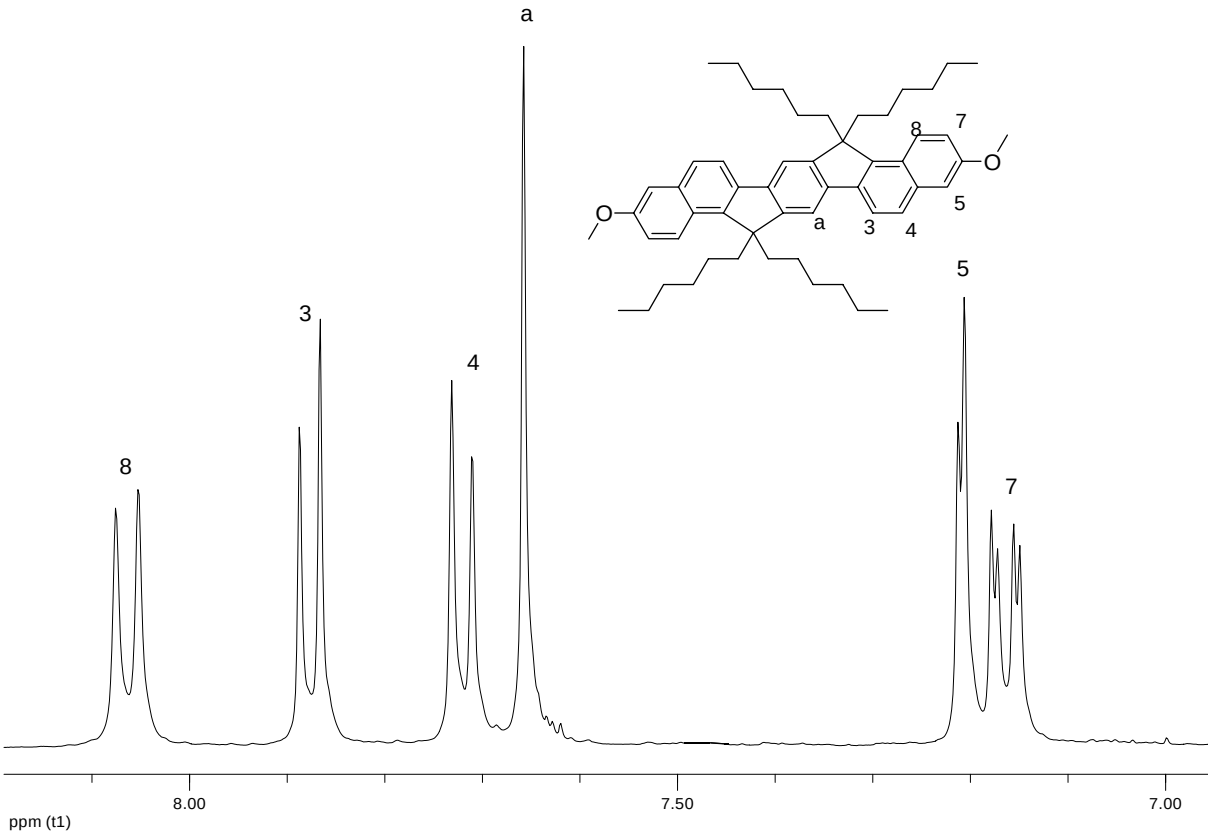

Figure 4.8: ^{1}H NMR spectrum of model compound **20** in $C_2D_2Cl_4$.

The measured coupling constantes of ^{3}J = 8.4 Hz are almost identical with the coupling of (3) and (4) in compound **14**. The ^{1}H-^{1}H COSY spectrum strengthens this assignment by showing a strong coupling pattern. The ^{1}H-^{1}H COSY-LR spectrum combined with measuring the coupling constances allows the identification of (7) followed by identifiying (8) via the ^{1}H-^{1}H COSY spectrum. Comparison of the two model compounds **15a** and **20** shows the proton signals of **15a** slightly upfield shifted (see Figure 4.10). Interestingly, proton (8) undergoes a dramatic shift on going from **15a** to **20**. However, the spectra show that for both model compounds the cyclization takes place exclusively in the α – position of the naphthyl group.

Therefore, it seems fair to assume a similar cyclization pattern for the polymer analogue ring closure reaction to polymers **6** and **9**. Due to the broad ^{1}H NMR signals of the step – ladder polymer **6**, a comparison of the spectrum to that of the model compound systems is not very substantial. Hence, Figure 4.11 compares the ^{13}C NMR spectra of model compound **15a** and the step – ladder polymer **6** confirming the regio – specific ring closure at the naphthyl moiety.

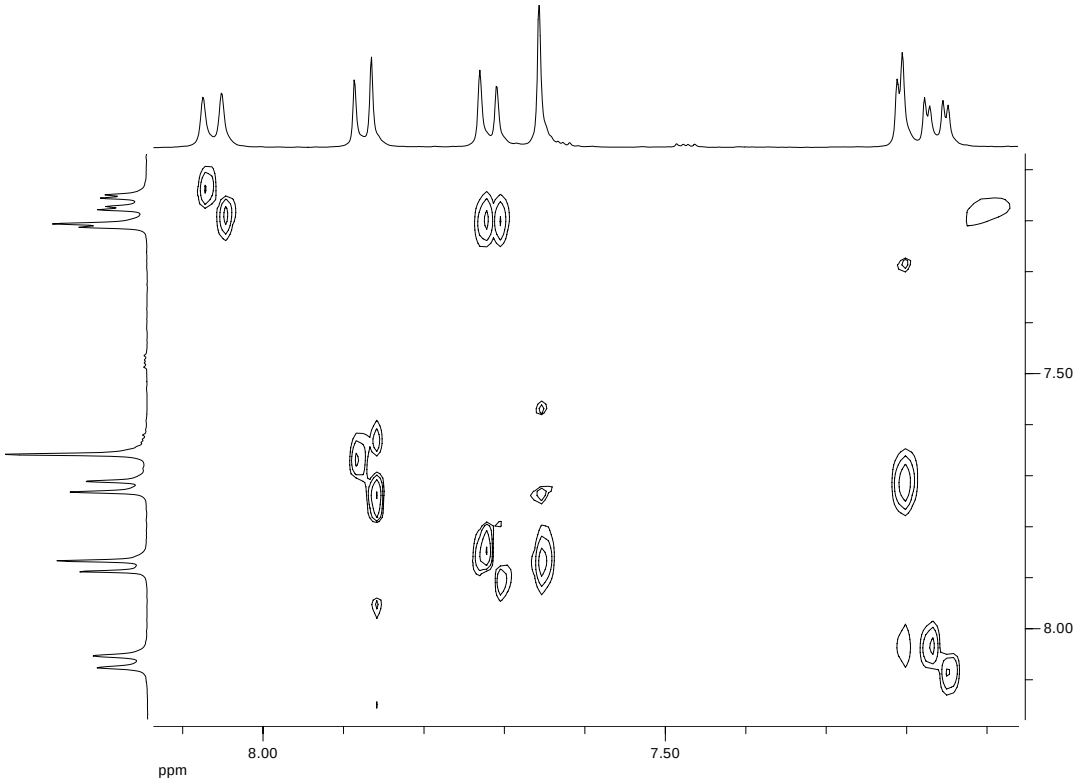

Figure 4.9: ^{1}H-^{1}H ROESY spectrum of model compound **20** in $C_2D_2Cl_4$.

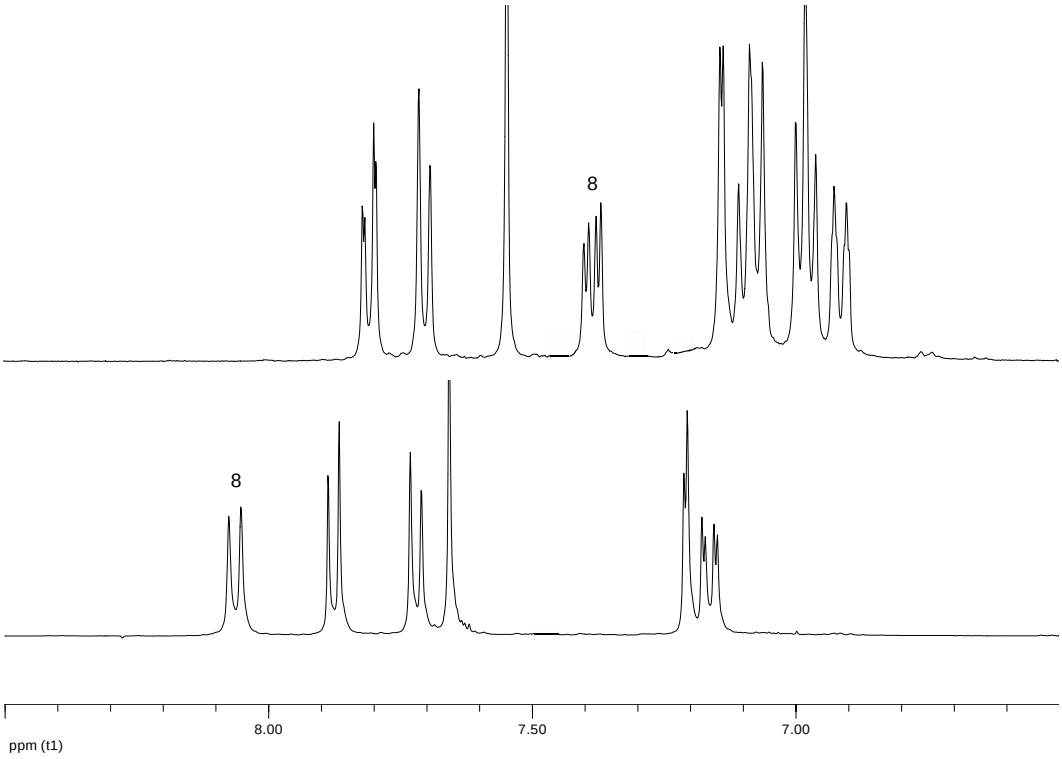

Figure 4.10: Comparsion of ^{1}H NMR spectra in the aromatic region for the model compounds **15a** and **20**.

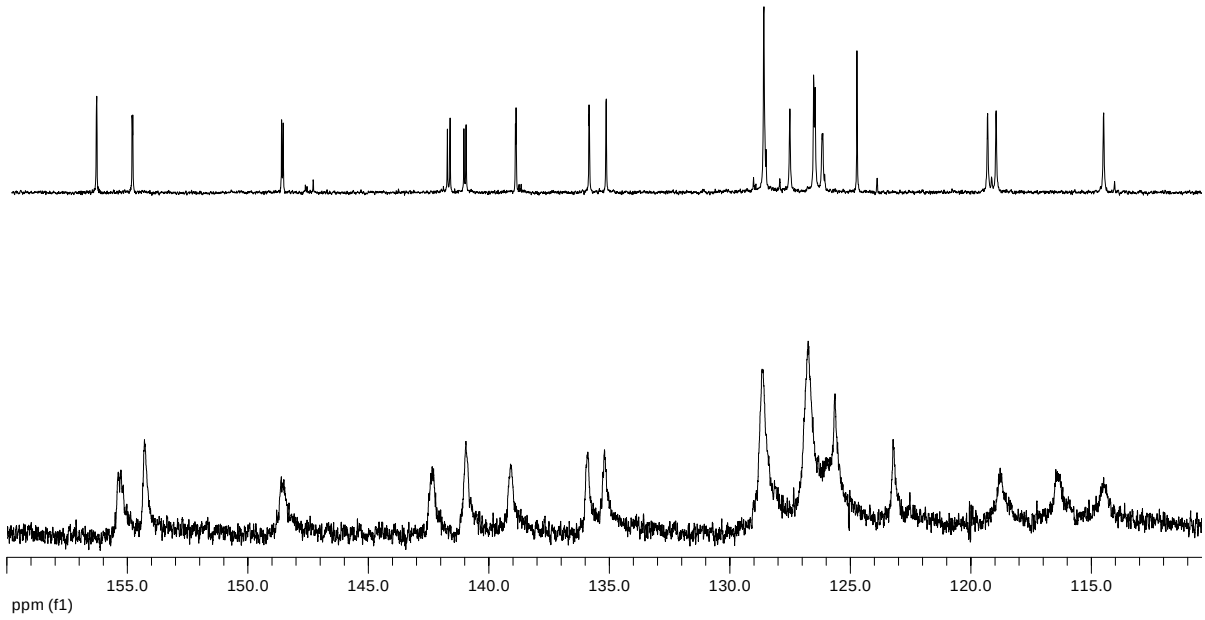

Figure 4.11: Comparsion of the ^{13}C NMR spectra (160 – 110 ppm) of model compound **15a** and polymer **6**.

4.2.3. X-ray Crystallography

To complete the characterization of **20** single crystalls were grown from THF. The X – ray investigations have been performed in the groups of Dr. Lehmann (MPI für Kohlenforschung, Mülheim) and Prof. Brauer (Bergische Universität Wuppertal).

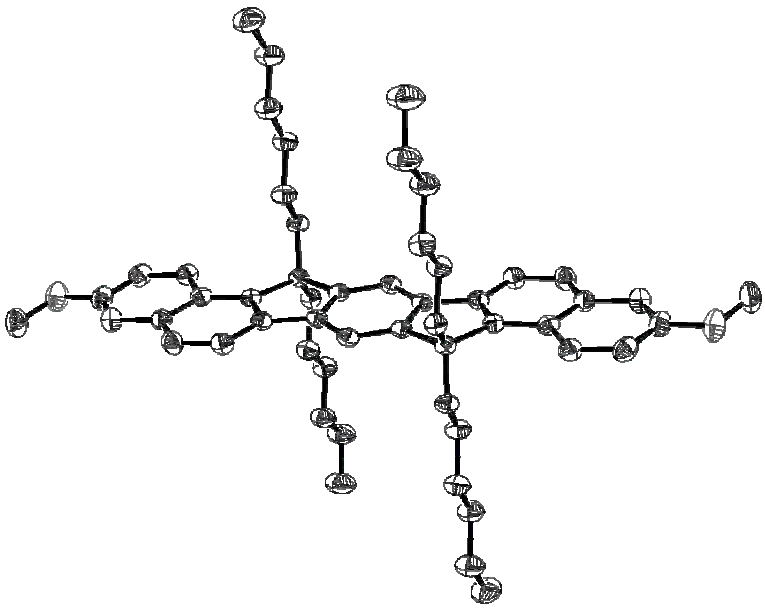

Figure 4.12: ORTEP plot of **20**.

Table 4.1 summarizes the most important crystallographic data. Figure 4.12 displays the expected cyclization in the α – position. The hexyl side – chains appear almost orthogonal to the backbone of the molecules. Investigations of the bond lengths and angles do not show any noticeable deviations.

Table 4.1: Crystal data and structure refinement of **20**

	20	
Empirical formula	$C_{54}H_{20}O_2$	
Color	colorless	
Formula weight	895.31 g · mol^{-1}	
Temperature	100 K	
Wavelength	0.71073 Å	
Crystal system	Triclinic	
Space group	**$P\bar{1}$, (no. 2)**	
Unit cell dimensions	a = 9.7465(4) Å	α= 78.985(3)°.
	b = 12.0082(7) Å	β= 84.870(2)°.
	c = 12.5014(6) Å	γ = 66.098(2)°.
Volume	1312.90(11) Å3	
Z	1	
Density (calculated)	1.132 Mg · m-3	
Absorption coefficient	0.068 mm-1	
F(000)	490 e	
Crystal size	0.27 x 0.20 x 0.18 mm3	
θ range for data collection	5.19 to 31.07°.	
Index ranges	-14 ≤ h ≤ 14, -17≤ k ≤ 17, -17 ≤ l ≤ 18	
Reflections collected	32145	
Independent reflections	8294 [Rint = 0.0828]	
Reflections with I>2σ(I)	6458	
Completeness to θ = 27.75°	98.4 %	
Absorption correction	None	
Refinement method	Full-matrix least-squares on F2	
Data / restraints / parameters	8294 / 0 / 301	
Goodness-of-fit on F2	1.019	
Final R indices [I>2σ(I)]	R1 = 0.0559	wR2 = 0.1375
R indices (all data)	R1 = 0.0757	wR2 = 0.1556
Largest diff. peak and hole	0.437 and -0.277 e · Å-3	

4.2.4. Optical Spectroscopy

4.2.4.1. UV/Vis and Photoluminescence Spectroscopy

The optical properties of the novel polymers and model compounds were recorded in both chloroform solution and as thin films. The data are summarized in Table 4.2. The solution UV/Vis and photoluminescence (PL) spectra of the polyketone (R/S)-**5** and the rigid step – ladder polymer (R/S)-**6** are shown in Figure 4.13. The UV/Vis spectrum of (R/S)-**5** exhibits a

broad structureless absorption band in the UV region with a maximum (λ_{max}) at 270 nm representing $\pi - \pi^*$ transistions and a long wavelength shoulder at 340 nm for $n - \pi^*$ transistions of the carbonyl chromophores. As expected, after cyclization of the polyketone to the rigid step – ladder polymer (R/S)-**6**, the UV/Vis shows additional intense, well resolved $\pi - \pi^*$ absorption bands at 360 and 380 nm, which are substantially red – shifted compared to the λ_{max} of the polyketone (R/S)-**5**. The well – resolved shape of the absorption bands is a characteristic feature of a rigid conjugated system with a coplanar configuration.

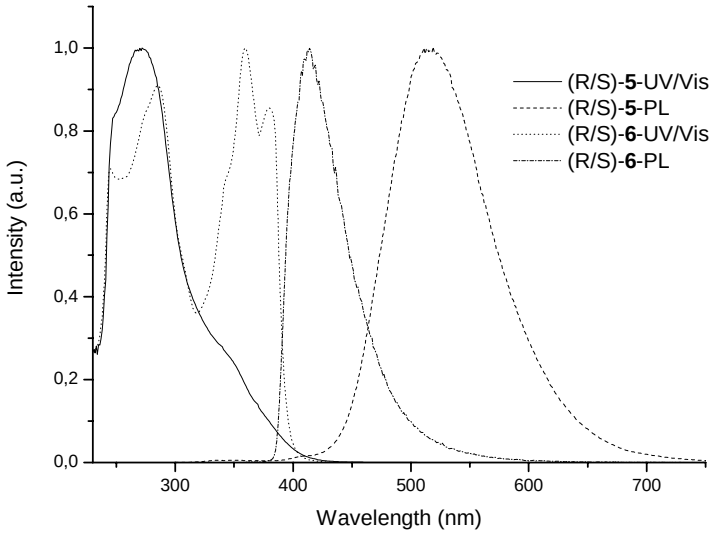

Figure 4.13: Absorption and emission spectra of polymers (R/S)-**5** and (R/S)-**6** in chlororform solution.

The PL emission of (R/S)-**6** is essentially featureless. The relatively small Stokes shift (2160 cm^{-1}) for (R/S)-**6** is consistent with a minimal geometry variation between the ground and the first excited state. The absorption and emission spectra of the step – ladder polymer **6** are dominated by the individual planarized segments since the distorted binaphthyl unit acts as an efficient conjugation barrier.[5;31;33] Therefore, the optical properties of the two model compounds **15a** and **20** were also investigated. The optical properties of **20** are almost identical to **15a** and for reasons of clarity not displayed in Figure 4.14. The UV spectrum of **15a** in dilute solution displays well – resolved absorption maxima at λ_{max} = 278, 353, and 373 nm which are quite similar to the UV/Vis spectrum of the step- ladder polymer **6**. The data shows only a small red – shift of around 7 nm by going from oligomer **15a** to polymer **6**. This

indicates only a weak interaction between two adjacent ladder units across the binaphthyl building block. Both model compounds **15a** and **20** exhibit an unstructured PL band with a maximum at around 400 nm. The larger Stokes of the polymer (R/S)-**6** (2160 cm^{-1}) compared to the model compound **15a** (1855 cm^{-1}) reflects some more conformational freedom in the polymer upon photo excitation, probably connected to the flexibility of the binaphthyl unit.

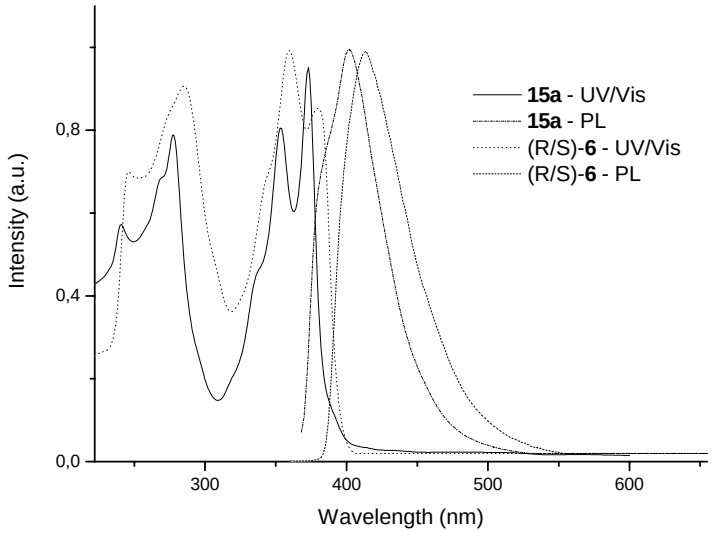

Figure 4.14: UV/Vis and PL spectra of the step –ladder polymer (R/S)-**6** and the model compound **15a** in chloroform solution.

All, these facts conclude for an essentially weak conjugative interaction between the ladder segments. This is consistent whit previous findings by Pu et al.[2;4] The expansion of the ladder segments between two binaphthyl moieties is expected to allow some tuning of the optical properties. Therefore, the extended step – ladder polymer (R/S)-**9** was also investigated. The UV/Vis spectrum of (R/S)-**9** shows well resolved absorption maxima (λ_{max}) at 425 and 452 nm. The maxima are almost identically to the values found for **MeLPPP** (see table 4.2), which indicates that the average length of the ladder segments reaches the effective conjugation length of **MeLPPP**. Compared to the step – ladder polymer (R/S)-**6** an distinct red – shift of the 0 – 0 band of 72 nm is observed.

Table 4.2: UV/Vis and PL data of polymers and the model compounds.

Polymer/ Oligomer	$\lambda_{max.}$ ($CHCl_3$-solution) (nm)		$\lambda_{max.}$ (film) (nm)	
	abs.	em.	abs	em.
5	270	414	273	460, 485
6	245, 286, 360, 380	414	361, 382	427, 458
9	425, 452	457, 486, 522	424, 452	462, 490, 526
15a	278,336,353,373	402	355,374	461
20	276, 335, 352, 372	400	n.m.	n.m.
MeLPPP	428, 458	460, 491, 531	426, 456	464, 494, 530

The PL spectrum of (R/S)-**9** displays three well – resolved PL bands at 464, 494 and 530 nm with a very small Stokes shift of 242 cm^{-1} (**MeLPPP**: 95 cm^{-1} derived from the solution data).

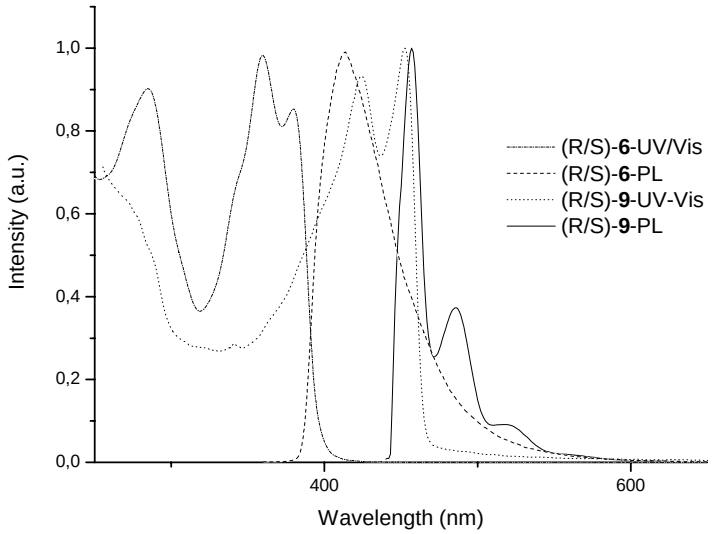

Figure 4.15: Absorption and emission spectra of polymers (R/S)-**6** and (R/S)-**9** in chloroform solution.

4.2.4.2. Chiroptical Methods

A characteristic property of chiral molecules is their ability to rotate linear polarized light. Linear polarized light can be seen as the superposition of left – and right circular polarized portions. The phenomenon of optical rotation has its origin in the fact that optically active materials have different refractive – indices for left and right circular polarized light ($n_l \neq n_r$).

n is defined as n = c/v, wherein c is the speed of light in vacuum and v is the velocity in the particular medium. The result is a different velocity of propagation for the left – and right polarized light. The consequence is a rotation of the polarization plane of the light. If the material absorbs at a special wavelength it has to be considered that also the extinction coefficients are different for left and right polarized light $\varepsilon_l \neq \varepsilon_r$. The difference between them is called circular dichroism $\Delta\varepsilon = \varepsilon_l - \varepsilon_r$. The outcome is that the projections of the electric field vectors differ in their velocity (angle-velocity) and their length and therefore lead to an elliptic polarization of the light. A plot of the circular dichroism versus the wavelength gives the CD spectrum.

The CD – spectrum of the optically active polyketone (R)-**5** and the corresponding UV/Vis spectrum are presented in Figure 4.16.

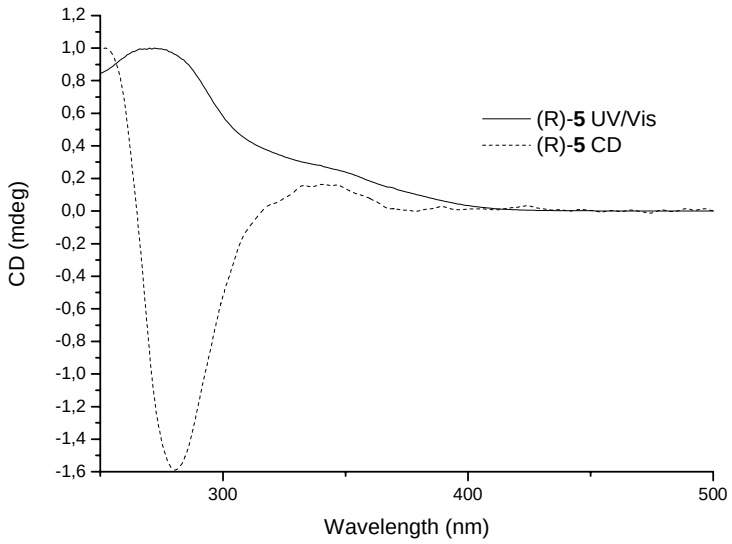

Figure 4.16: CD and UV/Vis spectra of polymer (R)-**5** in chloroform solution.

All data were obtained in dilute chloroform solution. In (R)-**5** there is an intense bisignate Cotton effect peaking at 278 nm. The spectrum resembles the CD – spectra of other polybinaphthyls and is characteristic for isolated binaphthyl - units.

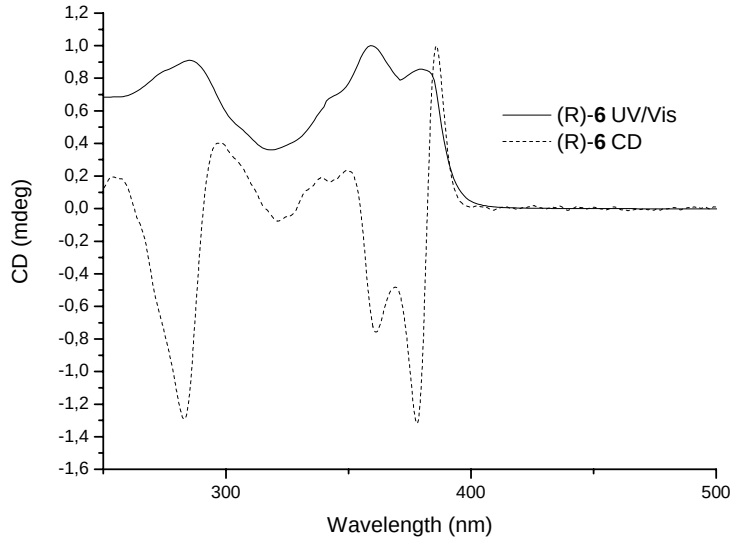

Figure 4.17: CD and UV/Vis spectra of polymer (R)-**6** in chloroform solution.

The spectrum of (R)-**6** is rather different and reflects the bathochromic shift of the UV/Vis spectrum on going from (R)-**5** to (R)-**6**. In analogy to the spectrum of (R)-**5** a first couplet with a positive peak at 290 nm is observed. The long wavelength region between 340 – 400 nm displays a series of well resolved bands. The signals can be interpreted as the superposition of two (or three) couplets with maxima/minima at 360, 378 and 385 nm, in good agreement with the absorption data (see Figure 4.17). The shape of the CD bands and the positions of the maxima in the $\pi - \pi^*$ transition reflect a strong exciton coupling between two dinaphthyl-benzene chromophores.[34;35] The sharp and well resolved signals also point towards a rigid, non-flexible arrangement of the chromophores. This finding indicates a helical conformation of the polymer backbone in the step – ladder polymer (R)-**6**.

4.3. Conclusion

A novel microwave – assisted non – aqueous Suzuki type cross – coupling reaction was applied to prepare a polyketone precursor (R)-**5**. It was subsequently cyclized in a polymer analogue Friedel – Crafts reaction, to give the step – ladder polymer (R)-**6**. To investigate the actual cyclization pattern of the polymer analogue reaction, two model compounds, resampling the repeating unit of poymer **6** were prepared. Extensive NMR spectroscopy and X – ray studies show that the cyclization exclusively occurs in the α – position of the

naphthalene unit. Also a statistical copolymer with extended chromophoric units between two binaphthyl units was prepared following the same synthetic strategy. The optical properties of all polymers and monodisperse model compounds were studied utilizing UV/Vis and PL spectroscopy. Through the statistical extension of the chromophoric units, it was possible to a certain degree to tune the optical properties. Furthermore, the optically active polymers (R)-**5** and (R)-**6** were examined by CD measurements, showing a well – structured CD spectrum for the step – ladder polymer (R)-**6**, which reflects a strong exciton coupling between adjacent chromophors. Such polymers of a stable helical conformation may find applications in areas such as chiral sensing, polarized light emission, nonlinear optics, or asymmetric catalysis.

4.4. Experimental Section

4.4.1. General Methods

For a general section concerning spectroscopic techniques and chemicals the reader is referred to chapter 2 of this thesis. CD – measurements have been carried out using a Jasco J-600 spectropolarimeter.

4.4.2. Synthesis

2,2'-Dioctyloxy-6,6'-dibromo-1,1'-binaphthyl-[(R)-**2]/[**(R/S)-**2]**

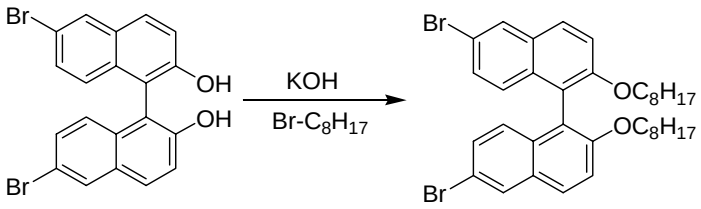

A solution of 6,6'-dibromo-1,1'-binaphthol (1) (10.0 g, 22.6 mmol) and KOH (3.6 g, 65 mmol) in anhydrous ethanol (200 mL) was degassed with argon and heated to reflux. Octylbromide (12.5 g, 65 mmol) was added slowly and the solution was refluxed for 12 hours. The reaction mixture was cooled down and filtered. The solid was then recrystallized from ethanol, filtered and dried under vacuum to afford **2** in 92 % yield. ^{1}H NMR (400 MHz, $C_2D_2Cl_4$, 25°C): δ = 7.94 (d, 2H, J = 1.9 Hz), 7.76 (d, 2H, J = 9.0 Hz), 7.34 (d, 2H, J = 9.0 Hz), 7.19 (dd, 2H, J = 1.9 Hz, J = 9.1 Hz), 6.92 (d, 2H, J = 9.0 Hz), 3.85 (m, 4H), 1.32 (m, 4H), 1.17 (m, 4H), 0.92 (m, 22H) ppm. ^{13}C NMR (100 MHz, CD_2Cl_4, 25 °C): δ = 155.1, 132.8, 130.3, 130.0, 129.5, 128.6, 127.5, 120.2, 117.3, 116.9, 69.8, 31.9, 29.5, 29.4, 29.3, 25.9, 22.9, 14.5 ppm. LR-MS (EI, 70eV): m/z = 44 (54.3), 444 (68.8), 668 [M^+] (100.0), 669 (38.3), 670 (46.2). Anal. Calcd. for $C_{36}H_{44}Br_2O_2$: C, 64.68; H, 6.63. Found: C, 64.68; H, 7.52.

2,2'-Dioctyloxy-1,1'-binaphthyl-6,6'-bis(4,4,5,5-tetramethyl-1,3,2-dioxaborolane) [(R)-**3**]/[(R/S)-**3**]

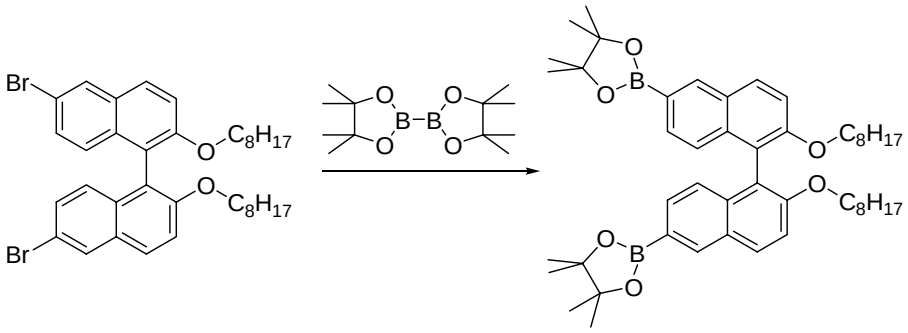

A two-neck roundflask was charged with 2,2'-dioctyloxy-6,6'-dibromo-1,1'-binaphthyl (2) (0.7 g, 1.05 mmol), Pd(dppf)Cl_2 (171 mg, 0.21 mmol), potassium acetate (1.03 g, 10.5 mmol) and sealed under argon. THF (35 mL) was added and stirred for 48 h at 80°C. The mixture was cooled down, water was added and extracted with chloroform. The combined organic layers were washed with water, dried over Na_2SO_4 and the solvent was removed under vacuum to give a brown oil. The crude mixture was purified by column chromatography on silica gel (95 % hexanes, 5 % ethyl acetate) to afford **3** as a thick yellow oil which solidified after a couple of weeks under atmospheric conditions in 85 % yield. ^{1}H NMR (400 MHz, $C_2D_2Cl_4$, 25°C): δ = 8.31 (s, 2H), 7.91 (d, 2H, *J* = 9.1 Hz), 7.46 (d, 2H, J = 8.6 Hz), 7.33 (d, 2H, J = 9.1 Hz), 7.00 (d, 2H, J = 8.6 Hz), 3.85 (m, 4H), 1.35 (m, 4H), 1.27 (s, 24H), 1.15 (m, 6H), 1.00 (m, 18H), 0.75 (t, 6H, J = 7.3 Hz) ppm. ^{13}C NMR (100 MHz, $C_2D_2Cl_4$, 25°C): δ = 155.9, 136.5, 136.1, 130.9, 130.2, 128.7, 124.8, 120.4, 116.0, 84.0, 69.9, 32.0, 29.7, 29.4, 25.9, 25.3, 25.2, 22.9, 14.5 ppm. LR-MS (EI, 70eV): m/z = 762 (45.6), 763 [M^+] (100.0), 764 (47.3). Anal. Calcd. for $C_{48}H_{68}B_2O_6$: C, 75.59; H, 8.99. Found: C, 74.58; H, 10.98.

Polyketone [(R**)-5]/[(**R/S**)-5]**

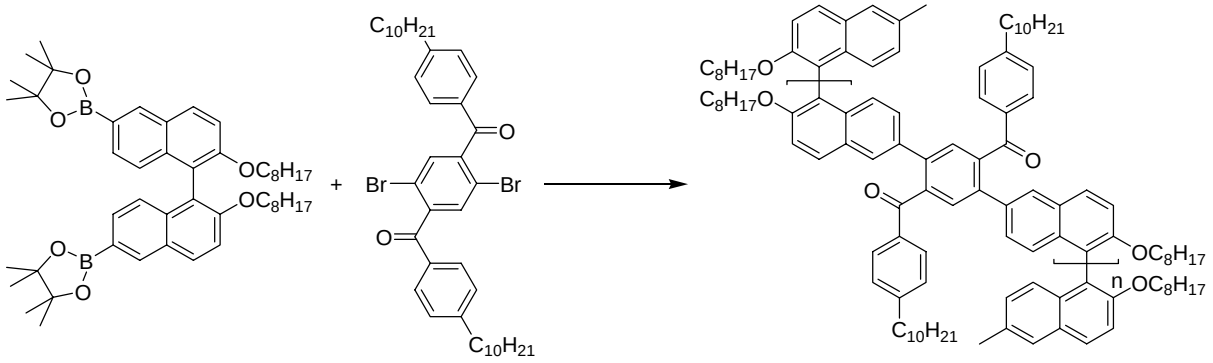

A dried 10 mL microwave-vessel equipped with a magnetic stirrer was charged with (**3**) (100 mg, 0.131 mmol), 1,4-bis(4',4''-decylbenzoyl)-2,5-dibromo-benzene (**4**), KOH (88 mg, 1.57

mmol) and $PdCl_2(PPh_3)_2$ (9.2 mg, 0.014 mmol). The vessel was filled with argon and evacuated several times. Then THF (3 mL) was added and the mixture irradiated in the microwave (300 W, 120 °C) for 12 min. Chloroform was added and the mixture extracted with 2 M HCl and water. The organic phase was dried over Na_2SO_4 and the solvent was removed. The residue was dissolved in chloroform, precipitated in methanol and soxhlet extracted with ethanol for one day and reprecipitated to methanol to give **5** as a grey solid in 45 % yield. GPC (vs polystyrene standards in THF) (**(R/S)-5**): M_n = 13,250, M_w/M_n = 1.6 (after extraction). GPC (vs polystyrene standards in THF) (**(R)-5**): M_n = 13,900, M_w/M_n = 1.6 (after extraction). ^{1}H NMR (400 MHz, $C_2D_2Cl_4$): δ =7.75 (s, 2H), 7.71 (d, 2H, J = 8.8 Hz), 7.63 (s, 2H), 7.60 (d, 4H, J = 7.6 Hz), 7.24 (d, 2H, J = 8.9 Hz), 7.12 (d, *J* = 8.7 Hz, 2H), 7.01 (d, 4H, *J* = 7.7 Hz), 6.85 (d, 2H, *J* = 8.6 Hz), 3.75 (m, 4H), 2.45 (m, 4H), 1.6 – 0.7 (m, 68H) ppm. ^{13}C NMR (100 MHz, CD_2Cl_4, 25°C): δ = 197.6 (C = O), 155.3, 149.0, 141.1, 139.7, 135.3, 134.3, 133.6, 130.5, 130.2, 129.5, 129.2, 128.4, 127.1, 126.0, 120.7, 116.7, 70.1, 36.1, 32.0, 31.8, 30.9, 29.7, 29.6, 29.6, 29.5, 29.4, 29.2, 25.8, 22.8, 22.7, 16.5, 14.2, 14.1 ppm.

Step-ladder polymer [(R)-**6]/[**(R/S)-**6]**

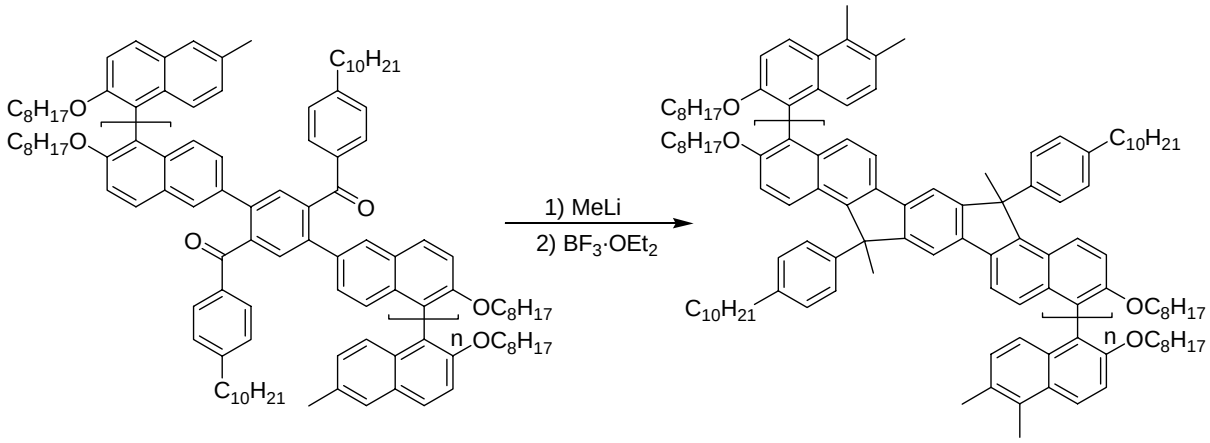

To a solution of (**5**) (140 mg, 0.13 mmol) in toluene (20 mL), MeLi (3.5 mL, 5.6 mmol) were added and stirred for 10 min. Then THF (15 mL) was added and the solution stirred for 16 h at room temperature. The reaction was quenched by adding ethanol (10 mL). The mixture was extracted with toluene until the aqueous layer was clear. The combined organic layers were washed with water, dried over Na_2SO_4, filtered and the solvent was removed under vacuum. The residue was dissolved in dichloromethane (15 mL) and $BF_3{\cdot}OEt_2$ (2 mL, 15.9 mmol) was added slowly. The mixture was stirred for 2 h under argon until ethanol (20 mL) and water (30 mL) were added. The organic layer was extracted with a $NaHCO_3$ solution and water. The

organic phase was dried over Na_2SO_4 and the solvent was removed. The residue was dissolved in chloroform and precipitated in methanol to afford **6** in 72 % yield. GPC (vs polystyrene standards in toluene) ((R/S)-**6**): M_n = 20,200, M_w/M_n = 2.0. GPC (vs polystyrene standards in THF) ((R)-**6**): M_n = 16,500, M_w/M_n = 1.6. ^{1}H NMR (400 MHz, $C_2D_2Cl_4$): δ = 7.7 – 6.6 (m, 18H), 3.75 (m, 4H), 2.6 (m, 4 H), 2.1 (m, 4H), 1.7 – 0.5 (m, 70H) ppm. ^{13}C NMR (100 MHz, $C_2D_2Cl_4$, 25°C): δ = 155.2, 154.2, 148.5, 142.3, 140.9, 139.0, 135.8, 135.1, 128.6, 128.6, 126.7, 126.6, 125.6, 123.1, 118.7, 116.3, 114.4, 70.1, 55.4, 35.8, 32.1, 31.8, 31.8, 31.3, 29.8, 29.7, 29.5, 29.2, 29.1, 25.8, 25.7, 22.8, 22.7, 22.7, 22.6, 14.2, 14.1 ppm.

Extended polyketone [(R/S**)-8]**

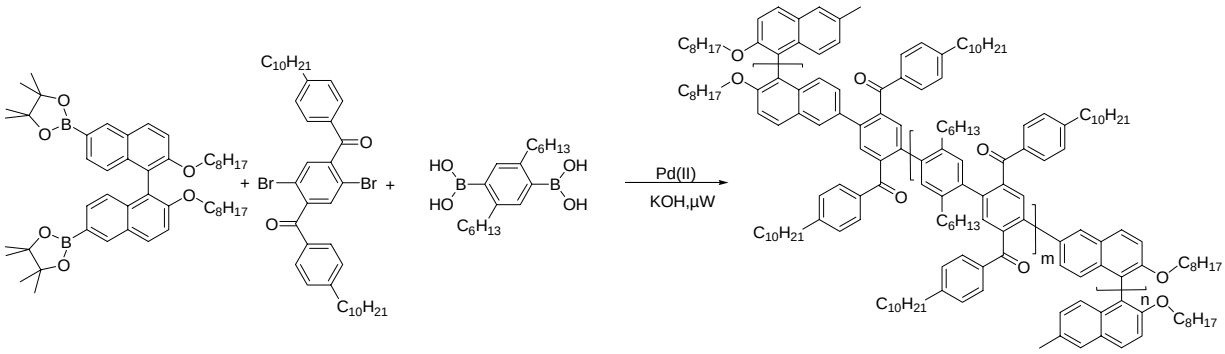

A dried 10 mL microwave-vessel equipped with a magnetic stirrer was charged with ((R/S)-**3**) (10.5 mg, 0.014 mmol), 1,4-bis-(4',4''-decylbenzoyl)-2,5-dibromo-benzene (**4**) (100 mg, 0.14 mmol), 1,4-di-hexyl-2,5-di-(boronic-acid)-phenyl (**7**) (41.4 mg, 0.124 mmol), KOH (93 mg, 1.66 mmol) and $PdCl_2(PPh_3)_2$ (19.4 mg, 0.03 mmol). The vessel was sealed under argon. Then THF (3 mL) was added and the mixture irradiated in the microwave (300 W, 120 °C) for 10 min. Chloroform was added and the mixture extracted with 2 M HCl and water. The organic phase was dried over Na_2SO_4 and the solvent was removed. The residue was dissolved in chloroform and precipitated in methanol to afford **8** (110 mg, 60 %, M_n = 10,608, PD = 1.9, GPC against PS-standards in THF) as a slightly grey powder. The precipitate was soxhlet extracted with ethanol for one day and reprecipitated to methanol to give (**8**) in 49 % yield as a grey solid. GPC (vs polystyrene standards in THF): M_n = 12,700, M_w/M_n = 1.6. ^{1}H NMR (400 MHz, $C_2D_2Cl_4$, 80°C): δ = 7.8 – 6.7 (m, 208H), 3.78 (m, 4H), 2.7 – 2.2 (m, 116H), 1.7 – 0.5 (m, 997H) ppm. ^{13}C NMR (100 MHz, $C_2D_2Cl_4$, 80°C): δ = 196.8, 148.7, 140.8, 138.9, 137.8, 137.5, 135.8, 131.0, 130.3, 129.8, 128.2, 36.1, 33.0, 32.0, 31.8, 31.0, 30.7, 29.8, 29.7, 29.5, 29.4, 29.2, 25.8, 22.8, 22.7, 14.2, 14.1 ppm.

Extended Stepp – ladder polymer [(R/S**)-9]**

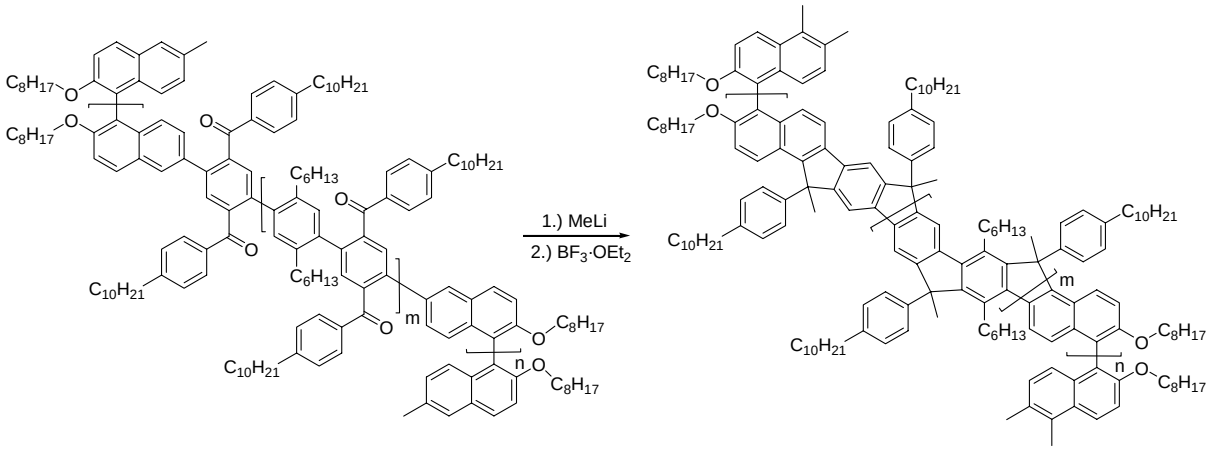

To a solution of (**8**) (120 mg) in toluene (20 mL), MeLi (3.5 mL, 5.6 mmol) were added and stirred for 10 min. Then THF (15 mL) was added and the solution stirred for 16 h at room temperature. A solution of ethanol/water (50 mL/100 mL) was added. The mixture was extracted with toluene until the aqueous layer was clear. The combined organic layers were washed with water, dried over Na_2SO_4, filtered, and the solvent was removed under vacuum. The residue was dissolved in dichlormethane (15 mL) and $BF_3{\cdot}OEt_2$ (2 mL, 15.9 mmol) was added slowly. The mixture was stirred for 2 h under argon. Then ethanol (20 mL) and water (30 mL) were added. The organic layer was extracted with a $NaHCO_3$ solution and water. The organic phase was dried over Na_2SO_4 and the solvent was removed. The residue was dissolved in chloroform and precipitated in methanol to afford (**9**) 85 % yield. GPC (vs polystyrene standards in THF): M_n = 16,600, M_w/M_n = 1.7. ^{1}H NMR (400 MHz, $C_2D_2Cl_4$, 25°C): δ = 7.9 – 6.4 (m, 122H), 3.80 (m, 4H), 3.1 – 0.1 (m, 836H) ppm. ^{13}C NMR (100 MHz, $C_2D_2Cl_4$, 25°C): δ = 155.9, 152.7, 143.3, 140.3, 138.6, 132.6, 128.3, 128.2, 126.7, 118.4, 54.3, 35.7, 32.0, 31.8, 31.3, 30.2, 29.7, 29.4, 25.7, 23.1, 22.8, 14.2, 14.1 ppm.

2-Bromo-6-ocytloxy-naphthalene (11)

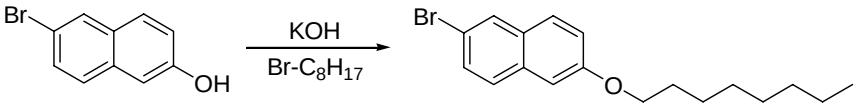

A solution of 2-bromo-6-naphthol (10.0 g, 44.8 mmol) and KOH (7.5 g, 134.5 mmol) in anhydrous ethanol (200 mL) was degassed with argon and heated to reflux. *n*-octylbromide (23.3 mL, 134.4 mmol) was added slowly and the solution was refluxed for 12 hours. The reaction mixture was cooled down and filtered. The solid was then stirred in water (200 mL) for 1 hour, filtered and dried under vacuum. Yield: 12.0 g (80 %). ^{1}H NMR (400 MHz, $CDCl_3$, 25°C): δ = 7.9 (s, 1H), 7.7 (d, 1H, J = 8.7 Hz), 7.6 (d, 1H, J = 8.7 Hz), 7.5 (dd, 1H,

J = 8.7 Hz, J = 2.0 Hz), 7.2 (dd, 1H, J = 8.7 Hz, J = 2.0 Hz), 7.1 (ps, 1H, J = 2.0 Hz), 4.1 (t, 2H, O-CH_2), 1.9 (q, 2H), 1.5 (q, 2H), 1.4 (m, 8H), 0.9 (t, 3H) ppm. ^{13}C NMR (100 MHz, $CDCl_3$ 25°C): δ = 157.4, 133.1, 129.9, 129.6, 129.5, 128.4, 128.3, 120.1, 116.9, 106.6, 68.1 (O-CH_2), 31.8, 29.4, 29.2, 29.2, 26.1, 14.1 ppm. LR-MS (EI, m/z): 222 (100.0), 224 (85.1), 334 (19.9), 336 [M^+] (23.2).

2-Octyloxy-6-yl-(4,4,5,5-tetramethyl-1,3,2-dioxaborolane)naphthalene (12)

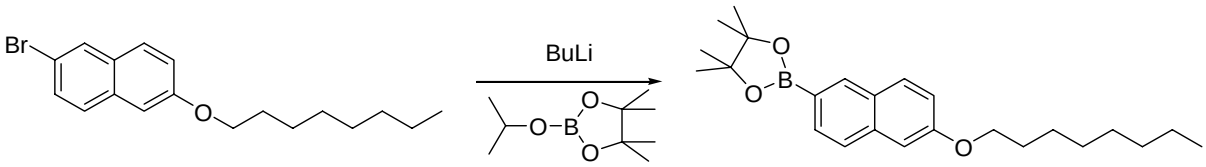

To a solution of (**11**) (5.0 g, 14.9 mmol) in diethylether (65 mL) at – 78 °C was added dropwise n-BuLi (16 mmol). The solution was stirred at – 78 °C for 30 minutes and then at 0°C for 2 h. The temperature was again lowered to – 78 °C and 2-isopropoxy-4,4,5,5-tetramethyl-1,3,2-dioxaborolane (4.3 g, 23 mmol) was added all at once. The solution was allowed to return to room temperature slowly and then stirred overnight before being poured into water. The water was then extracted with dichloromethane, which was subsequently washed with water and brine, dried over $MgSO_4$ and the solvent was removed by rotary evaporation. The residue was purified by column chromatography on silica gel with (98 % hexanes, 2 % ethyl-acetate) as eluent to give a pale yellow solid (3.0 g, 53 %). ^{1}H NMR (400 MHz, $CDCl_3$, 25°C): δ = 8.3 (s, 1H), 7.8 (d, 1H, J = 8.1 Hz), 7.75 (d, 1H, J = 9.2 Hz), 7.7 (d, 1H, J = 8.1 Hz), 7.8 (d, 1H, J = 8.1 Hz), 7.15 (m, 2H), 4.1 (t, 2H, J = 6.6 Hz), 1.85 (quin., 2H, J = 6.6 Hz, J = 7.6 Hz), 1.5 (quin., 2H, J = 8.1 Hz, J = 7.1 Hz), 1.4 (s, 12H), 1.3 (m, 8H), 0.9 (t, 3H) ppm.^{13}C NMR (100 MHz, $CDCl_3$ 25°C): δ = 158.1, 136.5, 136.0, 131.0, 130.1, 128.3, 125.8, 124.2, 119.0, 106.4, 83.7, 68.0, 31.8, 29.4, 29.2, 29.2, 26.1, 24.9, 22.6, 14.0 ppm. LR-MS (EI, m/z): 170 (54.1), 270 (43.2), 382 [M^+] (100.0).

4',4''-Didecyl-2,5-bis(4,4,5,5-tetramethyl-1,3,2-dioxaborolato)-terephthalophenone (13)

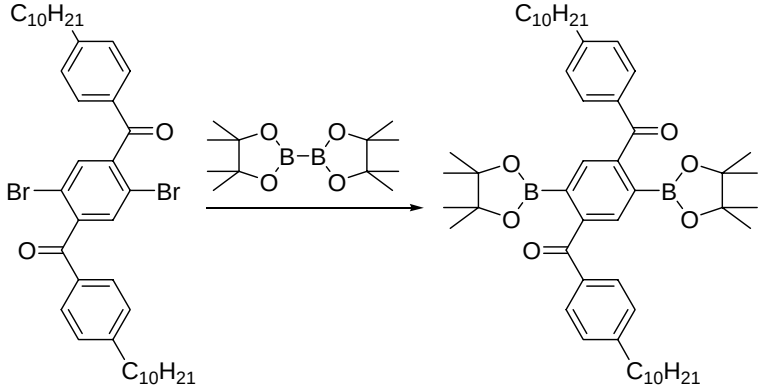

A mixture of 1,4-bis-(4,4'-decylbenzoyl)-2,5-dibromo-benzene (100 mg, 0.14 mmol), bis(pinacolato)diborolane (140 mg, 0.55 mmol), Pd(dppf)Cl_2 (45 mg, 0.56 mmol) and potassium acetate (165 mg, 1.68 mmol) in THF (4 mL) was stirred at 80°C for 24 h. The mixture was extracted with dichloromethane and washed with water and brine several times. The solvent was removed under reduced pressure. The residue was was recrystallized from hexanes to give **13** in 70 % yield. ^{1}H NMR (400 MHz, $C_2D_2Cl_2$, 25 °C): δ = 7.77 (s, 2H), 7.60 (d, 4H, J = 8.1 Hz), 7.18 (d, 4H, J = 8.1 Hz), 2.58 (t, 4H, J = 7.6 Hz), 1.53 (m, 4H), 1.20 (m, 30H), 0.95 (m, 24H), 0.80 (t, 6H, J = 6.8 Hz) ppm. ^{13}C NMR (100 MHz, $CDCl_3$, 25°C): δ = 198.2, 149.3, 145.8, 135.9, 133.3, 130.5, 128.8, 84.6, 36.3, 32.3, 32.2, 31.5, 29.8, 29.8, 29.7, 29.6, 29.4, 24.6, 23.0, 14.5 ppm. LR-MS (EI, m/z): 760 (65.2), 761 (100.0), 819 [M^+] (6.2).

1,4-Bis(6-octyloxynaphth-2-yl)-2,5-bis-(4-decyclbenzoyl)benzene (14)a

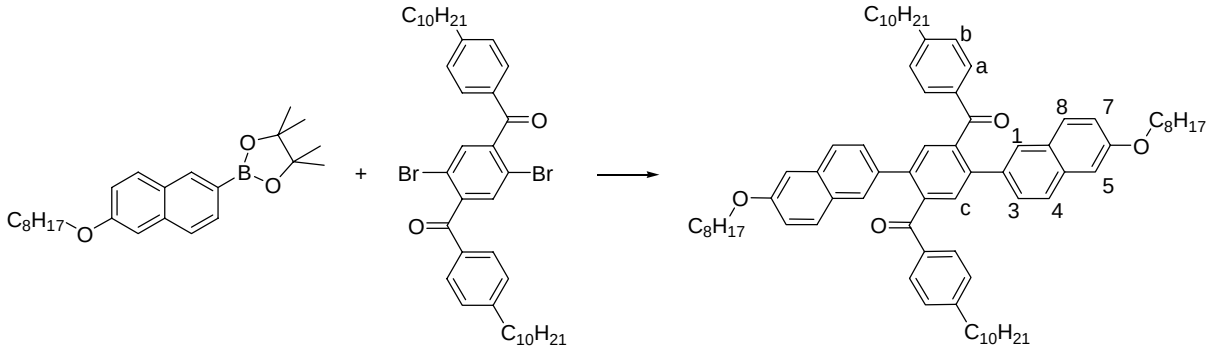

A dried 80 mL microwave-vessel equipped with a magnetic stirrer was charged with 1,4-bis-(4',4''-decylbenzoyl)-2,5-dibromo-benzene (339 mg, 0.47 mmol), **4** (447 mg, 1.17 mmol), KOH (309 mg, 5.5 mmol) and $PdCl_2(PPh_3)_2$ (65.6 mg, 0.09 mmol). The vessel was filled with argon and evacuated several times. Then THF (21 mL) was added and the mixture irradiated in the microwave (300 W, 120 °C) for 30 min. Chloroform was added and the mixture

extracted with 2 M HCl, brine and water. The organic phase was dried over Na_2SO_4 and the solvent was removed. The residue was dissolved in chloroform, precipitated in methanol, filtered of and purified by column chromatography on silica gel (95 % hexanes, 5 % ethyl-acetate). The received slightly yellow solid was recrystalized from ethyl-acetate to give (**6**) as a colorless powder (320 mg, 63.5 %). ^{1}H NMR (400 MHz, $CDCl_3$): δ = 7.76 (d, 2H, J = 1.4 Hz, H-1), 7.74 (s, 2H, H-a), 7.69 (d, 4H, J = 8.1 Hz, H-b), 7.64 (d, 2H, J = 9.0 Hz, H-8), 7.57 (d, 2H, J = 8.5 Hz, H-4), 7.44 (dd, 2H, J = 1.5 Hz, J = 8.4 Hz, H-3), 7.12 (dd, 2H, J = 2.1 Hz, J = 9.0 Hz, H-7), 7.07 (d, 2H, J = 8.1 Hz, H-c), 7.02 (d, 2H, J = 2.1 Hz, H-5), 4.05 (t, 4H, J = 6.6 Hz, O-CH_2), 2.5 (t, 4H, J = 7.6 Hz, -Ar-CH_2), 1.9 (quint., 4H, J = 6.62 Hz, J = 7.8 Hz, O-CH_2-$\underline{C}H_2$), 1.5 (m, 8H), 1.4-1.2 (m, 44H), 0.9 (2t, 12H, CH_3) ppm. ^{13}C NMR (100 MHz, $CDCl_3$): δ = 197.7, 157.9, 149.2, 141.1, 139.7, 135.2, 134.5, 134.0, 130.6, 130.2, 129.7, 128.8, 128.5, 128.4, 127.6, 127.0, 119.7, 107.2, 68.6, 36.1, 32.0, 32.0, 30.9, 29.7, 29.7, 29.5, 29.6, 29.5, 29.4, 29.4, 29.3, 26.3, 22.8, 22.8, 14.2, 14.1 ppm. IR (neat) ν (cm^{-1}): 3030, 2954, 2923, 2848, 2360, 1656 (C=O), 1602, 1196. FD-MS: 1076.5 (100.00).

1,4-Bis(6-octyloxynaphth-2-yl)-2,5-bis-(4-decyclbenzoyl)benzene (14)b

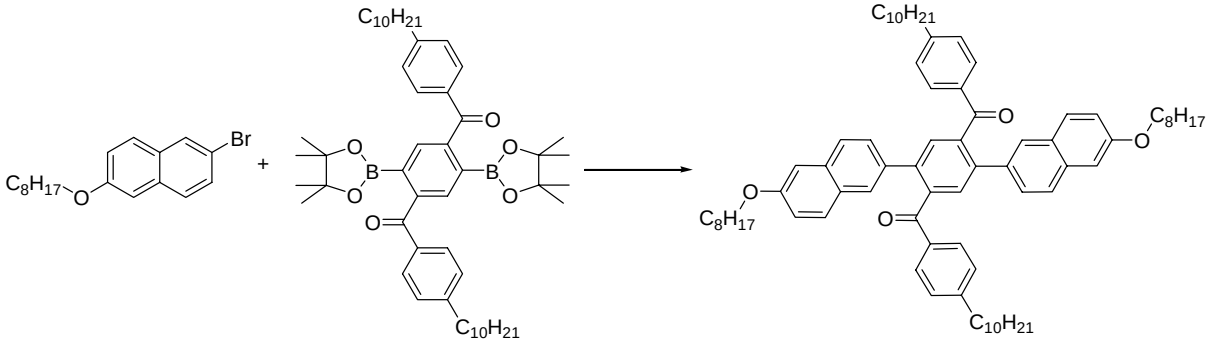

The synthetic procedure was similar to that described on the page before. The spectroscopic data are similar to the above described values.

Ladder oligomer (15a)

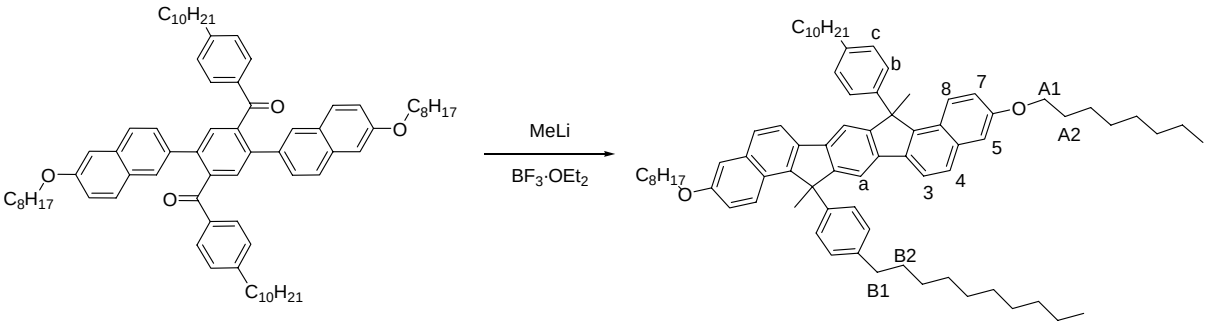

A stirred solution of (**13**) (130 mg, 0.121 mmol) in toluene (20 mL) was treated with Methyllithium (2 mL, 3.2 mmol) stirred for 15 min. and THF (15 mL) was also added. The mixture was stirred for 16 h at room temperature and quenched carefully with ethanol and water. The organic layer was isolated and washed with water, dried over Na_2SO_4 and the solvent was removed by rotary evaporation. The crude product was redissolved in dichloromethane (15 mL) and treated with borontrifluoride etherate (2 mL). The solution was stirred at room temperature for two hours and then ethanol (20 mL) followed by water (30 mL) was added to quench the excess borontrifluoride etherate. Chloroform was added and the organic layer was washed several times with a $NaHCO_3$ solution and water, dried over Na_2SO_4 and the solvent was removed by rotary evaporation. The residue was purified by column chromatography on silica gel (98 % hexanes, 2 % ethyl-acetate) to afford 14 as a colorless to slightly yellow oil in 92 % yield. ^{1}H NMR (400 MHz, $C_2D_2Cl_4$, 25°C): δ = 7.81 (dd, 2H, J = 1.7 Hz, J = 8.4 Hz, H-3), 7.71 (d, 2H, J = 8.4 Hz, H-4), 7.55 (s, 2H, H-a), 7.38 (dd, 2H, J = 3.7 Hz, J = 9.2 Hz, H-8), 7.17 (d, 2H, J = 2.2 Hz, H-5), 7.11 (pt, 4H, J = 8.1 Hz, H-b), 7.00 (pt, 4H, J = 8.0 Hz, H-c), 6.93 (dd, 2H, J = 2.2 Hz, J = 9.2 Hz, H-7), 4.00 (t, 4H, J = 6.5 Hz, A1), 2.50 (t, 4H, J = 7.5 Hz, B1), 2.00 (s, 6H, CH_3(bridge)), 1.76 (quin., 4H, J = 6.7 Hz, A2), 1.55 (m, 4H, B2), 1.43 (m, 8H), 1.26 (m, 20H), 0.85 (m, 12H) ppm. ^{13}C NMR (100 MHz, $C_2D_2Cl_4$, 25°C): δ = 156.4, 155.0, 154.9, 148.7, 148.7, 141.9, 141.8, 141.2, 141.1, 139.0, 139.0, 136.0, 136.0, 135.3, 128.7, 127.7, 126.7, 126.6, 126.3, 126.3, 124.9, 119.5, 119.1, 114.6, 108.5, 68.2, 55.1, 35.8, 32.1, 32.1, 31.7, 31.5, 31.5, 30.5, 30.0, 29.8, 29.7, 29.6, 29.6, 29.5, 29.5, 26.4, 25.6, 25.6, 23.0, 14.5 ppm.

2,5-Dibromo-dimethyl-terephthalate (17)

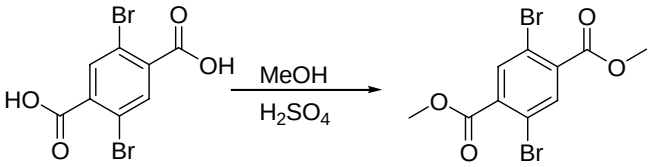

2,5-dibromo-terephthalic acid (4.0 g, 12.3 mmol) was stirred in methanol (60 mL), sulfuric acid (2 mL) was added and the mixture was heated to reflux for 24 h. The mixture was poured into water and extracted with dichlormethane. The solvent was removed under reduced pressure and the residue recrystallized from dichlormethane/heptane to afford **17** in 91 % yield as white crystalls. ^{1}H NMR (400 MHz, $CDCl_3$, 25°C): δ = 7.96 (s, 2H), 3.86 (s, 6H) ppm.^{13}C NMR (100 MHz, $CDCl_3$, 25°C): δ = 164.8, 136.8, 135.6, 120.5, 74.5, 74.2, 73.9, 53.4 ppm. LR-MS (EI, m/z): 321 (100.0), 224 (323 (49.8), 350 (41.2), 352 [M^+] (78.5), 354 (40.3). Anal. Calcd. for $C_{10}H_8Br_2O_4$: C, 34.12; H, 2.29. Found: C, 34.15; H, 2.18.

2,5-Bis(6-methoxynaphth-2-yl)-terephthalic acid dimethyl ester (19)

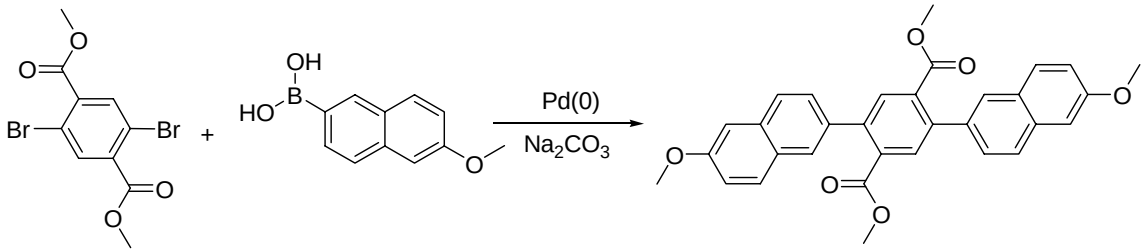

A dried 50 mL Schlenk flask was charged with **1** (150 mg, 0.43 mmol), 6-methoxy-2-boronic-acid-naphthalene (216 mg, 1.07 mmol) and K_2CO_3 (177 mg, 1.28 mmol). Degassed toluene (5 mL) and water (2.5 mL) was added and the mixture heated to 80°C for 30 min. Then $(PPh_3)_4Pd$ (20 mg, 20 µmol), dissolved in toluene were added and the mixture was stirred for 48 h. The mixture was poured into water, extracted with chloroform and the organic layer dried over Na_2SO_4. After the solvent was removed, the crude product was recrystallized from THF to afford a white powder in 84 % yield. ^{1}H NMR (400 MHz, CD_2Cl_4, 80°C): δ = 7.88 (s, 2H), 7.74 (d, 6H, J = 9.1 Hz), 7.42 (dd, 2H, J = 1.6 Hz, J = 8.3 Hz), 7.17 (m, 4H), 3.91 (s, 6H), 3.61 (s, 6H). ^{13}C NMR (100 MHz, $CDCl_3$ 25°C): δ = 168.4, 158.4, 141.2, 135.5, 134.2, 133.6, 132.4, 129.9, 129.0, 127.5, 127.3, 126.7, 119.3, 106.6, 55.7, 52.3 ppm. IR (neat) ν (cm^-

[1]): 2929, 1716 (C=O), 1630, 1499, 1380, 1273, 1242, 854, 828. LR-MS (EI, m/z): 506 [M^+] (100.0). Anal. Calcd. for $C_{32}H_{26}O_6$: C, 75.88; H, 5.17. Found: C, 74.13; H, 4.51.

Ladder oligomer (20)

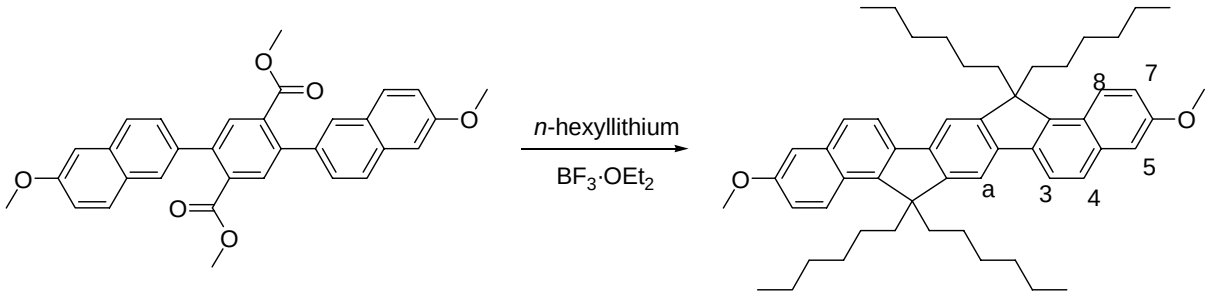

An excess of *n*-hexyl lithium (3 mL, 1.6 M in hexane) was added to a solution of **4** (250 mg, 0.49 mmol) in THF (30 mL) and stirred for 16 h at room temperature. Chloroform was added, and the solution washed with 2 N HCl. The organic phase was dried with Na_2SO_4, and the solvent was removed by rotary evaporation. The residue was redisolved in dichlormethane, treated with an excess of boron trifluoride and stirred for 3 h. Then an ethanol/water mixture (70 mL, 5:2) was added and the organic layer washed with water and diluted $NaHCO_3$-solution. The solvent was removed by rotary evaporation. The residue was purified by column chromatography on silica gel with toluene/hexanes (5:95) as eluent to afford **5** as white crystals (55 %). ^{1}H NMR (400 MHz, CD_2Cl_4, 25°C): δ = 8.06 (d, 2H, J = 9.2 Hz, H-3), 7.88 (d, 2H, J = 8.4 Hz, H-8), 7.72 (d, 2H, J = 8.4 Hz, H-7), 7.66 (s, 2H, H-a), 7.21 (d, 2H, J = 2.5 Hz, H-5), 7.16 (dd, 2H, J = 2.5 Hz, J = 9.1 Hz, H-4), 3.89 (s, 6H, OCH_3), 2.40 (m, 4H), 2.21 (m, 4H), 0.86 (m, 12H), 0.57 (t, 6H, J = 6.8 Hz), 0.38 (m, 4H) ppm. ^{13}C NMR (100 MHz, CD_2Cl_4, 25°C): δ = 156.5, 151.2, 144.9, 140.7, 137.9, 134.8, 127.1, 126.2, 125.4, 119.3, 118.6, 112.6, 108.1, 57.1, 55.6, 40.8, 31.6, 29.7, 23.7, 22.6, 14.2 ppm. LR-MS (EI, m/z): 750 (100.0), 751 [M^+] (59.3), 752 (7.0). Anal. Calcd. for $C_{54}H_{70}O_2$: C, 86.35; H, 9.39. Found: C, 86.02; H, 9.25.

References and Notes

[1] B. S. Nehls, E. Preis, S. Füldner, T. Farrell, U. Scherf, *Macromolecules* **2005,** *38*, 687.

[2] L. Pu, *Chem.Rev.* **1998,** *98*, 2405.

[3] L. Pu, *Chem.Rev.* **2004,** *104*, 1687.

[4] H. C. Zhang, L. Pu, *Tetrahedron* **2003,** *59*, 1703.

[5] H. C. Zhang, L. Pu, *Macromolecules* **2004,** *37*, 2695.

[6] D. Cai, D. Hughes, T. Verhoeven, P. Reider, *Org.Synth.* **1998,** *76*, 1.

[7] J. C. Ostrowski, R. A. Hudack, M. R. Robinson, S. Wang, G. C. Bazan, *Chem.Eur.J.* **2001,** *7*, 4500.

[8] C. S. Wang, H. S. Fei, Y. Qui, Y. Yang, Z. Q. Wei, *Appl.Phys.Lett.* **1999,** *74*, 19.

[9] M. Suarez, G. B. Schuster, *J.Am.Chem.Soc.* **1995,** *117*, 6732.

[10] Y. F. Zhang, *J.Org.Chem.* **1995,** *60*, 7192.

[11] N. P. M. Huck, W. F. Jager, B. Delange, B. L. Feringa, *Science* **1997,** *276*, 341.

[12] N. P. M. Huck, W. F. Jager, B. Delange, B. L. Feringa, *Science* **1996,** *273*, 1686.

[13] M. Schadt, *Ann.Rev.Mater.* **1997,** *27*, 305.

[14] G. P. Dado, S. H. Gellman, *J.Am.Chem.Soc.* **1994,** *116*, 1054.

[15] D. S. Schlitzer, B. M. Novak, *J.Am.Chem.Soc.* **1998,** *120*, 2196.

[16] J. S. Moore, C. B. Gorman, R. H. Grubbs, *J.Am.Chem.Soc.* **1991,** *113*, 1712.

[17] E. Peters, M. P. T. Christiaans, R. A. J. Janssen, H. F. Schoo, H. P. J. M. Dekkers, E. W. Meijer, *J.Am.Chem.Soc.* **1997,** *119*, 9909.

[18] R. B. Prince, L. Brunsveld, E. W. Meijer, J. S. Moore, *Angew.Chem.Int.Ed.* **2000,** *39*, 228.

[19] Y. J. Dai, T. J. Katz, D. A. Nichols, *Angew.Chem.Int.Ed.* **1996,** *35*, 2109.

[20] M. B. Goldfinger, K. B. Crawford, T. M. Swager, *J.Am.Chem.Soc.* **1997,** *119*, 4578.

[21] T. Rabe, M. Hoping, D. Schneider, E. Becker, H. H. Johannes, W. Kowalsky, T. Weimann, J. Wang, P. Hinze, B. S. Nehls, U. Scherf, T. Farrell, T. Riedl, *Adv.Funct.Mater.* **2005,** *15*, 1188.

[22] Q. Hu, D. Vitharana, G. Liu, V. Jain, M. Wagaman, L. Zhang, T. R. Lee, L. Pu, *Macromolecules* **1996,** *29*, 1082.

[23] M. Noji, K. Nakajima, K. Koga, *Tetrahedron Lett.* **1994,** *35*, 7983.

[24] G. D. Y. Sogah, D. J. Cram, *J.Am.Chem.Soc.* **1979,** *101*, 3035.

[25] T. Hattori, K. Sakurai, N. Koike, S. Miyano, H. Goto, F. Ishiya, N. Harada, *J.Am.Chem.Soc.* **1998,** *120*, 9086.

[26] H. Benmansour, T. Shioya, Y. Sato, G. C. Bazan, *Adv.Funct.Mater.* **2003,** *13*, 883.

[27] T. Ishiyama, M. Murata, N. Miyaura, *J.Org.Chem.* **1995,** *60*, 7508.

[28] U. Scherf, K. Müllen, *Macromol.Rapid Commun.* **1991,** 489.

[29] U. Scherf, E. J. W. List, *Adv.Mater.* **2002,** *14*, 477.

[30] G. Fytas, H. G. Nothofer, U. Scherf, D. Vlassopoulos, G. Meier, *Macromolecules* **2001,** *35*, 481.

[31] Q. Hu, D. Vitharana, G. Liu, V. Jain, L. Pu, *Macromolecules* **1996,** *29*, 5075.

[32] J. Jacob, J. Zhang, A. C. Grimsdale, K. Müllen, M. Gaal, E. J. W. List, *Macromolecules* **2003,** *36*, 8240.

[33] S. F. Mason, *Molecular Optical Activity and the Chiral Discriminations*, Cambridge University Press, New York **1982,** p. 72.

[34] B. Köhler, V. Enkelmann, M. Oda, S. Pieraccini, G. P. Spada, U. Scherf, *Chem.Eur.J.* **2001,** *7*, 3000.

[35] N. Harada, K. Nakannishi, *Circular Dichrotic Spectroscopy - Exciton Coupling in Organic Spectroscopy*, Oxford University Press, Oxford **1983**.

5. Statistical Binapthyl 9,9-dioctyl-fluorene copolymers

5.1. Introduction and Motivation

Polyfluorenes (PF) are a class of organic semiconductors that have been intensively investigated over the past few years,[1;2] as they combine efficient blue photo – or electroluminescence with the possibility of chain alignment in the liquid crystalline phase, and allowing the design of light emitting diodes (LEDs) with linearly polarized emission.[3;4] They have also received attention due to their very promising performance in organic solid state lasers[5;6] and photovoltaic devices.[7] The photophysical properties of PFs are known to vary strongly with the morphology of the films. Therefore, a particular interest has been devoted to the packing behaviour of the polymer chains in solid state films, especially in the case of poly(9,9-dioctylfluorene) (PFO). For this polymers, in addition to the regular glassy α–phase , a second, so called β-phase has been identified. This phase is characterized by high intrachain order with nearly no distortion between adjacent fluorene units.[8] The planarization is driven by a unique side – chain ordering (side chain crystallization) leading to an increased π – conjugation within the polymer chain if compared to the distorted glassy state.[9] Characteristic for the β-phase is a distinct red-shift of absorption and emission and a remarkably well – resolved vibronic progression both in absorption and emission.

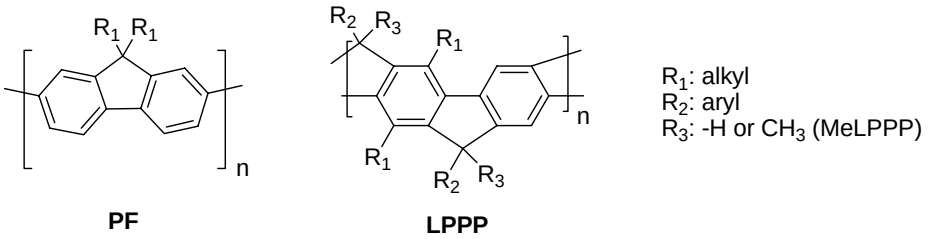

Scheme 5.1: Structure of 9,9-dialkyl-polyfluorene and a planarized PPP-type ladder polymer (**LPPP**).

A comparison to PPP – type polymers with a fully planarized backbone (ladder – type PPP; LPPP) shows very similar absorption and emission characteristics for the β – phase of polyfluorene and LPPP. In PFO films, the glassy α – and the β – phase can coexist and therefore their absorption and emission spectra are superimposed and it can be difficult to separate the contributions unless one phase dominates. However, Ariu et al. noticed a strong fraction of luminescence from the β – phase, even when their contribution to the absorption is low, indicating that an efficient energy migration towards the lower energy sites of the β – phase excited states occurs.[10;11] The actual concentration of the β – phase was found to depend strongly on the used solvent and post – deposition treatment.[10;12] It has been shown that PFO films containing even low fractions of the β – phase suffer from a serious deterioration of the low – temperature PL quantum efficiency, most probably due to an increased amount of accessible quenching polarons.[11] This quenching effect is expected to be even more dramatic in organic solid - state lasers at high excitation densities, necessary to reach the lasing threshold, which are several orders of magnitude higher than those used in PL measurements or OLEDs. In addition, any absorption introduced by polaronic species – although very small, is particularly detrimental in lasing applications, as this losses to the laser waveguide, considerably affecting the threshold. So, even if the influence of β – phase PF in conventional PL experiments may be negligible, it is a major issue for organic lasers. Therefore, the elimination of β – formation is of fundamental interest and promises particular improvements for organic thin film lasers.

During recent years many approaches have been employed to reduce the tendency of PFs to aggregate, like the introduction of bulky - or dendronized side groups.[13;14] However, our herein presented strategy is the introduction of distorted 1,1'-binaphthyl main – chain units into the PFO backbone.

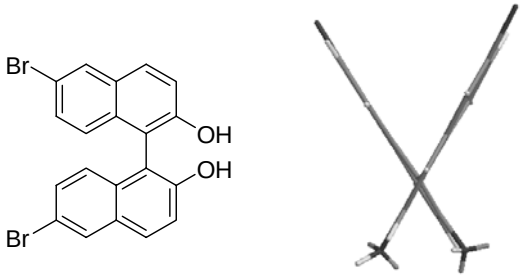

Scheme 5.2: Structure of 6,6'-dibromo-2,2'-dihydroxy-1,1'-binaphthyl and top view of a MM2 – optimized geometry model.

The idea stems from the perception, that non – planar building blocks disturb the regular polymer structure and therefore suppress interchain interactions. The randomly distributed binaphthyl units within the PFO chain should alter the packing in the solid state and facilitate the formation of the amorphous glassy state.[15-17]

5.2. Results and Discussion

5.2.1. Monomer and Polymer Synthesis

The first step towards the desired class of copolymers is the synthesis of suitable monomers as outlined in Scheme 5.3. 9,9-Dioctyl-2,7-dibromofluorene was obtained by alkylation of 2,7-dibromofluorene under basic conditions.[19] The preparation of compound **4** has already been described in chapter 4. Further studies have shown that melting of the monomers under high vacuum is suitable to eliminate even traces of alcohols, which may remain from the work-up procedure. Residues of protic compounds lead to a soft dehalogenation of the dibromo monomers as side reaction during the aryl – aryl coupling after the Yamamoto reaction, thus limiting the molecular weight of the obtained polymers.

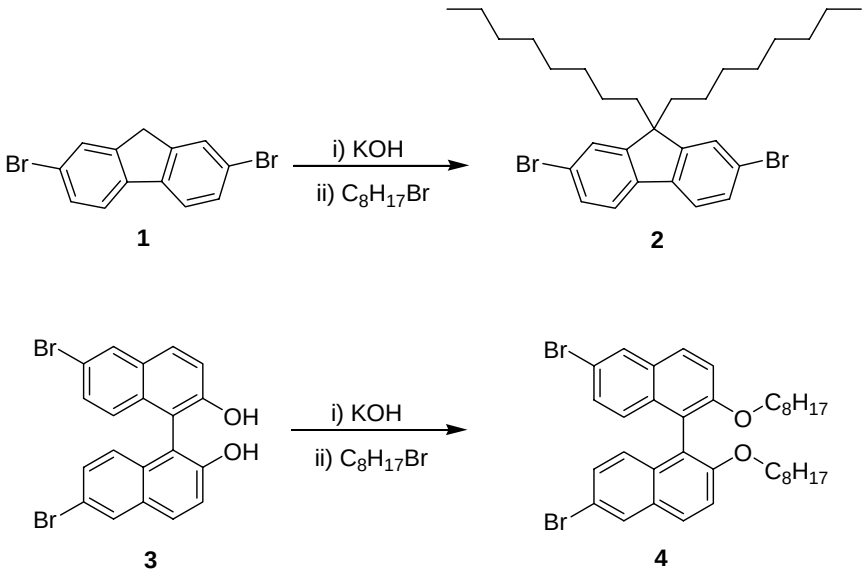

Scheme 5.3: Synthetic route towards the monomers **2** and **4**.

It was anticipated that the Ni(0)-mediated aryl-aryl coupling protocol would be suitable to prepare high molecular weight fluorene copolymers containing randomly incorporated binaphthyl spacers. Polymer preparation has been carried out utilizing conventional and

microwave – assisted protocols. It was shown in earlier investigations that microwave – assisted reactions give the desired polymers in high yields and molecular weights within 10 – 12 min.[20-22] However, to provide polymers in a multigram scale it was more convenient to prepare them via conventional protocols. Both kinds of reactions utilize $Ni(COD)_2$ /bipyridine as the catalytic system.[19] Motivated by investigations of Hagberg et al. the solvent system was changed from DMF/toluene mixtures to pure THF to stabilize the reactive nickel species. This change resulted in increased molecular weights and more convenient handling.[23]

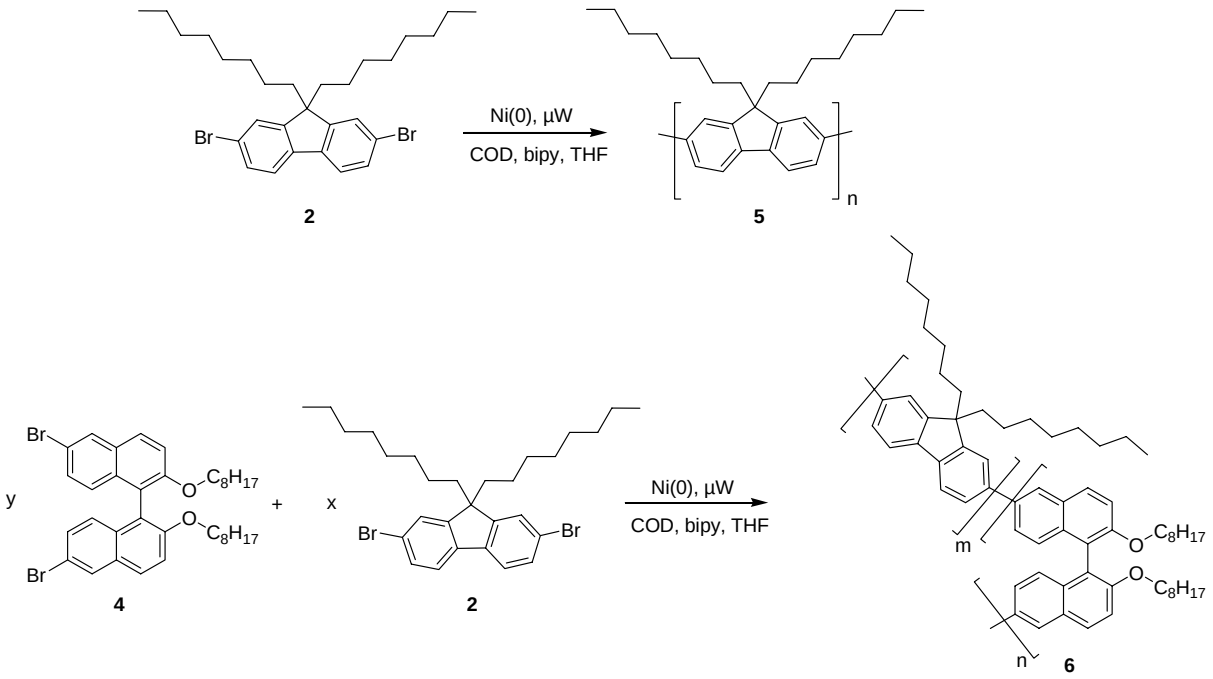

Scheme 5.4: Molecular structures of PFO (**5**) and the statistical copolymers incorporating binaphthyl spacers BNPFO (**6**).

Different copolymers were synthesized simply by using varying feed ratios of the comonomers **2** and **4** (see Table 5.1). The molecular weights were determined by routine size exclusion chromatography measurements. Therein the number average molecular weights were determined to be in the range of M_n = 90,000 – 140,000 g/mol with polydispersities between 1.6 and 2.1, (after extraction with ethyl acetate).

Table 5.1: Feed ratios for the homopolymer **5**, the statistical copolymers **6a - 6c** and copolymer compositions, predicted and estimated byNMR spectroscopy.

Name	x (mmol)	y (mmol)	y/(x+y) (%)	n/(m+n) (%)	Mn	PD
PFO (**5**)	2.01	0			190,000	2.4
BNPFO-5% (**6a**)	2.01	0.11	5.19	4.24	90,000	2.1
BNPFO-10% (**6b**)	2.01	0.22	9.87	9.44	160,000	2.2
BNPFO-15% (**6c**)	2.01	0.30	12.99	12.05	128,000	1.6

Figure 5.1 displays the ^{1}H NMR spectrum of **6b** for better understanding. The amount of incorporated binaphthyl units was calculated by comparing the relative integrals of the –O-CH_2 proton signal at $\delta = 3.9$ ppm from the binaphthyl moiety to the sum of the aryl and the alkyl proton signals, respectively. The average value of these two numbers gives the incorporated amount of binaphthyl units.

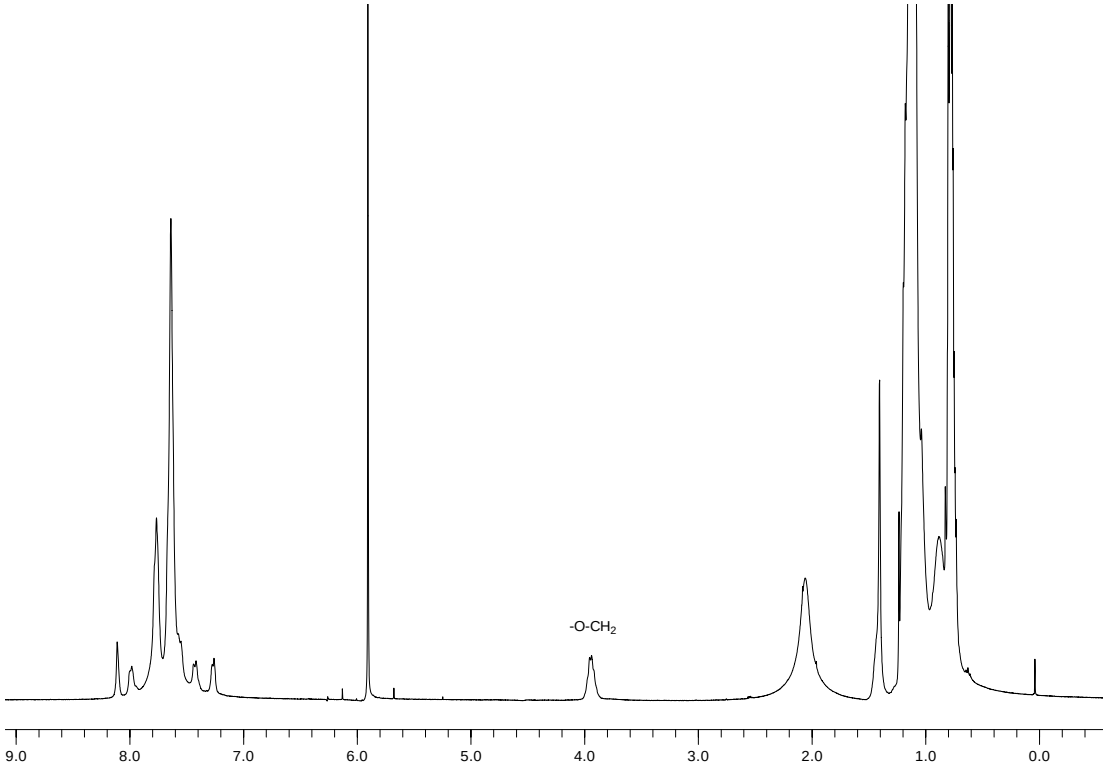

Figure 5.1: ^{1}H NMR spectrum of **6b** in $C_2D_2Cl_4$.

The percentage of incorporated binaphthyl units seems to be slightly lower than predicted from the monomer feed ratio (see Table 5.1). However, this trend was not reproducible for a further series of copolymers. Furthermore, it has to be mentioned that the integration of the broad signals is difficult especially for overlapping signals.

5.2.2. Thermal Properties

The thermal properties of polyfluorenes are remarkably interesting due to the occurence of liquid crystalline phases.[24] Thermogravimetric analysis showed that all herein presented polymers are thermally very stable up to 400 – 450°C. The thermal properties were further investigated by differential scanning calorimetry (DSC) in the range of 0 – 300°C with a heating and cooling rate of 10°C min^{-1}. The standard PFO sample showed two endothermic signals at 170°C and at 251°C, which were assigned to a liquid crystalline (T_{LC}) and a clearing transition (T_M) into the isotropic state. According to the literature a glass transition peak at 51°C is expected, which has not been observed within our experiments.[25] Incorporation of the binaphthyl units has a dramatic effect on the thermal properties of the resulting polymers, even at low concentrations. Incorporation of about 4 % gives a pronounced glass transition temperature of T_G = 78°C and a shifted T_{LC} at 147°C.

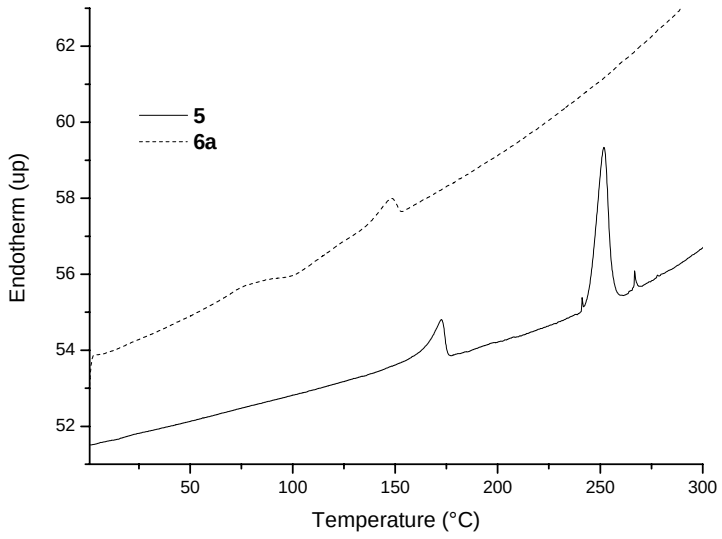

Figure 5.2: DCS traces (second heating) of PFO (**5**) and BN/PFO (4%) (**6a**).

The shift to lower T_{LC} temperatures is in good agreement with the literature which stresses that the length of a polymer has a direct influences of T_{LC}. In this case the binaphthyl unit can be seen as an interrupting unit giving virtually shortend chains (see Figure 5.2). None of the novel polymers **6a-6c** displays a melting peak. Incorporation of higher amounts of binaphthyl leads to copolymers which loose the liquid crystalline transition completely (not depicted) and content slightly increased glass transition temperatures of 82°C (**6b**) and 83°C (**6c**), respectively.

The fact that polymers with higher concentrations of the binaphthyl unit form stable amorphous glasses with little discernable tendency to crystallize (as determined by DSC) was encouraging for further applications (see paragraph 5.3), as generally microcrystallization has detrimental effects on PL efficiencies.

5.2.3. Optical Properties

As mentioned in the introduction, one of the most compelling problems of polyfluorenes with *n*-alkyl side chains is the influence of solid state packing effects. However, the thermal properties presented in the paragraph before encouraged us to expect improved electronic and optical properties. Due to their glassy behavior the β – phase formation should be suppressed. The simpliest way to investigate the β – phase formation is the examination of the optical properties. The first conclusion is that the initially distorted polyfluorene backbone becomes planarized during the β – phase formation. Previous work stresses that the driving force for this unique packing behavior is the solid state packing of the *n*-alkyl side chains (side chain crystallization). The new fluorene- type copolymers should alter the optical properties, due to the suppressed β – phase formation.

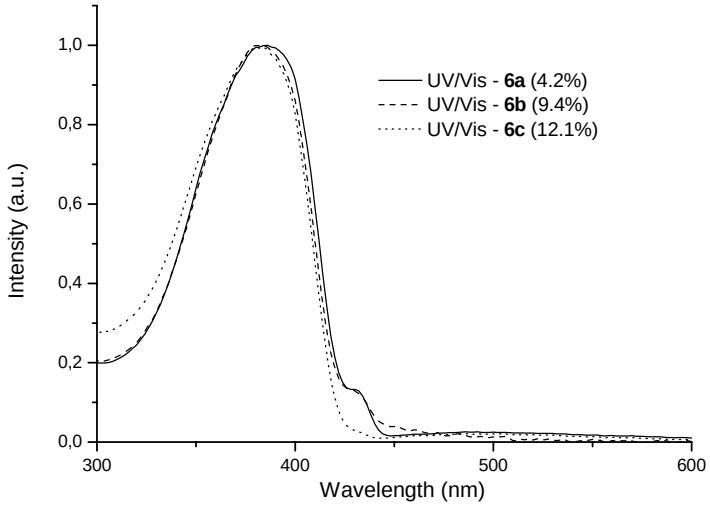

Figure 5.3: UV/Vis spectra of polymers **6a-6c** in chloroform solution.

Usually small β – phase fractions are not easy to detect via absorption spectroscopy.[11] However, for the herein presented copolymers **6a** – **6c** even in dilute chloroform solution an additional absorption peak at circa 435 nm appeared, which has to be assigned to the 0-0 absorption band of the β - phase (2_1 helix).[12] This peak occurs at a lower energy than the

HOMO-LUMO transition peak of PFO α – phase. Increasing amounts of the binaphthyl unit decrease the intensity of this peak until it almost disappears.

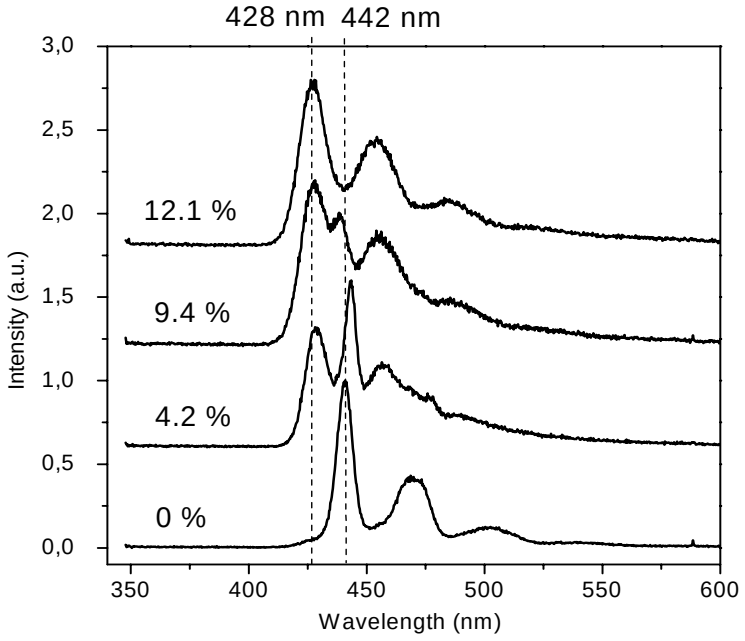

Figure 5.4: Low temperature (T = 30 K) photoluminescence spectra of PFO **5** and copolymers **6a-6c** in thin films.

To get a more detailed insight, low temperature photoluminescence measurements on films spin coated from toluene were performed. Using toluene as the solvent is known to yield films with only small fractions of the β – phase.[10] Nevertheless, Figure 5.4 clearly shows that the film formed from the PFO homopolymer (**5**) exhibited strong PL features originating from the PFO β – phase, with the main transition located around λ = 442 nm. This confirms an efficient energy transfer from the glassy α – phase to the energetically lower β – phase. Similar PL spectra have also been found in previous studies by Ariu et al. Figure 5.4 also displays the corresponding spectra for the copolymers **6a** to **6c**. Interestingly sample **6a** with 4.2 % binaphthyl spacer groups showed both contributions due to the α – (λ = 428 nm) and β – phase (λ = 442 nm). With increasing binaphthyl concentration, the PL contribution due to the β – phase became weaker and is not seen for a concentration of 12.1 % binaphthyl units. In fact, the PL spectrum of **6c** is almost identical to pure α – phase polyfluorenes. It seems that the binaphthyl groups effectively prevent the side chain crystallization responsible for the β –

phase formation. The optical and thermal properties encouraged us to test the novel copolymers as gain media for optically pumped lasers. The studies have been carried out in the group of Prof. W. Kowalsky (TU Braunschweig) and are presented in the following paragraph.

5.3. Threshold Reduction in Polymer Lasers Based on Poly-(9,9-dioctylfluorene) with Statistical Incorporated Binaphthyl Units.

As already mentioned in paragraph 5.1 polyfluorene derivatives have attracted widespread attention as the active gain media in organic polymer lasers.[5;6] Due to the improved optical properties of **6a** – **6c** as compared to standard PFO distributed feedback laser devices have been built using the new binaphthyl containing fluorene – type copolymers. A more detailed introduction to distributed feedback lasers has already been given in chapter 3.

5.3.1. Results and Discussion

Distributed feedback lasers based on polymers **5** and **6(a-c)** as active gain media have been prepared on SiO_2/Si substrates. The grating periods have been varied between 240 and 290 nm. With an effective refractive index of about 1.65 in films (thickness: 200 nm), the gratings function as second order DFB resonators. Further details on the device fabrication can be found in the literature.[18] Figure 5.5 displays the laser emission spectra for a DFB laser based on a film of polymer **6c**. The laser emission could be tuned from 435 nm ($\Lambda = 260$ nm) to 465 nm ($\Lambda = 290$ nm) by varying the grating period.

The lowest threshold energy densities of about 3 μJ/cm² were observed at lasing wavelength close to the ASE maximum at 446.3 nm (Figure 5.6), indicating a maximum gain.

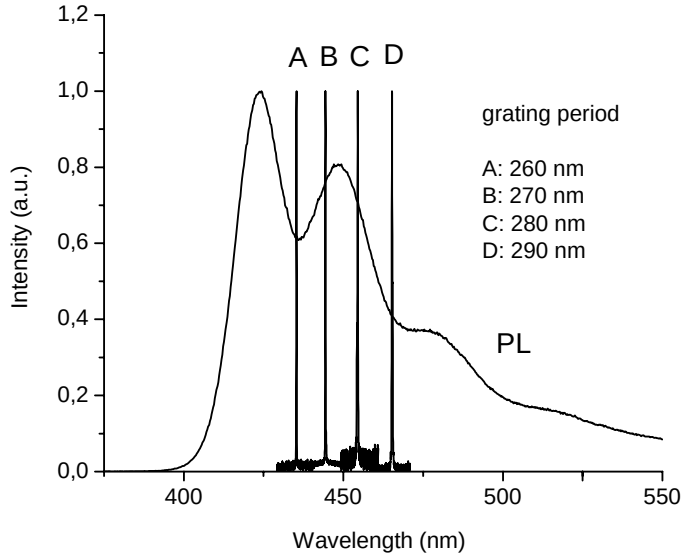

Figure 5.5: Photoluminescence and DFB laser emission spectra for polymer **6c**.

The minimum threshold energy densities for the DFB lasers built with **5** and **6(a-c)** are depicted in Figure 5.7. The threshold minimum for the standard PFO (**5**) was found to be 11.7 μJ/cm² (λ_{ex} = 452 nm).

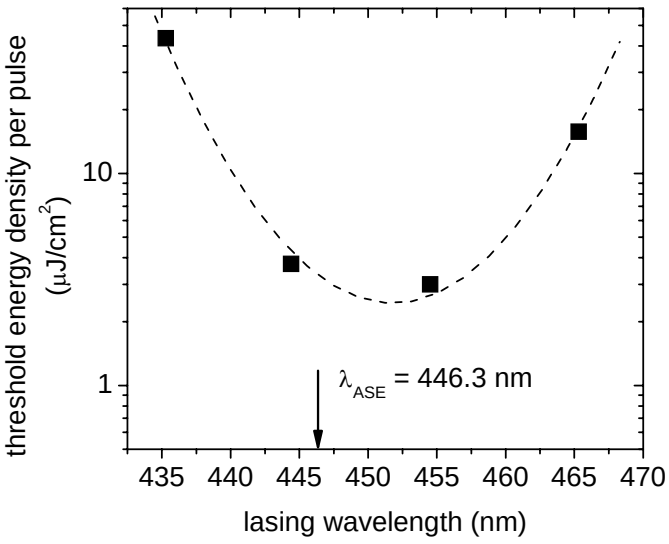

Figure 5.6: Threshold energy densities vs. emission wavelength for **6c**. The dashed line is a polynominal fit as a guide to the eyes.

Heliotis et al have reported threshold values of 64 μJ/cm² for second order DFB lasers based on PFO.[6] Our lower threshold values may be attributable either to the higher quality of the gratings or the special excitation conditions (in our case 335 nm pulses with 1 ns duration). Since, luminescence decay times of 400 – 800 ps have been reported for PFO films,[10] the excitation conditions should play a central role.

Towards higher binaphthyl concentrations in the copolymer the laser threshold decreases significantly to 3 μJ/cm² for the derivative **6c** (see Figure 5.7). These findings support our conclusion that the binaphthyl groups suppress the β-phase formation leading to an increased device performance.

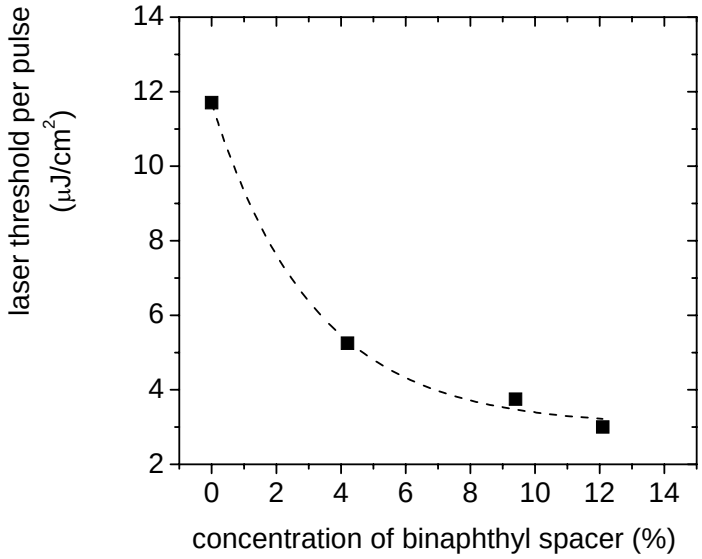

Scheme 5.7: Minimum threshold energy densities for the DFB laser with varying binaphthyl concentrations.

The threshold reduction by a factor of four reflects the benefit of our approach of designing PF – type copolymers with improved optical and electronic properties. Furthermore, initial results have shown that the photostability of films as well as solutions is increased by the incorporation of binaphthyl units.

5.4. Conclusion

A new series of fluorene – type copolymers, incorporating binaphthyl units, in order to suppress the β – phase formation have been introduced. Low temperature PL measurements showed that an increasing binaphthyl concentration decreases the β – phase emission, which was no longer observable for concentrations of 12.1 %. The beneficial effect of the suppressed β – phase formation for organic semiconductor lasers was reflected in drastically lowered threshold values going from 11.7 μJ cm^{-2} for pure PFO (**5**) to 3 μJ cm^{-2} for the copolymer **6c** with 12.1 % binaphthyl units. These results render the new materials highly attractive as gain materials in organic solid state lasers. For the future these materials will also be used as host materials for dye - doped lasers as well as a matrix polymer for new electrophosphorescent metal complexes.

5.5. Experimental Section

5.5.1. General Methods

For a general section concerning spectroscopic techniques and chemicals the reader is referred to chapter 2 of this thesis.

Synthesis of compounds **3** and **4** has already been described in chapter 4.

5.5.2. Synthesis

2,7-Dibromo-9,9-di-*n*-octyl-fluorene (1)

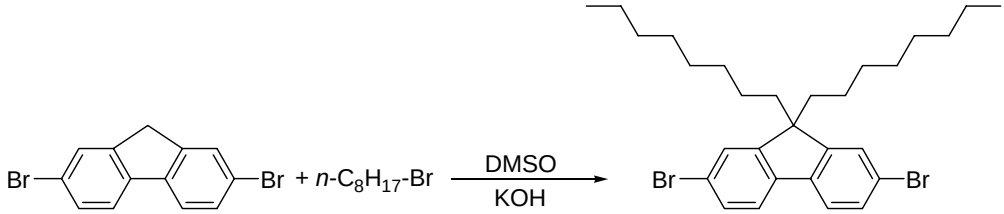

To a solution of 2,7-dibromofluorene (33 g, 102 mmol) and tetrabutylammonium bromide (9.9 g, 31 mmol) in DMSO (75 mL) an aqueous sodium hydroxide solution (40 mL, 50%) and *n* - octylbromide (43.3 g, 225 mmol) were added. The mixture was stirred at 80°C for 2 h and then poured into water (100 mL). The mixture was extracted two times with diethylether and the combined organic phases were washed with brine, water and dried over Na_2SO_4. Upon evaporating off the solvent the residue was purified via column chromatography with hexane as eluent to afford a colorless oil, which was stirred under high vacuum and subsequently solidified to afford **1** (88 %). ^{1}H NMR (400 MHz, $C_2D_2Cl_4$, 80°C): δ = 7.4 – 7.55 (m, 6 H, Ar-H), 1.82 – 1.97 (m, 4 H, Ar-CH_2), 1.10 (q, 4 H, CH_2), 0.97 – 1.05 (m, 8 H, γ/δ CH_2), 0.76 (t, 6 H, CH_3), 0.52 – 0.61 (m, 4 H, ß-CH_2-) ppm. ^{13}C NMR (100 MHz, $C_2D_2Cl_4$, 80 °C): δ = 152.3, 138.8, 129.8, 125.9, 121.0, 120.9, 54.2, 39.9, 31.1, 29.9, 29.2, 28.9, 23.2, 22.2, 13.5 ppm. LR-MS (EI, m/z): 57 (100.0), 323 (22.2), 546 (22.2), 548 [M^+] (28.0).

Poly-(9,9-di-*n*-octylfluorene-2,7-diyl) (PFO) (5)

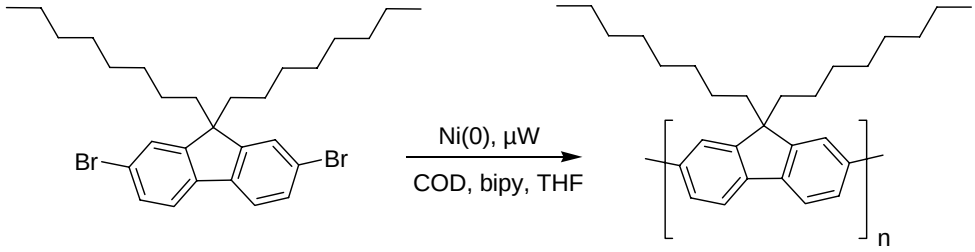

A flame dried 100 mL Schlenk-flask was charged under argon with 2,7-dibromo-9,9-di-*n*-octylfluorene (2.0 mmol, 1 eq), $Ni(COD)_2$ (4.8 mmol, 2.4 eq.) and 2,2'-bipyridyl (4.8 mmol, 2.4 eq). COD (3 mmol, 1.5 eq) and THF (40 mL) were added and the mixture heated to 80°C for three days. The solution was poured into 2N HCl and extracted with chloroform. The organic layer was washed with conc. EDTA solution, dried over Na_2SO_4 and the solvent was removed by rotary evaporation. The residue was taken up in chloroform and precipitated into methanol. The crude solid was extracted with ethyl acetate for two days and then reprecipitated into methanol to yield 5 in 81 % yield as yellow plates. GPC (vs polystyrene standards in THF) (**5**): M_n = 190,000; M_w/M_n = 2.4 (after extraction). ^{1}H NMR (400 MHz, $CDCl_3$, 25 °C): δ = 7.87-7.58 (bm, 6H), 1.29-1.00 (bm, 28H), 0.82 (bt, 6H, J = 7.2 Hz, -CH_3). ^{13}C NMR (100 MHz, $CDCl_3$, 25 °C): δ = 151.8, 140.5, 140.0, 126.2, 121.5, 120.0, 55.4, 40.4, 31.8, 30.0, 29.2, 28.0, 23.9, 22.6, 14.0.

Statistical (9,9-di-*n*-octylfluorene-2,7-diyl) / (2,2'-dioctyloxy-binaphthyl-6,6'-diyl) copolymers (BNPFO) (6a – 6c).

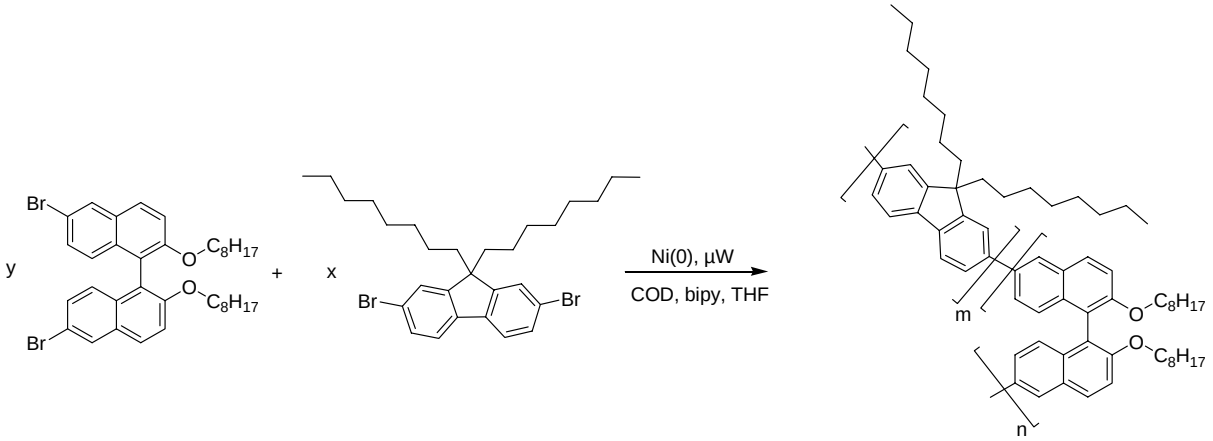

All statistical copolymers were prepared according to the procedure outlined for **5** utilizing suitable monomer ratios. The polymers were precipitated in methanol, Soxhlet - extracted with ethyl acetate for two days, and reprecipitated into methanol. The yields are in the range of 75 – 85 %. No NMR listings are given, due to the fact that no clear assignment of the

signals is possible. Experimental data can be found in the following table. y/(x+y) gives the feed ratio, while n/(n+m) gives the actual amount of binaphtyl (determined by ^{1}H NMR spectroscopy).

Name	x (mmol)	y (mmol)	y/(x+y) (%)	n/(m+n) (%)	Mn	PD
BNPFO-5% (**6a**)	2.01	0.11	5.19	4.24	90,000	2.1
BNPFO-10% (**6b**)	2.01	0.22	9.87	9.44	160,000	2.2
BNPFO-15% (**6c**)	2.01	0.30	12.99	12.05	128,000	1.6

References and Notes

[1] U. Scherf, E. J. W. List, *Adv.Mater.* **2002,** *14*, 477.

[2] D. Neher, *Macromol.Rapid Commun.* **2001,** *22*, 1365.

[3] M. Grell, W. Knoll, D. Lupo, A. Meisel, T. Miteva, D. Neher, H. G. Nothofer, U. Scherf, A. Yasuda, *Adv.Mater.* **2001,** *11*, 671.

[4] T. Miteva, A. Meisel, W. Knoll, H. G. Nothofer, U. Scherf, D. C. Müller, K. Meerholz, A. Yasuda, D. Neher, *Adv.Mater.* **2001,** *13*, 577.

[5] G. Heliotis, G. A. Turnbull, I. D. W. Samuel, D. D. C. Bradley, *Appl.Phys.Lett.* **2002,** *81*, 415.

[6] G. Heliotis, R. Xia, G. A. Turnbull, P. Andrew, W. L. Barnes, I. D. W. Samuel, D. D. C. Bradley, *Adv.Funct.Mater.* **2004,** *14*, 91.

[7] J. J. M. Halls, A. C. Arias, J. D. Mackenzie, W. S. Wu, M. Inbasekaran, W. W. Wu, E. P. Woo, *Appl.Phys.Lett.* **1998,** *73*, 629.

[8] M. Grell, D. D. C. Bradley, X. Long, T. Chamberlain, M. Inbasekaran, E. P. Woo, M. Soliman, *Acta Polym.* **1998,** *49*, 439.

[9] M. Grell, D. D. C. Bradley, G. Ungar, J. Hill, K. S. Whitehead, *Macromolecules* **1999,** *32*, 5810.

[10] A. L. T. Kahn, P. Sreearunothai, L. M. Herz, M. J. Banach, A. Köhler, *Phys.Rev.B* **2004,** *69*, 8520.

[11] M. Ariu, D. G. Lidzey, M. Sims, A. J. Cadby, P. A. Lane, D. D. C. Bradley, *J.Phys.Condens.Mater* **2002,** *14*, 9975.

[12] A. J. Cadby, P. A. Lane, H. Mellor, S. J. Martin, M. Grell, C. Giebeler, D. D. C. Bradley, *Phys.Rev.B* **2000,** *62*, 15604.

[13] S. Setayesh, A. C. Grimsdale, T. Weil, V. Enkelmann, K. Müllen, F. Meghdadi, E. J. W. List, G. Leising, *J.Am.Chem.Soc.* **2001,** *123*, 946.

[14] D. Marsitzky, R. Vestberg, P. Blainey, B. T. Tang, C. J. Hawker, K. R. Carter, *J.Am.Chem.Soc.* **2001,** *123*, 6995.

[15] A. K. Y. Jen, Y. Liu, Q. Hu, L. Pu, *Appl.Phys.Lett.* **1999,** *75*, 3745.

[16] J. C. Ostrowski, R. A. Hudack, M. R. Robinson, S. Wang, G. C. Bazan, *Chem.Eur.J.* **2001,** *7*, 4500.

[17] L. Pu, *Chem.Rev.* **1998,** *98*, 2405.

[18] T. Rabe, M. Hoping, D. Schneider, E. Becker, H. H. Johannes, W. Kowalsky, T. Weimann, J. Wang, P. Hinze, B. S. Nehls, U. Scherf, T. Farrell, T. Riedl, *Adv.Funct.Mater.* **2005,** *15*, 1188.

[19] H. G. Nothofer, PhD-Thesis, Flüssigkristalline Polyfluorene, Universität Potsdam, **2001**.

[20] K. R. Carter, *Macromolecules* **2002,** *35*, 6757.

[21] B. S. Nehls, Diplomarbeit, Mikrowellenunterstützte Synthese von Polyarylenen, Bergische Universität Wuppertal, **2003**.

[22] F. Galbrecht, X. H. Yang, B. S. Nehls, D. Neher, T. Farrell, U. Scherf, *Chem.Commun.* **2005,** 2378.

[23] E. C. Hagberg, D. A. Olson, V. V. Sheares, *Macromolecules* **2004,** *37*, 4748.

[24] J. I. Lee, G. Klaerner, R. D. Miller, *Chem.Mater.* **1999,** *9*, 1083.

[25] J. Ding, G. Day, G. Robertson, J. Roovers, *Macromolecules* **2002,** *35*, 3474.

6. Binaphthyl – and Biphenyl – Based Cruciforms

6.1. Introduction and Motivation

During the last decade there was a strong interest in finding organic chromophores that form stable glasses, e.g. for an application as emissive layers of evaporation – or solution – processed OLEDs.[1-4] Amorphous glasses eliminate complications related to grain boundaries or ill defined metal – organic interfaces, that are associated with crystalline materials.[5] With regard to organic materials, amorphous polymers are well known to match these criteria. However, the used methods of polymerization[6] and polycondensation provide materials with a certain polydispersity. In contrast, small molecules can easily be purified via standard organic methodologies. It has become quite clear that the nano – and macroscopic order in π – conjugated systems is extremely important, for the bulk properties of organic semiconductors, and the solid – state morphology often determines the efficiency of electronic and optoelectronic devices. For example in the case of organic light emitting diodes (OLEDs) the formation of aggregates leads to luminescence quenching and therefore has a great impact on the device stability.[5] Such processes represent a serious drawback of polymer based OLEDs and solid – state lasers. To suppress the crystallization of aromatic molecules long aliphatic side – chains can be attached.[7] Unfortunately, these non – polarizable groups reduce the charge transport ability of the bulk material. Then, in the case of organic light emitting diodes (OLEDs) the devices need to be operated at elevated potentials, which lowers their lifetimes under operating conditions.[8] Alternative approaches take advantage from the idea that the non – planarity of organic molecules can suppress the molecular packing. Typical representative molecular examples include starburst structures[9;10], spiro - type [11;12] and tetrahedral arrangements[13;14], or binaphthyl - based molecules.[15;16]

On the other hand, efficient intra – and intermolecular interaction can greatly enhance the charge carrier mobility. Corresponding poly – and oligomers that encourage substantial π - π overlap are often excellent charge transporting components for OFETs.

These general considerations in mind a series of novel oligomers with the *ortho* – tetraaryl motif were investigated. From earlier examinations it is assumed that such compounds should adopt a "folded" conformation as a result of intramolecular interactions.[17;18] Whether the driving force is really $\pi - \pi$ stacking or just a solid state packing effect is still not fully clear. To our knowledge, no previous study has probed the solution conformation of *ortho* – quarteraryls. Such data would be very useful to identify the driving forces, which induce torsionally flexible molecules to adopt a folded structure.

6.2. Binaphthyl Based Cruciforms

The binaphthyl unit as a non – planar aromatic building block, has already been introduced within this thesis was now used as the central core of the herein presented *ortho*- oligoaryls. The versatile and well developed substitution chemistry of binaphthyls give a good basis to start.[19] Most publications dealing with binaphthyl compounds utilize 2,2'-binaphthol as the starting material. They have found widespread applications in stereoselective synthesis[19-21], for chiral recognition[22;23], and in materials science, e.g. as the emitting layer in OLEDs.[15;16;24;25]

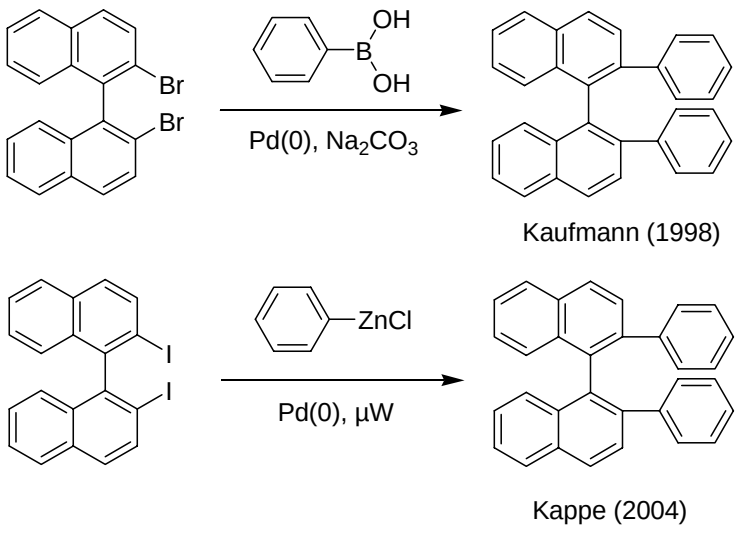

Scheme 6.1: Different approaches towards 2,2'-bis-arylated binaphthyl derivatives.

However, 2,2' -dialkoxy binaphthyls bear some disadvantages. The strong electron donating functionality influences the electronic properties. Further the chemical robustness can suffer on the weaker stability of the alkoxy group. Unfortunately, due to the absence of general and

efficient methods for the preparation of binaphthyls bearing aryl groups at positions 2 and 2', there is only a limited number of reports on their application.[26;27] At first Schilling and Kaufmann studied the arylation of racemic 2,2'-dibromide binaphthyl via a Suzuki protocol with benzeneboronic acid in the presence of Na_2CO_3 (see Scheme 6.1).[28] However, the desired 2,2'-dibenzene-1,1-binaphthyl was only observed in traces (< 3 %), while dehydrohalogenated or dehydroboronated derivatives were obtained as the main products (20 – 70 %). Later work by Kasak et al. reported increased yields of up to 50 % starting from the 2,2'-diiodo binaphthyl derivative.[29] Unfortunately, this procedure leads to a loss of the stereochemical information giving racemic products. A very recent publication by the Kappe group describes the stereoconservative access to 2,2'-diaryl-binaphthyl substituted systems via a microwave assisted Negishi coupling, utilizing again 2,2'-diiodo binaphthyl in very high yields.[30] However, this procedure did not work well with the more conveniently available ditriflate or dibromide derivatives.

The terminus "cruciform" also used for our molecules is related to a series of molecules presented by the groups of Nuckolls and Bunz.[31-34] However, their "cruciform" molecules contain four phenylene vinylene or phenylene ethynylene arms which are connected in a central core leading to flat molecules with neglectable torsion of the individual arms. In contrast the herein presented "cruciforms" are linked through an *ortho-ortho* biaryl unit leading to sterically restrained non – planar molecules.

6.2.1. Synthesis and Characterization

Scheme 6.2 shows the synthetic strategy towards our binaphthyl based cruciform molecules. Earlier studies have shown nearly quantitative reactions for step one, the substitution in the 6,6'-position of the binaphthyl system. However, step three, the biarylation of the bistriflate derivative, was known to be very difficult. Therefore a simpler compound **7** was used as a model compound to optimize the appropriate reaction conditions. The starting triflate **5** was commercially available or could be prepared via reaction of 2,2'-binaphthol with trifluoromethanesulfonic anhydride according to the literature.[35] Several synthetic methods towards the desired cruciform model **7** were tested, including Suzuki and Negishi type – cross – coupling reactions. The best results were obtained via a new Kumada/Grignard – type variant reported by the Knochel group.[36] The commercially available magnesium organyl **6** was stirred with a huge excess of lithium chloride and then added to **5** to afford compound **7** with maximum yields of circa 10 %.

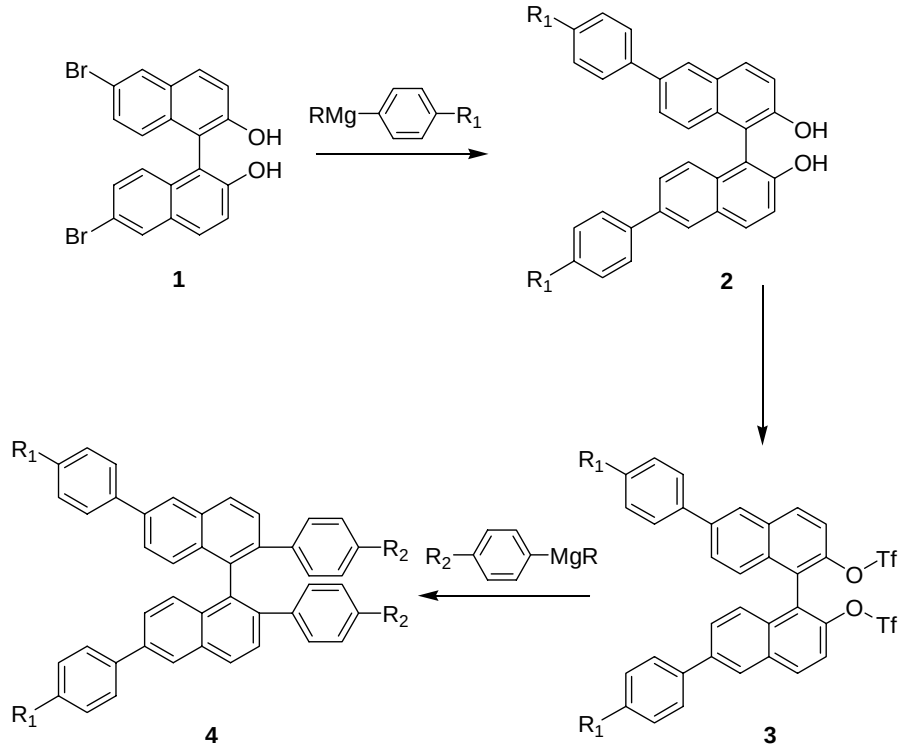

Scheme 6.2: Planned synthetic route towards the tetrasubstituted binaphthyl cruciform **4**.

Even a very careful addition of **6** gave mainly the homocoupled 1,6-di-*tert*-butyl-biphenyl, which has been isolated and characterized as well. The desired compound **7** was purified by thin – layer chromatography and characterized via NMR spectroscopy, MS spectrometry and X – ray crystallography.

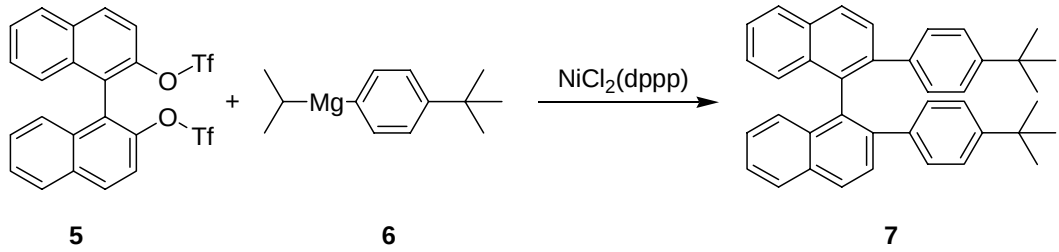

Scheme 6.3: Synthetic access to a 2,2'-biarylated binaphthyl **7**.

Figure 6.1 shows the aromatic region of the ^{1}H NMR spectrum of **7** in $C_2D_2Cl_4$. Two directly coupled signals show a remarkably upfield shift up to $\delta = 6.18$ ppm and $\delta = 6.77$ ppm and are assigned as protons (a) and (b). Such a strong upfield shift is usually attributed to a pronounced anisotropic effect of neighboured phenyl rings. This kind of shielding effect due to the increasing overlap of aromatic rings is also reported for conformationally rigid

carbohelicenes.[37-39] A similar upfield shift has also been reported in fluorenyl – substituted polyolefins in which the flexible fluorenyl substituents adopt a cofacial arrangement.[40] This behaviour is quite interesting, because usually such locked conformations are triggered by solvophobic, electrostatic, hydrogen – bonding or metal – ligand interaction effects.[38;41-44]

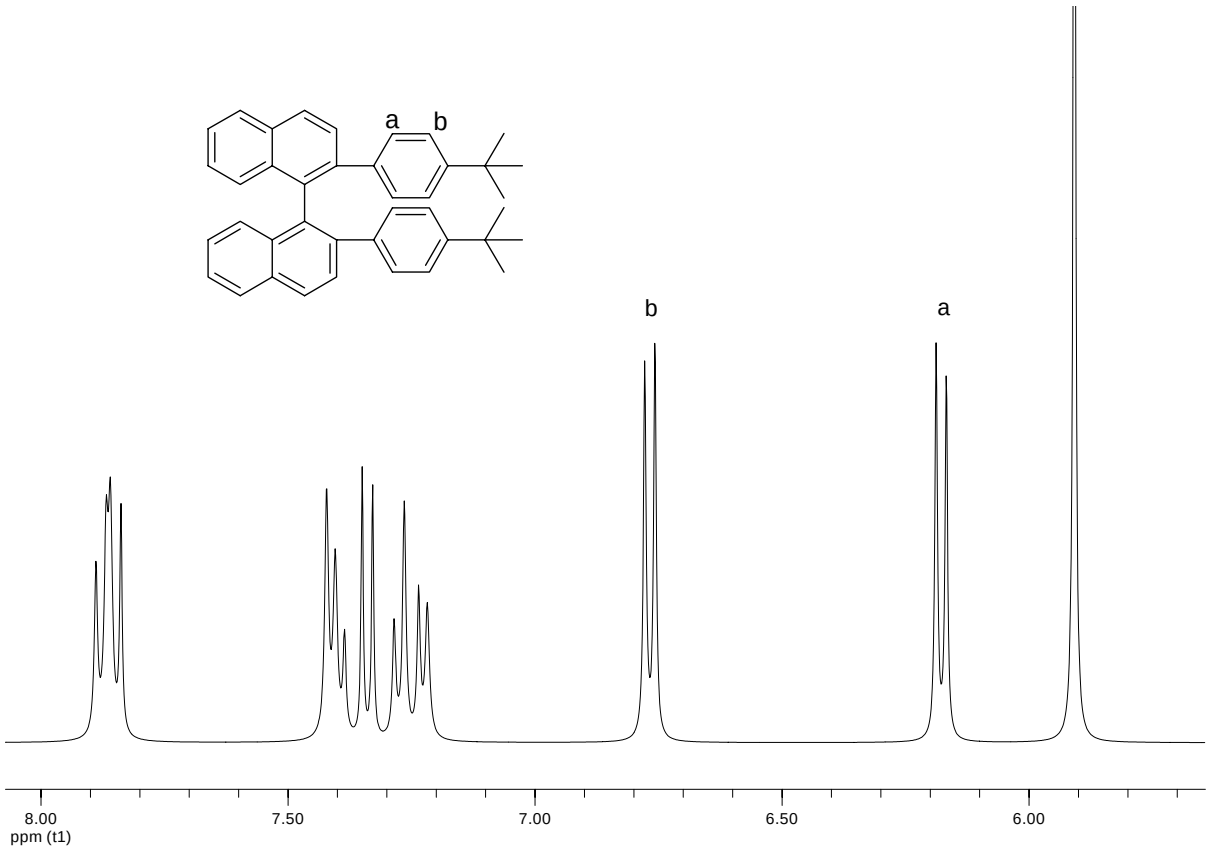

Figure 6.1: Aromatic region of the ^{1}H NMR spectrum of **7** in $C_2Cl_4D_2$.

To get more information of the molecular conformation in the solid state a single crystal was grown from THF and the structure resolved by Prof. D. J. Brauer (Bergische Universität Wuppertal). Figure 6.2 does not show the hydrogens for clarity and demonstrates the twist around the central aryl – aryl bond. Further details can be found in Table 6.1. Figure 6.3 shows clearly the folded formation and the overlapping phenyl rings. This shows similarities to the solution behaviour for the structure in the solid state.

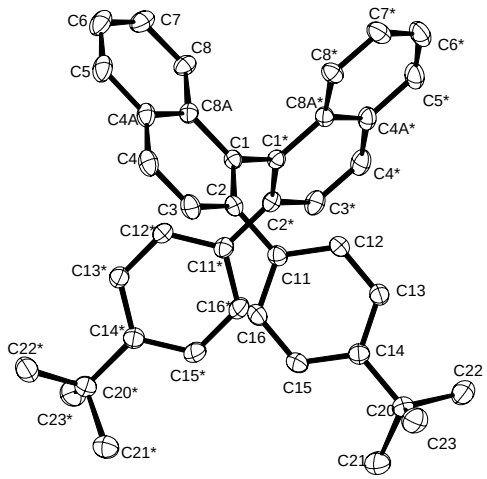

Figure 6.2: X – Ray structure of compound **7**.

Hereby, the interring distance between the offset phenyl rings is of special interest. Offset parallel geometries are believed to be favourable for π - π interactions.[45] Within this chapter the term "π - π interaction" is used to denote non – covalent interactions between π – systems.

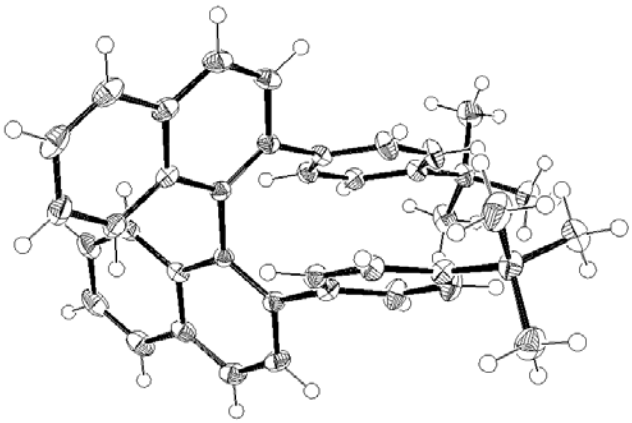

Figure 6.3: Side on view of compound **7**.

It is still under debate at which distance π - π interactions fulfil the criteria to provide a real interaction. So, it has been suggested that carbon - carbon distances < 3.6 Å are considered to give strong π - π interactions.[46] However, in truth it is difficult to unambiguously acertain if such interactions are present.[47] The closest contact of the two phenyl rings is given between

C11* and C11 with a distance of 3.31 Å. This distance fulfils the criteria given before. Therefore, in combination with the solution NMR results one can conclude for a intramolecular folding which is driven by π - π interactions.

6.2.2. Conclusion

According to literature the diaryl substitution at the 2,2'-position via the "triflate" route is very hard to realize and just gave poor yields. Therefore, the primary plan to synthesize tetrasubstituted binaphthyl cruciforms seemed not to be attractive any longer. However, during the investigations new ideas have appeared. If the weak accessibility of the 2,2'-substituted binaphthyl derivatives is governed by the steric situation of the binaphthyl moiety, it should be possible to obtain a related *ortho*-tetra aryl oligomer by changing the central core to a biphenyl building block. This class of cruciforms would open the door to a novel series of "tetraarm" oligoaryls and allow a more detailed investigation of the folding process.

6.3. Biphenyl Based Terphenyl-Cruciforms

Going from a binaphthyl to a biphenyl core unit should lead to systems with a much higher conformational flexibility.

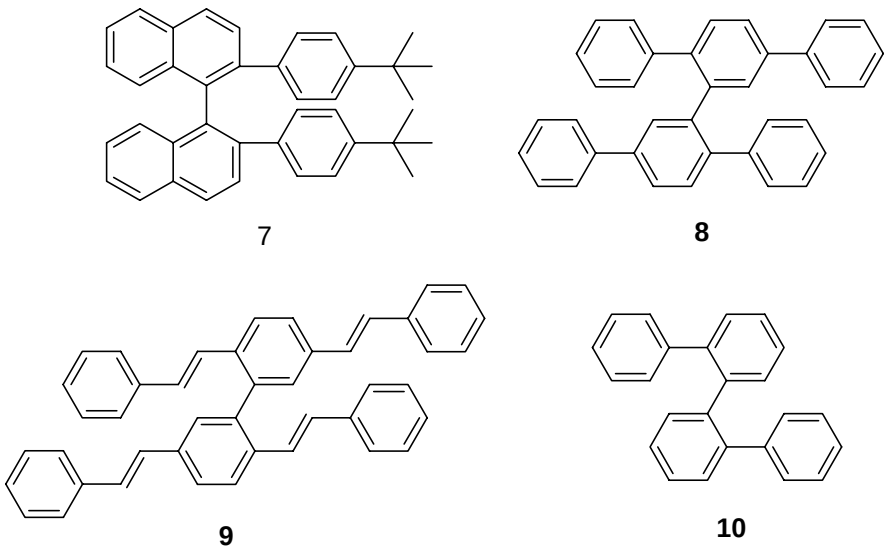

Figure 6.4: Possible relatives of the binaphthyl cruciforms utilizing a biphenyl core.

During the herein presented investigations also the Ma group used such biphenyl cores in the synthesis of phenylene vinylene based cruciforms like compound **9**. They stated that the

molecule shows a 70° twist between the planes of both phenylene vinylene arms. However, due to the vinylene group the distance between the phenyl rings is too large to adopt a folded conformation. Very simple tetraaryl cruciforms as **8** and **10** have already been synthesized.[48] Herein, we present an efficient synthetic strategy towards cruciform, π – conjugated oligomers based on the 2,5,2',5'-tetra-arylsubstituted-1,1'-biphenyl core.

6.3.1. Synthesis of the Biphenyl Based Terphenyl Cruciforms

The key step in the synthesis of the cruciform structure utilizes the different reactivity of aromatic bromo and chloro groups in a Suzuki-type aryl-aryl cross coupling reaction.[49;50] The reaction of 2.4 equivalents of 4-*tert*-butyl-benzene-boronic acid (**11**) with 1,4-dibromo-2-chloro-benzene (**12**) allows the selective coupling of the two bromo and boronic acid groups leaving the chloro group in place for further modifications.

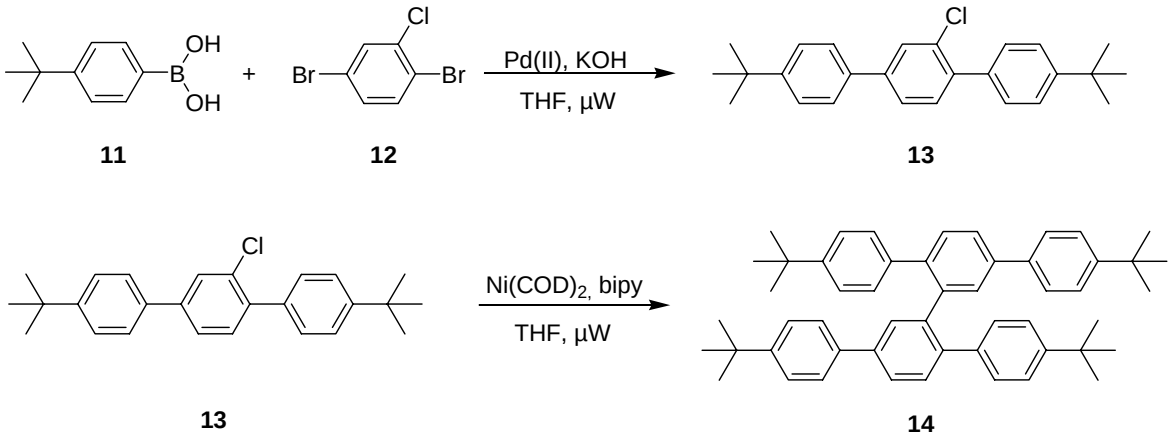

Scheme 6.4: Our synthetic strategy towards the biphenyl based cruciforms.

The reaction was carried out using a microwave assisted procedure utilizing $Pd(PPh_3)_2Cl_2$ as the catalyst and powdered KOH as the base.[51] All solid materials were weighed into a 10 mL microwave vessel and sealed under argon. THF was added and the reaction irradiated with microwaves (300 W, 115°C) for 12 min. Purification of the chloro – substituted cruciform precursor was accomplished by column chromatography to give **13** in 95 % yield.

The desired cruciform 2,5,2',5'-tetrakis(4-*tert*-butylphenyl)-1,1'-biphenyl (**14**)[48] was obtained via a Nickel – mediated microwave – assisted Yamamoto type coupling of **13**.[52;53] Contrary to earlier investigations a new variant using THF as the solvent at temperatures of about 130°C has been found to be superior.[54] The pure cruciform **14** was realized in 82 % yield after column chromatography.

Two related model compounds were synthesized as outlined in Scheme 6.5. Particularly the "half" cruciform molecule **18** should help in the conformational analysis, especially if such *ortho*-quarterphenyl systems generally adopt a folded conformation. Hence using a microwave – assisted Suzuki coupling, the linear 4,4'-bis-(4-*tert*-butylphenyl)benzene (**16**) and the *ortho*-quarterphenyl derivatives 2,2'-bis(4-*tert*-butylphenyl)-1,1'-biphenyl (**18**) were prepared in the reaction of **11** with 1,4-dibromo-benzene (**15**) and 2,2'-dibromo-1,1'-biphenyl (**16**) respectively. Both compounds were isolated in good yields of 90 % (**16**) or 82 % (**18**) respectively.

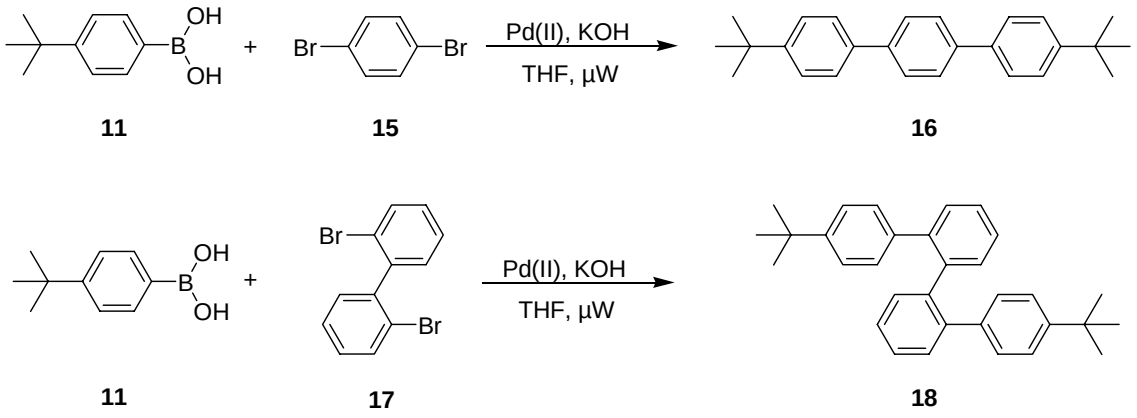

Scheme 6.5: Synthesis of the model compounds **16** and **18**.

6.3.2. NMR Spectroscopy

Compounds **14**, **16** and **18** display a very good solubility in common organic solvents, which allowed a detailed characterization of the materials by solution NMR spectroscopy. Figure 6.5 shows the aromatic region of the proton NMR spectrum of the cruciform **14** and the model compound **18**. Similar to the ^{1}H spectrum of **7** (Figure 6.1) the most notable feature is the upfield shifted position of two directly coupled doublets. For **18** they are found at $\delta = 6.35$ ppm and 6.88 ppm with a coupling constant of $J = 8.2$ Hz and represent the four protons of the 4-*tert*-butylphenyl units. Therefore it can be proposed that the *ortho*-quarterphenyl **18** forms a "folded" conformation without an external driving force, whereby the outer *tert*-butylphenyls adopt an offset π – stacked arrangement in solution.

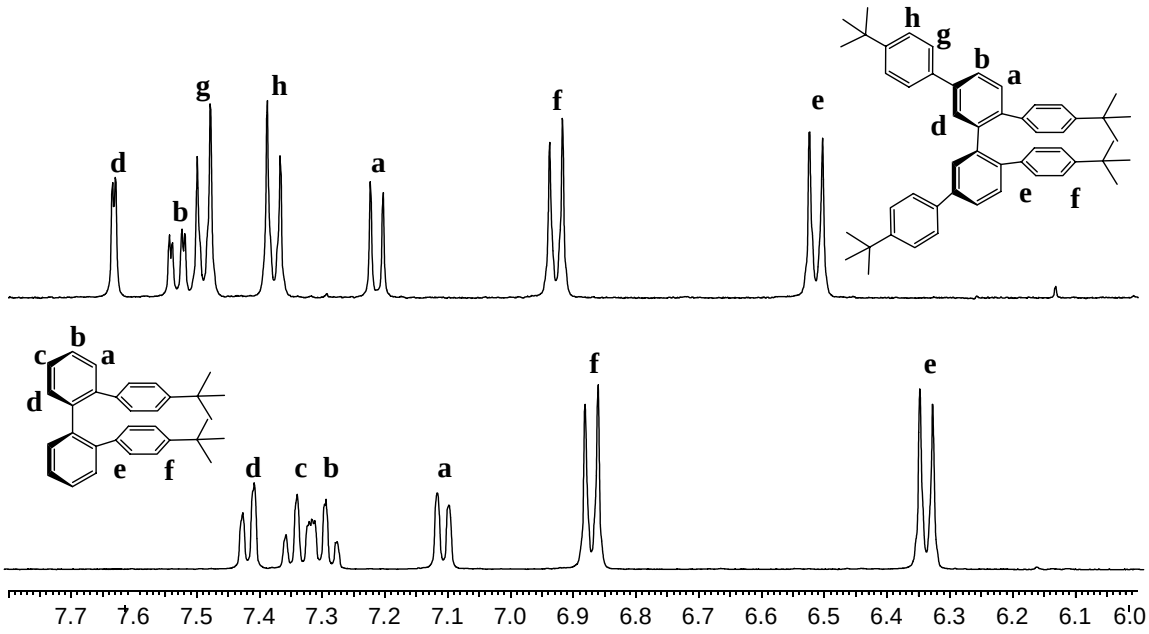

Figure 6.5: ^{1}H NMR spectra of **14** and **18** in $C_2D_2Cl_4$.

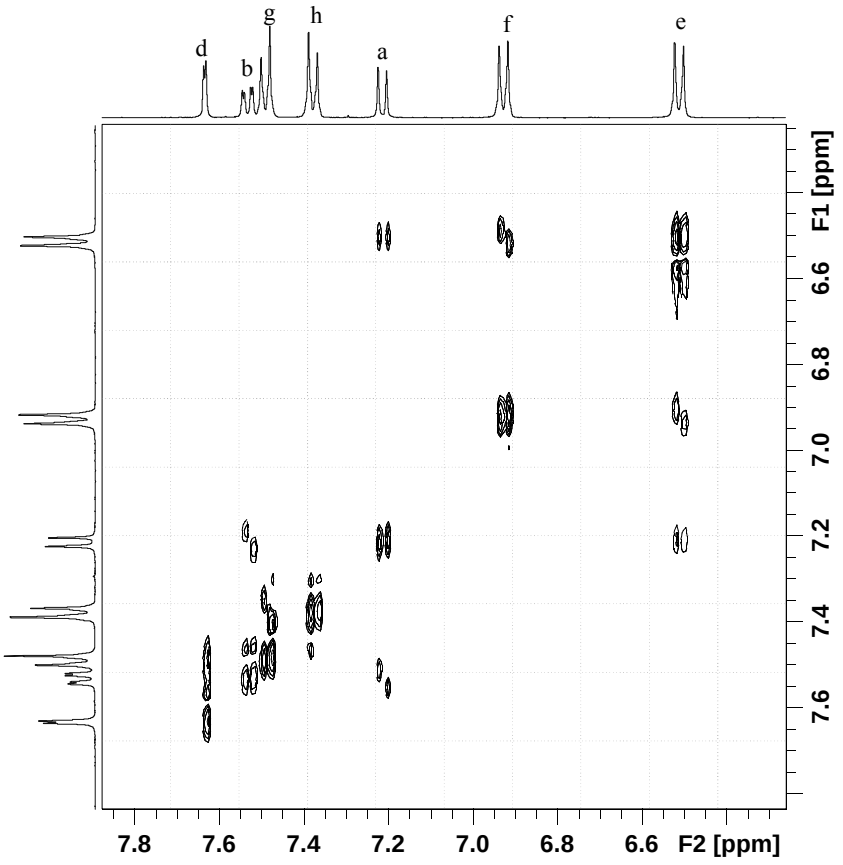

Figure 6.6: ^{1}H-^{1}H ROESY NMR spectrum of **14** in $C_2D_2Cl_4$.

A slight tilt between the corresponding *tert*-butylphenyl rings results in a larger upfield shift of the two protons (labelled e in Figure 6.5) closest to the central biphenyl unit. Analysis of the NMR spectra allows a full assignment of the structure based on the proposed coiled conformation and is presented in Figure 6.5. The similarities between the ^{1}H NMR spectra of **14** and that of **18** suggest that the cruciform **14** also adopts a "folded" conformation in solution. This again is reflected by a pair of two upfield shifted doublets at δ = 6.51 and 6.93 ppm. Also ^{1}H-^{1}H ROESY and ^{1}H-^{1}H COSY experiments have been carried out. The ^{1}H-^{1}H ROESY spectrum in Figure 6.6 shows clearly a through – space coupling between signal a (δ = 7.21 ppm) from the central core and the neighboured phenyl proton e (δ = 6.35 ppm).

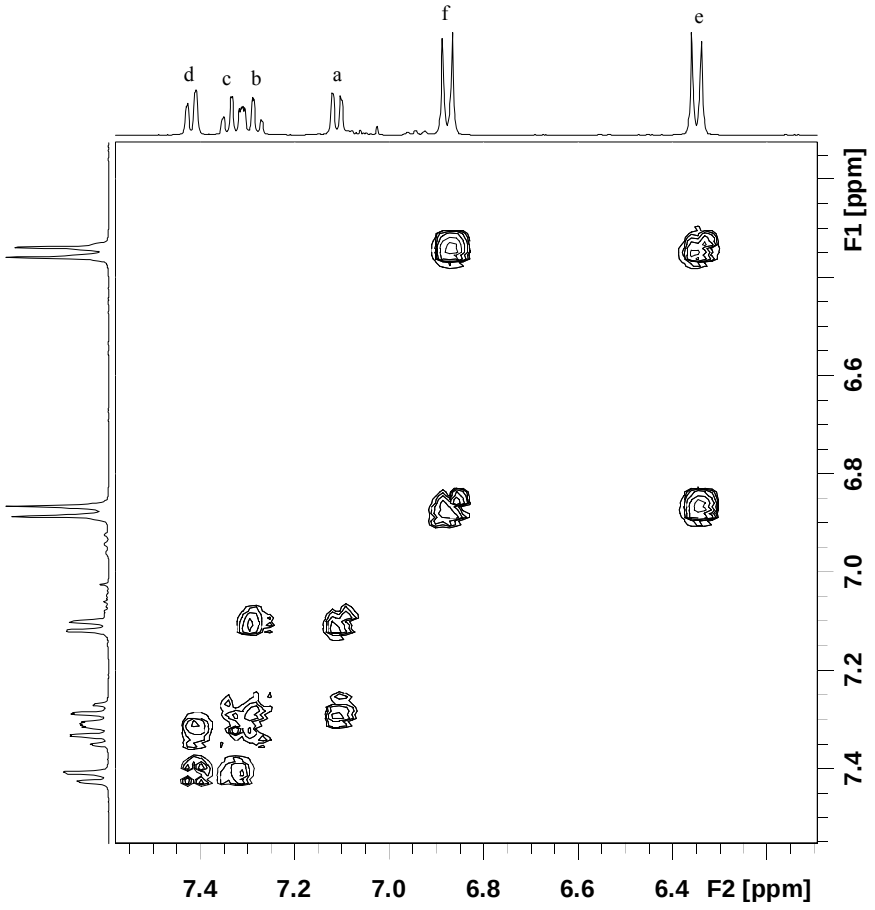

Figure 6.7: ^{1}H-^{1}H COSY spectrum of **18** in $C_2D_2Cl_4$.

Additionally conducted ^{1}H-^{1}H COSY (depicted for **18**), ^{1}H-^{1}H COSYLR and ^{13}C NMR examinations allowed an unambiguous assignment of all protons in the molecule. Further experiments utilizing different solvents and variable temperatures have showed that the folded conformation is remarkably stable up to 70°C and indifferent versus the type of solvent.

6.3.3. X – Ray Crystallography

For X – ray crystallographic studies single crystalline specimen of **14** and **18** were grown and their structures solved (Figures 6.8 and 6.9). The X – ray investigations have been performed in the groups of Dr. C. W. Lehmann (MPI für Kohlenforschung, Mülheim) and Prof. D. J. Brauer (Bergische Universität Wuppertal). Compound **14** displays a crystallographic C_2 symmetry and each molecule lies within the contact range of ten neighboring molecules. No crystallographic symmetry is imposed on the molecular structure of **18**, which exhibits a molecular coordination number of twelve.

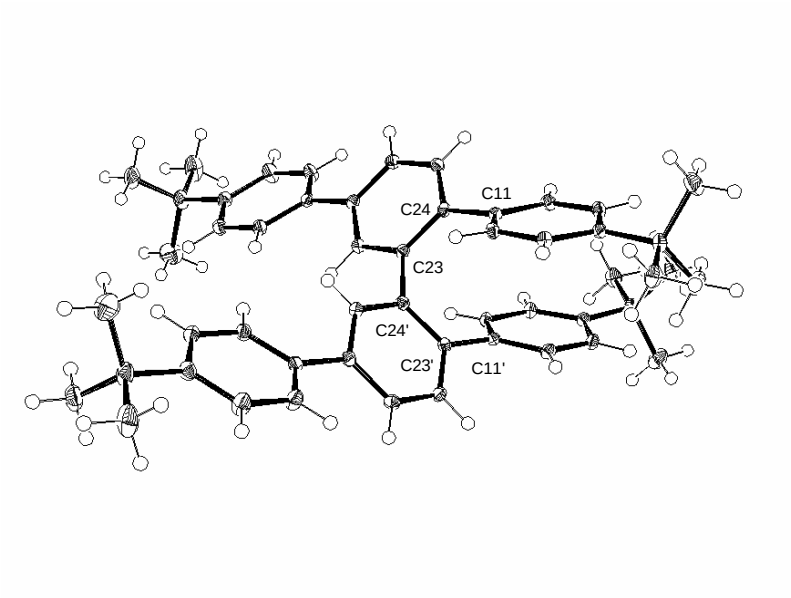

Figure 6.8: ORTEP plot representation of **14**.

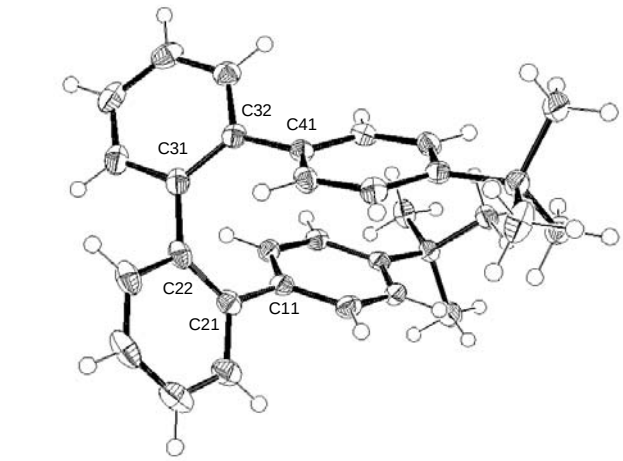

Figure 6.9: ORTEP plot of **18**.

As shown in the Figures, both **14** and **18** adopt a folded helical like conformation in their crystals.The two overlapping *tert*-butylphenyl rings of **14** display a dihedral angle of 6.5° formed by their planes. In analogy to the investigations of **7** the inter ring distances between the offset phenyl rings are of special interest. The closest contact is observed between C11 - C11' [3.16 Å] among other spacings in the range of 3.4 – 3.6 Å.

Table 6.1: Crystal data and structure refinement of **7**, **14** and **18**.

	7	**14**	**18**
Empirical formula	$C_{40}H_{38}$	$C_{52}H_{58}$	$C_{32}H_{34}$
Color	colorless	colorless	colorless
Formula weight	518.70 g · mol-1	682.98 g · mol-1	418.59 g · mol-1
Temperature	100 K	100 K	100 K
Wavelength	0.71073 Å	0.71073 Å	1.54178 Å
Crystal system	Monoclinic	Monoclinic	Monoclinic
Space group	**C2/c, (no. 15)**	**C2/c, (no. 15)**	**$P2_1/c$, (no. 14)**
Unit cell dimensions	a = 18.0571(4) Å α= 90°. b = 13.2349(3) Å β= 98.1380(10)°. c = 12.4742(2) Å γ = 90°.	a = 26.1849(6) Å α= 90°. b = 15.8390(4) Å β = 103.7280(10)°. c = 10.0760(2) Å γ = 90°.	a = 7.68070(10) Å α= 90°. b = 13.23650(10) Å β = 93.2000(10)°. c = 24.2500(3) Å γ = 90°.
Volume	2951.11(10) Å3	4059.57(16) Å3	2461.55(5) Å3
Z	4	4	4
Density (calculated)	1.167 Mg · m-3	1.117 Mg · m-3	1.130 Mg · m-3
Absorption coefficient	0.066 mm-1	0.062 mm-1	0.471 mm-1
F(000)	1112 e	1480 e	904 e
Crystal size	0.50 x 0.22 x 0.12 mm3	0.16 x 0.16 x 0.08 mm3	0.26 x 0.18 x 0.12 mm3
θ range for data collection	3.30 to 31.04°.	3.03 to 31.66°.	3.65 to 69.16°.
Index ranges	-26 ≤ h ≤ 26, -19≤ k ≤ 19, -18 ≤ l ≤ 18	-38 ≤ h ≤ 38, -23≤ k ≤ 23, -14 ≤ l ≤ 14	-8 ≤ h ≤ 7, -16≤ k ≤ 15, -29 ≤ l ≤ 27
Reflections collected	38686	57798	15596
Independent reflections	4700 [Rint = 0.0473]	6800 [Rint = 0.0966]	4157 [Rint = 0.0386]
Reflections with I>2σ(I)	4199	4994	4081
Completeness to θ = 27.75°	99.4 %	99.8 %	90.3 %
Absorption correction	Semi-empirical from equivalents	None	Gaussian
Max. and min. transmission	1 and 1		0.95 and 0.89
Refinement method	Full-matrix least-squares on F2	Full-matrix least-squares on F2	Full-matrix least-squares on F2
Data / restraints / parameters	4700 / 0 / 184	6800 / 0 / 241	4157 / 0 / 296
Goodness-of-fit on F2	1.104	1.069	1.070
Final R indices [I>2σ(I)]	R1 = 0.0586, wR2 = 0.1485	R1 = 0.0636, wR2 = 0.1381	R1 = 0.0424, wR2 = 0.1072
R indices (all data)	R1 = 0.0654, wR2 = 0.1530	R1 = 0.0946, wR2 = 0.1529	R1 = 0.0431, wR2 = 0.1078
Largest diff. peak and hole	0.413 and -0.191 e · Å-3	0.455 and -0.260 e · Å-3	0.222 and -0.217 e · Å-3

Here it should be mentioned that the van der Waals diameter of a carbon atom is given with 3.4 Å. The planes of the 4-*tert*-butylphenyl units of the model compound **18** are distinctly less parallel shown by a dihedral angle of 16.1°. The shortest contact [C11 – C41; 3.14 Å]

compares very well with the cruciform **14** and is again remarkably shorter if compared to the binaphthyl cruciform [C11 – C11'; 3.31 Å], described in Chapter 6.2. In accordance with the higher twist of the aryl planes in **18** compared to **14**, the number of additional interring C – C distances less than 3.6 Å is reduced to four compared to six in **14**.

The reduced tilt angle in **14** is accompanied by an increased distortion of the central biphenyl core. Thus the torsion angle of **14** [C24 - C23 – C23' – C24'; 63.0°] is obviously increased compared to the torsion within **18** [C32 – C31 – C22 – C21; 56.4°]. The internal twist of the binaphthyl cruciform **7** even reaches 68.3° [C2 – C1 – C1' – C2'].

The number of publications which include crystallographic data of *ortho* – oligoaryls that adopt such a helical or "folded" solid state pattern are relatively rare.[17;55-57] Interestingly, none of the older reports defines exactly the driving forces for the folding (π - π stacking or a simple solid state packing). Despite the close approach of the two *tert*-butylphenyl rings in **14** and **18** in the solid state, it is still speculative to conclude for the kind of driving forces only based on the crystallographic data. However, the herein presented results of combined NMR and X – ray investigations are the first report with a direct comparison between dilute solution and solid state conformation. Summarized it can be concluded that the *ortho*-quarter-phenyl motif reveals strong π - π related interactions both in solution and in the solid state.

6.3.4. Thermal Properties

Thermal stability is one of the prerequisites for materials when considered as components for electronic or optoelectronic devices. Their degeneration is often linked with morphological changes within the active layers. Therefore the thermal behaviour of oligomers **14** and **18** was studied by Differential Scanning Calorimetry (DSC) in the range from – 20° up to 300°C. The heating and cooling rates were constantly at 10 K/min. Figure 6.10 shows the DSC traces of the model **18**. During the first heating cycle an endothermic peak due to melting was observed at 97°C. No crystallization was observed when **18** was cooled down to room temperature and a glass was formed. Following heating cycles show a glass transition temperature T_g of 34°C and reflect the morphological stability of the glassy state. The DSC traces for a recrystallized sample of the cruciform **14** are shown in Figure 6.11. The first heating cycle shows a pronounced endothermic peak at 275°C which is assigned as the melting transition. Again, in analogy to the model compound **18**, the following heating cycles display a glass transition temperature which is positioned at 135°C. Furthermore, a new exothermic signal at ~ 244°C was attributed to recrystallization, followed by the melting transition at 275 – 278°C.

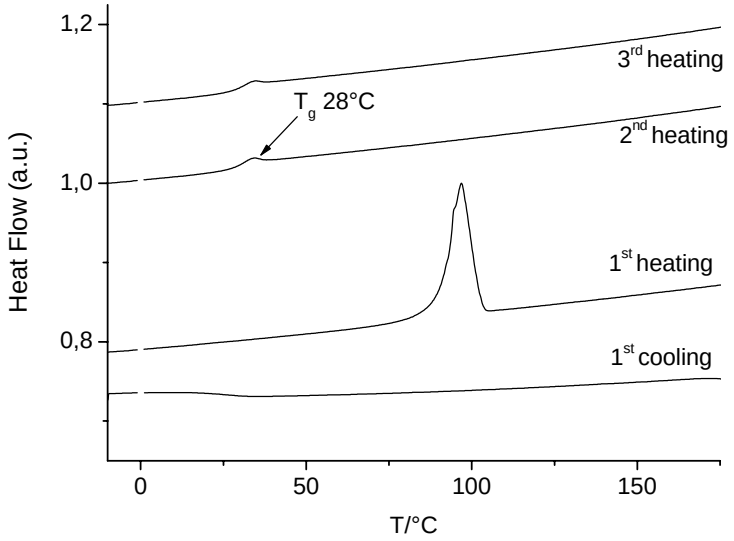

Figure 6.10: DSC traces for compound **18**.

This thermal behaviour is reproducible even after several repeated heating/cooling cycles. The comparison with **18** shows that the larger symmetric molecule exhibits a drastically increased T_g but also tends to recrystallize at temperatures > 220 °C. Although the glassy state of **14** is not stable at temperatures above 220 °C the T_g can be acknowledged as quite high. Therefore further modifications of the molecule could allow a suppression of the recrystallization.

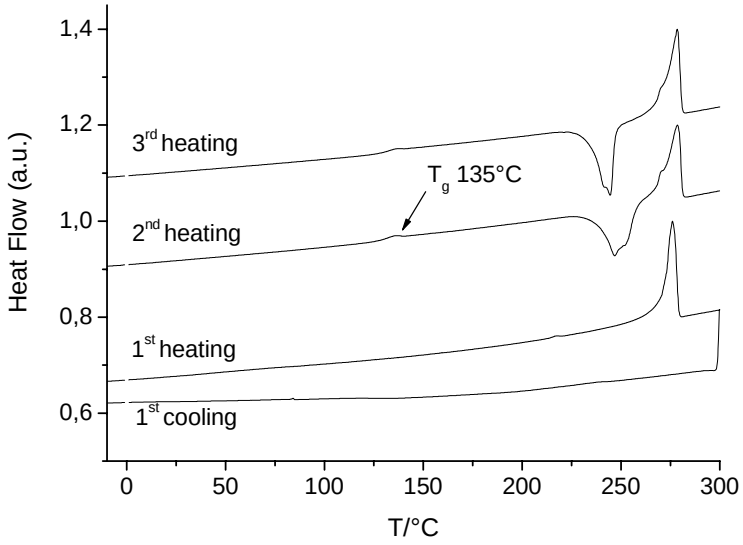

Figure 6.11: DSC traces for **14**.

6.3.5. Optical Properties

The optical properties of the terphenyl cruciform **14** and the linear terphenyl analogue **16** were examined both in dilute solution and as spin cast film. The data is listed in Table 6.2.

Table 6.2: Absorption and emission maxima of **14** and **16**.

Oligomer	$\lambda_{max.}$ ($CHCl_3$-solution) (nm)		$\lambda_{max.}$ (film) (nm)	
	abs.	em.	abs	em.
14	281	394	277	406
16	287	336	280	356

The isolated "arm" **16** shows the typical behaviour of *para*-terphenyls in general, exhibiting a broad and featureless absorption spectrum with a maximum at 287 nm (see Figure 6.12).[58;59] The PL spectrum of **16** on the other hand is much more resolved and displays a $0-0$ transition at 336 nm accompanied by vibronic side bands at 352 and 368 nm.

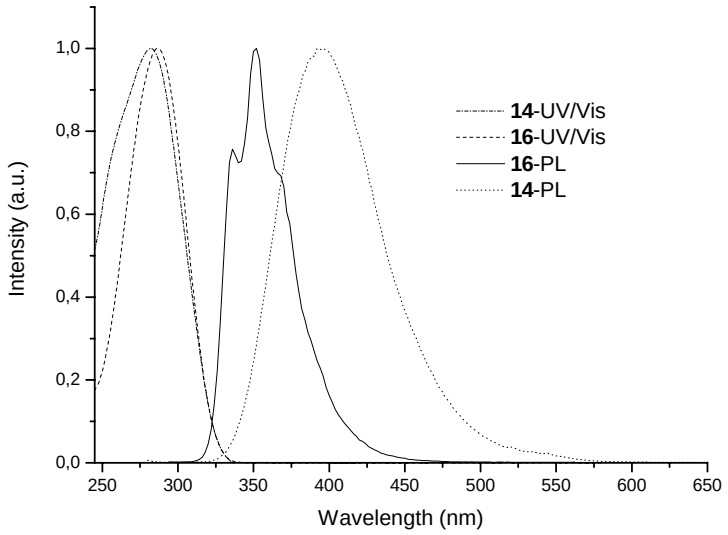

Figure 6.12: UV/Vis and PL spectra of **14** and **16** in chloroform solution.

These optical features are characteristic for chromophores that adopt a distorted ground state and a more planar conformation in their first excited singlet state. In agreement with the topology change between ground and excited state compound **16** possesses a relatively large Stokes shift of 5081 cm^{-1}. This is in good agreement with earlier studies on unsubstituted terphenyl which displayed a Stokes shift of about 4850 cm^{-1}.[58] The influence of the

para - substitution of the outer phenyl rings seems to be weak. The solid state properties of **16** are similar to those in solution. The absorption band remains featureless and the emission maximum is red – shifted by only 20 nm, which is attributed to the change of the environment on going from dilute solution to thin films.

Berlman et al. investigated the electronic spectra of a wide series of oligophenyls in a comprehensive study.[58] The most compelling result is that the substitution of the central ring in a terphenyl system gives a substantial disturbance to the planarity of the chromophore.

The absorption spectrum of the cruciform dimer **14** is very broad and similar to the linear analogue **16**. The slightly blue shifted absorption maximum at 281 nm is consistent with an increase in the distortion within the terphenyl arms of **14** as a consequence of the increased steric hinderance. On the other hand, the emission spectrum of **14** is rather different compared to **16**. The shape is much broader without vibronic finestructure and bathochromically shifted by circa 60 nm, giving an emission maximum at 394 nm and a large Stokes shift of 10,250 cm^{-1}. Photoluminescence quantum yields (PLQYs) of **14** were determined both in chloroform solution and thin films. The solution measurements were conducted versus anthracene in ethanol as the standard and gave a PLQY of only 12.5 %. The corresponding film measurement, utilizing an integrating sphere, gave a value of only 6 %. The very poor quantum yields reflect the dominance of non – radiative relaxation paths. Due to the somewhat increased distortion of the terphenyl chromophor also a blue shift of the PL compared to the linear analogue **16** could be expected. Such hypochromic effects have been reported for π – stacked base pairs in DNA or in polymers with π – stacked subunits.[40;60] However, the distinctly red – shifted PL of **14** clearly indicates the occurrence of intramolecular excited state dimers, so called excimers. The above described observation of folded conformations may support this conclusion. More in depth studies including time – resolved fluorescence experiments are required to fully elucidate these effects.

6.3.6. Synthesis and Characterization of Extended Biphenyl - Based Cruciforms

Despite the twisted structure **14** shows a disadvantageous tendency to crystallize. The synthesis of extended biphenyl - based cruciforms could lead to more glassy materials and followed an analogue route as presented in Scheme 6.4.

1,4-dibromo-2-chloro-benzene (**12**) was coupled via a Suzuki type cross coupling reaction with 4-trimethylsilyl-phenyleneboronic acid (**19**) to give 1-chloro-2,5-(trimethylsilyl-

phenyl)benzene (**20**) in more than 75 % yield after recrystallization from heptane/ dichloromethane.

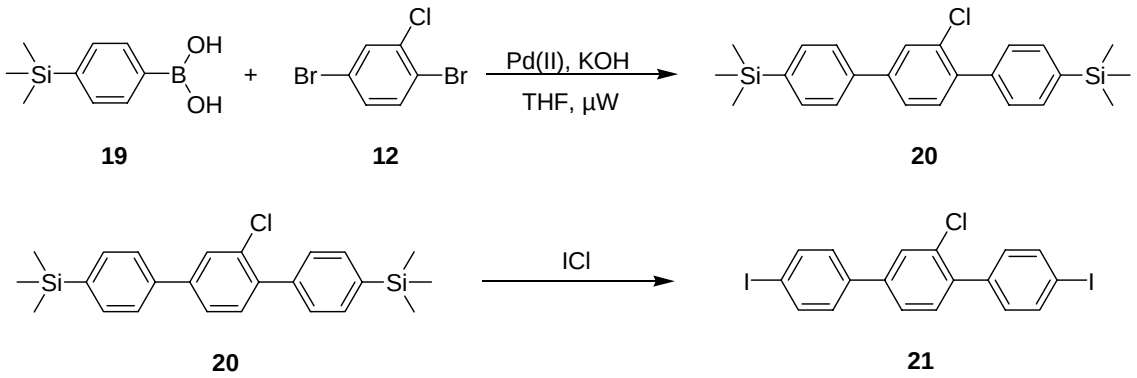

Scheme 6.6: Preparation of the terphenyl educt **21**.

The TMS – protected terphenyl **20** was subsequently converted to the diiodo derivative **21** by treating **20** with ICl in yields close to 90 %.

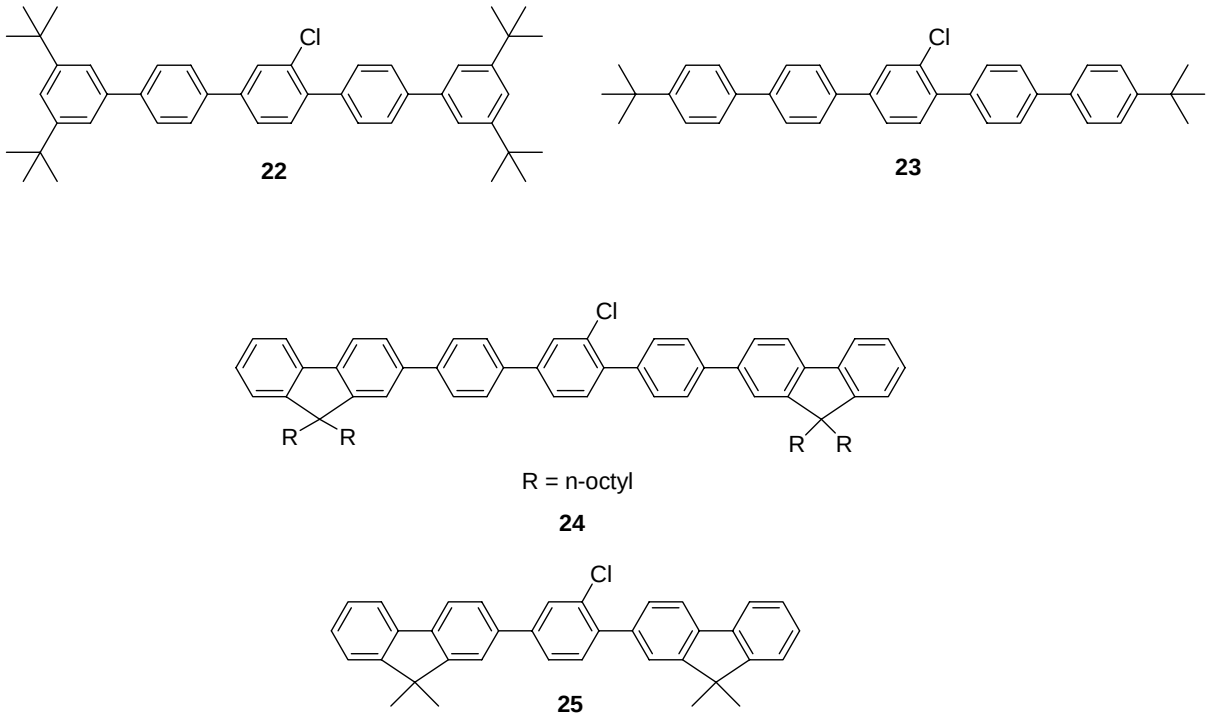

Scheme 6.7: Stuctures of the chloroaryl building blocks **22-25**.

The following Suzuki –type cross – coupling with a variety of different arylboronic esters gave the desired educts (**22-24**) in reasonable yields. **25** was prepared via direct coupling of 9,9-dimethyl fluorene-2-(4,4,5,5-tetramethyl-1,3,2-dioxaborolane) and **12**. All used arylboronic esters are commercially available or described in the experimental part. The "speciality" of **25** is the methylene bridge between the outer phenyl rings, so that the intramolecular folding should be hindered. The synthetic protocol for the preparation of the corresponding cruciform dimers is similar to the preparation of **14**, using a microwave assisted Yamamoto – type coupling reaction. Scheme 6.8 depicts the resulting cruciform molecules. Unfortunaly, the coupling of **23** could not be realised in a sufficient way, which may be explained by the extremely low solubility of **23** in THF or DMF/toluene mixtures. All other cruciforms were obtained in reasonable yields and purified via column chromatography.

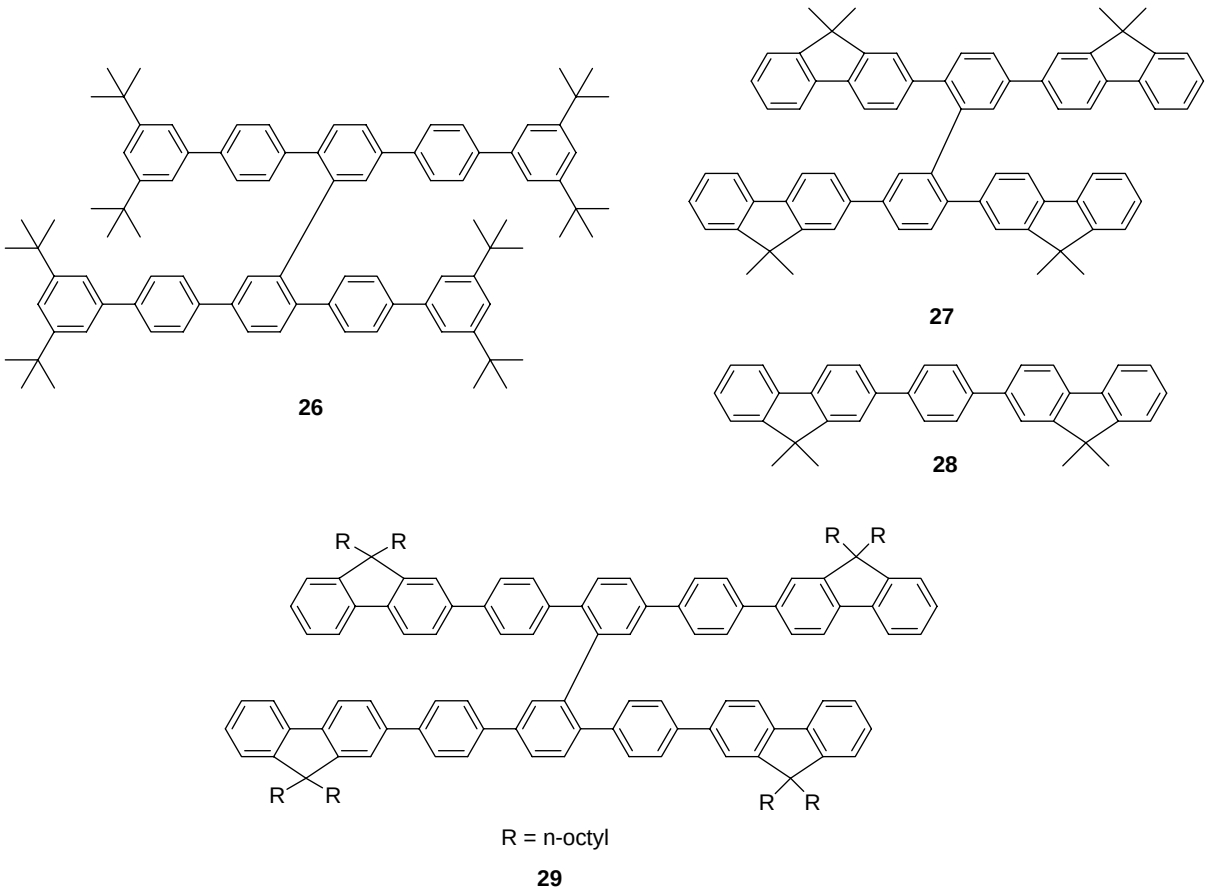

26 **27** **28** **29**

Scheme 6.8: Molecular structures of the cruciform dimers **26, 27**, **29** and the dehalogenated byproduct **28**.

In the coupling of **25** the dehalogenated terphenyl **28** has been isolated as a by – product. Structural integrity of all herein presented compounds was proved via NMR spectroscopy and MS spectrometry. Cruciforms **26** and **27** form white powdery materials, but several attempts to grow single crystals failed, so that no X – ray studies could be conducted so far. **29** forms a glassy, nearly transparent solid and shows no tendency to crystallize at all.

Due to their good solubility in common solvents extensive NMR studies of the cruciform dimers have been conducted.

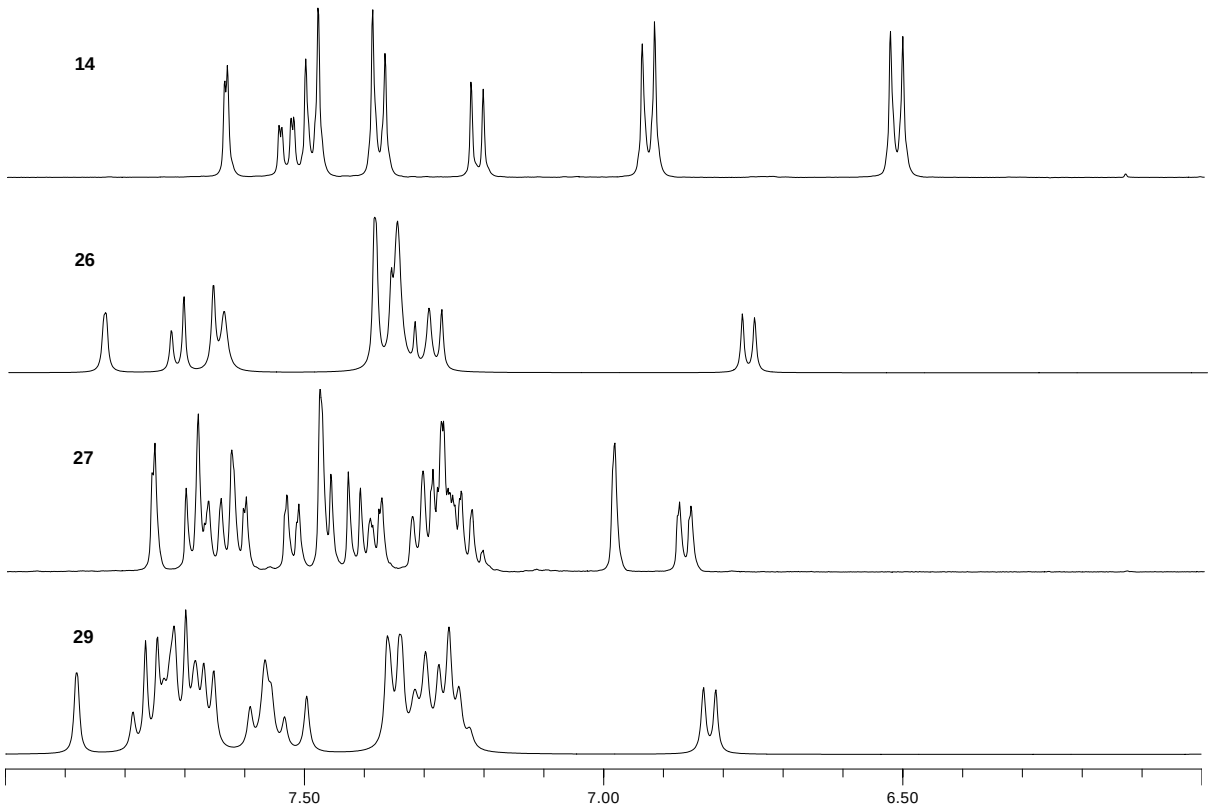

Figure 6.14: ^{1}H NMR (aromatic region 8.00 – 6.00) of **14**, **26**, **27** and **29**.

The pentaphenyl cruciform **26** is the most related structure to the archetype cruciform **14**. Figure 6.14 shows a remarkably decreased upfield shift for **26**, which is attributed to a weaker interaction between the overlapping rings. This can be explained by the increased steric repulsion of the outer *tert*-butyl groups. Nevertheless, the representive signal pattern of the π - π stacked arms can still be found. Molecule **27** exhibits, despite the presence of the methylene bridges, two sharp and upfield shifted signals at δ = 6.98 (s) and 6.87 (d) ppm (see also figure 6.15). Even **27** adopts a folded conformation. The protons of the fluorene in *ortho* – position (e1) and (e2) (see Figure 6.15) are clearly separated, wherein (e2) is more

directed to the neighboured aromatic system below. Proton (f) shows a distinct downfield shift if compared to the cruciforms **14** and **26** and could be assigned via ^{1}H-^{1}H COSY measurements (see Figure 6.15).

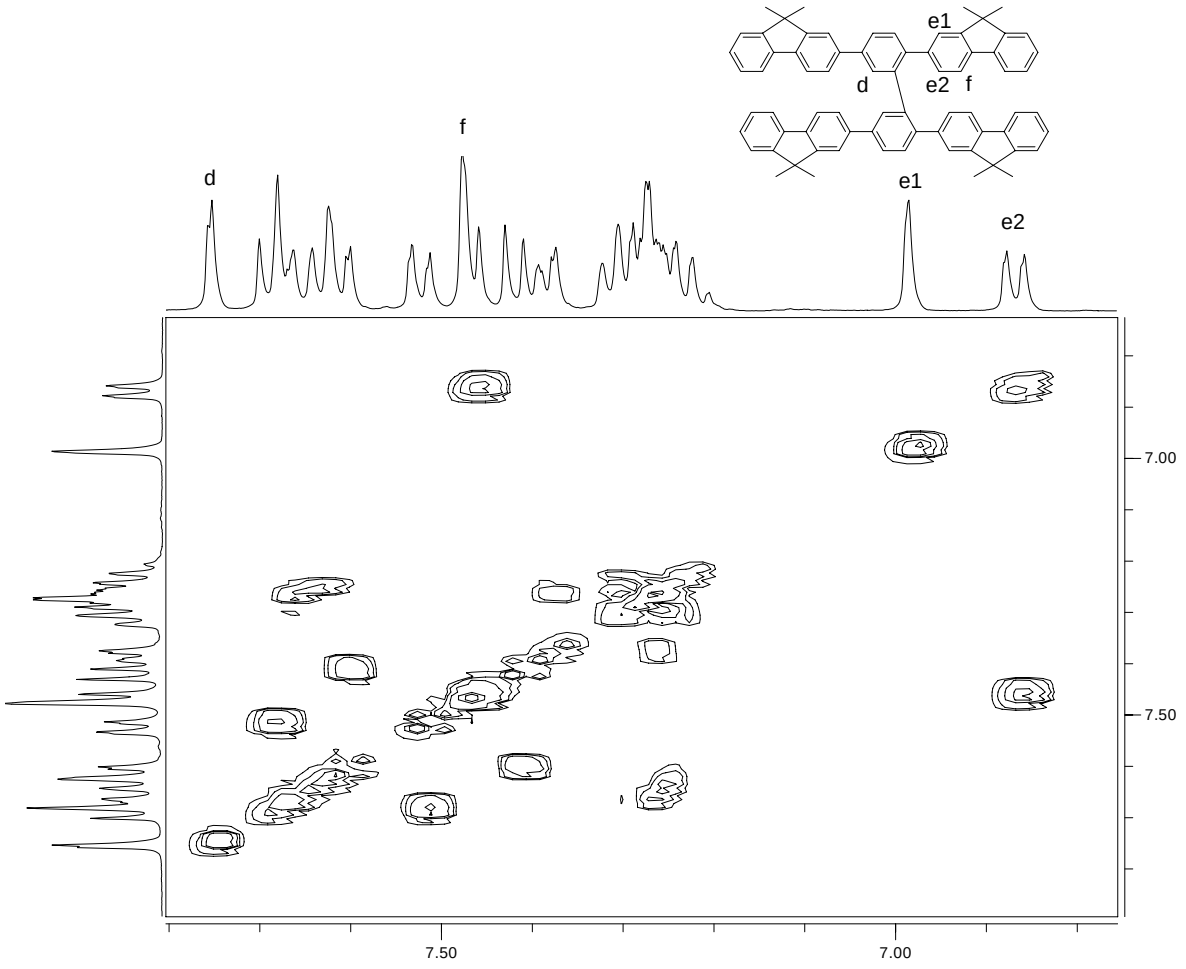

Figure 6.15: ^{1}H-^{1}H COSY spectrum of **27** in $C_2D_2Cl_4$.

^{1}H NMR measurements of cruciform **29** as the most extended representative also show a clearly upfield shifted doublet at $\delta = 6.82$ ppm. This shift is quite close to the shift in **26** indicating a comparable situation. Also, the long alkyl chains of **29** do not avoid the intramolecular folding.

6.3.7. Thermal Properties

The tunability of the thermal properties was one of the major concerns of extending the dimension of the cruciform dimers. Compounds **26**, **27** and **29** were studied by DSC in the range of – 20°C to 300°C, using a heating rate of 10 K/min. **26** displayed no morphological

change at all regardless of sample history. Also no T_g below 300°C was obtained. Cruciform **27** showed a series of signals during the first heating cycle in the range between 140 – 190°C. However, these signals were not reproducible during the following heating and cooling. Only an endothermic transition at ~ 160°C occurs during the heating and is attributed to the melting transistion. The DSC of **29** showed a reproducible glass transition temperature T_g of 45 – 50°C even after several temperature cycles. No crystallization was observed when **29** has been cooled down to – 20°C at different cooling rates.

6.3.8. Optical Properties

The absorption and emission spectra of all oligomers were examined both in dilute chloroform solution and as spin – cast films. The collected data are presented in Table 6.3.

Table 6.3: Optical Data of the extended cruciform series.

Oligomer	$\lambda_{max.}$ ($CHCl_3$-solution) (nm)		$\lambda_{max.}$ (film) (nm)	
	abs.	em.	abs.	em.
14	281	394	277	406
16	287	336, 352	280	356
26	308	391	306	403
27	325	395	348	410
28	329	380, 400, 422	351	395, 414, 439
29	333	395	343	421

All compounds are well soluble in chloroform and have been investigated in dilute solutions initially. All absorption spectra show the expected broad and structureless shape indicating the twisted ground state. The signal maxima shift bathochromically in order with the extended conjugation length from 281 nm for **14** to 333 nm for **29**. The solution PL spectra on the other hand reveal a very surprising feature. The PL maxima of all investigated cruciform dimers practically remain around 395 nm and exhibit a rather broad shape. A much faster converging PL compared to the UV/Vis with increasing length of the chromophore was already observed for other oligomer systems.[61;62] The photoluminescence quantum yields PLQYs are distinctly increased on going from **14** (12.5 %) to **29** (> 90 %) with intermediate values (ca. 70 %) for the two pentaphenyl chromophores. All solution PLQYs were measured using antracene in ethanol as the standard. The remarkably decreased PLQY of **14** is of special interest. In accordance to the NMR results the tendency for folding and excimer formation should be rather strong, if compared to the more extended cruciforms. The intramolecular

interaction of two arms leads to a pronounced PL quenching. This effect should be much less in the extended cruciform oligomers.

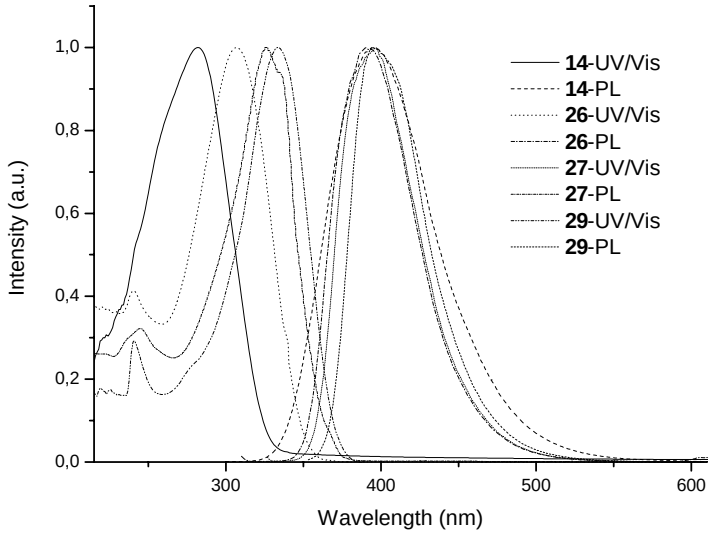

Figure 6.16: UV/Vis and PL spectra of **14**, **26**, **27** and **29** in dilute chloroform solution.

For a better understanding also the dehalogenated chromophores **16** and **28** have been investigated and compared with their corresponding cruciforms. Both molecules show a broad and structureless absorption spectrum very similar to their cruciform relatives.

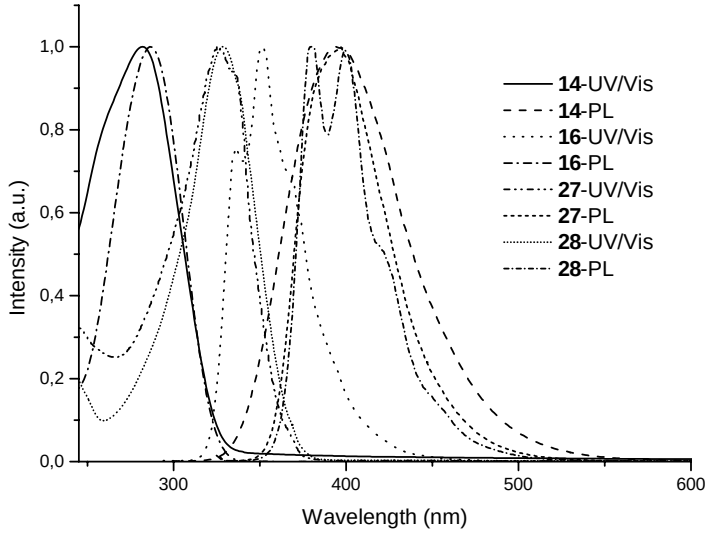

Figure 6.17: Comparison of the isolated chromophores with their corresponding cruciforms.

These results clearly indicate that the absorption of the cruciform dimers is mainly governed by the size of the individual arms. However, the PL spectra of the cruciforms show a distinct difference to the "isolated" chromophores. The single chromophores **16** and **28** display a pronounced PL fine structure, while the cruciform dimers give broad, structure less spectra and red – shifted PL spectra. These facts let assume the formation of intramolecular.
UV/Vis measurements of thin films show only slight deviations compared to the spectra in dilute chloroform solution (see table 6.3). The PLQY of the films were measured using an integrating sphere. Similar to the solution PLQYs the value for **14** (< 5 %) is drastically lower if compared to the extended cruciforms. The largest system **29** already exhibits PLQY values of ~ 30 %.

6.4. Conclusion

In summary, a novel and highly efficient synthetic route towards 2,5,2',5'-tetra-arylsubstituted-1,1'-biphenyl compounds has been introduced utilizing a sequence of Suzuki and Yamamoto – type coupling reactions. Examination of the X – ray and NMR data reveals the presence of an intramolecularly folded conformation driven by strong π - π interactions of two (oligo)aryl arms of the cruciform dimers, both in solution and solid state. Structural modifications, such as extension of the conjugation length or the attachment of side – chains allow a fine tuning of the optical and thermal properties. The absorption in solution was shifted from 281 nm for the terphenyl dimer **14** to 333 nm for a heptaphenyl dimer **29**. However, the photoluminescence spectra nearly reveal unchanged upon changing the chromophore length. The red – shifted PL and large Stokes shifts are probably related to the formation of intramolecular excimers as a result of strong π - π interaction. On – going synthetic work involves the synthesis and characterization of related cruciform oligoaryls with structurally modified arms including 4,4'-dialkyltriphenylamine and oligothiophenes as building blocks. Moreover, such cruciform oligoaryls will be incorporated into polymers.

6.5. Experimental Section

6.5.1. General Methods

For a general section concerning spectroscopic techniques and chemicals the reader is referred to chapter 2 of this thesis.

6.5.2. Synthesis

2,2'-Bis(4-*tert*-butylphenyl)-1,1'-binaphthyl (7)

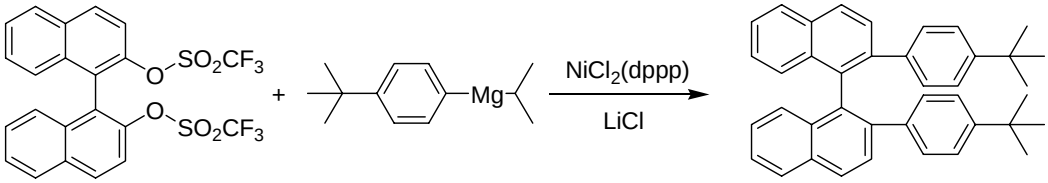

A dried 10 mL reaction vial was charged under argon with *iso*-propyl-4-*tert*-butylphenyl magnesium (4 mmol, 2 mL of a 2M solution), LiCl (150 mg, 3.54 mmol) and stirred at – 15°C for 30 min in THF (5 mL). This solution was added slowly to a stirred mixture of 1,1'-binaphthyl-2,2'-bistriflate (500 mg, 0.9 mmol) and $NiCl_2$(dppp) (50 mg, 0.09 mmol) in THF (5 mL) at – 15°C. After 1 h the reaction was allowed to warm up to room temperature and stirred for 12 h at ambient temperature before quenched with 2N HCl. The mixture was poured into water and then extracted with dichloromethane, which was subsequently washed with water and brine, dried over Na_2SO_4 and the solvent was removed by rotary evaporation. The residue was purified by thin layer chromatography on silica gel with hexanes/ethyl acetate (97:3) as eluent to give **7** in 10% yield. ^{1}H NMR (400 MHz, $C_2D_2Cl_4$, 80°C): δ = 7.88 (d, 2H, J = 8.2 Hz), 7.85 (d, 2H, J = 8.5 Hz), 7.40 (m, 2H), 7.34 (d, 2H, J = 8.5 Hz), 7.29 – 7.20 (m, 4H), 6.77 (d, 4H, J = 8.3 Hz), 6.18 (d, 4H, J = 8.3 Hz), 1.15 (s, 18H) ppm. ^{13}C NMR (100 MHz, $C_2D_2Cl_4$, 80 °C): δ = 139.4, 138.2, 134.8, 134.2, 132.4, 129.1, 128.9, 128.7, 128.2, 127.7, 126.6, 125.6, 124.6, 124.1, 34.4, 31.5, 31.4 ppm. LR-MS (EI, 70eV): m/z = 57 (98.21), 519 [M^+] (100.0).

4,4'-Di(*tert*-butyl)biphenyl

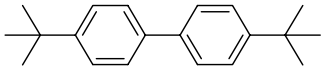

^{1}H NMR (400 MHz, $C_2D_2Cl_4$, 80 °C): δ = 7.50 (d, 2H, J = 8.2 Hz), 7.41 (d, 2H, J = 8.2 Hz), 1.32 (s, 18H) ppm. ^{13}C NMR (100 MHz, $C_2D_2Cl_4$, 80 °C): δ = 150.3, 137.9, 126.7, 126.0, 34.7, 31.7 ppm. LR-MS (EI, 70eV): m/z = 251 (100.0), 266 [M^+] (54.9).

1-Chloro-2,5-(4-*tert*-butylphenyl)benzene via a non-aqueous microwave procedure (13).

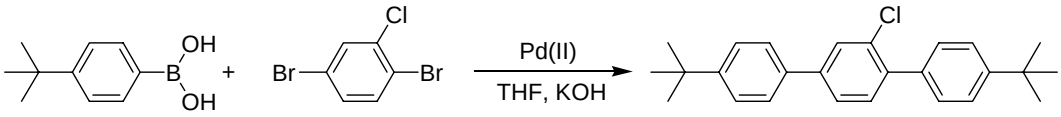

A dried 10 mL microwave tube was charged with 1-chloro-2,5-dibromo-benzene (**12**) (0.1g, 0.37 mmol), 4-*tert*-butyl-phenylboronic acid (**11**) (0.14g, 0.79 mmol), KOH (0.12g, 2.14 mmol), $PdCl_2(PPh_3)_2$ (0.013 g, 0.02 mmol) and sealed under argon. Dry THF (4 mL) was added and the reaction was irradiated with microwaves (300 W) for 10 min with air-cooling to keep the temperature between 110 and 115°C. The mixture was poured into water and then extracted with dichloromethane, which was subsequently washed with water and brine, dried over $MgSO_4$ and the solvent was removed by rotary evaporation. The residue was purified by column chromatography on silica gel with hexanes/ethylacetate (99:1) as eluent to give **13** in 95% yield. ^{1}H NMR (400 MHz, $C_2D_2Cl_4$, 80 °C): δ = 7.64 (d, 1H, J = 1.9Hz), 7.52 (m, 3H), 7.43 (m, 6H), 7.37 (d, 1H, J = 8.0 Hz), 1.34 (s, 9H), 1.33 (s, 9H) ppm. ^{13}C NMR (100 MHz, $C_2D_2Cl_4$, 80 °C): δ = 151.3, 150.7, 141.3, 138.9, 136.3, 136.0, 132.9, 132.1, 129.4, 128.4, 126.8, 126.2, 125.5, 125.3, 34.8, 34.8, 31.7, 31.6 ppm. LR-MS (EI, 70eV): m/z = 361 (79.4), 376 [M^+] (100.0), 377 (38.3). FD-MS: 377.0 (100.0). Anal. Calcd. for $C_{26}H_{29}Cl$: C, 82.84; H, 7.75. Found: C, 82.81; H, 7.46.

1,1´-Biphenyl-2,5,2´,5´-tetra-(4-*tert*-butylphenyl) via Yamamoto coupling (14).

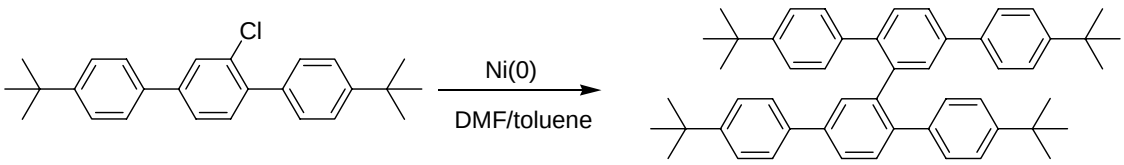

A dried 10 mL microwave tube was charged with **13** (0.10g, 0.27 mmol), $Ni(COD)_2$ (109mg, 0.40 mmol), 2,2'-bipyridyl (62mg, 0.40 mmol), COD (43mg, 0.40 mmol) and sealed under argon. Dry THF (4mL) was added and the reaction was irradiated with microwaves (300 W) for 12 min at a temperature of 130°C. The mixture was poured into water and then extracted

with dichloromethane, which was subsequently washed with 2 N HCl, water and brine, dried over Na_2SO_4 and the solvent was removed by rotary evaporation. The residue was purified by column chromatography on silica gel with hexanes/toluene (95:5) as eluent to give **14** in 82 % yield. ^{1}H NMR (400 MHz, $C_2D_2Cl_4$, 80 °C): δ = 7.63 (d, 2H, J = 1.73 Hz), 7.53 (dd, 2H, J = 8.2 Hz, 1.8 Hz), 7.49 (d, 4H, J = 8.4 Hz), 7.38 (d, 4H, J = 8.4 Hz), 7.21 (d, 2H, J = 8.1), 6.93 (d, 4H, J = 8.3 Hz), 6.51 (d, 4H, J = 8.5 Hz), 1.29 (s, 18H), 1.23 (s, 18H) ppm. ^{13}C NMR (100 MHz, $C_2D_2Cl_4$, 80 °C): δ = 150.7, 148.9, 140.5, 139.8, 139.3, 137.8, 137.5, 130.6, 130.5, 128.9, 126.8, 126.1, 126.0, 124.8, 34.7, 34.5, 31.6 ppm. LR-MS (EI, 70eV): m/z = 57 (85.8), 682 [M^+] (100.0). FD-MS: 683,8 (100.0). Anal. Calcd. for $C_{52}H_{58}$: C, 91.44; H, 8.56. Found: C, 90.75; H, 8.12.

4,4''-Di-(*tert*-butyl)terphenyl via a non-aqueous microwave procedure (16)

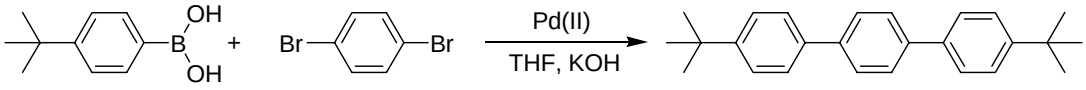

Compound **16** was prepared by a method similar to that used for **13** utilizing 1,4-dibromo-benzene (**15**). The crude product was purified by column chromatography on silica gel with hexanes/toluene (97:3) as eluent to give **16** in 90 % yield. ^{1}H NMR (400 MHz, $C_2D_2Cl_4$, 80 °C): δ = 7.63 (s, 4H), 7.56 (dd, 4H, J = 1.8 Hz, J = 6.5 Hz), 7.43 (dd, 4H, J = 1.9 Hz, J = 6.5 Hz), 1.35 (s, 18H) ppm. ^{13}C NMR (100 MHz, $C_2D_2Cl_4$, 80 °C): δ = 150.7, 139.7, 137.7, 127.3, 126.8, 126.0, 34.9, 31.6 ppm. LR-MS (EI, 70eV): m/z = 57 (100.0), 71 (60.2), 342 [M^+] (20.5), 343 (5.8). FD-MS: 342.9 (100.0). Anal. Calcd. for $C_{26}H_{30}$: C, 91.17; H, 8.83. Found: C, 91.12; H, 9.00.

2',2''-Bis(4-*tert*-butylphenyl)-1',1''-biphenyl via a non-aqueous microwave procedure (18)

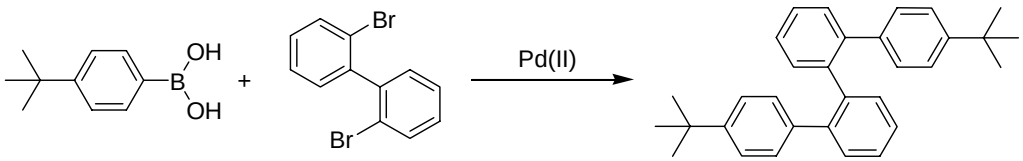

Compound **8** was prepared in the same manner as used for **13** utilizing 2,2'-dibromo-biphenyl (**17**) (0.04g, 1,28 mmol). Purification was carried out via column chromatography on silica gel with hexanes/toluene (95:5) as eluent to give **18** in 82 % yield. ^{1}H NMR (400 MHz, $C_2D_2Cl_4$, 25°C): δ = 7.42 (dd, 2H, J = 1.6Hz, J = 7.4Hz), 7.31 (dtd, 4H, J = 1.5 Hz, J = 7.3 Hz, J = 18.1 Hz), 7.11 (dd, 2H, J = 1.4 Hz, J = 7.5 Hz), 6.88 (d, 4H, J = 8.2 Hz), 6.35 (d, 4H, J =

8.2 Hz), 1.25 (s, 18H) ppm. ^{13}C NMR (100 MHz, $C_2D_2Cl_4$, 25°C): δ = 148.6, 140.9, 140.4, 137.9, 132.1, 129.9, 128.7, 127.8, 127.4, 124.6, 34.5, 31.7 ppm. FD-MS: 419.0 (100.0). Anal. Calcd. for $C_{32}H_{34}$: C, 91.81; H, 8.19. Found: C, 91.88; H, 8.51.

1-Chloro-2,5-bis(4-trimethylsilyl-phenyl)benzene via a conventional Suzuki cross-coupling (20)

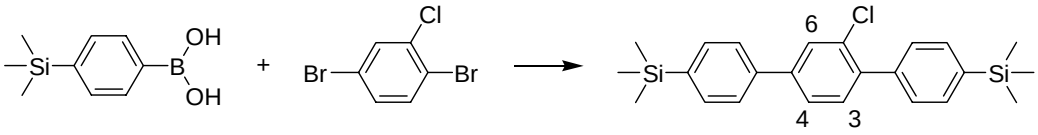

Compound **20** was prepared by a method similar to that used for **13** utilizing 1-trimethylsilylbenzene 4-boronic acid (**19**). The crude product was recrystallized from dichlormethane/heptane to afford **20** in 75 % yield. ^{1}H NMR (400 MHz, $C_2D_2Cl_4$, 25 °C): δ = 7.69 (d, 1H, J = 1.7 Hz, H-6), 7.58 (m, 6H), 7.53 (dd, 1H, J = 1.7Hz, J = 8.0 Hz, H-4), 7.46 (d, 2H, J = 7.9 Hz), 7.39 (d, 1H, J = 7. 9Hz, H-3), 0.29 (s, 9H, -CH_3), 0.28 (s, 9H, -CH_3) ppm. ^{13}C NMR (100 MHz, $C_2D_2Cl_4$, 25 °C): δ = 141.7, 140.6, 140.1, 139.6, 139.4, 139.3, 134.3, 133.4, 133.0, 132.1, 129.0, 128.7, 126.5, 125.8, - 0.7, - 0.7 ppm. MS (EI, m/z): 73 (63.8), 393 (100.0), 395 (53.6), 408 (88.4), 409 (33.6), 410 [M^+] (42.3). Anal. Calcd. for $C_{24}H_{29}ClSi_2$: C, 70.46; H, 7.14. Found: C, 69.90; H, 7.72.

1-Chloro-2,5-bis(4-iodo-phenyl)benzene (21).

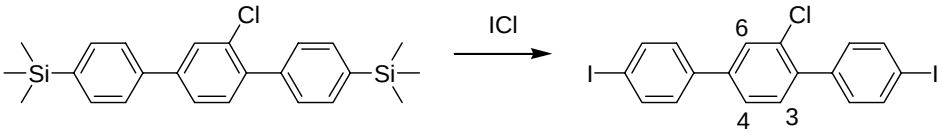

20 (1.67 g, 4.08 mmol) was dissolved in dichloromethane (20 mL), ICl (9.0 mL, 8.98 mmol, 1 M solution) in dichloromethane was added at 0°C within 1 h. After 2 h of stirring and warming up to room temperature a 1 M solution of sodium disulfite (20 mL) was added. The mixture was extracted into dichloromethane, washed with water and brine and dried over Na_2SO_4. The residue was recrystallized from heptane to afford 1.88 g (89 %) of **21**. ^{1}H NMR (400 MHz, $C_2D_2Cl_4$, 25 °C): δ = 7.73 (dd, 4 H, J = 2.7 Hz, J = 8.4 Hz), 7.60 (d, 1 H, J = 1.7 Hz, H-6), 7.43 (dd, 1 H, J = 1.7 Hz, J = 8.0 Hz, H-4), 7.31 (d, 1 H, J = 8.1, H-3), 7.28 (d, 2 H, J = 8.4 Hz), 7.17 (d, 2 H, J = 8.3 Hz) ppm. ^{13}C NMR (100 MHz, $C_2D_2Cl_4$, 25 °C): δ = 141.0, 138.9, 138.6, 138.5, 138.4, 137.6, 133.0, 131.9, 131.6, 129.1, 128.5, 125.7, 94.4, 94.2 ppm. MS (EI, m/z): 226 (60.2), 353 (31.5), 516 [M^+] (100.0). Anal. Calcd. for $C_{18}H_{11}ClI_2$: C, 41.85; H, 2.15. Found: C, 41.83; H, 2.37.

2''-Chloro-3,5,3'''',5''''-tetra(*tert*-butyl)-pentaphenyl (22).

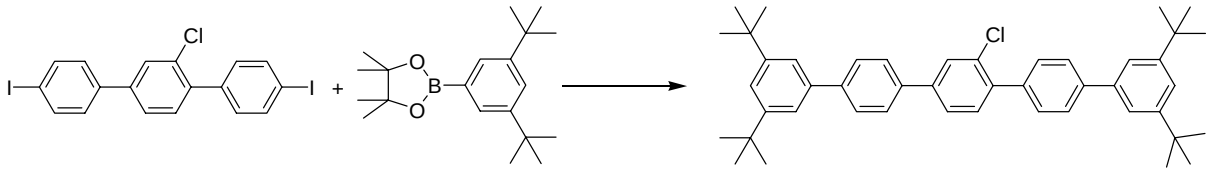

Compound **22** was prepared by a method similar to that used for **13** utilizing **21** and 3,5-di-*tert*-butylphenyl-(4,4,5,5-tetramethyl-1,3,2-dioxaborolane). Purification was carried out via recrystalization from a mixture of dichloromethane and heptane to give **22** in 77 % yield. ^{1}H NMR (400 MHz, $C_2D_2Cl_4$, 25 °C): δ = 7.76 (d, 1 H, J = 1.7Hz), 7.67 (m, 6 H), 7.59 (dd, 1H, J = 1.8 Hz, J = 8.1 Hz), 7.56 (d, 2 H, J = 8.2Hz), 7.47 (d, 1 H, J = 8.0 Hz), 7.44 (dd, 1 H, J = 1.5 Hz, J = 8.2 Hz), 7.40 (m, 2 H), 1.36 (s, 36 H) ppm. ^{13}C NMR (100 MHz, $C_2D_2Cl_4$, 25 °C): δ = 151.4, 142.2, 141.7, 141.4, 139.7, 139.5, 139.0, 137.9, 137.8, 133.1, 132.1, 130.2, 128.6, 128.1, 127.6, 127.2, 1257.2, 125.8, 122.2, 122.2, 121.6, 35.2, 31.9 ppm. LR-MS (EI, m/z): 57 (100.0), 640 (29.7), 641 (14.4), 642 [M^+] (12.3). FD-MS: 641.7 (100.0). Anal. Calcd. for $C_{46}H_{53}Cl$: C, 86.14; H, 8.33. Found: C, 84.96; H, 5.59.

2''-Chloro-4,4''''-di(*tert*-butyl)-pentaphenyl (23).

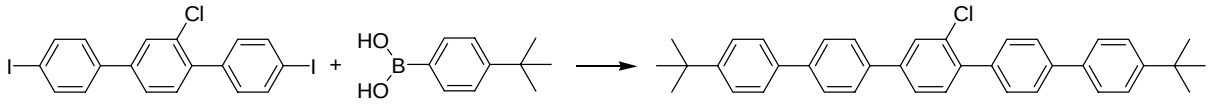

Compound **23** was prepared by a method similar to that used for **13** utilizing **21** and *para* - *tert*-butyl-phenyl-boronic-acid (**11**). Purification was carried out via chromatography (hexanes/toluene 85:15) to give **23** in 83 % yield. ^{1}H NMR (400 MHz, $C_2D_2Cl_4$, 80 °C): δ = 7.76 (d, 1H, J = 1.7 Hz), 7.66 (m, 6H), 7.57 (m, 7H), 7.45 (pd, 5 H, J = 8.4Hz), 1.35 (s, 18 H) ppm. ^{13}C NMR (100 MHz, $C_2D_2Cl_4$, 80 °C): δ = 151.0, 150.9, 141.4, 140.8, 140.4, 139.2, 138.0, 137.9, 137.6, 137.4, 133.2, 132.0, 130.1, 128.6, 127.6, 127.5, 126.9, 126.8, 126.7, 126.0, 126.0, 125.6, 34.7, 31.6 ppm. LR-MS (EI, m/z): 57 (100.0), 528 (36.9), 529 [M^+] (14.6), 530 (13.8). FD-MS: 529.4 (100.00). Anal. Calcd. for $C_{38}H_{37}Cl$: C, 86.25; H, 7.05. Found: C, 85.12; H, 4.72.

9,9-Dimethyl fluorene-2-(4,4,5,5-tetramethyl-1,3,2-dioxaborolane)

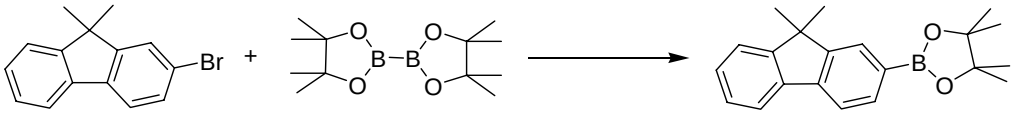

A mixture of 2-bromo-9,9-dimethyl-fluorene (3.59 g, 13.2 mmol), bis(pinacolato)diborolane (5 g, 19.6 mmol), Pd(dppf)Cl_2 (1.07 g, 1.30 mmol) and potassium acetate (6.4 g, 65.2 mmol) in THF (60 mL) was stirred under argon at 80°C for 48 h. The mixture was extracted with dichloromethane and washed with water and brine several times. The solvent was removed under reduced pressure. The residue was purified via column chromatography with hexanes/ethyl acetate (95:5) to give 2-pinacolato-boronic-ester-9,9-dimethyl-fluorene in 85 % yield. ^{1}H NMR (400 MHz, $C_2D_2Cl_4$, 25 °C): δ = 7.87 (s, 1H), 7.80 (d, 1H, J = 7.6Hz), 7.73 (m, 1H), 7.70 (d, 1H, J = 7.5Hz), 7.42 (m, 1H), 7.31 (m, 2H), 1.49 (s, 6H), 1.34 (s, 12H) ppm. ^{13}C NMR (100 MHz, $C_2D_2Cl_4$, 25 °C): δ = 154.5, 153.0, 142.4, 139.2, 134.2, 129.1, 128.2, 127.3, 123.0, 120.8, 119.6, 84.0, 47.1, 27.5, 25.3 ppm. LR-MS (EI, m/z): 305 (74.7), 306 (15.3), 319 (23.8), 320 [M^+] (100.0), 321 (23.5). Anal. Calcd. for $C_{21}H_{25}BO_2$: C, 78.76; H, 7.87. Found: C, 78.93; H, 8.21.

2-bromo-9,9-di-*n*-octyl-fluorene

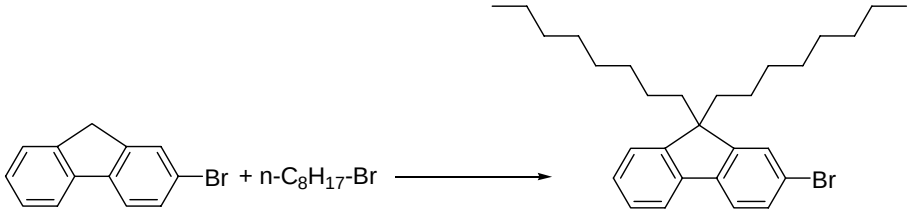

To a solution of 2-bromo-fluorene (25 g, 102 mmol) and tetrabutyl-ammoniumbromide (9.9 g, 31 mmol) in DMSO (75 mL) were added an aqueous sodiumhydroxide solution (40 mL, 50%) and *n*-octylbromide (43.3 g, 225). The mixture was stirred at 80°C for 2 h and then poured into water (100 mL). The mixture was extracted two times with diethylether and the combined organic phases were washed with brine, water and dried over Na_2SO_4. Upon evaporating off the solvent the residue was purified via column chromatography with hexane as eluent to afford 2-bromo-9,9-di-n-octyl-fluorene (86 %) as a colorless oil. ^{1}H NMR (400 MHz, $CDCl_3$, 25 °C): δ = 7.59 (td, 1H, J = 2.6 Hz, J = 5.2 Hz), 7.49 (d, 1H, J = 7.9 Hz), 7.41 (d, 1H, J = 1.5 Hz), 7.38 (dd, 1H, J = 1.5 Hz, J = 8.0 Hz), 7.25 (m, 3H), 1.85 (m, 4H), 1.05 (m, 20H), 0.76 (t, 6H, J = 7.1 Hz), 0.57 (m, 4H) ppm. ^{13}C NMR (100 MHz, $CDCl_3$, 25 °C): δ = 153.4, 150.6, 140.4, 140.1, 130.1, 127.8, 127.1, 126.4, 123.3, 121.3, 121.1, 120.0, 55.6,

40.3, 32.1, 30.2, 29.5, 29.5, 24.0, 22.9, 14.7 ppm. LR-MS (EI, m/z): 42 (61.9), 57 (98.0), 470 [M^+] (100.0).

(9,9-di-*n*-octylfluorene)-2-(4,4',5,5'-tetramethyl-1,3,2-dioxaborolane)

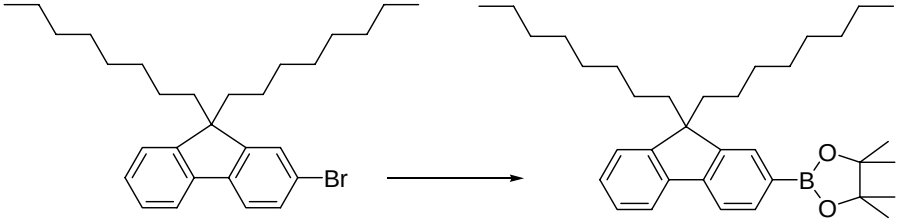

A flame dried 1000 mL flask was charged with **24** (14 g, 30 mmol) and sealed under argon. THF (450 mL) was added and the mixture cooled to -78°C. n-BuLi (84 mmol) was added, stirred for 10 min. and was then allowed to reach 0°C. The solution was cooled again to - 78°C, 2-isopropoxy-4,4',5,5'-tetramethyl-1,3,2-dioxaborolane (65 mmol) was added, then warmed up to room temperature and stirred for 24 h. The mixture was poured into water and extracted with chloroform. The organic layer was washed with brine, water and dried over Na_2SO_4. The solution was evaporated to dryness and the residue purified by chromatography using (hexanes/ethyl-acetate 95:5). After the solvent was removed, the remaining oil was recrytallized from ethanol to afford 2-(9,9-di-n-octylfluorene)-4,4',5,5'-tetramethyl-1,3,2-dioxaborolane as a white solid in 55 % yield. ^{1}H NMR (400 MHz, $CDCl_3$, 25 °C): δ = 7.74 (d, 1H, J = 7.7 Hz), 7.71 (s, 1H), 7.67 (m, 1H), 7.63 (d, 1H, J = 7.5 Hz), 7.27 (m, 3H), 1.91 (m, 4H), 1.31 (s, 12H), 1.14 (m, 4H,) 0.99 (m, 16H), 0.76 (t, 6H, J=7.1Hz),0.58 (m, 4H) ppm. ^{13}C NMR (100 MHz, $CDCl_3$, 25 °C): δ = 151.6, 150.2, 144.2, 141.0, 133.8, 129.3, 127.8, 126.9, 123.4, 120.4, 119.2, 83.9, 55.2, 40.3, 32.5, 32.1, 30.3, 29.5, 25.3, 24.0, 22.9, 14.5 ppm. LR-MS (EI, m/z): 101 (99.7), 404 (75.4), 517 [M^+] (100.0).

2'-Chloro-4,4''-bis(9,9-di-*n*-octyl-fluorene-2-yl)-terphenyl (24)

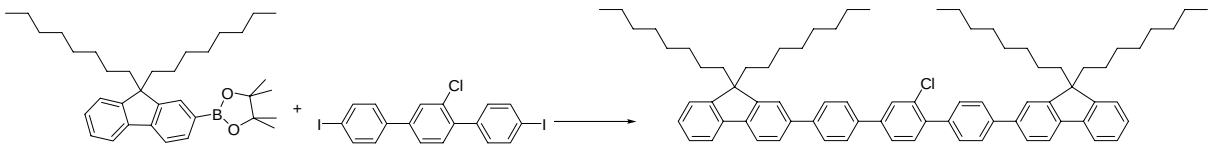

The compound was prepared by a method analogous to that used for compound **13** utilizing 2 - (9,9-di-n-octylfluorene)-4,4',5,5'-tetramethyl-1,3,2-dioxaborolane. After work up a white slightly brownish solid was isolated which was recrystallized from dichloromethane/ethanol to afford **24** as a white solid in 69 % yield. ^{1}H NMR (400 MHz, $C_2D_2Cl_4$, 25 °C): δ = 7.66-7.80 (m, 11H), 7.56-7.64 (m, 7H), 7.47 (d, 1H, J=7.9Hz), 7.22-7.38 (m, 6H), 1.98 (m, 8H),

0.8-1.3 (m, 40H), 0.75 (t, 12H, J = 7.1 Hz), 0.7 (m, 8H) ppm. ^{13}C NMR (100 MHz, $C_2D_2Cl_4$, 25 °C): δ = 151.8, 151.8, 151.3, 141.4, 140.9, 140.9, 140.9, 140.8, 140.8, 139.2, 139.1, 139.0, 138.1, 137.9, 133.1, 132.1, 130.2, 128.6, 127.9, 127.6, 127.4, 127.0, 126.0, 125.8, 123.3, 121.5, 120.3, 120.1, 55.3, 40.5, 40.4, 32.0, 30.3, 29.5, 24.1, 22.9, 14.4 ppm. FD-MS: 1042.6 (100.00). Anal. Calcd. for $C_{36}H_{29}Cl$: C, 87.60; H, 9.00. Found: C, 87.70; H, 10.15.

1-Chloro-2,5-bis(9,9-dimethyl fluorene-2-yl) benzene (25).

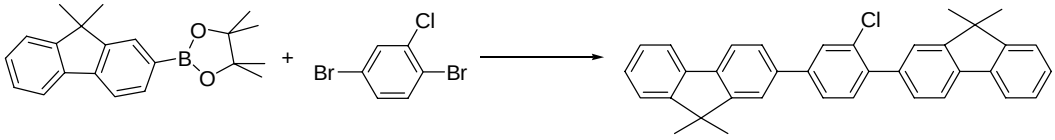

The compound was prepared by a method analogous to that used for compound **13** utilizing 9,9-dimethyl fluorene-2-(4,4,5,5-tetramethyl-1,3,2-dioxaborolane). After the work up a white slightly brownish solid was isolated which was recrystallized from dichloromethane/ethanol to afford **25** as a white solid in 69 % yield. ^{1}H NMR (400 MHz, $C_2D_2Cl_4$, 25 °C): δ = 7.78 (d, 1H, J = 1.6 Hz), 7.75 (dd, 2H, J = 2.4 Hz, J = 7.8 Hz), 7.72 (dd, 2H, J = 1.2Hz, J = 7.0Hz), 7.65 (d, 1H, J = 1.1Hz), 7.62 (dd, 1H, J = 7.9 Hz, J = 1.6 Hz), 7.56 (m, 2H), 7.48 (d, 1H, J = 7.93 Hz), 7.46 (dd, 1H, J=1.4Hz, J=7.8Hz), 7.42 (dd, 1H, J = 6.3 Hz, J = 1.4 Hz), 7.31 (m, 4H), 1.50 (d, 12H, J = 5.26 Hz) ppm. ^{13}C NMR (100 MHz, $C_2D_2Cl_4$, 25 °C): δ = 154.9, 154.4, 154.3, 153.8, 142.3, 139.8, 139.4, 139.1, 138.9, 138.9, 138.7, 138.3, 133.2, 132.0, 128.8, 128.6, 127.8, 127.7, 127.3, 127.3, 126.3, 125.8, 124.2, 122.9, 122.9, 121.4, 120.7, 120.4, 120.4, 119.8, 47.2, 47.2, 27.5, 27.4 ppm. LR-MS (EI, m/z): 83 (54.4), 481 (36.8), 496 (100.0), 497 [M^+] (39.5), 498 (38.3), 499 (11.5). FD-MS: 497.0 (100.00). Anal. Calcd. for $C_{36}H_{29}Cl$: C, 86.99; H, 5.88. Found: C, 86.03; H, 5.92.

Pentaphenyl dimer (26).

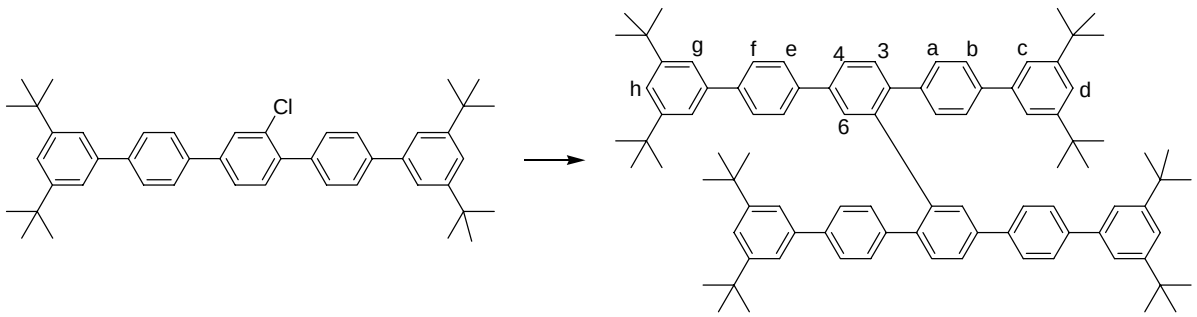

A flame-dried microwave tube was charged with **22** (50 mg, 0.08 mmol), $Ni(COD)_2$ (65 mg, 0.24 mmol), 2,2'-bipyridyl (37.5 mg, 0.24 mmol) and sealed under argon. THF (3 mL) and COD (26 mg, 0.24 mmol) were added. The tube was microwave irradiated (300 W) to hold a

temperature of 120°C for 15 min. The mixture was poured into 2N HCl extracted with dichloromethane, which was subsequently washed with conc. titriplex solution and water, dried over Na_2SO_4 and the solvent was removed. The residue was purified by chromatography (hexanes/toluene 95:5) a to afford **26** in 70 % yield as a white powder, which was recrystallized from dichloromethane/heptane. ^{1}H NMR (400 MHz, $C_2D_2Cl_4$, 25 °C): δ = 7.84 (d, 2H, J = 1.7 Hz, H-6), 7.72 (d, 4H, J = 8.4 Hz, H-e), 7.65 (m, 2H/4H, H-4/H-f), 7.39 (d, 4H, J = 1.6 Hz, C-h/C-d), 7.35 (m, 4H, H-c/H-g), 7.31 (d, 2H, J = 8.1 Hz, H-3), 7.28 (d, 4H, J = 8.2 Hz, H-b), 6.77 (d, 4H, J = 8.2 Hz, H-a), 1.32 (s, 18H), 1.31 (s, 18H) ppm. ^{13}C NMR (100 MHz, $C_2D_2Cl_4$, 25 °C): δ = 151.4, 151.3, 141.7, 140.7, 140.1, 140.1, 140.0, 139.7, 139.5, 139.0, 130.8, 130.4, 129.9, 128.0, 127.5, 126.7, 126.3, 122.1, 122.0, 121.6, 121.4, 35.25, 35. 2, 31.9 ppm. FD-MS: 1212.1 (100.00). Anal. Calcd. for $C_{92}H_{106}$: C, 91.18; H, 8.82. Found: C, 91.56; H, 8.12.

Tetrafluorenyl pentaphenyl dimer (27)

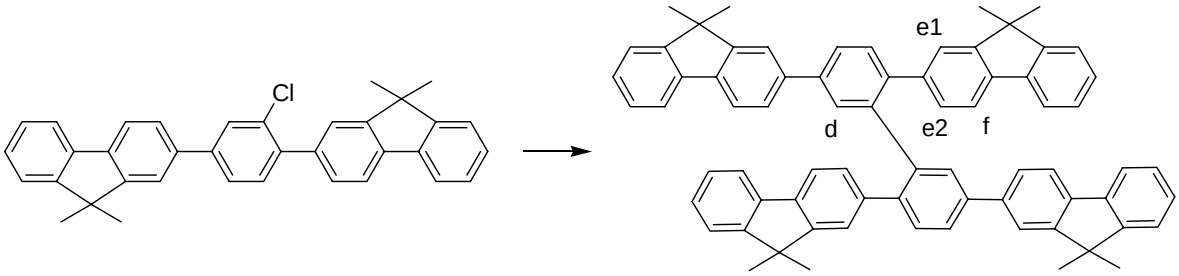

Compound **27** was prepared by a method similar to that used for **26** utilizing **25**. Purification was carried out via chromatography over silica gel using (hexanes/toluene 90:10). After the solvent was removed, the remaining solid was recrystallized from pentane to give **27** in 77 % yield. ^{1}H NMR (400 MHz, $C_2D_2Cl_4$, 80 °C): δ = 7.75 (s, 2H, H-d), 7.72 – 7.57 (m, 8H), 7.52 (d, 2H, J = 7.9 Hz), 7.47 (m, 4H), 7.44 – 7.36 (m, 4H), 7.35 – 7.18 (m, 10H), 6.90 (s, 2H, H-e1), 6.87 (d, 2H, J = 7.8 Hz, H-e2), 1.55 – 1.44 (m, 6H), 1.42 – 1.36 (m, 6H), 1.24 – 1.14 (m, 12H). ^{13}C NMR (100 MHz, $C_2D_2Cl_4$, 80 °C): δ = 154.7, 154.2, 152.9, 154.2, 140.8, 140.4, 140.4, 139.9, 139.7, 139.2, 139.0, 138.8, 137.4, 131.0, 130.8, 128.4, 127.7, 127.4, 127.3, 127.1, 126.6, 126.3, 124.4, 123.0, 122.9, 121.6, 120.6, 120.4, 120.4, 119., 47.2, 46.6, 32.2, 29.3, 27.6, 27.5, 27.4, 27.2, 23.0, 14.5 ppm. LR-MS (EI, m/z): 922 (100.0), 923 [M^+] (78.8), 924 (29.2). FD-MS: 922.6 (100.0). Anal. Calcd. for $C_{72}H_{58}$: C, 93.67; H, 6.33. Found: C, 92.98; H, 5.80.

1,4-bis(9,9-dimethyl-flourene-2-yl)benzene (28)

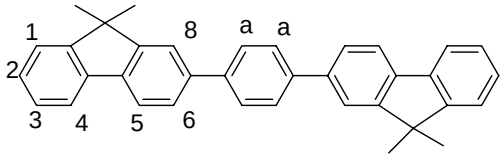

28 was isolated during the work-up procedure of **27** in 12 % yield. ^{1}H NMR (400 MHz, $C_2D_2Cl_4$, 80 °C): δ = 7.75 (d, 2 H, J(5-6) = 7.8 Hz, H-5), 7.26 (ps, 4 H, J(a-6) = 1.1 Hz, H-a), 7.70 (pdd, 2 H, J = 6.5 Hz, J = 7.1 Hz, J = 2.9 Hz, H-4), 7.67 (ps, 2 H, J(8-6) = 1.6 Hz, H-8), 7.60 (dd, 2 H, J (6-5) = 7.8 Hz, J(6-8) = 1.6, H-6), 7.43 (m, 2 H, J = 2.3, J = 6.3, J = 7.7, H-1), 7.30 (m, 4 H, J = 1.6, J = 6.3, J = 2.2, H-2, H-3), 1.52 (s, 6 H, -CH_3) ppm. ^{13}C NMR (100 MHz, $C_2D_2Cl_4$, 80 °C): δ = 154.6, 154.2, 140.4, 139.8, 139.0, 138.8, 127.8, 127.7, 127.3, 126.3, 123.0, 121.5, 120.7, 120.4, 47.2, 30.0, 27.6 ppm. LR-MS (EI, m/z): 447 (34.36), 462 [M^+] (100.0), 463 (68.0), 464 (12.9). Anal. Calcd. for $C_{36}H_{30}$: C, 93.46; H, 6.54. Found: C, 88.18; H, 10.06.

Tetrafluorenyl heptaphenyl dimer (29)

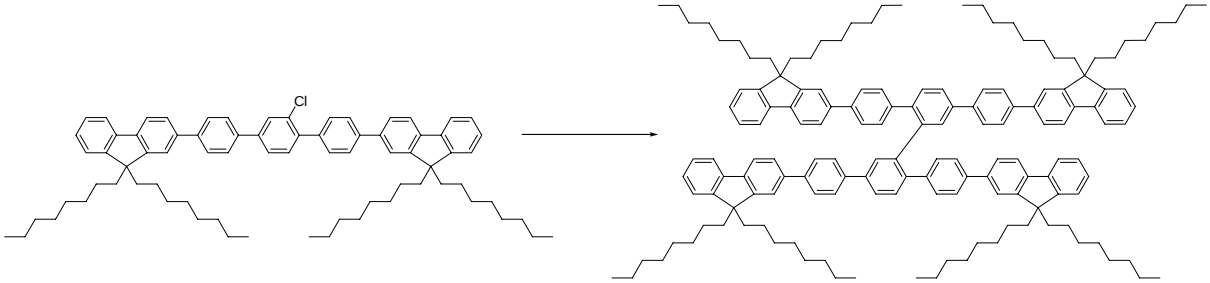

Compound **29** was prepared by a method similar to that used for **26** utilizing **24**. Purification was carried out via chromatography over silica gel using (hexanes/toluene 90:10) to give **29** in 77 % yield. ^{1}H NMR (400 MHz, $C_2D_2Cl_4$, 25 °C): δ = 7.88 (s, 2H), 7.80 – 7.64 (m, 18H), 7.61 – 7.52 (m, 6H), 7.50 (s, 2H), 7.32 – 7.21 (m, 12H), 6.82 (d, 2H, J = 8.2 Hz), 1.93 (m, 16H), 1.16 – 0.95 (m, 82H), 0.77 – 0.69 (m, 26H), 0.68 – 0.60 (m, 12H) ppm. ^{13}C NMR (100 MHz, $C_2D_2Cl_4$, 25 °C): δ = 151.8, 151.3, 151.2, 140.9, 140.8, 140.6, 140.6, 140.0, 139.8, 139.6, 139.5, 139.3, 139.1, 130.5, 129.9, 127.8, 127.6, 127.4, 127.3, 127.0, 126.6, 126.4, 126.0, 125.9, 123.3, 121.6, 120.2, 120.0, 55.3, 40.4, 32.0, 30.3, 30.0, 29.5, 24.1, 22.9, 14.4 ppm. FD-MS: 2015.7 (100.00). Anal. Calcd. for $C_{152}H_{186}$: C, 90.69; H, 9.31. Found: C, 90.23; H, 9.73.

References and Notes

[1] P. Strohriegel, J. V. Grazulevicius, *Adv.Mater.* **2002**, *14*, 1439.

[2] Y. Shirota, *J.Mater.Chem.* **2005,** *15*, 75.

[3] Y. Shirota, *J.Mater.Chem.* **2000**, *10*, 1.

[4] G. Hughes, M. R. Bryce, *J.Mater.Chem.* **2005**, *15*, 94.

[5] M. D. Joswick, I. H. Cambell, N. N. Barashkov, J. P. Ferraris, *J.Appl.Phys.* **1996**, *80*, 2883.

[6] G. Odian, *Principles of Polymerization*, Wiley, New York **1991**.

[7] F. Garnier, A. Yasar, R. Hajilaoui, G. Horowitz, F. Deloffre, B. Servet, S. Ries, P. Alnot, *J.Am.Chem.Soc.* **1993**, *115*, 8716.

[8] S. Doi, M. Kuwabara, T. Noguchi, T. Ohnishi, *Synthetic Metals* **1993**, *55-57*, 4174.

[9] K. Okumoto, Y. Shirota, *Chem.Mater.* **2003**, *15*, 699.

[10] J. Blochwitz, M. Pfeiffer, K. Leo, *Synthetic Metals* **2002**, *127*, 169.

[11] N. Johansson, J. Salbeck, J. Bauer, F. Weissörtel, P. Bröms, A. Andersson, W. R. Salaneck, *Adv.Mater.* **1998**, *10*, 1136.

[12] T. Spehr, R. Pudzich, T. Fuhrmann, J. Salbeck, *Organic Electronics* **2003**, *4*, 61.

[13] M. R. Robinson, S. Wang, G. C. Bazan, Y. Cao, *Adv.Mater.* **2000**, *12*, 1701.

[14] X. M. Liu, H. He, J. Huang, J. Xu, *Chem.Mater.* **2005**, *17*, 434.

[15] J. C. Ostrowski, R. A. Hudack, M. R. Robinson, S. Wang, G. C. Bazan, *Chem.Eur.J.* **2001**, *7*, 4500.

[16] H. Benmansour, T. Shioya, Y. Sato, G. C. Bazan, *Adv.Funct.Mater.* **2003**, *13*, 883.

[17] A. Almutairi, F. S. Tham, M. J. Marsella, *Tetrahedron* **2004**, *60*, 7187.

[18] M. J. Marsella, K. Yoon, A. Almutairi, S. K. Butt, F. S. Tham, *J.Am.Chem.Soc.* **2003**, *125*, 13928.

[19] L. Pu, *Chem.Rev.* **1998**, *98*, 2405.

[20] Berthod M., G. Mignani, G. Woodward, M. Lemaire, *Chem.Rev.* **2005**, *105*, 1801.

[21] R. Noyori, *Asymmetric Catalysis in Organic Synthesis*, Wiley, New York **1994**.

[22] L. Pu, *Chem.Rev.* **2004**, *104*, 1687.

[23] S. G. Telfer, R. Kuroda, *Coord.Chem.Rev.* **2003**, *242*, 33.

[24] A. K. Y. Jen, Y. Liu, Q. Hu, L. Pu, *Appl.Phys.Lett.* **1999**, *75*, 3745.

[25] L. Pu, *Macromol.Rapid Commun.* **2000**, *21*, 795.

[26] E. G. Ijpeij, F. H. Beijer, H. J. Arts, C. Newton, J. G. de Vries, G. J. M. Gruter, *J.Org.Chem.* **2002**, *67*, 169.

[27] D. L. An, T. Nakano, A. Orita, J. Otera, *Angew.Chem.Int.Ed.* **2002**, *41*, 171.

[28] B. Schilling, D. E. Kaufmann, *Eur.J.Org Chem.* **1998**, 701.

[29] P. Kasak, H. Brath, M. Dubovska, M. Juricek, M. Putala, *Tetrahdron Lett.* **2004**, *45*, 791.

[30] K. Krascsenicsova, P. Walla, P. Kasak, G. Uray, C. O. Kappe, M. Putala, *Chem.Commun.* **2004**, 2606.

[31] J. N. Wilson, K. I. Hardcastle, M. Josowicz, U. H. F. Bunz, *Tetrahedron* **2004**, *60*, 7157.

[32] J. E. Klare, G. S. Tulevski, K. Sugo, A. de Picciotto, K. A. White, C. Nuckolls, *J.Am.Chem.Soc.* **2003**, *125*, 6030.

[33] J. N. Wilson, M. D. Smith, V. Enkelmann, U. H. F. Bunz, *Chem.Commun.* **2004**, 1700.

[34] J. N. Wilson, M. Josowicz, Y. Wang, U. H. F. Bunz, *Chem.Commun.* **2003**, 2962.

[35] Y. Uozumi, A. Tanahashi, S. Y. Lee, T. Hayashi, *J.Org.Chem.* **1993**, *58*, 1945.

[36] A. Krasovsky, P. Knochel, *Angew.Chem.* **2004**, *116*, 3396.

[37] J. E. Field, T. J. Hill, D. Venkataraman, *J.Org.Chem.* **2003**, *68*, 6071.

[38] T. J. Katz, *Angew.Chem.Int.Ed.* **2000**, *39*, 1921.

[39] A. E. Rowan, J. M. Nolte, *Angew.Chem.Int.Ed.* **1998**, *37*, 63.

[40] T. Nakano, T. Yade, *J.Am.Chem.Soc.* **2003**, *125*, 15474.

[41] A. Orita, D. L. An, T. Nakano, J. Yaruva, N. Ma, J. Otera, *Chem.Eur.J.* **2002**, *8*, 2005.

[42] R. E. Abed, B. B. Hassine, J. P. Genet, M. Gorsane, A. Marinetti, *Eur.J.Org Chem.* **2004**, 1517.

[43] L. A. Cuccia, J. M. Lehn, J. C. Homo, M. Schmutz, *Angew.Chem.Int.Ed.* **2000**, *39*, 233.

[44] R. B. Prince, T. Okada, J. S. Moore, *Angew.Chem.Int.Ed.* **1999**, *38*, 233.

[45] C. A. Hunter, J. K. M. Saunders, *J.Am.Chem.Soc.* **1990**, *112*, 5525.

[46] C. Janiak, *J.Chem.Soc.Dalton Trans.* **2000**, 3885.

[47] K. M. Guckian, B. A. Schweitzer, R. X. F. Ren, C. J. Sheils, D. C. Tohmassebi, E. T. Kool, *J.Am.Chem.Soc.* **2000**, *122*, 2213.

[48] E. Ibuki, S. Ozasa, Y. Fujioka, H. Kitamura, *Chem.Pharm.Bull.* **1980**, *28*, 1468.

[49] A. Suzuki, *J.Organomet.Chem.* **1999**, *576*, 147.

[50] A. Suzuki, *J.Organomet.Chem.* **2002**, *653*, 83.

[51] B. S. Nehls, E. Preis, S. Füldner, T. Farrell, U. Scherf, *Macromolecules* **2005**, *38*, 687.

[52] K. R. Carter, *Macromolecules* **2002**, *35*, 6757.

[53] B. S. Nehls, Diplomarbeit, Mikrowellenunterstützte Synthese von Polyarylenen, Bergische Universität Wuppertal, **2003**.

[54] F. Galbrecht, X. H. Yang, B. S. Nehls, D. Neher, T. Farrell, U. Scherf, *Chem.Commun.* **2005**, 2378.

[55] A. J. Blake, P. A. Cooke, K. J. Doyle, S. Gair, N. S. Simpkins, *Tetrahdron Lett.* **1998**, *39*, 9093.

[56] L. Tong, H. Lau, D. M. Ho, R. A. Pascal Jr, *J.Am.Chem.Soc.* **1998**, *120*, 6000.

[57] T. Motomura, H. Nakamura, M. Suginome, M. Murakami, Y. Ito, *Bull.Chem.Soc.Jpn.* **2005**, 142.

[58] I. B. Berlman, H. O. Wirth, O. J. Steingraber, *J.Phys.Chem.* **1971**, *75*, 318.

[59] I. B. Berlman, *J.Chem.Phys.* **1970**, *52*, 5616.

[60] G. B. Schuster, *Acc.Chem.Res.* **2000**, *33*, 253.

[61] R. Güntner, PhD thesis, Oligomere und Blockcopolymere auf Fluorenbasis, BU-Wuppertal, **2004**.

[62] G. Klaerner, R. D. Miller, *Macromolecules* **1998**, *31*, 2007.

List of Symbols and Abbreviations

bipy	2,2'-Bipyridyl
COSY	correlated spectroscopy
δ	chemical shift
DMF	*N*, *N* – Dimethylformamide
d	doublett
DSC	Differential Scanning Calorimetry
eq.	equivalent
h	hours
HOMO	highest occupied molecular orbital
IR	infra red
LUMO	lowest unoccupied molecular orbital
MeLPPP	methylated – ladder poly(*para*-phenylene)
min	minutes
M_n	Number average molecular weight [$g \cdot mol^{-1}$]
M_w	Weight average molecular weight [$g \cdot mol^{-1}$]
NMR	nuclear magnetic resonance
n.m.	not measured
OFET	organic field effect transistor
OLED	organic light emitting diode
PD	polydispersity
PF	polyfluorene
PL	photoluminescence
ppm	parts per million
PPP	poly(*para*-phenylene)
q	quartett
THF	tetrahydrofuran
t	triplett

List of Publications

- H. Cheun, F. Galbrecht, B. S. Nehls, U. Scherf, M. J. Winokur, Temperature dependent spectroscopy of poly[9,9-bis-(2-ethyl)-hexylfluorene]/(9,9-di-*n*-octylfluorene) copolymers, *submitted*.

- K. Becker, J. M. Lupton, J. Feldmann, B. S. Nehls, F. Galbrecht, D. Q. Gao, U. Scherf, On chain fluorenone defect emission from single polyfluorene molecules: The ultimate evidence against excimer formation as the origin of the green fluorescence band, *Adv. Funct. Mater, accepted*.

- B. S. Nehls, F. Galbrecht, C. W. Lehmann, D. J. Brauer, T. Farrell, U. Scherf, Synthesis, Spectroscopy and medium Independent π- π Assisted Folding of an Oligophenyl Based Cruciform, *Org. Biomol. Chem.*, **2005**, *3*, 3213.

- T. Rabe, M. Hoping, D. Schneider, E. Becker, H. H. Johannes, W. Kowalsky, T. Weimann, J. Wang, P. Hinze, B. S. Nehls, U. Scherf, T. Farrell, T. Riedl, Threshold reduction in polymer lasers based on poly (9,9-dioctylfluorene) with statistical binaphthyl units, *Adv. Funct. Mater*., **2005**, *15*, 1188.

- F. Galbrecht, X. H. Yang, B. S. Nehls, D. Neher, T. Farrell, U. Scherf, Semiconducting polyfluorenes with electrophosphorescent on chain platinum-salen chromophores, *Chem. Commun.*, **2005**, 2378.

- B. S. Nehls, S. Füldner, E. Preis, T. Farrell, U. Scherf, Microwave – Assisted Synthesis of 1,5- and 2,6 Linked Naphthylene – Based Ladder Polymers, *Macromolecules*, **2005**, *38*, 687.

- B. S. Nehls, U. Asawapirom, S. Füldner, E. Preis, T. Farrell, U. Scherf, Semiconducting Polymers via Microwave-Assisted Suzuki and Stille Cross Coupling Reactions, *Adv. Funct. Mater.*, **2004**, *14*, 352.

Acknowledgment

- An erster Stelle danke ich Prof. Dr. U. Scherf für die vielseitige finanzielle und fachliche Unterstützung. Ebenso für die Möglichkeit eine Vielzahl von Konferenzen zu besuchen und einen Teil meiner Arbeit im Ausland durchführen zu dürfen.

- Prof. Dr. A. Monkman, Prof. Dr. M. Bryce und den jeweiligen Arbeitskreisen in Durham, UK sei ganz herzlich gedankt für die freundliche Aufnahme und die damit verbundene tolle Zeit in England.

- Für die finanzielle Unterstützung bedanke ich mich ganz herzlich beim Verband der chemischen Industrie und in besonderer Weise bei Frau Dr. Kiefer für die freundliche Betreuung.

- Meinem Laborkollegen Frank Galbrecht gilt ein besonderer Dank für die schöne Zeit im Labor, endlos viele Diskussionen über Gott und die Welt und einer Menge Spaß. Ebenfalls danke ich Dr. Tony Farrell für viele chemische Hilfestellungen, Ideen und seine tatkräftige Unterstützung. Ein weiterer Dank geht an unseren „Laborzuwachs“ Torsten Bünnagel für die Hilfe bei allen möglichen Computerproblemen und der ein oder anderen humoristischen Erzählung.

- Ein großes Dankeschön geht an alle weiteren Mitarbeiter der Scherf – Gruppe (Reihenfolge ohne Wertung): Sybille Allard, Sylwia Adamczyk, Askin Bilge, Patrick Casper, Bianca Enz, Michael Forster, Deqing Gao, Saulius Grigalevicius, Ligita Grigaleviciene, Anke Helfer, Christof Kudla, Eduard Preis, Benjamin Souharce, Guoli Tu, Argiri Tsami und meinen Praktikanten Sven Weber.

- Ilka Polanz sei herzlich gedankt für die Messung von unzähligen NMR und MS Proben, sowie die Hilfestellungen bei der Bearbeitung der Spektren.

- Prof. Dr. D.J. Brauer (Lehrstuhl für Anorganische Chemie) und Dr. C.W. Lehmann (MPI – Mülheim) danke ich für die Messung der Kristallstrukturen, die in dieser Arbeit präsentiert werden.

- Dem Arbeitskreis von Prof. Dr. W. Kowalsky (TU – Braunschweig) und allen voran Dr. T. Riedl und Dipl. Ing. T. Rabe sei gedankt für den Bau der sehr guten DFB Laser.

- Last but not least danke ich meiner Familie und all meinen Freunden, die mich das ganze Studium über begleitet haben.